

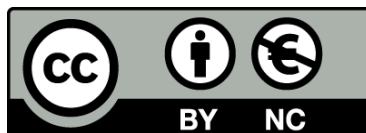


UNIVERSITAT DE
BARCELONA

Identification of novel NEK9 substrates and functions through the use of genetically engineered mice

Novel roles in the control of the centrosome cycle

Paula Martínez Delgado



Aquesta tesi doctoral està subjecta a la llicència [Reconeixement- NoComercial 4.0. Espanya de Creative Commons](#).

Esta tesis doctoral está sujeta a la licencia [Reconocimiento - NoComercial 4.0. España de Creative Commons](#).

This doctoral thesis is licensed under the [Creative Commons Attribution-NonCommercial 4.0. Spain License](#).

UNIVERSIDAD DE BARCELONA
FACULTAD DE FARMACIA Y CIENCIAS DE LA ALIMENTACIÓN

**IDENTIFICATION OF NOVEL NEK9
SUBSTRATES AND FUNCTIONS THROUGH THE
USE OF GENETICALLY ENGINEERED MICE**

NOVEL ROLES IN THE CONTROL OF THE CENTROSOME CYCLE

Paula Martínez Delgado, 2018



INSTITUTE
FOR RESEARCH
IN BIOMEDICINE



UNIVERSITAT DE
BARCELONA

UNIVERSIDAD DE BARCELONA
FACULTAD DE FARMACIA Y CIENCIAS DE LA ALIMENTACIÓN
Departamento de Bioquímica y Fisiología
Programa de Doctorado en Biomedicina

**IDENTIFICATION OF NOVEL NEK9
SUBSTRATES AND FUNCTIONS THROUGH THE
USE OF GENETICALLY ENGINEERED MICE**

NOVEL ROLES IN THE CONTROL OF THE CENTROSOME CYCLE

Memoria presentada por Paula Martínez Delgado para optar al
título de doctor por la Universidad de Barcelona

Dr. Joan Roig Amorós

Dr. Carme Caelles Franch

Paula Martínez Delgado



A mis padres

Y como no sabía que era imposible....

lo hice.

AGRADECIMIENTOS

Después de un intenso período de 5 años, hoy es el día. Han sido unos años de aprendizaje intenso, no solo en el campo científico, sino también a nivel personal. Realizar este trabajo ha tenido un gran impacto en mí y es por eso que me gustaría agradecer a todas aquellas personas que de una manera u otra han participado, leyendo, opinando, corrigiendo, apoyando, teniéndome paciencia, dándome ánimo, acompañando en los momentos de crisis y en los de felicidad, porque sin su valiosa aportación no hubiera sido posible este trabajo.

Gracias para empezar a Joan, mi jefe, por haber confiado en mí, por la orientación, el seguimiento continuo, por la motivación y el apoyo desde el principio hasta el final, que ha sido especialmente complicado.

A Carme y a Jens, mi tutora y el que casi puedo considerar como mi segundo jefe, por los sabios consejos. A Travis y Lluisa, miembros de mi TAC, por las útiles discusiones sobre el proyecto y las buenas recomendaciones.

Gracias a Lúdia Bardia y Anna LLadó de Microscopía, me habéis ayudado a usar todos los microscopios posibles, gracias por vuestra paciencia. A Neus Prats y su equipo de Histología por la ayuda con ratones. A Pepe Reina, Cayetano González, Renata Basto y Ciaran Morrison por los anticuerpos y la ayuda.

Gracias a Gonzalo Fernández-Miranda, por enseñarme infinidad de cosas y por su gran colaboración en la parte más complicada del proyecto, los malditos embriones. Por la ayuda en esta parte, gracias también a Embryotools, sobre todo a Ivette.

Gracias a los que estaban cuando llegué, en concreto millones de gracias Susana y Cristina Vila, por la paciencia que tuvisteis conmigo al llegar al lab, la nueva que no se entera de nada, y por todo lo que me habéis ayudado y enseñando después, tanto dentro como fuera del lab.

A las Nurias, porque han dado vida al lab, mientras una no para de reír la otra habla sola y come pasta con queso, imposible aburrirse. No hubieran sido iguales los días sin escuchar ¿sabes que me ha pasado? ¿a ver, tú qué harías? De Nuria Gallisá, o las mil veces que Nuria Campos se caga en satán.

Quisiera hacer extensiva mi gratitud al resto de mis compañeros del cuquilab, Andrea, Toni, Patri y Anghara porque un buen ambiente y unas risas hacen más ameno el trabajo. Y como no, a los lüderzitos, Nico, Sabine, Carlos, Rosa, Artur, Francisco, Marta, Ricardo, Cristina, Aamir, Ilaria, Joel, Nina y Fabian, por los consejos, los momentos vividos y por hacerme sentir una más de vuestro grupo. ¡Se os va otro buitre, ahora durará más la comida!

Al grupo de Shond@s, que aparecieron de la nada y se convirtieron en todo. La semana se hacen más cortas esperando el Viernes de Gargoleo. Infinitas gracias Berni, Pablo, Henar, Marc, los hermanos Teruel, Carlitos V, Carlos Pérez, Cristina, Gabi, Miguel, Paola, Pedro y Pepe. Bueno a vosotras tres, Ana Irma, Lorena y Lucía os doy las gracias a parte, porque sois de lo mejor que me ha dado Barcelona, gracias por las noches de fiesta, las tardes de café y cotilleo, las risas y los llantos, en definitiva, gracias por estar ahí siempre, porque aquí solo nos tenemos a nosotras.

A los andaluces en Barcelona, que me han dado mucho y que fueron de tanta ayuda cuando más lo necesitaba, especialmente a Pedro, Kiko, Juan Andrés, Almudena y como no a Enrique, de las mejores personas que he conocido en mi vida, un amigo, un hermano y un padre a la vez, que ha estado ahí siempre para todo y que espero que siga estando.

A mis amig@s de Sevilla, aunque la distancia ha hecho que los haya visto poco estos últimos años, cuando os veo es como si el tiempo no pasara y

habéis estado ahí compartiendo malos y buenos momentos, en especial a Álvaro, Maca, Ali, Noelia, Estrella, Mada, María, Amparo y Anle. ¡Aunque haga nuevas amigas, como vosotras nunca habrá nadie!

A mis compañeros Biotecs, en especial a las Elenas y a María, mi compañera de batallas, mi confidente y la mejor amiga que se puede tener.

Mil veces gracias a Pablo, por estar siempre a mi lado, por su cariño y comprensión, por aguantar mis días malos y darme tantos buenos, por traerme chocolate cuando lo necesitaba y por tantos y tantos otros detalles. Nada como alguien que te quiera cuando estás insoportable. Gracias también por llevarme ese día a la Gárgola, que me cambió la vida en Barcelona para mucho mejor.

Gracias mis abuelos que ya no están, sé que estarían muy orgullosos de mí y a mi abuela que espero que siga mucho tiempo viéndome crecer.

Y por supuesto a los que más han sufrido, mis padres, que son el pilar fundamental de todo lo que hoy soy, que me han apoyado desde el primer momento que me planteé emprender esta aventura, a pesar del disgusto que era para ellos tenerme lejos. Por el esfuerzo en darme una buena educación, tanto académica como de la vida, por sus ejemplos de perseverancia y constancia que los caracterizan y me han infundado siempre, por su incondicional apoyo y su cariño y por el dineral que les he costado (menos mal que soy solo una). Todo este trabajo y que esté donde estoy ahora ha sido posible gracias a ellos.

A todos vosotros y muchas otras personas que de una manera u otra han pasado por mi vida durante estos años,

¡GRACIAS!

RESUMEN

La mitosis es un proceso que asegura la distribución correcta de los cromosomas entre dos células recién generadas, está regulada por dos procesos principales, la degradación y la fosforilación de proteínas por diferentes quinasas mitóticas. CDK1 es el principal regulador de la mitosis, pero en las últimas décadas se ha demostrado que las proteínas de la familia Aurora o Polo o NIMA desempeñan un papel clave en la mitosis.

El objetivo de esta tesis es identificar nuevas funciones de Nek9, una quinasa de la familia NIMA, durante el ciclo celular y más específicamente durante las fases tardías de la mitosis. Nuestro objetivo es caracterizar nuevos sustratos y funciones de la quinasa mediante el uso de diferentes líneas celulares y ratones genéticamente modificados que nos permiten interferir con la expresión de Nek9.

El centrosoma actúa como el principal centro organizador de microtúbulos de la célula para mantener el citoesqueleto en interfase y para organizar el huso bipolar en la mitosis, su ciclo de duplicación va en sintonía con el ciclo celular. Cuando la célula entra en mitosis, los centrosomas duplicados se separan ensamblando el huso mitótico para segregar los cromosomas y para mantener la estabilidad genómica. Sin embargo, diferentes aberraciones ocurren con frecuencia en el centrosoma y a menudo conducen a la formación anormal del huso mitótico, que puede dar como resultado una segregación cromosómica anormal y, como consecuencia, tumorogénesis, microcefalia o ciliopatías.

Nek9 está inactiva en interfase y se activa en los centrosomas durante la mitosis mediante un mecanismo de dos pasos mediado por Plk1 y CDK1. Una vez activo, Nek9 se puede unir a Nek6 y Nek7 y fosforilarlas induciendo a su vez su activación. Nuestro grupo ha demostrado que Nek6/7 fosforilan

la quinesina Eg5, modulando la acumulación de Eg5 en los centrosomas y su separación durante la profase. Nek9 también fosforila el adaptador NEDD1 / GCP-WD, independientemente de Nek6/7, lo que contribuye a su reclutamiento en el centrosoma y, en consecuencia, al reclutamiento del complejo de nucleación de microtúbulos formado por γ -tubulina.

Aquí mostramos que los animales con un único alelo Nek9 KO están sanos y son fértiles. Sin embargo, los cruces entre ellos no dan lugar a ningún animal KO homocigoto, lo que indica que la eliminación de Nek9 es letal durante el desarrollo embrionario. Además, los embriones procedentes de estos cruces tienen una mayor frecuencia de defectos mitóticos que provocan la muerte durante los primeros días de desarrollo.

Como Nek9 es importante para el correcto desarrollo de la mitosis, queríamos ver si la expresión en heterocigosis daba como resultado tumores que afectan la viabilidad de los animales. Se han observado algunas diferencias en la esperanza de vida libre de tumores entre los heterocigotos con cierta incidencia de cáncer y aneuploidía.

Por otro lado, la eliminación de la expresión de Nek9 en células conduce a la aparición de mitosis anormales, aneuploidía y múltiples centrosomas, tanto en fibroblastos embrionarios de ratón genéticamente modificados como en células humanas teniendo como consecuencia la acumulación de centrobina, una proteína presente en los procentriolos.

En la presente tesis describimos posibles nuevas funciones y sustratos de Nek9 en el ciclo del centrosoma, íntimamente ligado al ciclo de división celular, tras interferir con su expresión de diferentes formas.

ABSTRACT

Mitosis is a process that ensure the correct distribution of the chromosomes between the two newly generated cells, is tightly regulated by two main processes, protein degradation controlled by the APC and protein phosphorylation by different mitotic kinases. CDK1 is the master regulator of mitosis but in the last decades proteins from the Aurora or Polo or the NIMA family have been shown to play key roles in mitosis.

The objective of this thesis is to identify new roles during the cell cycle and more specifically the late phases of mitosis of Nek9, a NIMA-related kinase. We aim to characterize new substrates and functions of the kinase by using different cell lines and genetically modified mice and interfering with Nek9 expression.

The centrosome acts as the major microtubule-organizing center (MTOC) of the cell to maintain cytoskeleton in interphase and to organize the bipolar spindle in mitosis, and its duplication cycle is coupled with the cell cycle. When the cell enters mitosis, the duplicated centrosomes separate to the spindle poles and assemble the bipolar mitotic spindle for accurate chromosome separation and to maintain genomic stability. However, centrosome aberrations occur frequently and often lead to abnormal mitotic spindle formation, which can result in abnormal chromosome segregation and as a consequence tumorigenesis, microcephaly or ciliopathies.

Nek9 is inactive during interphase and activated at centrosomes and spindle poles during mitosis by a two-step mechanism mediated by Plk1 and CDK1. Once active, Nek9 is able to bind Nek6 and Nek7 and directly phosphorylate these kinases inducing in turn their activation. Our group has shown that Nek6/7 phosphorylates the kinesin Eg5 at Ser1033 in the C-

terminal domain, modulating the accumulation of Eg5 at or around centrosomes and their separation during prophase. Nek9 also phosphorylates the adapter NEDD1/GCP-WD, independently of Nek6/7, contributing to its recruitment to the centrosome and in consequence, to the recruitment of the microtubule nucleating complex formed by γ -tubulin to the same organelle. Thus, Nek9, Nek7 and Nek6 regulate different aspects of the centrosome machinery during the entry in mitosis and have a role in spindle organization and correct mitotic progression.

Here we show that animals with a single Nek9 KO allele are healthy and fertile but intercrosses between them have not resulted in any homozygous null animals among born offspring indicating that the deletion of Nek9 is embryonic lethal. Also embryos obtained from these intercrosses had a higher frequency of mitotic abnormalities that result in death during the first days of development.

As Nek9 is important for the proper development of mitosis we checked whether the expression in heterozygosity of Nek9 results in tumors affecting the viability of the animals. Some differences in tumor-free lifespan between heterozygous and wild type animals have been observed, with the appearance of tumors and aneuploidy. In addition, elimination of Nek9 expression lead to the apparition of abnormal mitosis, aneuploidy and multiple centrosomes both in genetically engineered MEFs and human cells, resulting in accumulation of centrin, a protein mostly associated with the daughter centrioles, in the amplified centrioles.

In the present thesis we describe possible new functions and substrates of Nek9 in the centrosome cycle, closely linked to the cell division cycle, after interfering with its expression using different strategies.

LIST OF ABBREVIATIONS

APC/C	Anaphase promoting complex/cyclosome
APS	Ammonium persulphate
BSA	Bovine serum albumin
CAK	CDKs Activating Kinase
CRISPR	Clustered regularly interspaced short palindromic repeats
DDR	DNA Damage Response
DMEM	Dulbecco's Modified Eagle's
DMSO	Dimethyl Sulfoxide
DSB	Double Strand Break
FBS	Fetal Bovine Serum
γ TuRC	γ -Tubulin Ring Complex
GFP	Green fluorescent protein
HU	Hydroxyurea
IF	Immunofluorescence
Kb	Kilobase pair(s)
Kif	Kinesin Family Member
LB	Luria-Bertani medium
LC/MS/MS	Liquid Chromatography/Mass Spectrometry
MAP	Microtubule associated protein
MEF	Embryonic Mice Fibroblast
MT	Microtubule
MTOC	Microtubule-organizing Center
NE	Nuclear Envelope

NEB	Nuclear Envelope Breakdown
NEDD1 down-	Neural precursor cell expressed, developmentally regulated 1
NEK	NIMA-related kinase
NHEJ	Non-homologous end joining
NIMA	Never-in-mitosis A
NLS	Nuclear Localization Signal
PBS	Phosphate buffered saline
PFA	Paraformaldehyde
PCM	Pericentriolar material
PCR	Polymerase chain reaction
PEI	Polyethyleneimine
Pen/Strep	Penicillin/streptomycin
PLK	Polo-like kinase
PP1	Protein phosphatase 1
RNase	Ribonuclease
RT	Room temperature
SAC	Spindle assembly checkpoint
SDS	Sodium dodecyl sulphate
SDS-PAGE	SDS polyacrylamide gel electrophoresis
SEM	Standard error of the mean
siRNA	Short interfering RNA
SPB	Spindle pole body
WB	Western Blot

TABLE OF CONTENTS

INTRODUCTION	23
➤ The cell cycle and mitosis	25
➤ Mitotic kinases	28
➤ The CDK family	29
➤ The Polo-like kinase family	32
➤ The Aurora family	38
➤ The NIMA family	41
➤ Neks in ciliogenesis and DNA Damage Response	43
➤ Other Neks	44
➤ Mitotic Neks	45
▪ Nek2	45
▪ Nek5	47
▪ Nek9	48
▪ Nek6 and Nek7	53
➤ Spindle formation	56
➤ TPX2	59
➤ Motor proteins	60
▪ The dynein complex	61
▪ Kinesins	62
➤ Centrosomes and centrioles	65
➤ Centrosome structure	66
➤ The Centrosome cycle	68
▪ Centrosome disengagement	69
▪ Centrosome duplication	73
▪ Centrosome maturation	75
▪ Centrosome disjunction	76
▪ Centrosome separation	77

➤ Centrosome duplication and the link with the cell cycle	78
➤ Centrosome amplification and cancer	80
➤ Centrobin	83
OBJECTIVES	87
MATERIALS AND METHODS	91
➤ Reagents	93
➤ Nek9-targeted mice	93
➤ Culture of embryos	94
➤ Mouse Embryonic Fibroblast (MEFs) culture	94
➤ Histopathologic Analyses	94
➤ Splenocytes isolation	95
➤ Metaphase spreads	95
➤ Plasmids	95
➤ Genomic DNA extraction and genotyping PCR	97
➤ Cell culture	98
➤ Transfection	99
➤ Drug treatments	99
➤ Lentiviral infection	100
➤ Cell extracts, immunoprecipitation and western blotting analysis	100
➤ Protein expression in bacteria	102
➤ Stable isotope labeling with amino acids in cell culture (SILAC)	102

➤ Kinase assay	103
➤ Time lapse microscopy	103
➤ Cell cycle analysis	104
➤ Immunocytochemistry	104
➤ CRISPR/SpCas9	105
➤ High throughput screening for Nek9 inhibitors	106
➤ Statistical Methods	106
RESULTS	107
➤ Elimination of Nek9 expression in mice	109
➤ Generation of Nek9 genetically modified mice	109
➤ Development of pre-implantation embryos lacking Nek9	110
➤ Characterization of <i>Nek9</i> ^{+/<i>trap</i>} mutant mice	115
➤ Cellular effects of eliminating Nek9 expression in Mouse Embryonic Fibroblasts (MEFs)	126
➤ Nek9 depletion results in mitotic arrest and aneuploidy	128
➤ Nek9 depletion results in the apparition of multiple centrosomes and aberrant mitotic figures	133
➤ Nek9-depleted cells contain an excess of Centrobin positive “daughter” centrioles	141
➤ Centrobin positive centrioles favor the production of shorter cilia and multi-ciliated cells	149
➤ Nek9 depletion in human cells	151
➤ Cell viability is affected upon Nek9 depletion	151
➤ U2OS but not HeLa cells phenocopied the effect on centrosomes of downregulating Nek9 levels observed in MEFs	152

➤ Centriole amplification upon Nek9 downregulation is Plk4-dependent	157
➤ Nek9 may control centriole number through centrobins	161
➤ Centrobins overexpression induces centriole amplification	162
➤ Study of the possible phosphorylation of centrobins by Nek9	164
➤ Nek9 interacts with centrobins	166
ADDITIONAL RESULTS	169
➤ High throughput screening for Nek9 inhibitors	171
➤ Nek9 may be involved in centriole disengagement	173
➤ CRISPR/cas9, an additional model for Nek9 disruption	175
DISCUSSION	177
➤ Nek9 null embryos die at early post-implantation stage	179
➤ Nek9 haploinsufficiency mouse model	182
➤ Impact in the centrosome duplication cycle after Nek9 cell abrogation	184
CONCLUSIONS	191
REFERENCES	195
SUPPLEMENTARY TABLES	223

INTRODUCTION

INTRODUCTION

The Cell Cycle and mitosis

The cell cycle can be divided into two different periods, interphase (I) and M phase. Interphase is the period between two mitosis and can be subdivided in G1, S and G2. **G1** starts just right after cell division and is considered the first growth phase. The **S** phase is the period comprising DNA and centrosomes duplication. **G2** is the second stage of cell growth and also the moment when cells prepare for division. On the other hand, the M phase is subdivided in two stages: mitosis and cytokinesis. **Mitosis**, first described by Walther Flemming in the late 1870's (Paweletz, 2001), is the process of chromosome segregation and nuclear division, while **cytokinesis** refers to the physical division of the cell in two daughter cells with exact genetic copies (Morgan, 2007).

Traditionally, it is considered that mitosis starts with chromosome condensation in **prophase**. The subsequent breakdown of the nuclear envelope (NE) initiates **prometaphase**, and at this stage the chromosomes become attached to and positioned on the mitotic spindle. Then, at **metaphase**, all chromosomes are aligned forming a plate at the middle of the spindle. At **anaphase** the two sister chromatids of the replicated chromosome migrate towards the opposing spindle poles. They do so in two steps, anaphase A, in which chromosomes are pulled toward the spindle poles by contraction of the kinetochore microtubules (MTs), and anaphase B, in which the spindles are pushed away from each other by the elongation of inter-spindle-pole microtubules. During **telophase** chromosomes decondense and the NE is reformed (Figure 1) (Maiato, 2010; Rhind and Russell, 2012).

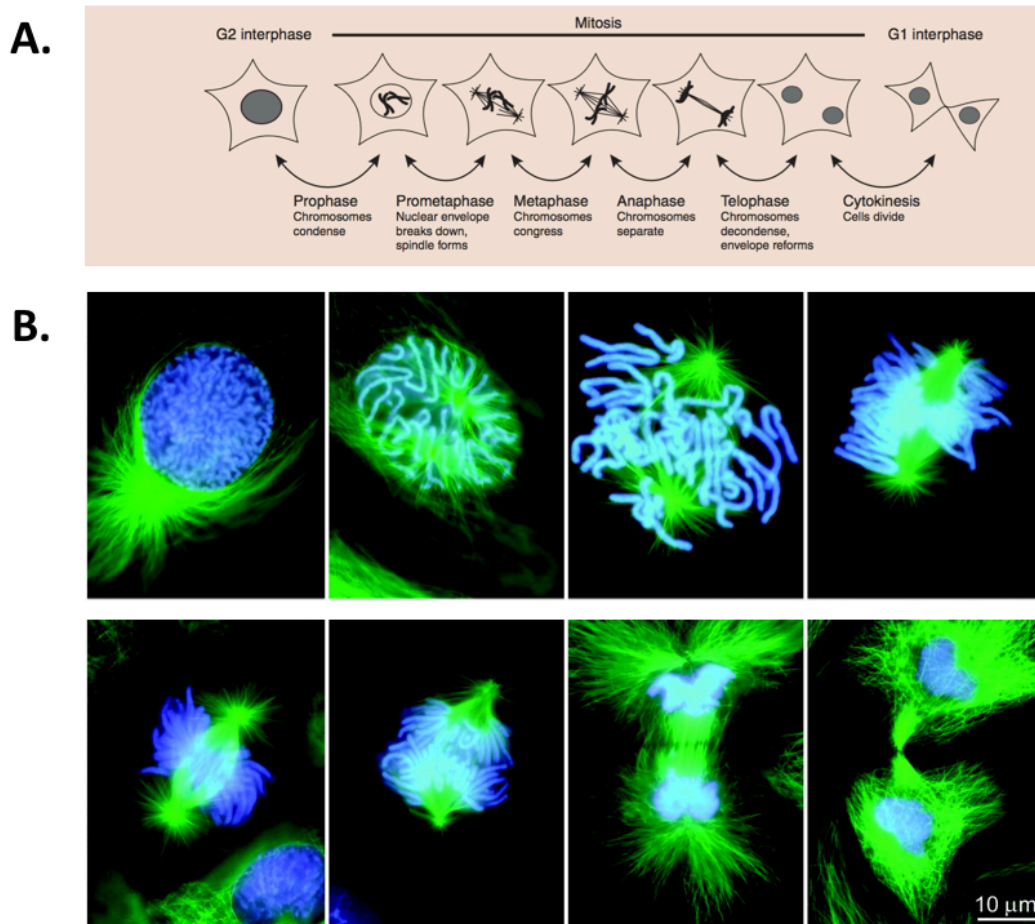


Figure 1: **A)** Cartoon of different mitotic phases, adapted from (Rhind and Russell, 2012); **B)** Fluorescence micrographs of mitosis in fixed cells showing microtubules (green) and chromosomes (blue) (Rieder and Khodjakov, 2003).

However, (Pines and Rieder, 2001) argued against the idea that mitosis starts with the initiation of chromosome condensation, because in some cells the chromosomes never condense and in others condensation takes place at the beginning of interphase. In addition, in many protists, ciliates, algae and fungi there is no nuclear envelope breakdown (NEB), whereas in other systems such as *Caenorhabditis elegans* the nucleus persists until anaphase. Furthermore, the formation of a metaphase plate is not a requirement for anaphase to begin even in higher organisms. In base of this, they suggested that mitosis can be subdivided into five transitional phases (Figure 2) independent of chromosome alignment and nuclear envelope breakdown

(NEB), characterized by the activity of defined cell-cycle regulators, the mitotic cyclin-dependent kinases (CDKs) and the anaphase-promoting complex/cyclosome (APC).

Transition one is characterized by the activity of CDK/cyclin A, Plk1 and Aurora A and is when chromatin condensate and centrosomes mature. In this phase, entry into mitosis can be arrested by the DNA damage checkpoint. **Transition two** or **entry into mitosis** is defined by the activation of CyclinB/CDK1, and at this moment cells cannot revert mitosis. **Transition three** is characterized by the presence of activated CDK1/cyclin B and Anaphase Promoting Complex (APC) being modulated by the kinetochore attachment checkpoint. In this stage the APC, promote degradation of cylin A but not of cyclin B or securin. This corresponds to prometaphase. **Transition four** or **mitotic exit in defined by** APC^{Cdc20} activation and in consequence cyclin B and securin are degraded. Finally, in **transition five** or **return to interphase** Cdc20 is degraded and replaced by Cdh1, which is then phosphorylated and degraded before DNA replication.

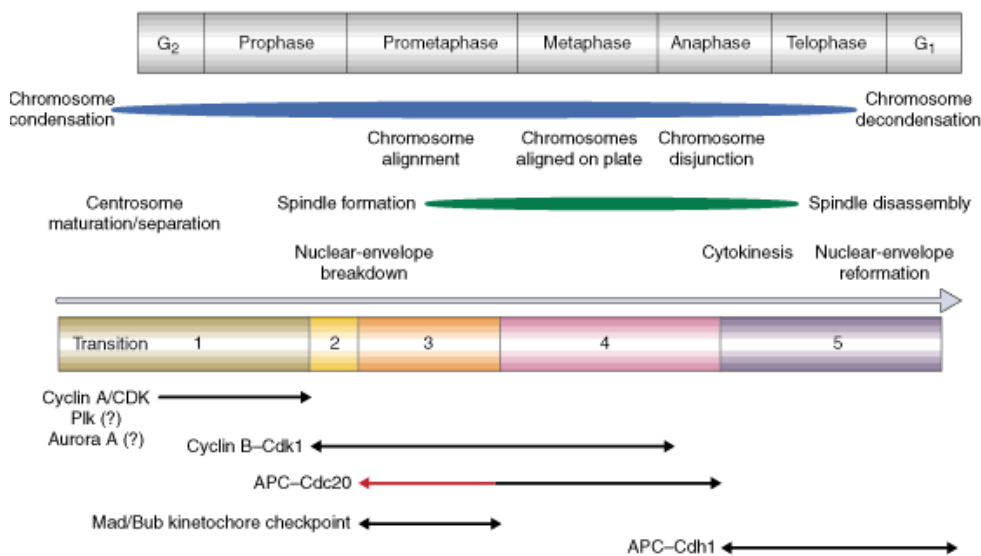


Figure 2: Comparison of the traditional phases of mitosis (top) and Pines and Rieder, 2001 proposed transitions (bottom).

Mitotic kinases

Protein phosphorylation was discovered as a regulatory mechanism by Krebs and Fischer in the late 1950s through their classic studies of glycogen phosphorylase (Cohen, 2002). Phosphorylation is considered one of the most important types of post-translational modification (PTM). The size and charge of covalently attached phosphates can induce conformational changes in the modified protein, and also allow specific and inducible recognition of phosphoproteins by phosphospecific-binding domains in other proteins, resulting in protein–protein interaction, essential for transducing signals intracellularly. However, phosphorylation can also cause a change in the subcellular location of a protein or create a phosphodegron, leading to ubiquitin-dependent protein degradation (Hunter, 2012). Attesting to the importance of kinases for eukaryotic cell signal transduction and metabolism, there are more than 500 human protein kinases recognized through their conserved sequence motifs. Deregulation of protein kinase is associated with a several disorders and the enzymes have become essential targets for cancer therapies, but to make them selective and specific is important to consider the structures of the kinase (Endicott et al., 2012).

All eukaryote protein kinases share a conserved core that contains twelve subdomains that were originally defined by Hanks and Hunter (Hanks and Hunter, 1995). Thereby, the structure of the catalytic domain is highly conserved, formed by an N-terminal and a C-terminal lobe with the substrate binding pocket located between them. The N-lobe is in charge of ATP coordination and proper positioning at the substrate-binding pocket. This domain includes the phosphate-binding loop (P-loop). The C-lobe contains the activation loop (T-loop), which has a function in ATP binding, and the catalytic loop, which include an acidic amino acid (proton acceptor) that

incorporates the remaining proton from the attacking substrate. (Endicott et al., 2012; Hunter, 2012; Kornev and Taylor, 2015; Taylor and Kornev, 2011).

Phosphate groups can be added to one of the three hydroxylated amino acids (Serine, Threonine and Tyrosine) through ATP hydrolysis. Serine and threonine, both aliphatic amino acids, are phosphorylated by the action of **Ser/Thr kinases** and dephosphorylated by **Ser/Thr phosphatases**. Phosphorylation of tyrosine, which contains an aromatic ring, requires enzymes with a larger catalytic site, which are the **Tyr kinases** and **Tyr phosphatases**. Only in a few cases enzymes present dual reactivity and can (de)phosphorylate both serine/threonine and tyrosine residues (Endicott et al., 2012).

Together with ubiquitin-mediated protein degradation, mitosis is guided by protein phosphorylation. In mammals, there are four families of kinases involved in mitosis: Cyclin Dependent Kinases (CDKs), Polo like kinases (Plks), Aurora kinases and NIMA kinases.

The CDK family

The CDKs are Ser/Thr protein kinases that bind cyclin subunits. CDKs activity is controlled by this binding as the catalytic pocket of CDKs is only accessible after it. Mammals contain 20 CDKs (CDK1 to 20) and 29 cyclin subunits. CDKs preferentially modify serine and threonine residues directly followed by a proline (S/TPX). In addition to their well-known function in cell cycle control, it is now evident that mammalian CDKs and cyclins play indispensable roles in processes such as transcription, epigenetic regulation, metabolism, stem cell self-renewal, neuronal functions and spermatogenesis (Lim and Kaldis, 2013; Malumbres and Barbacid, 2005).

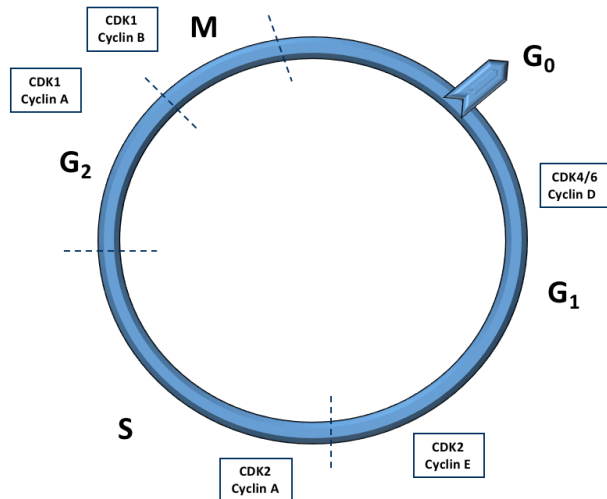


Figure 3: CDKs and respective cyclins involved in cell cycle

Mitotic signals initially induce in G₁ the synthesis of the D-type cyclins and possibly the proper folding and transport of **CDK4** and **CDK6** to the nucleus. Active complexes phosphorylate members of the retinoblastoma (Rb) protein family, which includes pRb, p107 and p130, that repress transcription by distinct mechanisms. In human cells, pRb contains 13 conserved sites that are phosphorylated by CDKs. CDK4 and CDK6 phosphorylate residues Ser807 and Ser811, priming it for further phosphorylation by these or other CDKs at other sites. pRb inactivation results in de-repression of multiple genes encoding proteins required for DNA synthesis or mitosis, such as E-type cyclins (E1 and E2), which in turn bind and activate CDK2.

CDK2–cyclin E complexes further phosphorylate these proteins, leading to their complete inactivation. CDK2 is subsequently activated by cyclin A2, and this complex is known to phosphorylate numerous proteins that are thought to be required for proper completion and exit from S phase (Malumbres and Barbacid, 2005; Sherr and Roberts, 2004). At the centrosome, CDK2 phosphorylates centrosomal NPM/B23 to promote centrosome licensing for S-phase duplication through still unknown

mechanisms. In fact, centrosome separation and duplication occur prematurely in *Cdk2*^{-/-} MEFs and are compromised in *Cdk4*^{-/-} MEFs. Additionally, ablation of *Cdk4* or *Cdk2* suppress centrosome amplification and chromosome instability in *p53*-null MEFs by abrogating excessive centriole duplication. Furthermore, hyperactive CDK2 and CDK4 promote the licensing of the centrosome duplication cycle in *p53*-null cells by hyperphosphorylating nucleophosmin (NPM) (Adon et al., 2010).

CDK1 binds to cyclin A at late G2 and cyclin B at mitosis, allowing phosphorylation of different substrates and the correct progression of centrosome maturation and separation, as well as entry into mitosis through the control of chromosome condensation, Golgi dynamics, nuclear envelope breakdown (NEB) and spindle formation. In addition to binding to the cyclin subunit, phosphorylation and dephosphorylation of CDK1 play a role in the control of kinase activity. Thus, phosphorylation at residues T14 and Y15 by the Wee1 and Myt1 kinases inhibits CDK1 whereas phosphorylation at T161 by CDKs Activating Kinases (CAKs) promotes the activation. During mitotic entry dephosphorylation by Cdc25 phosphatase rescues CDK1 activity. Once CDK1 is active, it phosphorylates cyclin B resulting in CDK1/cyclin shuttling to the nucleus. At metaphase CDK1 activity is shut down, due to cyclin B degradation by the APC complex, and its substrates begin to be dephosphorylated to allow chromosome segregation, chromosome decondensation, re-assembly of the NE and cytokinesis (Malumbres, 2014).

Tumour-associated cell cycle defects are often mediated by alterations in cyclin-dependent kinase (CDK) activity. Recent studies have revealed that CDK1 is the only CDK essential for cell cycle (Santamaría et al., 2007) and interphase CDKs are only essential for proliferation of specialized cells, but in normal conditions different CDK/cyclin pairs control different phases of

the cell cycle (Figure 3). Thus, selective CDK inhibition may provide therapeutic benefit against certain human neoplasias (Malumbres and Barbacid, 2009).

The Polo-like kinase family

The polo-family serine/threonine kinases were first described in mutants that failed to undergo a normal mitosis in *Drosophila melanogaster* (*polo*) (Llamazares et al., 1991; Sunkel and Glover, 1988). They have been shown to have key roles in cell cycle progression, the response to genotoxic stress and neuron biology and are controlled at the level of protein synthesis and stability, by the action of upstream kinases and phosphatases, and by localization to specific subcellular structures (Archambault and Glover, 2009; Barr et al., 2004; de Cárcer et al., 2011; Zitouni et al., 2014).

Plks are characterized by the presence of an N-terminal protein kinase domain and a C-terminal polo-box domain (PBD) which is composed usually of two Polo-Box (PB) motifs involved in substrate binding and regulation of kinase activity. The family can be divided into three different subfamilies. Plk1 subfamily which contains the mammalian Plk1 and *Drosophila polo*, the Plk2 subfamily containing Plk2, Plk3 and Plk5 and finally the SAK subfamily that contains *Drosophila* SAK and mammalian Plk4 (Figure 4) (de Cárcer et al., 2011; Weerdt and Medema, 2006).

INTRODUCTION

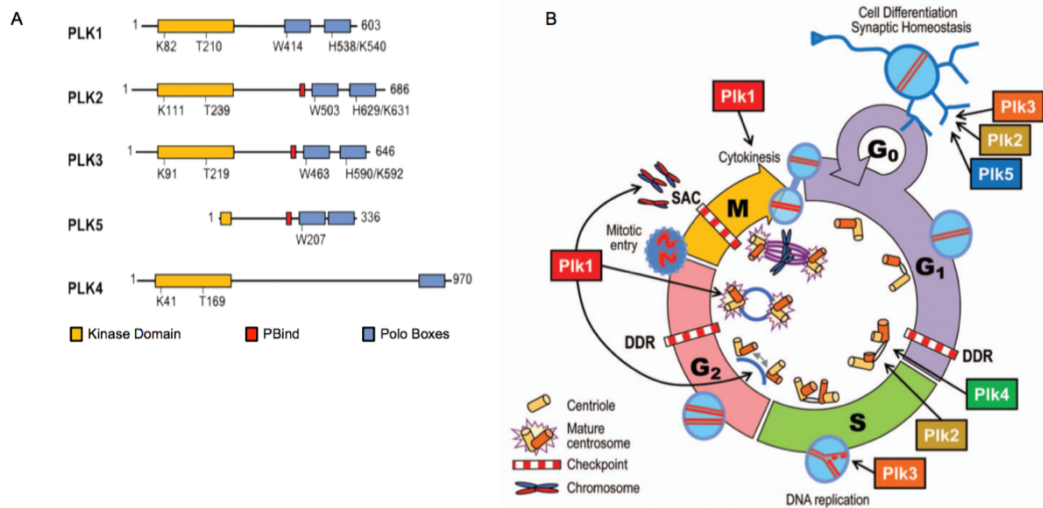


Figure 4: **A)** The human Plk family and its domains; **B)** Schematic representation of the functions of the Plk family members along the cell cycle. Adapted from (de Cárcer *et al*, 2011b).

The founding member of the family, **Plk1**, is a master regulator of cell division. This kinase controls centrosome maturation, mitotic entry, spindle assembly, correct microtubules attachment to kinetochores, the regulation of the APC/C, cytokinesis and centrosome disengagement. Accordingly, to its functions, Plk1 localizes to the cytoplasm and centrosomes in interphase and accumulates at centrosomes during prophase, at kinetochores in prometaphase and metaphase, is recruited to the central spindle in anaphase and accumulates at midbody during telophase.

Plk1 promotes mitotic entry by activating Cyclin B/Cdk1 in different ways. First, Plk1 phosphorylate the phosphatase Cdc25C in a nuclear export signal sequence, thereby leading to its nuclear translocation and activation. At the same time, Plk1 phosphorylates Cyclin B/CDK-inhibiting kinases Wee1 and Myt1 promoting their degradation. Furthermore, Plk1 phosphorylates Cyclin B at centrosomes, the first site at which Cyclin B/CDK1 is activated, on a serine residue (Ser147) that is located within a nuclear-export signal, thereby promoting the nuclear accumulation of cyclin

B (Barr et al., 2004). Afterwards it is required for centrosome maturation controlling the recruitment of γ -tubulin and other PCM proteins, such as Nedd1, pericentrin, Cep192, Kizuna or CDK5RAP2 to the centrosomes, required for spindle formation (Haren et al., 2009; Oshimori et al., 2006).

Binding of Plk1 to PBIP1 is crucial for localizing Plk1 to the kinetochores where it can phosphorylate BubR1, thus stabilizing kinetochore-microtubule interactions, or PICH, required for the spindle assembly checkpoint (Baumann et al., 2007; Elowe et al., 2007; Kang et al., 2006). Finally, some cytokinetic substrates of Plk1, such as Rock2, Mlkp2 or NudC, a component of the dynactin complex have been described (Barr et al., 2004).

Inhibition of Plk1 function by RNA interference or small-molecule inhibitors such as BI2536 results in failure to establish a bipolar spindle and to properly attach kinetochores to microtubules. Plk1 is an essential gene as Plk1-null mice die at the morula stage due to a massive mitotic arrest (Lu et al., 2008a; Wachowicz et al., 2016).

Similar to many other protein kinases, Plks are activated by phosphorylation within a short region of the catalytic domain, the so-called T-loop (or activation-loop) (Barr et al., 2004). Plk1 is activated at the G2/M transition and its activity reaches peak levels in mitosis. Plk1 activation requires phosphorylation at Thr210. During G2, Aurora-A, in complex with its cofactor hBora, phosphorylates Plk1 at Thr-210. Activated Plk1 phosphorylates Cdc25C and Wee1, which induces activation of cyclin B-Cdk1 complexes and promotes mitotic entry. (Macûrek et al., 2008; Seki et al., 2008). Plk1 is then degraded at the start of anaphase after ubiquitination by the anaphase promoting complex (APC) (Weerdt and Medema, 2006).

The PBD contributes to substrate specificity and to the changes in subcellular localization of Plk1. The PBD of Plk1 binds sequence motifs of phosphorylated serine or threonine followed by a proline [pS/pT]PX with some preference for S[pS/pT]PX (Elia et al., 2003). Two models for how PBD might function to direct Plk1 kinase activity have been described. In the first one, called “processive phosphorylation model”, the PBD binds to one extreme of the protein and Plk1 phosphorylates at another site of the same protein. On the other hand, in the “distributive phosphorylation model” the PBD binds to a protein that acts as scaffold and then Plk1 phosphorylates a different protein (Lowery et al., 2005).

In mammals, an altered expression of Plk1 is associated with tumorigenesis. For this reason, Plk1 has been proposed as a cancer therapeutic target, being tested some of its inhibitors in clinical trials. Interestingly, despite Plk1 known role during mitotic entry, these inhibitors arrest cells in prometaphase but not in G2, showing the kinase is dispensable for the G2/M transition. However, although PLK1 displays some oncogenic activity, all Plks may also function as tumor suppressors (de Cárcer et al., 2011; Strebhardt and Ullrich, 2006)

Plk2 (also known as SNK) has a very similar structure to Plk1. It contains a kinase domain and two polo-boxes in the polo-box domain. It only differs in the Pbind domain, a domain that it uses to bind to some of its substrates in non-proliferative tissues where the priming kinases may not be present. Plk2 is broadly expressed in different tissues, proliferating and non-proliferating, such as post-mitotic neurons. Its expression increases in G1 and early S phase at centrosomes, where it acts as a regulator (de Cárcer et al., 2011). Overexpression and depletion of Plk2 lead to an increase and decrease of centrosome numbers, respectively, indicating that Plk2 is

required for centriole duplication during S phase. Plk2 is a nonessential gene, as *Plk2*^{-/-} embryos are viable. However, Plk2 does play a role in cell cycle progression since *Plk2*^{-/-} embryos do show slightly retarded growth and skeletal development. Cultured *Plk2*^{-/-} embryonic fibroblasts grow less and show delayed entry into S phase (Weerdt and Medema, 2006). In addition, Plk2 binds and phosphorylates NPM/B23 (Nucleophosmin) on serine 4 in S-phase, which is necessary for centriole duplication (Krause and Hoffmann, 2010). Plk2 indirectly activates ROCK2 via phosphorylating nucleophosmin (NPM), and Plk4 functions downstream of ROCK2 to drive centrosome amplification in the arrested cells (Ling et al., 2015).

Plk3 (also named FNK or PRK) is required at the G₁-S phase transition, where it promotes the accumulation of cyclin E and activation of Cdc25A, favoring DNA replication. It has also been proposed that Plk3 might sense genotoxic stress (de Cárcer et al., 2011).

Plk4 (also known as SAK) structurally differs from the other members of the Plk family, because it does not have the canonical two polo-boxes conforming a polo-box domain. Instead, Plk4 possesses a unique central region called the “cryptic polo box”, with two tandem, homodimerized polo boxes, PB1-PB2. This C-terminal polo box (PB3) is required for binding the centriolar protein Cep152 as well as robust centriole targeting. Thus, it facilitates oligomerization, targeting, and promotes *trans*-autophosphorylation, limiting centriole duplication to once per cell cycle (Slevin et al., 2012). Plk4 plays an essential role in centrosome duplication. Overexpression of Plk4 leads to an excessive formation of centrioles and depletion of Plk4 by RNAi prevents centriole formation causing mitotic defects (Bettencourt-Dias et al., 2005). *Plk4*^{-/-} mice die at E7.5 showing

Plk4 as essential for post-gastrulative embryonic development (Hudson et al., 2001).

Abnormal expression of Plk4 has been linked with genomic instability and a predisposition to tumorigenesis and thus Plk4 abundance must be tightly regulated in order to correctly control centrosome number and maintain genome integrity. Plk4 is a low-abundance kinase whose stability is directly linked to the activity of the enzyme, with active Plk4 phosphorylating itself to promote its own destruction through the ubiquitin–proteasome pathway. The SCF (Skp/Cullin/F-box) E3 ligase associates with phosphorylated Plk4 through the F-box protein β -TrCP. Phosphorylation of two residues within the β -TrCP-binding motif of Plk4 promotes the binding of β -TrCP and subsequent ubiquitylation and destruction of the kinase (Cunha-Ferreira et al., 2009; Holland et al., 2012; Sillibourne et al., 2010)

It was recently described that ROCK2, Plk2 and Plk4 induce centrosome amplification in arrested cells by a lineal pathway. Plk2 phosphorylates NPM on Ser4, which promotes phosphorylation of NPM on Thr199 by CDK2-cyclin E (or cyclin A). NPM acquires a high binding affinity to ROCK2 by Thr199 phosphorylation, which leads to facilitation of NPM to interact with ROCK2 at centrosomes. ROCK2 then either directly or indirectly acts on Plk4, which in turn acts on its targets, leading to induction of centrosome re-duplication (Ling et al., 2015).

Finally, **Plk5**, which lacks kinase activity, is only expressed in a few non-proliferative tissues, as in the central nervous system. It is mostly transcribed in cerebellum where is functionally important (de Cárcer et al., 2011).

The Aurora family

The original *aurora* allele was identified in a screen for *Drosophila* mutants that were defective in spindle-pole behavior (Glover et al., 1995). The mammalian genomes contain three genes encoding Aurora kinases called Aurora A, B and C. The three Aurora kinases are serine/threonine kinases and have a N-terminal domain, a kinase domain and a C-terminal domain. Aurora A and B share 71% identity in the C-term catalytic domain. Despite the similarity, the three mammalian Aurora kinases have very distinct localizations and functions. The expression levels of human Auroras are high in certain types of cancer, which has increased the interest to this family of kinases as potential drug targets for the development of new anti-cancer therapies (Carmena and Earnshaw, 2003).

Aurora A levels increases during late S/early G2 reaching a peak in early mitosis. Low levels of Aurora A have also been reported on the midbody late in mitosis. The APC initiates Aurora-A degradation in anaphase B but only completes it in G1 phase. Aurora A is present on duplicated centrosomes from late S phase until early G1 phase and it is also detectable on spindle microtubules during mitosis. It participates in several crucial mitotic processes, such as the mitotic entry, by activation of Plk1 and CDK1, through phosphorylation and activation of Cdc25, the phosphatase that reverts CDK1/cyclin B inactivation by phosphorylation, but is also necessary for proper centrosome maturation and separation (Barr and Gergely, 2007; Vader and Lens, 2008). Aurora A also has roles in microtubule organization and it coordinates centrosome independent and chromatin dependent spindle assembly (Meunier and Vernos, 2015).

The kinase activity of Aurora A is regulated by autocatalytic phosphorylation of Thr288 in its T-loop but this is facilitated by cofactors. At centrosomes, two proteins bind Aurora A and facilitate its activation and

its centrosomal localization: **Ajuba** and **Bora**. Bora is nuclear during interphase, but during the G2/M transition is translocated to the cytoplasm in a CDK1 dependent manner. Bora interacts with Plk1 and controls the accessibility of its activation loop for phosphorylation and activation by Aurora A. Phosphorylation of Plk1 lead to the activation of cyclin-dependent kinase 1 and mitotic entry. Aurora-A can also directly activate Cdc25B by phosphorylation at Ser-353. During mitosis, active Cdk1 primes hBora for interaction with and phosphorylation by Plk1, which, in turn, leads to proteasomal degradation of Bora. Aurora-A is now free to interact with TPX2, a complex that is necessary for bipolar spindle assembly (Chan et al., 2008; Hutterer et al., 2006; Seki et al., 2008).

Moreover, **TPX2** is another important Aurora A cofactor. TPX2 is a Microtubule Associate Protein (MAP) regulated by the RanGTP pathway that has a role in microtubules stabilization and Aurora A activation (see below). After NEBD Ran–GTP releases TPX2 from importin that then binds Aurora A at the centrosome and targets it to the microtubules proximal to the pole. Binding of TPX2 to Aurora-A not only induces it to adopt an active conformation by autophosphorylation but also prevents dephosphorylation of Thr288 by protein phosphatase 1 (PP1). TPX2 is also required for localization of the kinase to the spindle after NEB (Bayliss et al., 2003; Gruss et al., 2001; Neumayer et al., 2014).

Aurora B, together with INCENP, Survivin and Borealin, forms the Chromosomal Passenger Complex (CPC). These subunits bind to Aurora B promoting its autophosphorylation and thus, its activation and recruitment to the centromeres at early mitosis. The kinase moves to the spindle midzone and finally, during cytokinesis accumulates at the midbody. Aurora B has a

role in controlling chromosome-microtubule interaction, cohesion, spindle stability and cytokinesis (Carmena et al., 2009; Vader and Lens, 2008).

Aurora C is a chromosomal passenger protein localizing first to centromeres and then to the midzone of mitotic cells that cooperates with Aurora B to regulate mitotic chromosome segregation and cytokinesis in mammalian cells (Bolanos-Garcia, 2005). It is differentially expressed in testis, with an important role in meiotic cells (Vader and Lens, 2008).

Thus, mitotic entry is conformed by a network of events in which every kinase supports the activation of the other ones (Figure 5). Cells decide to enter or not into mitosis in late G2. Mechanisms as the G2 checkpoint ensure that the cells are ready to start mitosis without damage. Mitotic entry is defined by an increased activity of CDK1/cyclin B and therefore, this protein complex is the final target of G2 checkpoint pathways. CDK1 activation is supported by the action of Aurora A and Plk1. Plk1 promotes the degradation of the CDK1 inhibitor Wee1 and the activation of the CDK1 activating phosphatase Cdc25C. At the same time Plk1 activity induces Aurora A accumulation at centrosomes at late G2. On the other hand, Aurora A activates Plk1 by phosphorylation at Thr210 and promotes the activation of Cdc25B phosphatase and cyclin B recruitment. Finally, Aurora A activation is also affected by CDK1 activity (Lens et al., 2010).

INTRODUCTION

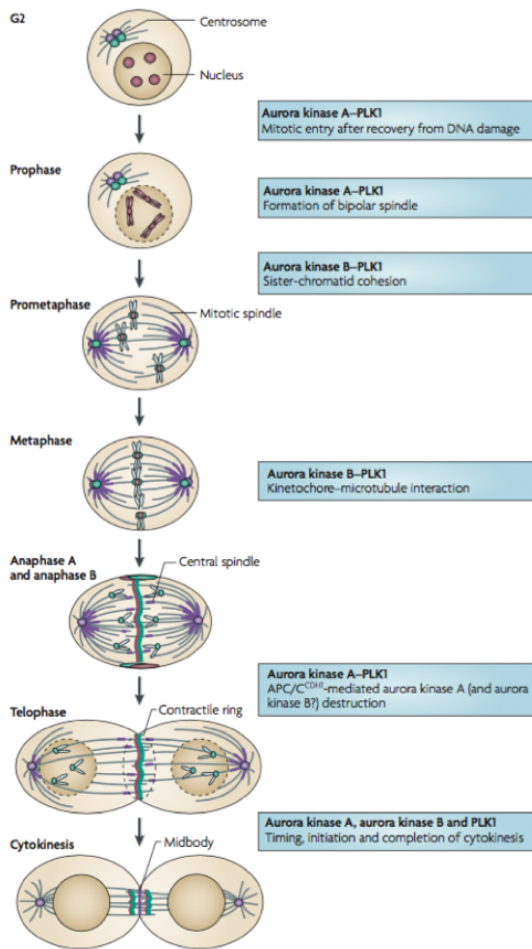


Figure 5: Localization of Plk1 (green), aurora A (purple) and aurora B (red) in mitosis and crosstalk between them (Lens et al., 2010).

The NIMA family

The NIMA-family of serine/threonine kinases is named after the NIMA kinase, identified in *Aspergillus nidulans* as the product of a gene that when mutated abrogated proliferation, arresting cells in G2 (hence the name nimA *never in mitosis A*). Overexpression of NIMA induced a pseudo-mitotic state with condensed chromosomes and aberrant spindles. Thus, NIMA was characterized as an essential protein for mitotic entry and progression in *Aspergillus*, regardless of cdc2 activation. Later on, NIMA was shown to control the nuclear import of Cdc2/cyclin B, chromatin condensation, spindle and nuclear envelope organization and cytokinesis in *Aspergillus* (O'Connell et al., 2003a)(O'regan et al., 2007).

NIMA-related kinases, or Neks are conserved across most eukaryotes. The number of Neks encoded within the genome varies from organism to organism with a correlation with complexity of the molecular structures that contribute to formation of cilia and flagella. Plant cells have around six Neks, *Drosophila* only two Neks (Nek2 and Niki), while *C. elegans* has four (Nek1-4). Fungi and yeast have only one member of the NIMA related kinase (Neks), but the family is expanded in ciliated organisms where it has been suggested to coordinate cilia with cell cycle. Examination of different genomes shows that there is a correlation between number of Neks in organisms and whether or not it has ciliated cells that divide (Quarmby and Mahjoub, 2005).

Mammalian cells contain 11 NIMA-family members (Figure 6) (Fry et al., 2012; O'Connell et al., 2003a) that have a N-terminal catalytic domain with high identity (40-50%) with the kinase domain of NIMA and a C-terminal regulatory domain, which is the most divergent part among them. Hence, they may share at least some of NIMA functions during mitosis but have also acquired novel regulatory roles, and different members of the family have been proposed to be involved in the control of the microtubule and ciliary machineries (Nek1, Nek8) and the response to DNA damage (Nek1, Nek10, Nek11). Nek2, Nek5, Nek9 and the highly similar Nek6 and Nek7 are involved in the control of the centrosomal cycle and of mitotic spindle formation (Fry et al., 2012, 2017; O'Connell et al., 2003b; O'regan et al., 2007).

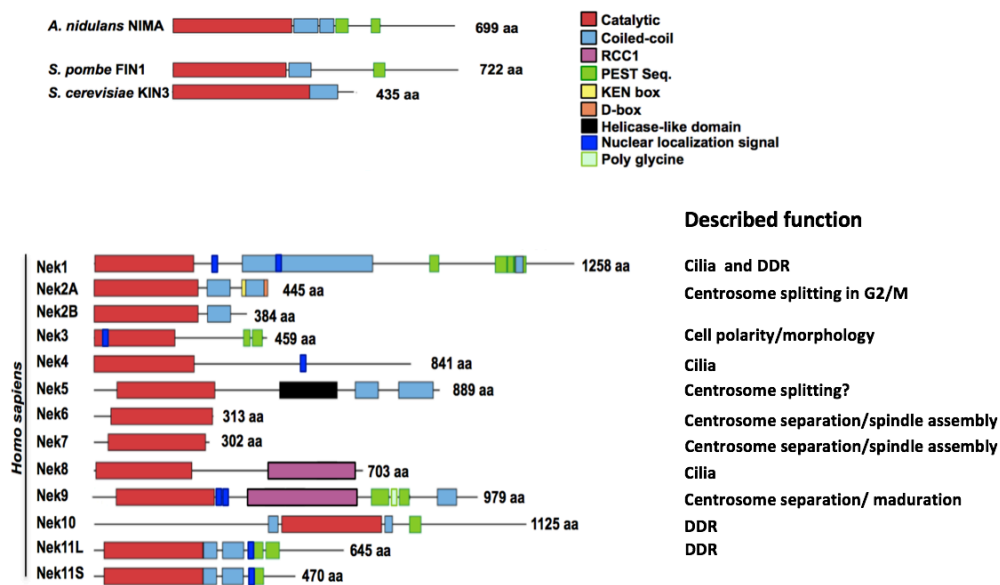


Figure 6: The NIMA-related kinases family (modified from O’Connell et al.,2003)

Neks in ciliogenesis and the DNA Damage Response

Nek1 is important for efficient DNA damage checkpoint control and for proper DNA damage repair (Chen et al., 2008) and its overexpression leads to abnormal chromatin condensation (Feige et al., 2006). On the other hand, Nek1 depletion in mice suggests a role of this protein in the kidney, as mice devoid of the kinase developed polycystic kidney disease (PKD), in addition to other defects like dwarfism and facial dysmorphism (Upadhyya et al., 2000). Nek1 is localized to the centrosome or the basal body region of the cilia and its overexpression inhibits ciliogenesis while its depletion causes defects in cilia assembly (Shalom et al. 2008). This strongly suggests a ciliary role for Nek1 and may explains the mice phenotype (Shalom et al., 2008).

Nek8, also localizes at centrosomes and basal body of primary cilia and defects in its function or localization result in ciliopathy, including kidney disorders (Otto et al., 2008). Nek8 targeted disruption in mice is lethal and causes defects in left-right asymmetry (Manning et al., 2013). In addition, may regulate local cytoskeletal structure in kidney tubule epithelial cells (Liu et al., 2002).

Nek10 is implicated in DDR by promoting MEK/ERK activation and G2/M arrest in response to UV radiation (Moniz et al., 2011).

Nek11 is an important component of the pathway enforcing the G2/M checkpoint. Under DNA damage is activated by direct Chk1 phosphorylation and when active it phosphorylates Cdc25a and triggers it for degradation, thus preventing entry into mitosis (Melixetian et al., 2009).

Other Neks

Nek3 is highly expressed in neurons and it may have some role in disorders where axonal degeneration is an important component, as Nek3 mutants results in a decrease of microtubule stability (Chang et al., 2009).

Nek4 has a role in microtubule regulation and a recent work on the Nek4 interactome indicates that this kinase could also be associated with the DDR or ciliogenesis (Basei et al., 2015; Doles and Hemann, 2010)

Mitotic Neks

Nek2

Nek2 is the most closely related Nek to *Aspergillus* NIMA, localizes to centrosomes and is a cell cycle-regulated kinase with maximal expression and activity in S and G2 (Fry et al., 1995, 1998a). Nek2 function is to disassemble the proteinaceous linker that connects the duplicated centrosomes at the onset of mitosis, called centrosome disjunction, to facilitate centrosome separation and the establishment of the mitotic spindle (Fry et al., 2012; O'Regan et al., 2007).

At the G₁/S transition vertebrates express two major splice variants, Nek2A and Nek2B that differ in their extreme C termini, which has important implications for their regulation, as the C terminus of Nek2A, but not Nek2B, contains both a binding site for protein phosphatase 1 and motifs that target the protein for ubiquitin-mediated degradation after mitotic entry. Importantly, Nek2A and Nek2B exhibit distinct patterns of cell-cycle-dependent expression. Both are present in low amounts in G₁, which increased in the S and G₂ phases. However, Nek2A disappears in prometaphase cells, whereas Nek2B remains elevated. APC/C mediated destruction of Nek2A occurs in early mitosis resulting in low Nek2A levels in M/G₁. The degradation of Nek2B does not occur during this time allowing Nek2B to persist throughout mitosis (Fletcher et al., 2005; Hames and Fry, 2002).

Nek2A activates by autophosphorylation in G₂, and it has been described that homodimerization of the protein is essential for this autophosphorylation and subsequent activation of the kinase (Fry, 2002). Interaction of Nek2A with protein phosphatase 1 (PP1) can lead to

dephosphorylation and inhibition of Nek2, suggesting that Nek2 may only become fully activated once PP1 is inactivated at the onset of mitosis. Besides autophosphorylation, Nek2 may be regulated by upstream kinases. The kinase can in fact be inactivated during interphase by a complex composed by Mst2 and PP1- γ . During the G2/M transition Mst2 is phosphorylated by Plk1, which liberates Mst2/Nek2A from the inhibitory effect of PP1- γ . Once liberated, Mst2 phosphorylates Nek2A promoting its activation. Finally, this phosphorylation allows Nek2 translocation to the centrosomes, where Mst2/Nek2A complex is stabilized by hSav1 (Mardin et al., 2010). Once it is activated at late G2, Nek2 phosphorylates proteins that constitute the intercentrosomal linker, such as C-Nap1 (Fry et al., 1998a), Rootletin, Centlein, Cep68 (Fang et al., 2014) and β -Catenin (Bahmanyar et al., 2008) promoting its dissolution. Cells lacking Nek2 fail to remove C-Nap1 from centrosomes upon mitotic entry (Mardin et al., 2010).

In addition, Nek2 also phosphorylates centrin, that can bind microtubules promoting microtubules stabilization and thus allowing organization of the microtubule network in interphase and bipolar spindle in mitosis (Jeffery et al., 2010a; Jeong et al., 2007a).

Besides its functions in centrosomes, Nek2A is associated to the kinetochores and is necessary for faithful chromosome segregation. Nek2A phosphorylates Hec1 and this phosphorylation is essential for a faithful chromosome attachment to spindle microtubule, which prevents chromosome instability during cell division (Du et al., 2008). Nek2A also phosphorylates human Sgo1 and such phosphorylation is essential for faithful chromosome congression in mitosis (Fu et al., 2007) Nek2A plays a defining role in spindle assembly checkpoint control by binding and phosphorylating Mad2 and Cdc20. In this way, Nek2 deregulation may

promote aneuploidy by disrupting the control of the mitotic checkpoint (Liu et al., 2010).

Nek2B is involved in maintenance of centrosome structure and spindle assembly since its depletion results in a delay in centrosome maturation, microtubules aster formation and mitotic delay. Upon exiting mitosis, cells exhibit mitotic defects such as the formation of multinucleated cells. Such phenotypes are not observed in cells that exit mitosis in the absence of Nek2A. These observations suggest that Nek2B may be required for the execution of mitotic exit (Fletcher et al., 2005; Uto and Sagata, 2000).

Additionally, a third Nek2 isoform has been identified in vertebrates. **Nek2C** is the result of an alternative splicing of Nek2A mRNA. Its function is unclear, but due to its nuclear localization in interphase, it may contribute to chromatin condensation during mitosis (Wu et al., 2007).

Nek5

Nek5 localizes to the proximal ends of centrioles and contributes not only to the loss of the centrosome linker but also to the integrity of the pericentriolar material (PCM) and centrosomal microtubule nucleation. Upon mitotic entry, Nek5-depleted cells retained centrosome linker components and exhibited delayed centrosome separation and defective chromosome segregation. Disassembly of the centrosome linker may be achieved through cooperation with Nek2, although how this happens remains to be determined (Prosser et al., 2015).

Nek9

Nek9 was originally identified by two independent works. It was purified during a search for protein kinases induced by IL-1, although it is not physiologically activated by the interleukin, and named Nek8 by error (Holland et al., 2002); and through coimmunoprecipitation with Nek6 from cultured cell lines and originally named Nercc1 (Roig et al., 2002a).

Nek9 is a 120 KDa protein with a 979 amino acids sequence. It is highly conserved in mammals, birds and amphibians. In fish and invertebrates it exist but is shorter and only 20 to 50% similar to human Nek9 (Parker et al., 2007). Nek9 has three main domains, an N-terminal kinase domain (residues 52- 308 in humans), a RCC1 domain (residues 347-726) that acts as an autoinhibitory domain and a non-catalytic C-terminal domain (761-979) containing different motifs and features, including a putative coiled coil (891-940) that is necessary for the oligomerization of Nek9 resulting in autophosphorylation and activation *in vitro* (Figure 7) (Roig et al., 2002a). This kinase domain is followed by a functional NLS with two classical nuclear localization motifs, although Nek9 is cytoplasmic. It follows the RCC1 domain, followed by nine consecutive glycine residues that possibly conform a flexible hinge, encompassed within a PEST sequence. An acidic serine/threonine/proline-rich segment (761–890) follows next, which includes two motifs that conform to the SH3-domain-binding sequence PXXP, and seven SP and TP sites motifs, putative Cdk1 phosphorylation sites (Holland et al., 2002; Roig et al., 2002a).

This protein is expressed in all tissues and cell lines studied at similar levels during the cell cycle. Nek9 activity requires the phosphorylation of a residue within its T-loop, Thr210. Nek9 is able to auto activate *in vitro* through the autophosphorylation of this residue. *In vivo* it is inactive during

interphase, and a small amount (5%) is activated in prophase and localizes at centrosomes and spindle poles during mitosis by a two-step mechanism mediated by Plk1 and CDK1 (Figure 7, Figure 8). Interestingly, a significant fraction of active Nek9 is associated with chromosomes and the midbody after the metaphase-anaphase transition, suggesting possible roles of Nek9 after metaphase (Bertran et al., 2011; Roig et al., 2005).

The Nek9 activation mechanism consists of a first phosphorylation by Cdk1 at Ser869 which allows the subsequent binding of the PBD of Plk1. Once bound, Plk1 phosphorylates Nek9 at different sites, among them the RCC1 domain, thus possibly releasing the kinase domain and allowing Thr210 phosphorylation and Nek9 activation. Once active, Nek9 may be able to autophosphorylate resulting in an amplification of the activation.

When Nek9 is active, it binds, phosphorylates and activates both Nek6 and Nek7 (Belham et al., 2003). This activation is important for the subsequent phosphorylation of the kinesin Eg5 at Ser1033, a site that, together with CDK1 site Thr926, controls accumulation of a pool of Eg5 at the centrosomes and is necessary for prophase centrosome separation and normal mitotic spindle formation (Bertran et al., 2011; Eibes et al., 2018; Rapley et al., 2008). Simultaneously, Nek9 directly regulates centrosome maturation and the ability of this organelle to nucleate enough microtubules to organize a normal spindle by phosphorylating the protein adaptor Nedd1/GCP-WD, controlling its centrosomal accumulation and thus the centrosomal content of γ TuRC, the major microtubule nucleating complex of the cell (Sdelci et al., 2012) (Figure 6, and see below).

Nek9 interacts with the multifunctional protein (and dynein light chain) LC8 through a KXTQT motif at the C-terminal domain of Nek9. This binding modulates Nek9 oligodimerization and autophosphorylation. In response to Nek9 activation and autophosphorylation, LC8 binding to Nek9

is disrupted, thus allowing Nek9 to interact with Nek6/7 and activate these two related kinases (Regué et al., 2011).

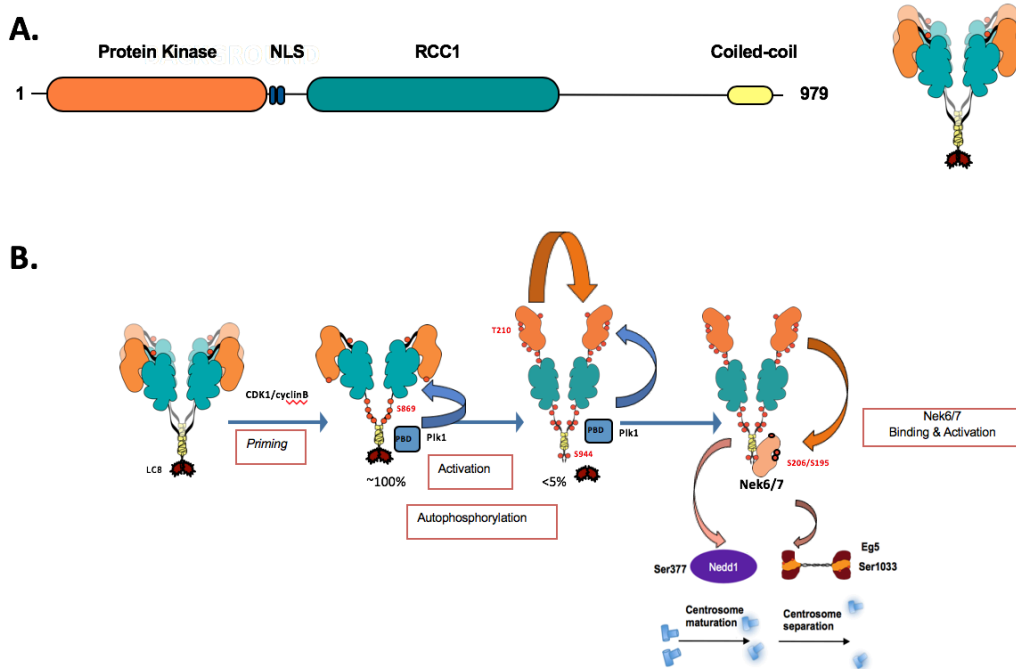


Figure 7: A) Nek9 cartoon representation and its dimerized form; **B)** Mechanism of Nek9 activation and the processes derived from it.

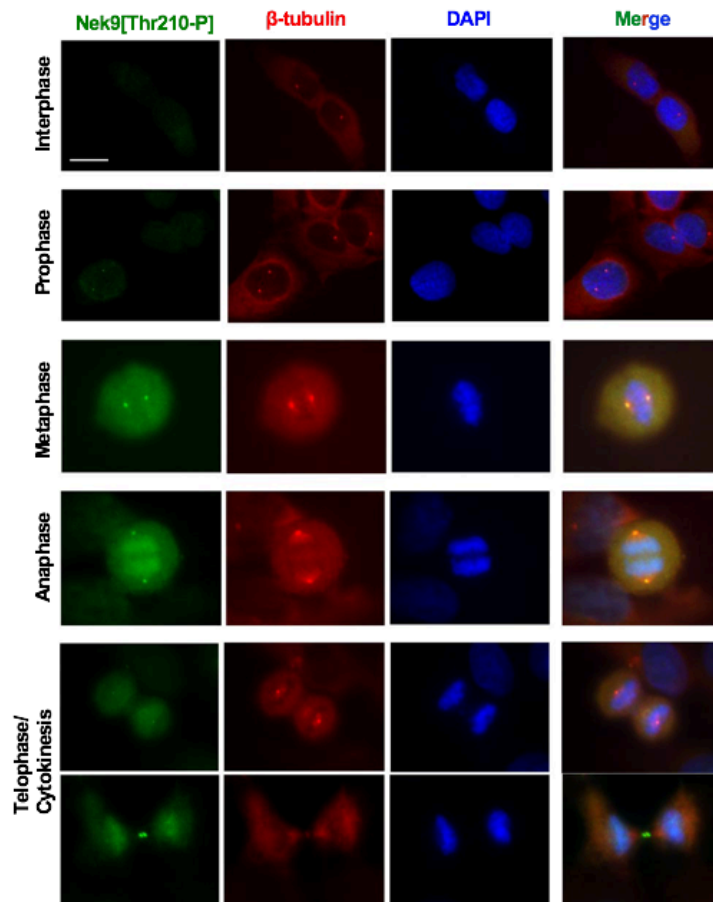


Figure 8: Localization of active Nek9 during cell cycle and different stages of mitosis (Roig et al., 2005).

Loss-of-function phenotypes for Nek9 by gene knockout have not been reported, although a number of observations indicate that interference with the protein kinase results in abnormal progression through the cell cycle, and specifically mitosis. Thus, overexpression of inactive Nek9 (Nek9[K81M]) is toxic for cells. They do not divide and can undergo apoptosis. The microinjection of antibodies against Nek9 during prophase leads to prometaphase arrest with nonaligned chromosomes and a disorganized spindle, abnormal mitosis and aneuploidy (Roig et al., 2002a). In parallel, immunodepletions of endogenous XNercc in *Xenopus laevis*

meiotic extracts interfere with both the formation of mitotic spindle and normal chromosome alignment (Roig et al., 2005).

Nek9 depletion in glioblastoma and kidney cancer cells by siRNA has been described in slower cellular growth due to prolonged G1 and S phase and induced cytokinesis failure and incorrect chromosome separation, characterized by the formation of giant micronucleated cells (Kaneta and Ullrich, 2013).

Nek9 is a component of the acentriolar MTOCs in mouse oocytes, which is critical for meiotic spindle stability and accurate chromosome segregation. Depletion of Nek9 in oocytes using specific morpholino dissociated γ -tubulin from the MTOCs with disrupted meiotic spindle structure and misaligned chromosomes resulting in SAC activation and meiotic arrest at the Pro-MI/MI stage (Yang et al., 2012).

In the present work we described that Nek9 KO mice are not viable and die at very early stages of embryonic development. In humans, Nek9 is essential during development based on the recent description of a Nek9 mutation (c.1489C>T; p.Arg497*) that cause a lethal recessive skeletal dysplasia, which is the first disorder to be associated with *NEK9* in humans to date (OMIM entry #617022). Characterization of patient fibroblasts showed a significant reduction in cell proliferation, a delay in cell cycle progression and a reduction in cilia number and length. Also the Nek9 orthologue in *C. elegans* is restricted to ciliated cells adding further support for a potential role of Nek9 in ciliary function (Casey et al., 2016). Furthermore, it was recently shown that somatic point mutations in Nek9 cause *Nevus comedonicos*. This rare disease is characterized by the presence of skin injuries similar to acne (Levinsohn et al., 2016).

Nek9 has also been identified as a crucial factor involved in cell-cycle progression in p53-deficient cancer cells, as its depletion selectively inhibited proliferation in p53-deficient cancer cells both in vitro and in vivo with G1 arrest and senescence-like features. Thus, Nek9 inhibition provide a possible way to selectively target cancer cells that lack functional p53 with the corresponding development of novel cancer therapies (Kurioka et al., 2014).

Apart from its mitotic functions, Nek9 binds and phosphorylates the dynein adaptor protein BicD2, although the function of this phosphorylation is not known(Holland et al., 2002).Besides, Nek9 may has a role in the nucleus as a fraction of Nek9 has been reported to be associated with the chromatin modulator FACT (Tan and Lee, 2004), in autophagy as depletion of the kinase impairs this process inhibiting the cargo recruitment to vesicles and vesicle trafficking (Behrends et al., 2010) and in the replication stress response (RSR) by promoting CHK1 activity as its depletion in cells leads to replication stress hypersensitivity, spontaneous accumulation of DNA damage and an impairment in recovery from replication arrest (Smith et al., 2014).

Nek6 and Nek7

Nek6 and Nek7 were identified as two NIMA-related kinases with a highly similar catalytic kinase domain (85% identical) and lacking the regulatory C-terminal domain typical of other Neks. They only differ in the N-terminal region of the protein, just before the kinase domain. They were identified first in mice (Kandli et al., 2000).

Later, they were described in humans as ribosomal protein kinase p70 S6 kinases (Belham et al., 2001; O'Regan and Fry, 2009) They are the shortest

members of the NIMA family and both of them bind and are activated by Nek9 (Belham et al., 2003; Roig et al., 2002a).

In metaphase, Nek6 is associated with spindle microtubules, in anaphase it localizes in the central spindle and it is found in the midbody when cells undergo cytokinesis. In contrast, Nek7 is localized to centrosomes either in interphase or mitosis (O'Regan and Fry, 2009).

Nek9 binds to, phosphorylates and activates Nek6/7 by direct phosphorylation at Ser206 and Ser195 respectively. Once active, Nek6 autophosphorylates at Ser137 and Ser202 causing a higher activation of the kinase (Belham et al., 2003). In parallel it has been described that Nek7 is also activated upon binding to the C-terminal domain of Nek9, that dimerises through a coiled-coil domain and could thereby bring together two molecules of Nek7 to promote autophosphorylation, releasing autoinhibition through Tyr97. The same happens in Nek6 with the analogous Tyr108 (Haq et al., 2015; Richards et al., 2009).

Nek6 and Nek7 have a number of different functions during mitosis related to the control of centrosome positioning, spindle assembly and cytokinesis. Upon Nek9 activation, Nek6 and Nek7 phosphorylate the kinesin Eg5 at Ser-1033 that, together with CDK1 phosphorylation at Thr-926, allows Eg5 to accumulate around centrosomes and stimulate their separation in prophase before nuclear envelope breakdown (Bertran et al., 2011; Rapley et al., 2008). Also, both Nek6 and Nek7 contribute to nuclear envelope breakdown through phosphorylation of the nuclear pore protein, Nup98 (Laurell et al., 2011). In prometaphase and metaphase, Nek6 promotes spindle assembly through phosphorylation of the heat shock protein, Hsp72 (O'Regan et al., 2015). Finally, several reports implicate Nek6 and Nek7 in the control of cytokinesis, possibly by phosphorylating

the kinesins Mklp2 and Kif14 (Cullati et al., 2017; Fry et al., 2017; O'Regan and Fry, 2009; Rapley et al., 2008; Salem et al., 2010).

Apart from mitosis, these kinases may have additional roles in interphase. For example, Nek7 has been shown to be important for primary cilia formation, as *Nek7*^{-/-} MEFs exhibit abnormal cilia numbers (Salem et al., 2010) and for regulating microtubules in interphase (Cohen et al., 2013). Furthermore, Nek6 and Nek7 have been implicated in the regulation of centrosome duplication and maturation, senescence, DNA damage response (Gupta et al., 2017; Kim et al., 2011; Lee et al., 2008; Tan et al., 2017) and in activation of the NLRP3 inflammasome (He et al., 2016).

Cell expression of Nek6/7 kinase inactive mutants or depletion by RNAi results in an increase of mitotic cells, multipolar and fragile spindles, abnormal chromosome segregation, multinucleation and cell death (Fry et al., 2017; O'Regan and Fry, 2009; Yin et al., 2003; Yissachar et al., 2006). Nek6 and Nek7 mRNAs are present in most tissues, both in human and mouse. However, the two kinases are expressed differentially during embryogenesis and in different regions of the adult nervous system (Feige and Motro, 2002). Nek6 knockout animals are born at Mendelian ratios and do not show an obvious phenotype, only an increased cardiac hypertrophy after transthoracic aorta constriction (Bian et al., 2014). Conversely, knockout of Nek7 results in late embryonic or perinatal lethality and severe growth retardation. In addition, Nek7 depleted MEFs present binuclear cells, tetraploidy, chromosomal instability, micronuclei and also differences in frequency of primary cilia. Thus, Nek7 has crucial functions during development that cannot be replaced by Nek6 (Salem et al., 2010). Nek6 low resolution and Nek7 high resolution structures have been solved. The structures show that both kinases are formed by a globular kinase domain

and a disordered N-terminal domain (Meirelles et al., 2011; Richards et al., 2009).

Spindle formation

The key components of the mitotic spindle are microtubules, chromosomes that consist of two sister chromatids tightly adhered at their centromere regions where each sister assembles a kinetochore that attaches the chromosome to spindle microtubules, centrosomes in cells that have them, and numerous cell division proteins.

There are three subpopulations of microtubules: kinetochore microtubules that connect chromosomes to spindle poles; interpolar microtubules that originate from opposite poles and interact in an antiparallel way stabilizing the bipolarity of the spindle, and astral microtubules that extend away from centrosomes into the cytoplasm and have a function in orientating and positioning the spindle within the cell (Figure 9) (Wittmann et al., 2001). Microtubules are polarized filaments composed by α - and β -tubulin heterodimer arranged linearly in a head-to-tail configuration within protofilaments. Thirteen parallel protofilaments associate laterally to form the cylindrical microtubule structure. Two are the fundamental properties of microtubules: their dynamic properties and their structural polarity. The dynamic properties allow microtubules to grow or shrink in the presence of GTP by the gain or loss of tubulin dimers at both ends. It is known as **dynamic stability**, which is defined by switching states from growth to shrink (catastrophe) and shrink to growth (rescue). It is regulated by microtubule-associated proteins (MAPs) (Desai and Mitchison*, 1997; Mitchison and Kirschner, 1984). The second important property of microtubules is their **polarity**. Because of the asymmetry of the tubulin dimer subunits, the minus ends and the plus ends of microtubules have

different dynamics. (Desai and Mitchison*, 1997). The microtubule plus ends (with β -tubulin exposed at their extremes) are highly dynamic, alternating states of shrinkage and growth. These ends are usually oriented towards the surface of the cell. However, minus ends (exposing α -tubulin monomers) are less dynamic, and although they can grow they do it slowly than plus ends. In cells, minus ends can be stabilized due to their association with the centrosome or other MTOCs. Different motor proteins, including dynein and a large set of kinesin-like proteins, recognize microtubules polarity and move their cargo (microtubules, chromosomes and other proteins) along them (Figure 9) (Wittmann et al., 2001).

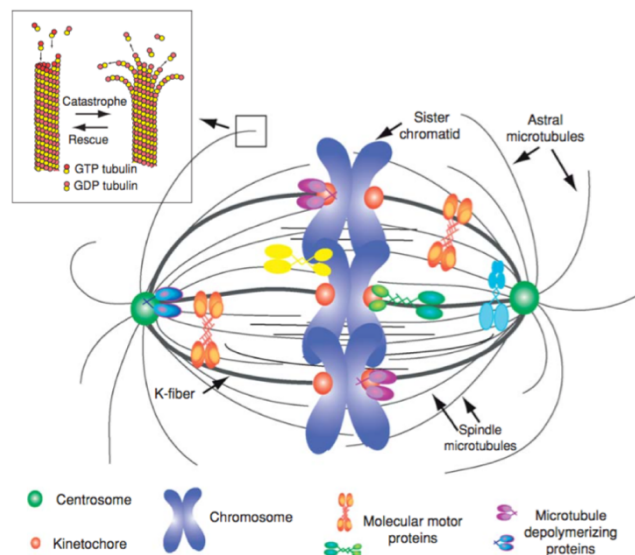


Figure 9: Key components of the mitotic spindle and the tubulin assembly-disassembly cycle (Walczak and Heald, 2008).

In mitosis, distinct complementary mechanisms drive nucleation and reorganization of microtubules for bipolar spindle assembly (Figure 10). The first model proposed is a **centrosome-based** microtubule nucleation, the “**search and capture**” model, in which centrosome nucleate microtubules till their plus ends are captured and stabilized by one of the sister kinetochores. Thus, chromosomes find a become bioriented at the equator of

the cell (Duncan and Wakefield, 2011; Kirschner and Mitchison, 1986; Walczak and Heald, 2008). In contrast to the “search and capture” pathway, in the “**self-assembly**” model microtubules are nucleated around chromosomes, independently of centrosomes, and sorted into an antiparallel array that generates the bipolar spindle. Microtubules nucleation and spindle assembly dependent of chromatin and kinetochores is mediate by **Ran GTPase** via localization of its guanine nucleotide exchange factor RCC1. Upon nuclear envelope breakdown, RCC1 bound to condensing chromatin generating a gradient of RanGTP in the vicinity of the chromosomes. (Duncan and Wakefield, 2011; Gruss et al., 2001; Hetzer et al., 2002). The kinetochores stabilize microtubules (k-fibers) originated around chromosomes and become oriented with the plus ends attached to the kinetochore and the minus ends focused at the spindle poles (Meunier and Vernos, 2011) which finally will be included in the centrosome-driven spindle, through cytoplasmic dynein via their capture by astral microtubules and at least seven different kinesins (Goshima et al., 2005; Maiato et al., 2004; Rieder, 2005; Rieder and Khodjakov, 2003). RanGTP releases import cargoes from importin β binding either in the interphase nucleus or surrounding chromosomes during mitosis, some of which are spindle assembly factors (SAFs) such as TPX2 and NuMA, , allowing the activation of proteins that function in spindle assembly (Dasso, 2002; Hetzer et al., 2002). The chromosomal passenger complex (**CPC**), consisting of Aurora B, INCENP, Survivin and Borealin has been also shown to be required for microtubule generation during spindle formation (Duncan and Wakefield, 2011; Tseng et al., 2010). Finally, another mechanism is **the augmin pathway**. The augmin hetero-complex is able to interact simultaneously with the γ TuRC subunit NEDD1 (Teixidó-Travesa et al., 2010) and pre-existing spindle microtubules facilitating intra-spindle microtubule nucleation (Duncan and Wakefield, 2011; Goshima et al., 2008) maintaining

polarized microtubule organization, even when noncentrosomal microtubules initiation is widespread (Kamasaki et al., 2013).

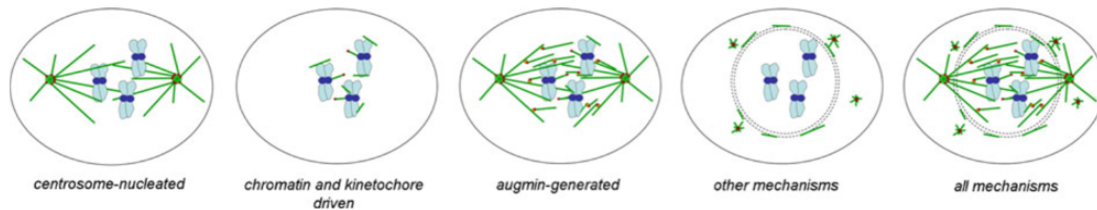


Figure 10: Mechanisms that contribute to mitotic spindle formation (Duncan and Wakefield, 2011).

TPX2

TPX2, a microtubule Associate Protein (MAP), was originally identified as a protein that targets the kinesin-12 family member Xklp2 to spindles in *Xenopus* egg extracts. TPX2 has a dynamic localization along the cell cycle. During interphase it localizes at the nucleus while after NEB it localizes at spindle poles which requires dynein activity, Eg5 and microtubule flux (Ma et al., 2010; Wittmann et al., 2000). Immunodepletion of TPX2 from mitotic egg extracts causes defects in spindle pole organization and centrosome-directed spindle assembly, and completely blocked microtubule growth in the absence of centrosomes (Gruss et al., 2001). It seems to be conserved in somatic cells having a crucial role in chromatin-mediated spindle assembly since TPX2 knockdown completely abolished chromosome-mediated microtubule nucleation in mammalian cells (Tulu et al., 2006).

The N-terminal of TPX2 mediates Aurora A activation, while its C-terminal mediates microtubule binding and TPX2 interaction with the motor protein Eg5 (Ma et al., 2011). TPX2 nuclear localization during interphase could be explained by the presence of two nuclear localization signals (NLS) recognized by importin- α . Despite its nuclear localization all TPX2 functions

described until now are cytoplasmic and exclusive to mitosis, with the only possible exception of a role for TPX2 in the DNA Damage Response in interphase. (Neumayer et al., 2012, 2014): During prophase, Eg5 localization and centrosome separation depend on TPX2, a pool of which localizes to the centrosomes before NEBD in a RHAMM- and Nek9-dependent manner. Nek9 phosphorylates TPX2 nuclear localization signal (NLS) preventing its interaction with importin and nuclear import (Eibes et al., 2018). Then, after NEB it localizes at spindle poles, which requires the activity of the dynein–dynactin complex. In anaphase TPX2 becomes relocalized from the spindle poles to the midbody (Wittmann et al., 2000). RanGTP releases TPX2 from importin, stimulating interaction between TPX2 and Aurora A kinase, which leads to activation of the kinase (by preventing dephosphorylation by PP1 phosphatases of Aurora A Thr288) and TPX2 phosphorylation. Aurora A subsequently phosphorylates the kinesin-5 Eg5 that promotes spindle bipolarity and TACC that promotes microtubule polymerization (Bayliss et al., 2003; Eyers et al., 2003; Tsai et al., 2003).

TPX2 interacts during mitosis with (Receptor for Hyaluronan Mediated Motility) RHAMM. This interaction is required for proper localization of TPX2 at centrosomes during mitosis and for activation of Aurora A (Chen et al., 2014).

Motor proteins

Motor proteins involved in assembly and maintenance of the mitotic spindle comprise two groups: the **dynein family**, which moves towards the minus ends of microtubules, and the **kinesin family**, which has members that move along the microtubules in both directions and can also play a role destabilizing them (Figure 11).

The dynein complex

Dynein belongs to the AAA+ superfamily of ATPases, associated with diverse activities. Dynein has a ring of six AAA+ modules that are linked together into one large polypeptide, along with several unique appendages that enable motor function.

Mammals have two differentiated dynein families, cytoplasmic and axonemal dynein. Axonemal dynein is present in cilia and flagella whereas cytoplasmic dynein has roles on intracellular trafficking and mitosis.

Cytoplasmic dynein transport cargos towards microtubule minus ends, which includes components of the centrosome, transcription factors and cytoskeletal filaments among others. It is also involved in clearing material from the periphery of the cell for degradation and recycling (Roberts et al., 2013). At cell division, cytoplasmic dynein participates in spindle assembly dependent of chromatin. Dynein functions include centrosome separation, centrosome tethering to the nuclear envelope and nuclear envelope breakdown by pulling nuclear membranes and associated proteins in a poleward manner along astral microtubules (Raaijmakers and Medema, 2014; Salina et al., 2002). Mammalian cytoplasmic dynein requires different adaptors, such as dynactin, for its motility: lissencephaly 1 (**LIS1**; also known as NUDF), nuclear distribution E (**NUDE**) and the **dynactin complex** (Kardon and Vale, 2009; Vallee et al., 2012).

BicD2 is a conserved, dimeric adapter protein. BicD2 N-terminal coiled coil domain is not only an adaptor, it is also required for dynein activation or motility, it facilitates the interaction between dynein and dynactin (Hoogenraad and Akhmanova, 2016; McKenney et al., 2014). BicD2 C-terminal part, apart from its interaction with dynactin subunit dynamitin, interacts with Rab6, a small GTPase present at Golgi. Rab6

interaction with BicD2 promotes BicD2 localization at Golgi during interphase (Hoogenraad et al., 2003). This BicD2 fragment also interacts with RanBP2 allowing its localization at NE during G2/M transition and is important for centrosome tethering to the NE (Splinter et al., 2010).

Furthermore, BicD2 C-terminal domain is able to interact directly with the N-terminal domain acquiring an inhibitory conformation of the protein that could control its interaction with dynein (Hoogenraad et al., 2003).

Kinesins

Kinesins are molecular motors that use the energy from hydrolysis of ATP to associate with microtubules and control the movement of chromosomes in the spindle. There are 14 families of kinesins, and most members possess two distinct functional domains: an ATP-hydrolyzing motor domain and a tail domain that can associate with the cargo. The motor domain is very well conserved among the different kinesins families while the tail domains are more divergent. Most kinesins translocate to the plus ends of the microtubule and possess an N-terminal motor domain. There are kinesins with the motor at the C-terminus that translocate to the minus end of the microtubule. Some kinesins are able to control microtubule dynamics through promoting polymerization, depolymerization or simply stopping polymerization (Cross and McAinsh, 2014; Vicente and Wordeman, 2015)

Eg5 (also known as Kif11 or kinesin 5) is a plus end directed kinesin, which is structured in an N-terminal motor domain, a central coiled coil domain called stalk and a globular C-terminal tail domain. The coiled coil domain permits the homotetramerization with two heads contacting one microtubule and the other pair of heads contacting a parallel or antiparallel microtubule, so that forcing two microtubules to glide with respect to each other (Kapitein et al., 2005). This activity is used to separate the centrosomes

during the beginning of mitosis and to maintain bipolar spindle (Ferenz et al., 2010). Eg5 localizes at spindle during mitosis with an important predominance at spindle poles. It has been suggested that Eg5 localization along the spindle is controlled by TPX2 and dynein (Wittmann et al., 2000). Inhibition of Eg5 either by RNAi (Weil et al., 2002) or with chemical inhibitors leads to monopolar spindle formation and failed chromosome segregation, suggesting that the kinesin could be a putative target for effective antimitotic drugs (Maliga et al., 2002; Mayer et al., 1999; Skoufias et al., 2006).

CDK1 phosphorylates Eg5 at Thr926. This phosphorylation is required for its spindle localization and binding to microtubules (Blangy et al., 1995). Moreover, a small amount of Eg5 is phosphorylated by Nek6/7 necessary for correct mitotic progression (Rapley et al., 2008), depending on the binding to TPX2 (Eibes et al., 2018).

During prometaphase through to metaphase, kinesin 12/HKLP2 plays a redundant role to Eg5, it compensates the loss of Eg5 in the prometaphase pathway for centrosome separation (Tanenbaum et al., 2009). Also, kinesin-14 HSET is a minus-end directed motor that generates an inward force during the formation of the spindle. The outward force created by Eg5 and kinesin 12 compensates this inward force to help maintain the spindle length. In addition, localization of Kinesin-7, 8 and 13 to the kinetochores and of Kinesin-4 and Kinesin-10 to the chromosome arms facilitates microtubule capture and chromosomal congression to the metaphase plate. During anaphase, sister chromatid separation and movement towards the spindle poles are facilitated by the Kinesin-7 and 13. During telophase, Kinesin-6 motors localize to the midbody and are involved in cytokinesis (Cross and McAinsh, 2014; Verhey and Hammond, 2009; Vicente and Wordeman, 2015).

INTRODUCTION

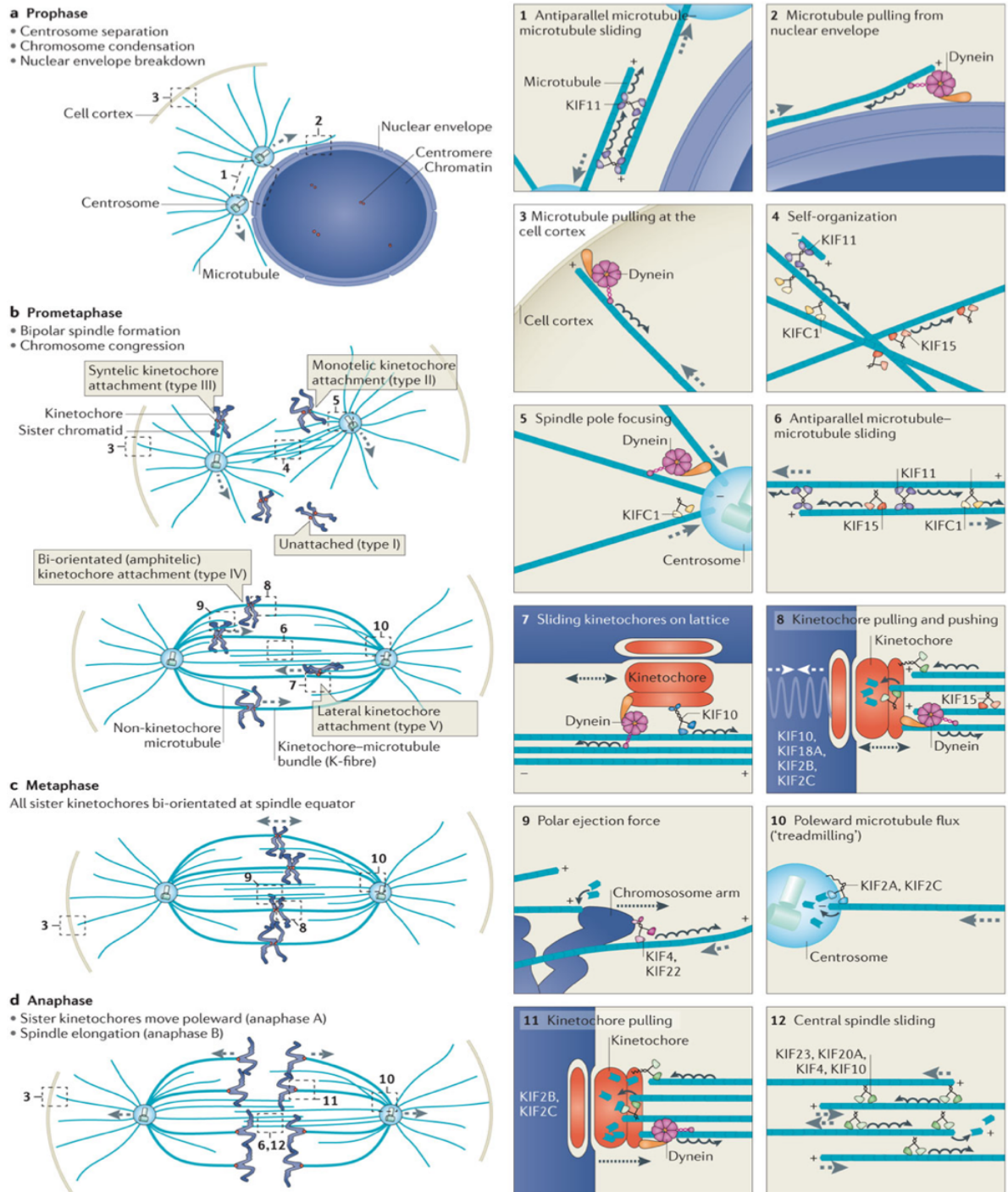


Figure 11: Schematic representation of all motor protein involved in mitotic events and their function at every stage (Cross and McAinsh, 2014).

Centrosomes and centrioles

The centrosome was first observed in the 1800s by Theodor Boveri and Édouard Van Beneden. They studied cell divisions in fertilized eggs of parasitic worms and discovered the existence of a spindle pole organizer during mitosis that continuously duplicates and acts as the main organizing centre for cellular division (Scheer, 2014). He also proposed that tumors developed as a consequence of chromosomal imbalances, and, furthermore, suggested that centrosome aberrations contribute considerably to that imbalance (Nigg et al., 2014).

The centrosome is known to act as the major microtubule organizing centre (MTOC) in proliferating animal somatic cells. It concentrates microtubule nucleating activities and physically anchors and organizes the microtubule network. It thus orchestrates different cellular processes, including the formation of the mitotic spindle in dividing cells, cell motility, signaling, adhesion, coordination of protein trafficking by the microtubule cytoskeleton and the acquisition of polarity. It also acts as the basal body for primary cilium formation in quiescent cells. Structural and numerical centrosome aberrations have long been implicated in cancer, and more recent genetic evidence directly links centrosomal proteins to ciliopathies, dwarfism and microcephaly (Banterle and Gönczy, 2017; Bettencourt-Dias, 2013; Bettencourt-Dias et al., 2011; Doxsey, 2001; Fırat-Karalar and Stearns, 2014; Gönczy, 2015; Nigg et al., 2014; Sluder, 2005).

In general, vertebrate centrosomes are thought to have evolved from internalization of basal bodies of unicellular organisms, and several eukaryotic non-ciliated cells including plants, some fungi, and mammalian oocytes lack apparent centriole structures (Bettencourt-Dias, 2013).

Centrosome structure

Originally, the centrosome was described as a special organ of cell division and a spindle pole organizer. Only decades later electron microscopy enable scientists to discover the beautiful architecture of centrioles within centrosomes (Azimzadeh and Marshall, 2010).

Structurally, it is highly conserved, at least among animal cells. A typical unduplicated centrosome is composed of two cylindrical centrioles (called mother and daughter centriole) arranged orthogonally to each other. Centrioles are microtubule-based organelles usually formed by a characteristic radial array of nine microtubule triplets (Figure 12). Starting from the inside, each triplet contains an A, B and C microtubule, with the A-microtubule being the only complete one that contains the full set of 13 protofilaments. The A-microtubule from one triplet is connected with the C-microtubule of the next triplet located clockwise via a A–C linker (Gönczy, 2012). Centriole size differs among species, being between 100 - 250 nm in diameter and 100 – 500 nm in length. For example, they are shorter in *Drosophila melanogaster* and *Caenorhabditis elegans* and are composed of nine microtubule doublets and singlets, respectively, instead of triplets. In some insects, the ninefold symmetry is lost, preserving however the ability to assemble cilia (Bettencourt-Dias, 2013; Bornens, 2012; Gönczy, 2015; Hatch and Stearns, 2010; Lüders and Stearns, 2007). The centriole is polarized along its long axis, with the base referred to as the proximal end and the tip as the distal end. Microtubules impose this polarity on the centriole being the microtubule plus ends at the distal end of the centrioles (Azimzadeh and Marshall, 2010; Winey and O’Toole, 2014).

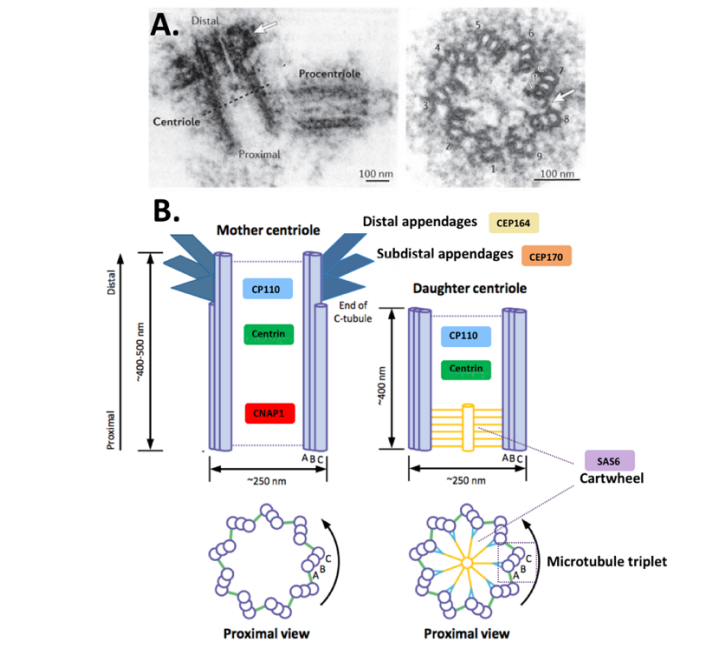


Figure 12: **A)** Ultrastructure of a resin-embedded centriole and procentriole and a cross-section illustrating the ninefold radial symmetry of microtubules (Gönczy, 2012); **B)** Structure of a mature parent centriole and a tightly associate procentriole (Gupta and Kitagawa).

Both centrioles differ in age and structure and are associated by interconnecting fibers. The older centriole (the mother centriole) is characterized by distal and subdistal appendages. Subdistal appendages function by anchoring microtubules, whereas distal appendages seem to be involved in anchoring the organelle to the cell membrane while performing its role as the basal body of cilia. Surprisingly, appendages are absent in *Drosophila* and *C. elegans*. However, several vertebrate centrosomal proteins are highly conserved in these species (Azimzadeh, 2014).

Centrioles are made of numerous proteins such as ninein, centrobilin, centrosomal P4.1- associated protein (CPAP) and HsSAS-6 that interact with and stabilize tubulins (Delgehyr et al. 2005; Gudi et al. 2011; Zheng et al. 2016).

The centrioles also organize the pericentriolar material (PCM), an electron-dense protein mass organized as radial layers that functions in microtubule

nucleation and anchoring roles of the centrosome. (Fu and Glover, 2012; Sonnen et al., 2012). CPAP is located at the interface between the centrioles and the PCM, followed by CEP192 and Cep120. CDK5RAP2 (Cyclin-dependent kinase 5 regulatory subunit-associated protein 2), NEDD1 (Neural precursor cell expressed developmentally down-regulated protein 1) and the microtubule nucleator complex γ -Tubulin Ring Complex (γ TuRC) are found at the outer layers. Pericentrin has an extended conformation and is organized radially, with the carboxy terminus pericentrin-AKAP450 centrosomal targeting (PACT) domain adjacent to the centriole wall and the amino terminus extending outward into the PCM.

The PCM undergoes dramatic changes during the cell cycle. During the transition from G2 to M the centrosome recruits several proteins. Induced by the activity of mitotic kinases, such as Plk1, several phosphorylation modifications take place and the centrosome increases the size and nucleation activity, a process known as centrosome maturation (see below) (Lüders, 2012).

The mitotic centrosome is organized in two parts; an inner part with a radial layer organization and an outer extended part organized like a cloud. In the human mitotic centrosome, the inner part of is organized in a similar manner as in interphase while the outer part contains CDK5RAP2, CEP192, γ TuRC and pericentrin (Fu and Glover, 2012; Lüders, 2012; Sonnen et al., 2012).

The Centrosome cycle

The centrosome and cell cycle are intricately linked to ensure that centrosome duplication is restricted to only once per each round of cell division (Hatch and Stearns, 2010; Nigg and Raff, 2009; Tsou and Stearns, 2006). The mechanism of centriole duplication can be summarized as comprising four discrete steps, namely centriole disengagement,

procentriole assembly, centrosome maturation and centrosome disjunction and separation (Figure 13).

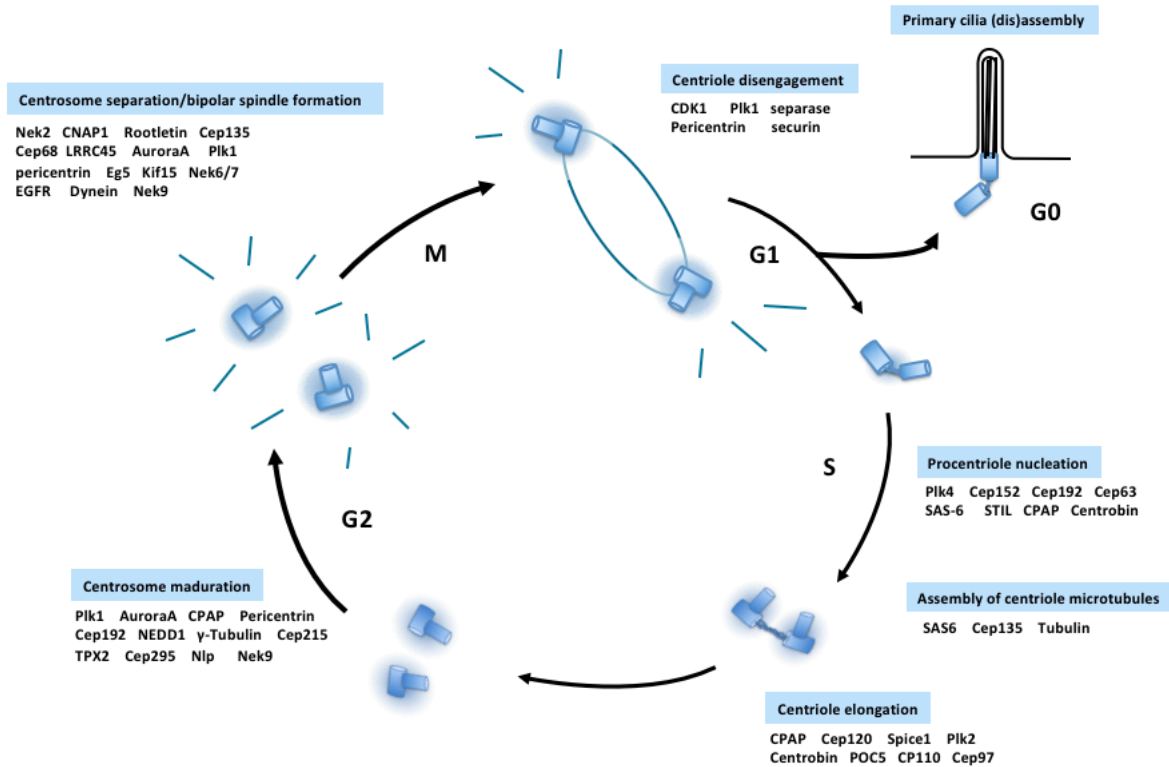


Figure 13: The centrosome cell cycle

Centrosome disengagement

During metaphase, each of the centrosomes that form the bipolar spindle is composed of a pair of centrioles arranged in a tight orthogonal conformation, that is thought to prevent centriole reduplication in the same cell cycle. At the end of mitosis or in early G1, the orthogonal arrangement of the centrioles is lost in a process known as ‘centriole disengagement’. This process licenses the centrioles for efficient centriole duplication at the proximal ends of each of the centrioles during S-phase (Tsou and Stearns 2006, Tsou et al. 2009). The licensing of centrioles is now recognized to depend on two main processes: centriole disengagement, which permits the

reduplication of the parent centriole, and centriole-to-centrosome conversion, which is required for the procentriole to acquire competence for duplication (Nigg and Holland, 2018).

Centriole disjoining is suggested to be controlled by two “centriole licensing pathways” respectively in early mitosis (Plk1-mediated) and in late mitosis, in anaphase/telophase transition (Plk1 and separase-mediated). At the onset of anaphase, Plk1 regulates the activation of separase, a cysteine protease that triggers sister chromatid separation.

By analogy to sister chromatid cohesion, Plk1 might promote a separase-independent removal of an hypothetical centriolar “glue” protein (ideally responsible for cohesion) in early mitosis, while in anaphase might recruit separase and mediate an anaphase-specific separase cleavage of this “glue” protein (Tsou and Stearns, 2006; Tsou et al., 2009). Separase induce centriole separation through the cleavage of cohesin and pericentrin. Pericentrin has to be phosphorylated by Plk1 to be a suitable substrate of separase in late mitosis. Phosphoresistant mutants of PCNT are not cleaved by separase and eventually inhibit centriole separation (Kim et al., 2015). In addition, expression of a non-cleavable PCNT mutant suppressed centriole disengagement (Lee and Rhee, 2012; Matsuo et al., 2012).

Cep215, also called CDK5Rap2, is tightly bound to centrioles through interactions with Cep152 and Cep192 and there are two distinct and independently localized pools of Cep215 at the centrosome. One interacts with Cep68 and contributes to the intercentriolar linker. Phosphorylation of Cep68 target it to degradation in early mitosis releasing this pool of Cep192. The second pool of Cep192 interacts with pericentrin and is more intimately associated with centrioles. In late mitosis, separase cleavage pericentrin, releasing Cep192 and promoting centriole

engagement lost. A non-degradable version of Cep68 (S332A) did not prevent linker disassembly so Cep68 but non-cleavable pericentrin did (Figure 14) (Pagan et al., 2015).

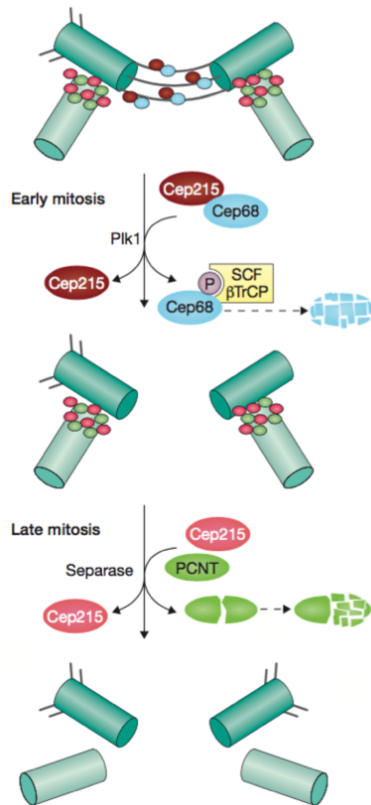


Figure 14: Cep215 has a dual role in centrosome cohesion (Fry, 2015).

Laser ablation of the daughter centrioles in S phase–arrested cells promoted a new duplication cycle on the mother centrioles, showing that the attachment of the daughter centriole to the wall of the mother inhibits formation of additional daughters. Under conditions when multiple daughters simultaneously form on a single mother, all of these daughters must be removed to induce reduplication. In addition, overexpression of the PCM protein pericentrin in S-arrested cells induces formation of numerous daughter centrioles meaning that the size of the PCM cloud associated with the mother centriole restricts the number of daughters that can form simultaneously (Loncarek et al., 2008).

Furthermore, it is known that Shugoshin 1 (Sgo1) is involved in controlling spindle pole integrity and centriole cohesion and that its function is at least mediated through phosphorylation by Plk1 (Wang et al., 2008) This suggest a dual pathway in which Plk1 promotes the stabilization of cohesion through sSgo targeting and phosphorylates factors that induce disengagement.

After centriole disengagement, the orthogonal link between the mother and daughter centriole is lost and the centriole pairs are tethered by a newly formed intercentriolar linkage that extends between the proximal ends that is composed of rootletin, β -Catenin, Cep68, Cep215, LRRC45 and C-Nap1 (Fry et al. 1998a, Bahe et al. 2005, Bahmanyar et al. 2008, Pagan et al. 2014). This allows each of the centrioles to go through the second requisite for duplication, acquisition of PCM, a process termed centriole-to-centrosome conversion, which is also governed by CDK1 and Plk1 (Fu et al., 2015a; Izquierdo et al., 2014; Wang et al., 2011b). This involves the acquisition of Cep295 for the recruitment of critical factors for duplication, such as Cep152. Proteins such as centrobins and Cep120, which are recruited to daughter centrioles in their first cell cycle, are gradually lost during the conversion. To become competent for ciliogenesis and MT anchoring, mother centrioles formed two cycles ago reach its final maturation by building distal and subdistal appendages (Loncarek and Bettencourt-Dias, 2017).

However, it has been described recently that Plk1 induces maturation and distancing of the daughter centriole allowing reduplication of the mother centriole even if the original daughter centriole is still orthogonal to it but there is around 80 nm distance, which is the distance centrioles normally reach during prophase (Shukla et al., 2015).

Centrosome duplication

At the initial stage of procentriole assembly, several proteins are recruited to form a central tube known as the cartwheel structure at the proximal ends of each of the licensed centriole, onto which microtubules are added to form the centriolar wall. Cep192, as well as the interacting proteins Cep152, Cep63, and Cep57, constitute a first module that plays a critical scaffolding function to recruit Plk4, the main centriole duplication factor, to the proximal region of the parental centriole to coordinate the process and identify the origin of centriole duplication (Arquint and Nigg, 2016; Banterle and Gönczy, 2017; Fırat-Karalar and Stearns, 2014; Fu et al., 2015b; Hatch and Stearns, 2010; Nigg and Holland, 2018; Nigg and Stearns, 2011; Sonnen et al., 2013).

In early G1 phase, Plk4 forms a ring around each parental centriole. Plk4 exist as homodimer and trans-autophosphorylation within the dimer triggers SCF- β TrCP-mediated proteolytic degradation (Cunha-Ferreira et al., 2009; Holland et al., 2012; Nigg and Holland, 2018). At this stage, STIL and SAS-6 proteins are not yet present, due to their degradation by APC/C^{Cdh}. With the silencing of the APC/C at the G1/S transition STIL binds PLK4 on the circumference of the mother centriole. Upon binding to STIL, Plk4 undergoes a conformational change and is activated through trans-autophosphorylation within the activation segment (Arquint and Nigg, 2016; Arquint et al., 2015; Lopes et al., 2015). Once active, Plk4 then phosphorylates STIL allowing the interaction and the recruitment of HsSAS-6 and cartwheel formation. HsSAS-6 homodimers finally oligodimerize to form a ring with nine homodimeric units conferring ninefold symmetry to the centrioles (Keller et al., 2014). Depletion of PLK4 or chemical inhibition

of the kinase results in rapid loss of STIL from centrioles, suggesting that PLK4 activity is required to maintain STIL at the site of centriole formation (Arquint and Nigg, 2016). Binding of Plk4 with STIL is regulated first, by CDK1-CyclinB, which binds STIL during mitosis, thus preventing interaction with Plk4 (Zitouni et al., 2016) and second, STIL levels are low during G1, when is targeted for degradation via APC/C^{Cdh1}. As for STIL, levels of HsSAS-6 are regulated by both APC/C^{Cdh1}- and Plk4- mediated phosphorylation of SCF/FBXW5, which prevents the targeting of HsSAS-6 for degradation, thus promoting of centriole assembly (Puklowski et al., 2011; Strnad et al., 2007). Centriolar HsSAS-6 feeds back positively on STIL and STIL also interacts with the tubulin-binding protein CPAP, recruiting it to the emerging procentriole. Overexpression of any one of the core components of the Plk4-STIL–Sas-6 module is sufficient to promote the formation of more than one centriole per mother centriole (Arquint and Nigg, 2016; Arquint et al., 2012; Banterle and Gönczy, 2017; Nigg and Holland, 2018).

Also, Cep135 interaction with HsSAS-6 serves to connect HsSAS-6 to CPAP making Cep 135 a promising candidate bridge between cartwheel and peripheral elements and its depletion leads to a significant reduction in centriole number (Lin et al., 2013). Daughter centrioles start to elongate in late S phase until they reach its full-length in G2-phase. Centrobin, SPICE, Cep120 and CPAP participate in the centriole elongation process through their interactions with tubulin (Banterle and Gönczy, 2017; Gudi et al., 2011; Zheng et al., 2016). CPAP controls the speed of microtubule growth during centriole assembly while CP110 and POC1 cap the distal tips of centrioles, resulting its depletion results in overly long centriolar microtubules (Banterle and Gönczy, 2017; Nigg and Holland, 2018; Schmidt et al., 2009; Zheng et al., 2016).

It was recently described a new role of Plk4 as a homeostatic clock that helps to ensure daughter centrioles grow to the correct size in fly embryos. If the centriole contains higher Plk4 levels at the beginning of S phase, this will impact the Plk4 recruitment rate and thus the rate by which Plk4 is subsequently lost from the centriole. On the contrary, reduced Plk4 levels at the beginning of S phase will result in lower recruitment and loss rates. Thus, initial recruitment of Plk4 could be sufficient to establish the centriolar Plk4 rate controlling proximal end Sas-6 incorporation period and centriole size (Aydogan et al., 2018).

Centrosome maturation

Newly formed centrioles in cycling cells undergo a maturation process that is almost two cell cycles long before they become competent to function as microtubule-organizing centers and basal bodies. As a result, each cell contains three generations of centrioles, only one of which is able to form cilia.

During G2/M centrosomes increase their size, recruit additional PCM proteins and assemble the appendages on the new parental centriole which allow for its transition from daughter to a mother centriole (Azimzadeh and Marshall, 2010). This process has long been known to be governed by Plk1 (Kong et al., 2014). Plk1 triggers the ordered assembly of an initial set of core scaffolding proteins (Cep152, CDK5RAP2 and Cep192) that subsequently recruit all other PCM components. First, Cep192 acts as a scaffold for Aurora A recruitment and activation, which make Plk1 active and ready to phosphorylate Cep192 triggering γ TuRC binding and microtubules nucleation (Joukov et al., 2014). The protein adaptor NEDD1/GCP-WD is phosphorylated by Nek9, acting downstream of Plk1, contributing to its recruitment to the centrosome and in consequence, to the recruitment of γ -tubulin in prophase (Sdelci et al., 2012).

Centrosome disjunction

After centriole disengagement the proximal ends of the two centrioles became tethered by filamentous centriole linkers to ensure centrosome cohesion. The proteinaceous filaments is mainly composed by two proteins: Rootletin and C-Nap1, although recently the proteins Cep68 and Cdk5Rap2 (Cep215) have also been described as part of the link (Bahe et al. 2005, Bahmanyar et al. 2008, Pagan et al. 2014).

During mitosis centrosomes must separate so the linker should be dissolved. Cep215, also called CDK5Rap2, is tightly bound to centrioles through interactions with Cep152 and Cep192 and there are two distinct and independently localized pools of Cep215 at the centrosome. One interacts with Cep68 and contributes to the intercentriolar linker. Phosphorylation of Cep68 targets it to degradation in early mitosis releasing this pool of Cep215. The second pool of Cep215 interacts with pericentrin and is more intimately associated with centrioles. In late mitosis, separase cleavage pericentrin, releasing Cep215 and promoting centriole engagement lost. A non-degradable version of Cep68 (S332A) did not prevent linker disassembly so Cep68 but non-cleavable pericentrin did (Figure 14) (Pagan et al., 2015).

The linker components C-Nap1 and rootletin are phosphorylated by Nek2A after Nek2A activation by Plk1 at late G2/early M phase. Nek2 phosphorylates the C-terminal of C-Nap1 to prevent its oligomerisation and interaction with the Cep135 (centrosomal protein of 135 kDa) and rootletin thereby disrupting the stability of the filamentous intercentriolar linker (Faragher and Fry, 2003; Fry et al., 1998b; Pagan et al., 2015; Yang et al., 2006). A physiological antagonist of Nek2 activity is the PP1 phosphatase, specifically the PP1 α isoform, which regulates centrosome cohesion through dephosphorylating C-Nap1 after mitosis (Meraldi and Nigg, 2001; Mi et al.,

2007).

Additionally, the maintenance of centrosomal integrity involves the activity of β -catenin, that can localize to the proximal and distal centriole ends and, moreover, between centrosomes acting like a docking protein for the recruitment of Rootletin and C-Nap1 (Bahmanyar et al., 2008).

Centrosome separation

Centrosomes then separate and move to the opposite side of the nucleus forming a bipolar spindle. There are two different pathways according the timing of centrosome separation; the prophase pathway, where centrosomes separate before NEB and the prometaphase pathway, where centrosomes complete separation after dissociation of the nuclear membrane. During the prophase pathway, kinesin-5 (Eg5/KIF11), cortical dynein and dynein bound to the NE are the main players. For the prometaphase pathway, the activity of KIF15 (also known as Kinesin-12 and HKLP2) plus microtubule-kinetochores pushing forces and actin cytoskeleton are required (Raaijmakers et al., 2012; Tanenbaum and Medema, 2010). Prophase centrosome separation optimizes spindle assembly and minimizes abnormal chromosome attachments that could end in aneuploidy (Silkworth et al., 2012).

Eg5 is a plus-end- directed member of the kinesin 5 family that is able to bind antiparallel microtubules emerging from both centrosomes and slide them apart. Eg5 loading at centrosomes is a required step for separation. This localization is regulated by the action of different protein kinases. CDK1 phosphorylates Eg5 at Thr926 promoting Eg5 binding to microtubules (Blangy et al., 1995). At the same time CDK1 and Plk1 drive the activation of the Nek9/Nek6/7 pathway, so once active, Nek6 and Nek7 phosphorylate Eg5 at Ser1033 promoting its accumulation at centrosomes (Bertran et al.,

2011). Recently, our group has shown that Eg5 localization and centrosome separation in prophase depend on the nuclear microtubule-associated protein TPX2, a pool of which localizes to the centrosomes before NEBD in a RHAMM- and Nek9-dependent manner. Nek9 phosphorylates TPX2 nuclear localization signal (NLS) preventing its interaction with importin and nuclear import (Eibes et al., 2018).

Centrosome duplication and the link with the cell cycle

The centrosome duplication cycle is coupled with cell cycle. When the cell enters mitosis, the duplicated centrosomes separate to the spindle poles and assemble the bipolar mitotic spindle for accurate chromosome separation and to maintain genomic stability. The two cycles might be coordinated so that when the chromosome cycle is delayed, the centrosome cycle stops, thereby avoiding the generation of extra centrosomes.

There are two coupling points, at the G1/S and G2/M transitions. At the G1/S transition, cyclin-dependent kinase 2 (CDK2) in a complex with cyclin E or cyclin A may trigger procentriole formation via phosphorylation of the centriolar coiled-coil protein of 110 kDa (CP110), the serine/threonine kinase MPS1 (also known as TTK) and the multifunctional protein nucleophosmin (Gönczy, 2015; Hinchcliffe and Sluder, 2001). Overexpression of a non-phosphorylatable form of nucleophosmin, inhibits disengagement, whereas depletion of nucleophosmin results in centrosome amplification (Okuda et al., 2000). Also, CDK2 inactivates APC/C^{CDH1} towards the end of G1 phase, preventing the degradation and thus leading to the accumulation of components needed for S phase entry, including HsSAS-6, STIL and CPAP. At G2/M transition, CDK1 leads to activation of the serine/threonine kinase Aurora A, which in turn

phosphorylates and activate Plk1 resulting in centriole–procentriole disengagement (Figure 15) (Gönczy, 2015; Hinchcliffe and Sluder, 2001).

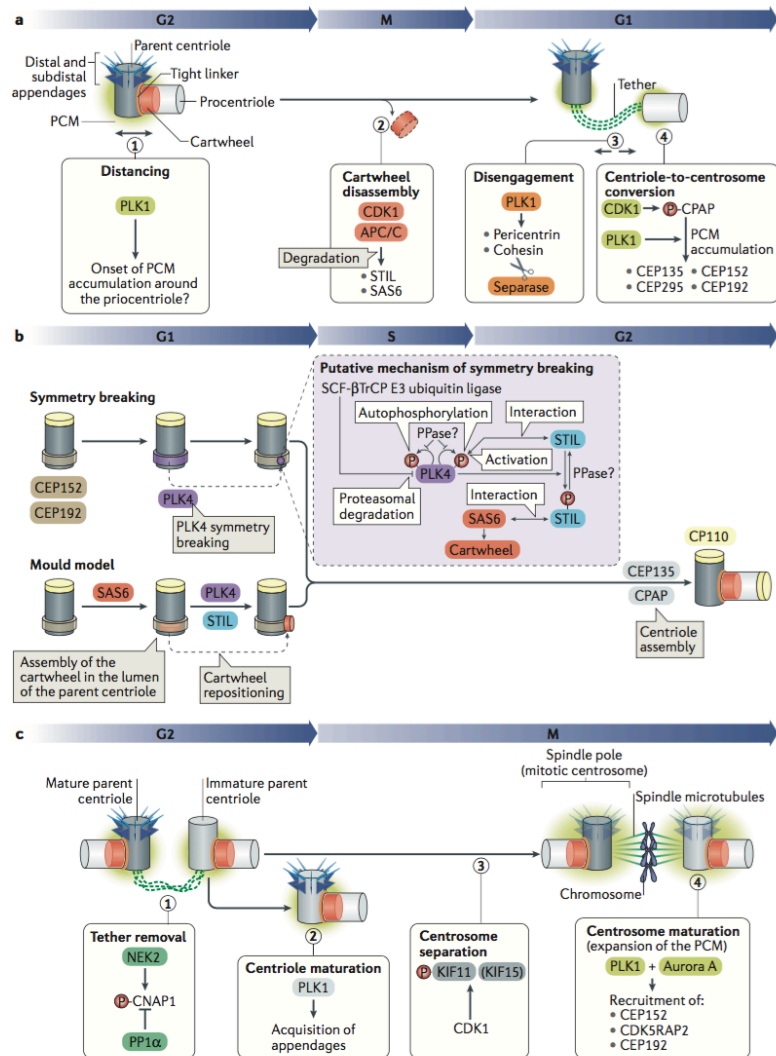


Figure 15: Key aspects of the centrosome duplication cycle (Nigg and Holland, 2018).

Centrosome amplification and cancer

Centrosome aberrations occur frequently and often lead to abnormal mitotic spindle formation, which can result in abnormal chromosome segregation and as a consequence tumorigenesis, microcephaly, dwarfism or ciliopathies (Bettencourt-Dias et al., 2011; Gönczy, 2015; Nigg et al., 2014).

Centrosome anomalies can be divided into structural alterations, originated from alterations in the levels or activity of centrosome proteins, and numerical alterations, due to an increase number of centrioles (Chan, 2011; Nigg and Holland, 2018). Correct centriole number is controlled in three ways: during each round of duplication only two new centrioles are assembled (numerical control); centriole duplication occurs once per cell cycle (temporal control); and the procentriole is formed in a site next to an existing centriole (spatial control).

Distinct mechanisms can lead to centrosome amplification. First, deregulation of the centrosome duplication cycle by overexpression of centriolar proteins or PCM components. Whereas genes encoding centrosome proteins are rarely mutated in human cancers, increased or decreased expression of centrosome proteins is more common (Chan, 2011; Gönczy, 2015; Nigg and Raff, 2009). Second, by perturbation of cell cycle progression, a prolonged G2 arrest by DNA damage (Inanç et al., 2010) results in Plk1 activation, centriole disengagement and premature centriole reduplication (Lončarek et al., 2010). Third, upon loss of existing centrioles and production of new ones by the novo pathway, that happen when all endogenous centrioles are destroyed, but is normally inhibited by the presence of even a single endogenous centriole (Loncarek and Khodjakov, 2009). Finally, as a result of tetraploidization, that results of cytokinesis failure, mitotic slippage, endoreduplication or cell fusion (Anderhub et al., 2012; Godinho and Pellman, 2014; Hatch and Stearns, 2010).

Centrosome amplification can specially contribute to abnormal chromosome segregation. To suppress multipolar spindles, the cell can silence the extra centrosomes, preventing them from forming a spindle pole and leaving only two centrosomes active. Alternatively, cells with supernumerary centrosomes often cluster them in anaphase to form a pseudo-bipolar spindle. However, a prior intermediate multipolar spindle, can result in merotelic microtubule-kinetochore (MT-KT) attachments, an error in which a single kinetochore is attached to microtubules emanating from both spindle poles, leading to lagging chromosomes and subsequently aneuploidy. This provides a direct mechanistic link between extra centrosomes and chromosome instability (CIN), two common characteristics of human solid tumors (Ganem and Pellman, 2012; Ganem et al., 2009). Clustering needs spindle tension, the actin cytoskeleton and the cell adhesion machinery, and is expected to require microtubule-associated proteins (MAPs) and motors that organize the spindle poles. The microtubule motor cytoplasmic dynein is an important factor for this clustering, together with NuMA, a spindle associated MAP and the minus-end-directed kinesin 14 motor protein HSET. Centrosome clustering is essential for the survival of cells with supernumerary centrosomes. Thus, the use of inhibitors that target centrosome clustering opens a new possible selective cancer therapeutic strategy (Kwon et al., 2008; Nigg, 2002; Quinyne et al., 2005).

Another source of mitotic errors comes from the incorrect timing of centrosome separation before cell division. Both accelerating and delaying centrosome separation increase the frequency of chromosome mis-segregation (Silkworth et al., 2012; Zhang et al., 2012). Centrosome amplification also can impair asymmetric cell division, for example in *Drosophila* neuroblasts leading to amplification of the neuroblast stem cell pool and subsequent tissue overgrowth.

The deleterious effects of extra centrosomes are not limited to mitosis, they can also alter the architecture of the interphase microtubule cytoskeleton. The presence of supernumerary centrosomes can affect cilia signaling and increase microtubule nucleation capacity, altering the activity of Rho GTPases which play an important role in the regulation of invasion and migration. Thus, centrosome amplification could also influence tumor biology independently of generating aneuploidy by altering cell shape, polarity or motility (Figure 16) (Godinho and Pellman, 2014; Nigg and Holland, 2018).

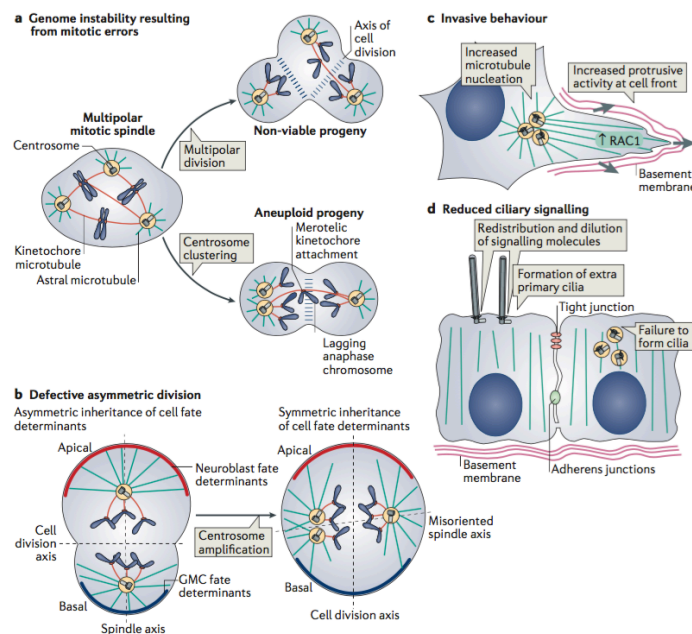


Figure 16: Mechanisms through which centrosome amplification can contribute to tumorigenesis (Nigg and Holland, 2018).

Centrobin

Centrobin (Centrosomal BRCA2 interacting protein) is a 903 residues protein containing a large coiled-coil domain in its center. It was identified in a proteomic analysis of purified human centrosomes (Andersen et al., 2003) and later through a yeast two-hybrid screen with the C terminus of the BRCA2 tumor suppressor, although the interaction with BRCA2 could not be verified (Zou et al., 2005).

Centrobin has ubiquitous expression in almost all cells, is preferentially localized to the daughter centriole of proliferating human cells, (Zou et al., 2005), although in mouse hippocampal cells, it localizes to both mother and daughter centrioles (Shin et al., 2015), and is required for centriole duplication. Centrobin is recruited to the procentrioles at the beginning of S phase. During S, G2, and M phases, there are two centrobin-positive centrioles, the newly assembled procentrioles. In G1, cells have one centrobin-positive centriole, the daughter centriole assembled in the previous cell cycle, that disappear in the next S phase (Zou et al., 2005). Centrobin interacts with tubulin directly, and centrobin–tubulin interaction is essential for the function of centrobin during centriole duplication. Centrobin is recruited to the procentriole via its direct interaction with tubulin, and it is dependent on hSAS-6 allowing the recruitment of other duplication proteins. Interaction with tubulin also facilitate centrobin function in centriole elongation and stabilization. (Gudi et al., 2011). It is also critical in the organization of microtubule network in both interphase and mitotic cells (Jeffery et al., 2010a; Jeong et al., 2007a).

Cep152 interacts with and recruits centrobin to site of centriole biogenesis. At the same time, centrobin interacts with (centrosomal P4.1–associated protein) CPAP, interaction critical for the recruitment of CPAP to

procentrioles to promote the elongation of daughter centrioles and for the persistence of CPAP on them for normal centriole biogenesis and integrity. Although depletion of centrobilin from cells did not have an effect on the centriolar levels of Cep152, it caused the degradation of CPAP from both the preexisting and newly formed centrioles. Loss of centrobilin-CPAP interaction happens at mitosis by an unknown mechanism targeting CPAP for degradation to restrict the centriole length during biogenesis. Conversely, centrobilin excess causes the accumulation of CPAP and defective long centrioles (Gudi et al., 2014, 2015).

Depletion of centrobilin by siRNA resulted in impaired cytokinesis, in centrosomes with one or no centriole and a range of spindle abnormalities due to unfocused spindle poles, detachment of centrosome from the mitotic spindle and less stable MT-KT attachments, resulting in spindle assembly checkpoint (SAC) activation and metaphase arrest. That demonstrates that centrobilin is essential for centriole biogenesis and integrity, acting as a regulator of microtubule dynamics and as a protein necessary for centrosome-spindle adhesion (Jeffery et al., 2010a; Zou et al., 2005). Furthermore, centrobilin is confirmed as an essential centriole duplication factor since a combination of centrobilin depletion by siRNA and HU-induced cell cycle arrest or Plk4 overexpression prevents centrosome amplification (Gudi et al., 2011). Mitotic defects with abnormal spindle formation were also observed in *centrobilin* suppressed early mouse embryos (Sonn et al., 2009). Unlike human cells, *Drosophila* centrobilin is not necessary for centriole duplication, depletion by siRNA or *Centrobilin* hemizyosity does not affect the centriole duplication process in *Drosophila* neuroblasts and *Drosophila* S2 cells (Jeffery et al., 2013)

In addition, in interphase cells centrobilin acts as a modulator of PCM components and microtubule nucleation activity of the centrosome since its

depletion results in an increase of microtubule nucleation and defects in microtubule stability, which trigger microtubules and PCM proteins recruitment around the centrosome (Jeffery et al., 2013).

Although, centrobilin is target to the daughter centriole by its C-terminal end, a fraction of cytoplasmic centrobilin can bind to microtubules transiently by Nek2 phosphorylation, allowing organization of microtubule network in interphase and bipolar spindle in mitosis (Jeffery et al., 2010a; Jeong et al., 2007a). On the other hand, centrobilin can be phosphorylated by Plk1, enhancing centrobilin activity for proper spindle formation during mitosis (Lee et al., 2010a).

Other new studies revealed the opposite effects of Nek2 and Plk1 phosphorylations on microtubule-stabilising activities of centrobilin. Since the Nek2 activity is highest at G2 phase, Nek2 phosphorylation antagonizes the MT-stabilizing activity of centrobilin prior to mitosis, having a function in cell spreading, migration and microtubule stabilization in interphase cells. When the cell enter mitosis, Plk1 phosphorylation promotes centrobilin microtubule stabilizing activity, which is critical for bipolar spindle formation (Park and Rhee, 2013).

Work in *Drosophila* neuroblasts revealed that in interphase, centrobilin (CNB) functions as a positive regulator of microtubule organizing center (MTOC), daughter centriole recruits PCM and forms an aster that is crucial for successful asymmetric cell division and that it is dependent of Plk1 phosphorylation. Its depletion impedes daughter centrioles to assemble an MTOC, whereas mother centrioles carrying ectopic CNB become active MTOCs (Januschke et al., 2013). Conversely, In *Drosophila* type I sensory neurons, CNB functions as a negative regulator of ciliogenesis. Although basal body capability is exclusive of

mother centrioles, CNB depletion allow daughter centrioles to template a defective ectopic axoneme. However, mother centrioles ectopically expressing CNB cannot function as basal bodies (Gottardo et al., 2015).

In *Drosophila* primary spermatocytes mothers and daughters centrioles become basal bodies, with equal signal of CNB, that assemble axoneme-based cilium-like structures, which are the precursors of sperm flagella. In a very recent study, CNB has been shown to be required in primary spermatocytes for centrioles to properly position and stabilize C-tubules, grow in length up to full-sized basal bodies, and template normal axonemes (Reina et al., 2018).

Recently, new roles for centrobilin as a positive regulator of vertebrate ciliogenesis have been identified by using CRISPR-Cas9 to ablate *CNTROB* in hTERT-RPE1 cells. The depletion increase frequency of monocentriolar and acentriolar cells. Besides, centrobilin loss abrogated primary ciliation upon serum starvation and it requires a C-terminal portion of centrobilin that interacts with CP110 and tubulin. Another signal of ciliary dysfunction is shown in centrobilin-depleted zebrafish embryos, that develop microcephaly, defects in laterality control and other morphological features (Ogungbenro et al., 2018).

An study in the Chinese Han population (Wang et al., 2012) revealed some genetic nucleotide polymorphisms of the human centrobilin that can be associated with breast cancer susceptibility. Also, a recent proteomic analysis (Gupta et al., 2015) of centrosome-cilium protein interactions show a interaction of centrobilin with FANCD2, an essential DNA inter-strand crosslink that has been shown to be mutated in some human ciliopathies (Johnson and Collis, 2016).

OBJECTIVES

OBJECTIVES

OBJECTIVES

The main objective of the thesis is to interfere with Nek9 using different approaches to find Nek9 unidentified substrates and functions.

Detailed objectives:

1. Study of the results of eliminating Nek9 expression during mice early embryonic development.
2. Study the phenotype resulting from Nek9 heterozygosis.
3. Study the effects of eliminating Nek9 expression from cells in cell growth, viability and the centrosome cycle.
4. Identify Nek9 substrates by monitoring phosphorylation sites on a proteome-wide scale by SILAC that could explain the observed phenotypes and relate their modification to possible new roles of Nek9.
5. High throughput screening for Nek9 inhibitors.

OBJECTIVES

MATERIALS AND METHODS

MATERIALS AND METHODS

Reagents

All reagents were obtained from Sigma-Aldrich unless otherwise indicated.

Nek9-targeted mice

Mice lacking Nek9 (B6.129-Nek9^{tm1a/H} and B6.129-Nek9^{tm1c};Cg-Tg(UBC-cre/ERT2)1Ejb/J) were generated in the IRB Barcelona mutant mouse core facility. Mouse embryonic stem (ES) cells were targeted with a Nek9 targeting construct that was designed and constructed using standard recombineering methods. The gene trapped allele (*trap*) was assembled by inserting a LACZ/NEO cassette surrounded by Frt sites between exon 1 and 2 plus loxP sequences flanking exon 2 of the murine Nek9 locus. The targeting vector was confirmed by sequencing and linearized vector was transfected into ES cells. Finally, ES cells injections were performed derived from C57B6/j mice. Injected blasts were re-implanted back into the oviduct of pseudo-pregnant foster mice. Chimeras were scored by coat colour analysis, and the chimeras showing the highest contribution from the ES cells were mated with C57B6/j wild-type mice. Agouti offspring obtained from these test-matings were screened for the presence of the mutation.

Mice lacking *p53* were a generous gift from Travis Stracker, who purchased from Jackson Laboratories (B6.129S2-Trp53^{tm1Tyj/J}; stock #002101)

All animals were maintained in strict accordance with the European Community (86/609/EEC) guidelines in the specific-pathogen-free (SPF) animal facilities in the Barcelona Science Park (PCB). Protocols were approved by the Animal Care and Use Committee of the PCB (IACUC; CEEA-PCB) in accordance with applicable legislation (Law 5/1995/GC; Order 214/1997/GC; Law 1201/2005/SG). All efforts were made to minimize animal suffering.

Culture of embryos

Females were superovulated with PMSG (National Hormone and Peptide Program-UCLA) and hCG (Sigma). Fertilized embryos at E1.5 were collected by flushing the uteri of pregnant females with M2 medium (Sigma) and cultured in vitro in potassium simplex optimized medium (KSOM; Chemicon International). Two-cell embryos were cultured in vitro for 2 days.

Mouse Embryonic Fibroblast (MEFs) culture

MEFs were obtained from E12.5 embryos and cultured following standard protocols in Dulbecco's modified Eagle's medium (DMEM) supplemented with 2 mM glutamine, 1% penicillin/streptomycin, and 10% fetal bovine serum (FBS).

The adenovirus expressing Cre recombinase (Ad5 CMV-Cre) was a gift from Gonzalo Fernandez-Miranda and was amplified using HEK 293 cells. Subsequently, MEFs were infected with adenoCre or treated with (Z)-4-Hydroxytamoxifen (H7904, Sigma) in confluence and in low serum conditions. Three days after infection cells were split into plates containing 10% FBS medium and then harvested at different time points for analysis. For rescue experiments MEFs were infected with retrovirus expressing pBabe vector. After infections, cells were selected in puromycin for 2 days.

Histopathologic Analyses

Tissues and organs that presented a macroscopic alteration at the necropsy were collected, fixed in 10% neutral buffered formalin and embedded in paraffin using standard procedures. Sections of 4 μ m sections were obtained and stained with hematoxylin and eosin (H/E). Finally, the histological analysis was performed in a blinded manner by a board-certified

veterinary pathologist. Blood smears were prepared using the wedge technique, followed by air-drying and Acridin Orange staining.

Splenocytes isolation

Spleens were removed from mice and were homogenized into a single-cell suspension using Dulbecco's phosphate buffered saline supplemented with 10% fetal bovine serum, designated wash buffer. Red blood cells were lysed by resuspending spleen cells in ammonium chloride-Tris (ACT) buffer and incubating at RT 5 min. Splenocytes were washed and resuspended in wash buffer. 2×10^6 cells were seed in complete media supplemented with cytokines LPS ($\mu\text{g/ml}$) and IL-4 (5ng/ml).

Metaphase spreads

Metaphase preparations were made using 0.075M KCl hypotonic treatment and 3:1 methanol/acetic acid fixation from MEFs or splenocytes after a 4h treatment with colcemid ($0.1 \mu\text{g/ml}$). Slides were stained with with Giemsa stain (Sigma Giemsa Stain, catalog #GS-500, dilute in water 1:20) for 30 minutes. Chromosomes were counted with an upright epifluorescence Nikon E600 microscope and CellCount software.

Plasmids

Different Nek9 and Nek6 expression plasmids were previously described (Belham et al., 2003; Roig et al., 2002b).

Different cDNAs were amplified by PCR from existing plasmids (Table 1). In some cases, the restricted fragment was introduced in an intermediate pCR 2.1-TOPO vector using the TOPO TA Cloning kit (Invitrogen) according to

the manufacturer's protocol. The cDNAs were digested from the vector and introduced in the desired plasmids.

Vector	Insert	5' Site	3' Site	Primer Forward	Primer Reverse
pEGFP-C3	centrobin	EcoRI	KpnI	aaaagaattcttATGGCAACATCAGCTGACAGCCC	tttgggtaccTCATCTCCAGACTCCCCCGG
pGEX-4T1	centrobin 1-200	EcoRI	Not I	aaaagaattcATGGCAACATCAGCTGACAGCCC	tttttgcggccgctcaACAATGCTTGCGGCGGGTATGC
pGEX-4T1	centrobin 590-903	EcoRI	Not I	aaaagaattcatgCAGGAGCCCGAGAAGGAGGAGAG	tttttgcggccgctCATCTCCAGACTCCCCCGG

Table 1: Sequences of primers to cloning.

Primers were synthesized by Sigma-Aldrich. Constructs were sequenced at MacroGen Inc.

Mini and midi plasmid DNA were prepared using Macherey-Nagel NucleoSpin Plasmid kit or Nucleobond Xtra Midi (Endotoxin-free) kits, respectively. In these procedures, plasmids were isolated according to the manufacturer's instructions. For miniprep, a single bacterial colony was used to inoculate 5 ml of LB broth with appropriate antibiotic and incubated shaking overnight at 37°C. 4 ml of the overnight culture was used for miniprep DNA extraction while 400 ml overnight culture was used for midiprep extractions. The resulting plasmids were resuspended in 50 µl and 160 µl Milli-Q water respectively.

pEGFP-C3 CNTROB	
Mutation	Primer 5'-3'
4A (T35A,S36A,S41A,S45A)	GAAGTGgCCgCCCAGCTCTATGCTgCTTTGCGCCTCgcCCGGCAG
4D (T35D,S36D,S41D,S45D)	GAAGTGgaCgaCCAGCTCTATGCTgaTTTGGCGCTCgaCCGGCAG
2A (S78A,S80A)	CGGCTTCGCCAAGAATTGAGTCGAgcCTTGgCAGTCGGATTGG
2D (S78D,S80D)	CGGCTTCGCCAAGAATTGAGTCGAgcCTTGgatGTCGGATTGG
S837A	CTACCTGAAGAGGCTGGAACACgcCGGGACTGATGGCCGAGGGG
K832M	GCTGAGGATCTCTGCTCTACCTGAtGAGGCTGGAACACAGCGGG
S837D	CTACCTGAAGAGGCTGGAACACgaCGGGACTGATGGCCGAGGGG

pBABE-puro	
Mutation	Primer 5'-3'
HindIII mutant	CTAGGCTTTTGCAAAAAGCTAACCATGACCGAGTACAAGC

Table 2: Sequences of primers for mutagenesis

Genomic DNA extraction and genotyping PCR

Ear punches from mice or MEFs Cells were incubated 1h at 95°C in 250 µl Hot Shot buffer followed by 250 µl Neutralization buffer. Genomic DNA obtained was used for PCR amplification of specific sequences (Table 3).

PCR reactions were all assembled in 20 µl, including 1 µl DNA. Amounts of primers, nucleotide mix (2.5 mM each dNTP), Taq polymerase buffer, Taq polymerase and MgCl₂ (NZY or Biotools) together with PCR conditions varied with primer set. For Nek9 embryos we performed a Nested PCR, with 10 µl DNA for the first round PCR and 1µl of first round PCR product as template for the second PCR using Thermo Scientific Phire Hot Start II DNA Polymerase.

p53	
Primer name	Primer sequence 5'-3'
P53comF	ACAGCGTGGTGGTACCTTAT
P53WTR	TATACTCAGAGCCGGCCT
P53MUTR	CTATCAGGACATAGCGTTGG

Nek9 Trap	
Primer name	Primer sequence 5'-3'
SF1	TCCTGAGATCAGGTCCCATC
KO5	GGCCACCCAAGTACCTTGGG
S2R	CTGACCTCTGAAGGGACGAC

Nek9 Flox	
Primer name	Primer sequence 5'-3'
FKWfw	CAGTTCTCCGCTGTACAGGTTCT
FRT2	GGAACCGAAGTTCCTATTCCGAAG
S4R2	CACCCCGCTGAGAACTGCTTAC

CRE	
Primer name	Primer sequence 5'-3'
Cre A	GACATGTTTCAGGGATCGCCAGGCG
Cre B	GACGGAAATCCATCGCTCGACCAG

Nek9 Δ	
Primer name	Primer sequence 5'-3'
FKWfw	CAGTTCTCCGCTGTACAGGTTCT
S2R	CTGACCTCTGAAGGGACGAC
S4R	ATGAACTGTCATTCCATGAGG

Table 3: Sequences of primers for sequencing

Cell culture

HeLa, U2OS, HEK 293T cells and Embryonic Mice Fibroblast cells were cultured in a 5% CO₂ atmosphere and 37°C in DMEM (Dulbecco's modified Eagle's medium) supplemented with 10% FBS (Fetal Bovine

Serum), L- glutamine (2mM), penicillin and streptomycin (100 IU/ml and 100 ug/ml, respectively).

The tetracycline-inducible U2OS myc-Plk4-WT cell line (U2OS:myc-Plk4-WT), previously described (Kleylein-Sohn et al., 2007) was a gift from Jens Lüders. Stable transformants were established by selection for 2-3 days with 1 mg/ml G418 (Invitrogen) and 50 µg/ml hygromycin (Merck) and then induced with 0,5ug/ul tetracycline.

To induce primary cilia formation in MEFs, cells were plated to be 70-80% confluent the next day, when they are supplemented with 0.1% FBS DMEM for up to 48 h.

Transfection

HEK 293T cells were transfected using different expression plasmids with LipofectamineTM 2000 according to the manufacturer instructions (Invitrogen) or with Polyethyleneimine (PEI) (Polyscience, Inc) (Boussif et al., 1995). HeLa, U2OS cells and RPE1 were transfected with LipofectamineTM 2000 according to the manufacturer instructions (Invitrogen). siRNA transfection was performed using LipofectamineTM RNAiMax according to the manufacturer's instructions.

The sequences of the siRNA duplex for targeting the different proteins were: Nek6, 5'-AAUAGCAGCUGUGAGUCUUGCCU-3' (Ambion) (O'Regan and Fry 2009); Nek7, 5'-AAUAGUGAUCUGAAGGAAGAGGUGG-3' (Invitrogen) and Nek9, 5'AAUAGCAGCUGUGAGUCUUGCCU-3' (Invitrogen).

Drug treatments

Cells were treated for the indicated times with the following inhibitors: nocodazole 250 ng/ml (Sigma); Bi2536 (100nM) (Axon Medchem); RO-

3306 9 μ M (Enzo); CentrinoneB 500nM (Medchemexpress) and Hydroxyurea 2mM (sigma).

Lentiviral infection

shRNA was delivered through lentiviral infection. HEK 293 cells were transfected with PEI using the plasmids for lentiviral assembly REV, RRE and VSVG, together with the corresponding pLKO.1-shRNA plasmids (Sigma MISSION shRNA Library). Empty pLKO.1 vector was used as a control. 24 hours after transfection, HEK cells were incubated at 30°C during 16 hours stimulating virus assembly and continuously medium was collected and filtered. HeLa cells were treated with the resulting media for two consecutive days and then selected with puromycin (1 μ g/ml) during 3 days.

The shRNA clones used for targeting the different proteins were Nek9 TRCN000000929 5'CCGGCCGAGGAATGGAAGGTTTAATCTC GAGATTAAACCTTCCATTCCTCGGTTTTT-3' and TRCN000000930 5'CCGGCCAAAGGAACTCAGACAGCAACTCGAGTTGCTGTCTGA GTTCCTT TGGTTTTT-3'.

Nek9 wt, Nek9 DRCC1 and Nek9 KM were cloned using BglIII and HindIII from Nek9 previously described plasmids (Belham et al., 2003; Roig et al., 2002b) into a pBABE-puro plasmid with a mutated HindIII site in the SV40 promoter (Table 2).

Cell extracts, immunoprecipitation and western blotting analysis

Cells were lysed with lysis buffer that contained 50mM Tris (pH 7.5), 100mM NaCl, 50mM NaF, 1mM DTT, 1mM EDTA, 1mM EGTA, 10 mM β - glycerophosphate, 2mM Na₃VO₄, 25nM calyculin A, 1% TX100, 0.5mM PMSF, 1 μ g/ml leupeptin, 1 μ g/ml aprotinin or with RIPA buffer. Cytosolic

fraction was obtained by centrifugation at 13200 rpm for 10 minutes. Protein concentrations were determined using the Bradford reagent (BioRad).

Immunoprecipitations were carried out with the indicated antibodies pre-bound to protein A/G dynabeads (Invitrogen). 1mg of lysate was incubated for 1h at 4°C and washed three times with lysis buffer. Immunoblotting was carried out after separation of proteins by SDS-PAGE and transfer to PVDF membranes (Immobilon-P Transfer Membrane, Millipore). Meanwhile, 20 µl of prewashed protein A/G beads (Santa Cruz) were incubated with 3-5 µg of primary antibody for 1-2 hours at 4°C with gentle agitation. Beads-antibody complex was washed twice with IP lysis buffer followed by incubation with 3-5 mg total cell extracts for a further 2-4 h. After incubation, beads-antibody-protein complex was spun down at 250 g for 3 min and supernatant discarded while beads-antibody- protein complex was washed 4-6 times in lysis buffer. The complexes were then boiled in 5x protein sample buffer for 10 min and pelleted at 12,000 g before immunoblot analysis of bound proteins.

Membranes were probed with the following antibodies: anti-Nek9, anti- Nek9[Thr210-P], anti-Nek6 and anti-Nek6[Ser206-P] polyclonal antibodies were produced as described (Belham et al., 2003; Roig et al., 2002b, 2005). Anti-GFP (1:1000) (Roche) (Invitrogen), anti-FLAG (1:1000) and anti-βtubulin (1:1000) (Sigma), anti-Nek6 (Abcam), anti-Nek7 (Abcam), anti-Plk4 (Abcam), anti-p53 (Cell Signalling), anti-centrin (Merk Millipore), anti-SAS-6 (Santa Cruz), anti-centrobin (Abcam), anti-active caspase 3 (R&D Systems) and anti-Aurora A (Abcam) were also used. Anti-SAS-6 and anti-CPAP were a gift from Renata Basto. Anti-centrobin was a

gift from Ciaran Morrison. Anti-Arl13b was a gift from Pepe Reina and Cayetano González.

Anti-centrin antibody resulted in some cases in multiple non-specific centrin *foci* in the cytoplasm making it difficult to quantify, so only ones that were clearly centrioles were considered in the quantifications.

Secondary antibodies were from Jackson Immuno Research Laboratories and were detected by ECL Chemiluminiscence (Thermo Scientific).

Protein expression in bacteria

pGEX-4T1Centrobin 1-200 and pGEX-4T1Centrobin 590-903 constructs were expressed in *E. coli* Rosetta™ 2 (DE3) induced with isopropil-β-D-thiogalctopyranoside (IPTG) for 8h at 37°C or 8h at RT respectively. GST fusion proteins were purified with glutathione-sepharose (GE Healthcare) following standard protocols and were eluted with 25 mM reduced glutathione. Purified proteins were resolved in SDS-PAGE acrylamide gels and stained with Coomassie blue (Sigma) to check protein presence, size and purity.

Stable isotope labeling with amino acids in cell culture (SILAC)

Two cells population of MEFs, Nek9^{+/+} and Nek9^{flox/flox} were grown in DMEM that contains the natural ‘light’ amino acid or the nonradioactive labeled ‘heavy’ amino acid form (¹²C₆ and ¹³C₆ L-lysine, respectively) (Thermo Scientific Pierce SILAC Protein Quantitation Kit-DNEM). After 6

passages cells reached 100% label incorporation of ¹³C6 L-lysine-labeled cells and were infected with Adcre to induce Nek9 depletion.

In collaboration with Dr. Judit Villen (University of Washington, Seattle, US), equal concentrations of cell lysate from both cell populations are combined for sample processing and subsequent protein separation by SDS-PAGE. Proteins are digested with trypsin to generate peptides for mass spectrometry (MS) and quantitation of isotopic peptide pairs. Unbiased quantitative comparison of changes in phosphosite composition after elimination of Nek9 has been carried out giving us a global view of phosphosites that depend on the kinase for their phosphorylation.

Kinase assay

Centrobin (1-200 and 590-903 constructs) phosphorylation assays were done by incubation of the purified protein in phosphorylation buffer (50mMMOPS at pH 7.4, 1 mM EGTA, 5 mM MgCl₂, 10 mM β-glycerophosphate), plus 100 mM ATP and [³²P] ATP at 30°C for 30 minutes in presence or absence of eluted recombinant Nek9 plus a 10 minutes incubation at 25°C with an exogenous substrate as H3. Reactions were terminated by addition of 5X Laemli buffer and boiling, and proteins were resolved by SDS-PAGE. Coomassie staining was used to visualize proteins and kinase activity was measured with a PhosphorImager system or with the specific α-Nek9[Thr210-P] antibody as indicated.

Time lapse microscopy

Automated Wide-field scanR microscope equipped with temperature and CO₂ incubation chamber was used to acquire time lapse imaging of MEFs cell using the 20x 0.45 phase contrast objective lens every 7 minutes for 24 hours with the CellIR software (Olympus Life Science Europe).

Software autofocus was used to adjust the z-focus with transmission channel and transmission acquisition was performed on single plane 12bits-images with an ORCA camera (Hamamatsu Photonics). Subsequent analysis was performed with ImageJ.

Spinning disk confocal microscopy with the Andor Revolution system, equipped with EMCCD camera technology was used to acquire time lapse imaging of stable U2OS GFP-centrin using the 100X objective lens every 5 min with a Z stack to encompass centrioles completely. Software autofocus was used to adjust the z-focus with transmission channel. Cy3, GFP (with filter cubes and excitation filters from AHF Analysentechnik) and transmission acquisition was performed on single plane 12bits-images with an ORCA camera (Hamamatsu Photonics). Subsequent analysis was performed with ImageJ.

Cell cycle analysis

0,5ml of PBS and 4,5 ml of ethanol 70% and fixed for 2 hours at -20°C. Subsequent centrifugation of the samples was followed by a wash in PBS and staining with a PBS solution containing 10% Triton X-100 (Sigma), 20 µg/ml propidium iodide (Sigma) and 2 mg/ml RNase A (DNAsa free-Sigma) at 37°C for 15 min. Cells were analysed using a Coulter XL analyser8 (Beckman Coulter).

Immunocytochemistry

Cells were grown on coverslips, rinsed with PBS and fixed with methanol at -20 °C for 15 minutes. After rinsing with PBS, cells were incubated with PBS containing 3% bovine serum albumin, 0.1% Triton-X and 0.02% azide. Primary antibodies used were: anti-γ-tubulin or βtubulin 1:500 (Sigma), anti-pericentrin 1:5000 (Abcam), anti-H3-P 1:200 (Cell

Signaling), anti-GFP 1:500 (Invitrogene), anti-FLAG 1:1000 (Sigma), anti-hSAS-6 1:200 (Santa Cruz), anti-centrin3 1:2000 (Mitchinson and Ohi lab), anti-centrin1 1:500 (Millipore) , anti-centrobin 1:500 (Abcam) anti-Cep164 1:500 (Proteintech), anti-C-Nap1 1:500 (Proteintech), anti-ARL13Rr 1:500 (Proteintech), anti-Cdk5Rap2 1:500 (Universal Biologicals), anti-Cep152 1:500 (GenTex) and anti-Nedd1 1:200 (Abcam). Primary antibodies were detected with Alexa Fluor 488 goat anti-rabbit or anti- mouse IgG and Alexa Fluor 555 goat anti-rabbit or anti-mouse IgG 1:500 (Invitrogen). DNA was stained with DAPI (0,01 mg/ml).

Images were acquired with an Orca AG camera (Hamamatsu) on a Leica DMI6000B microscope equipped with 1.4 NA 63x and 100x oil immersion objectives. AF6000 software (Leica) was used for image acquisition and edited using Fiji (Image J). Confocal images were obtained using a Leica DM2500 spectral confocal microscope.

Quantification of fluorescence intensities at centrosomes was performed with Fiji on non-saturated images acquired with constant exposure. We measured a circular area around centrosome and an adjacent area with the same dimension to subtract the background. All the values were normalized to the median of each control.

CRISPR/Cas9

A gRNA 5'CACCGTACCACGCTGCTGATTGAGC-3' (IDT DNA) to direct cleavage exon 2 of Nek9 was cloned in a pSpCas9(BB)-2A-GFP (PX458) vector (available from Addgene, vector #48138), that co-expresses SpCas9, gRNA, and GFP. The vector contains two BbsI cleavage sites that allow for the insertion of annealed oligonucleotides containing the gRNA target sequence. After transfection, fluorescent U2OS cells were directly sorted into individual wells of a 96-well plate. After 2–4 weeks, when single

cell has grown into large colonies, cells were harvest and processed by WB to check for Nek9 depletion.

High throughput screening for Nek9 inhibitors

In collaboration with PLACEBO, the Platform Austria for Chemical Biology at the Ce-M-M-, the Research Center for Molecular medicine of the Austrian Academy of Sciences and using PLACEBO available equipment we have screen PLACEBO library of chemicals for their capability to interfere with recombinant Nek9 autoactivation and phosphorylation of its substrate Nek7 in the presence of ATP/Mg²⁺. The modification of biotinylated Nek7 was detected using an available antibody that specifically recognizes phosphorylated Nek7 and streptavidin-coated AlphaScreen Donor beads plus AlphaScreen Protein A Acceptor beads (from PerkinElmer). The kinase reaction and Alpha detection has been performed in a Packard Proxi 384-well microplate with control buffer o tested compound with Nek9 solution and Biotin-Nek7 solution containing ATP, incubated for 60 min at RT and when a mix with EDTA/donor and acceptor beads/Antibody mixture for alpha detection was added.

The plate was incubated ON and read in an EnVision Multimode late reader (PerkinElmer) using Wallac EnVision Manager.

Statistical Methods

Asterisks indicate statistically significant difference with the corresponding controls as determined using the two-tailed Mann-Whitney t test unless indicated otherwise (*p<0.05; **p<0.01; ***p<0.001).

Values = mean ± SD.

RESULTS

RESULTS

Elimination of Nek9 expression in mice

Previous work in our group showed that interference with Nek9 in different systems has major effects in cell division and reduces viability, suggesting that Nek9 has key roles during mitotic progression and more specifically spindle organization (Roig et al., 2002a, 2005). Completely abolishing the phosphorylation of specific substrates of Nek9 or of its downstream effectors Nek6/7 (the adaptor Nedd1 and the kinesin Eg5, respectively) impedes (Sdelci et al., 2012) or strongly hinders (Bertran et al., 2011) the completion of mitosis. In addition, and although it is clear that some Nek9 functions are independent of Nek6 and Nek7 (Sdelci et al., 2012), downregulation of either Nek6 or Nek7 has also been shown to interfere with normal mitosis and microtubule dynamics (Cohen et al., 2013; O'Regan and Fry, 2009; Yissachar et al., 2006). In mice, lack of Nek7 has been previously shown to lead to lethality in late embryogenesis or at early postnatal stages and to severe growth retardation (He et al., 2016; Salem et al., 2010). Embryonary fibroblasts derived from *Nek7*^{-/-} embryos show increase tendency for chromosomal lagging and abnormalities in primary cilia number (Salem et al., 2010). In contrast, Nek6-deficient mice have no observable phenotype at early stages of life (our unpublished results), possibly as a result of compensation by Nek7. To better study this as well as the importance of the kinases in organism development and homeostasis, we have generated mouse models with disrupted Nek9, Nek7 and Nek6 expression and started their characterization.

Generation of Nek9 genetically modified mice

In order to complete disrupt Nek9 expression, with the assistance of the Mutant Mouse Facility of the IRB Barcelona, we generated mice containing a "knockout-first" targeted gene trap allele (*tm1a* or *trap*). Nek9 exon 2 was flanked with loxP sequences and a reporter-tagged insertion

allele (frt- *lacZ* -neo-frt cassette) was inserted effectively making it a *Nek9* null mutation. This allele was additionally converted to a "floxed" conditional knockout (tm1c or *flox*) allele through crossing with mice expressing the site-specific recombinase Flpo. This conditional knockout can be converted to a deletion allele (tm1d or Δ) through the action of the recombinase Cre (Figure 17A). To gain further control of this step, conditional knockout *Nek9^{flox/flox}* mice was crossed with animals ubiquitously expressing a tamoxifen-inducible *cre* activity (Cre-ERT2) under the UBC promoter (B6.Cg-Tg(UBC-cre/ERT2)1Ejb/J) resulting in *Nek9^{flox/flox};UBC-cre/ERT2* animals. Mutant Estrogen Receptor (ERT2) ligand-binding domain fusions with Cre recombinase are a key tool for spatio-temporally controlled genetic recombination with the *Cre/lox* system. CreERT2 is efficiently activated in a concentration-dependent manner by the Tamoxifen metabolite *trans*-4-OH-Tamoxifen (*trans*-4-OHT).

Development of pre-implantation embryos lacking *Nek9*

Our results show that animals carrying a single KO-first allele (*Nek9^{+trap}* effectively *Nek9^{+/-}*) are healthy at birth and fertile. We intercrossed *Nek9^{+trap}* mice and analyzed their progeny. No homozygous null animals (*Nek9^{trap/trap}*, effectively *Nek9^{-/-}*) were born and no homozygous viable embryos were observed at mid gestation, suggesting early embryonic lethality. A small number (6%) of nonviable reabsorbed *Nek9^{trap/trap}* embryos were observed at E12.5 suggesting post-implantation lethality (Figure 17).

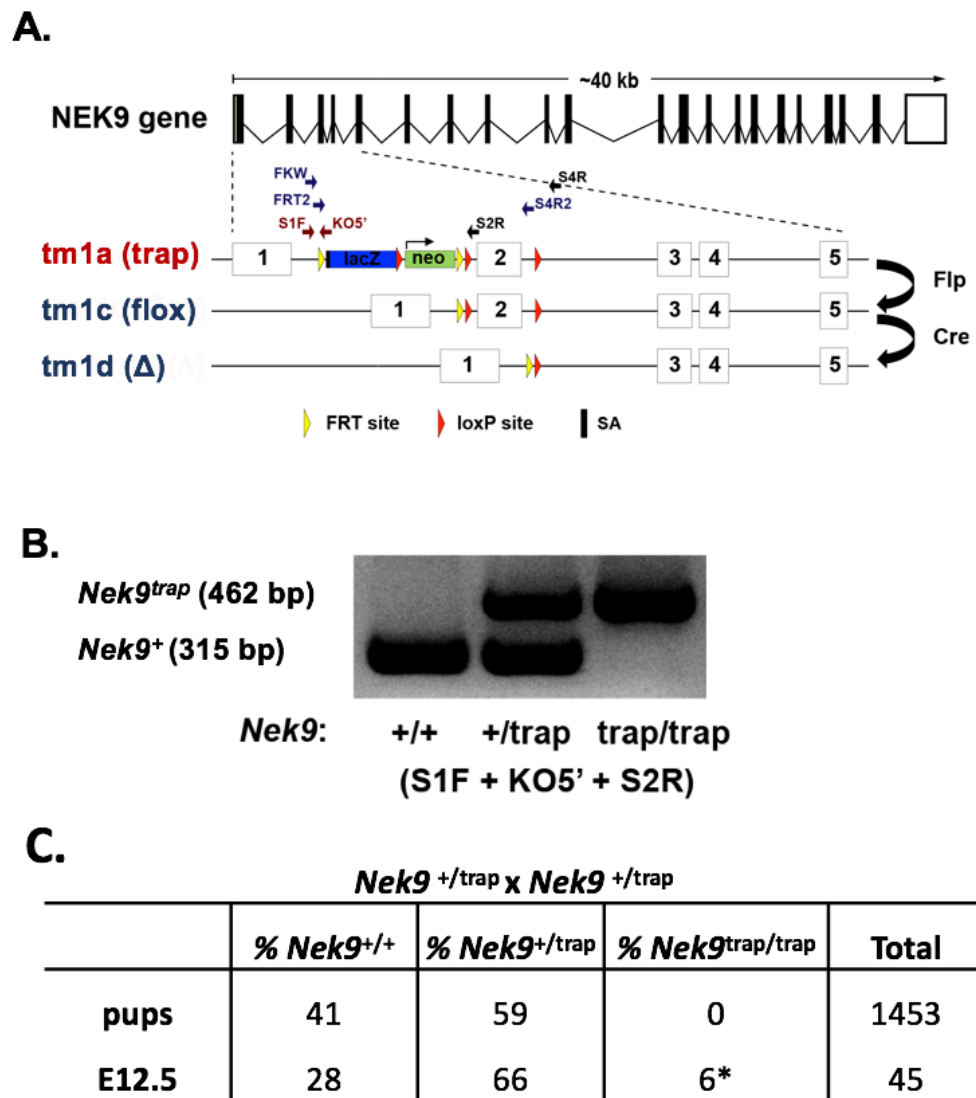


Figure 17: Generation of *Nek9* genetically modified mice. **A)** Schematic of the *Nek9* alleles used in this study. The position of the oligonucleotides used for genotyping is shown as numbered arrows (see Table 3 in material and methods); **B)** Representative PCR of *Nek9*⁺ (WT) and *Nek9*^{trap} mice alleles; **C)** Results from *Nek9*^{+/trap} intercrosses, observed number of genotyped pups or E12.5 embryos. Asterisk indicate non-viable partially reabsorbed embryos.

RESULTS

To determine the cellular and molecular basis of this, in collaboration with Dr. Gonzalo Fernández-Miranda (IRB Barcelona), Ivette Vanrell and Dr. Nuno Costa-Borges (Embryotools S.L.) we extracted embryos from $Nek9^{+/trap}$ intercrosses at E1.5 (when expected to be at the one- or two-cell stages) and cultured them *in vitro* for 3 days (E4.5, until wild type embryos reach blastocyst stage). We initially quantified embryo viability from $Nek9^{+/+}$ x $Nek9^{+/+}$, $Nek9^{+/+}$ x $Nek9^{+/trap}$ and $Nek9^{+/trap}$ x $Nek9^{+/trap}$ intercrosses. As we expected, embryos from control and $Nek9^{+/+}$ x $Nek9^{+/trap}$ intercrosses mostly developed normally reaching either the morula or blastocyst stage. However, $Nek9^{+/trap}$ intercrosses resulted in a considerable part of the embryos becoming inviable at different stages of development, from 2 cells to morula, possibly corresponding to $Nek9^{trap/trap}$ embryos (Figure 18A).

RESULTS

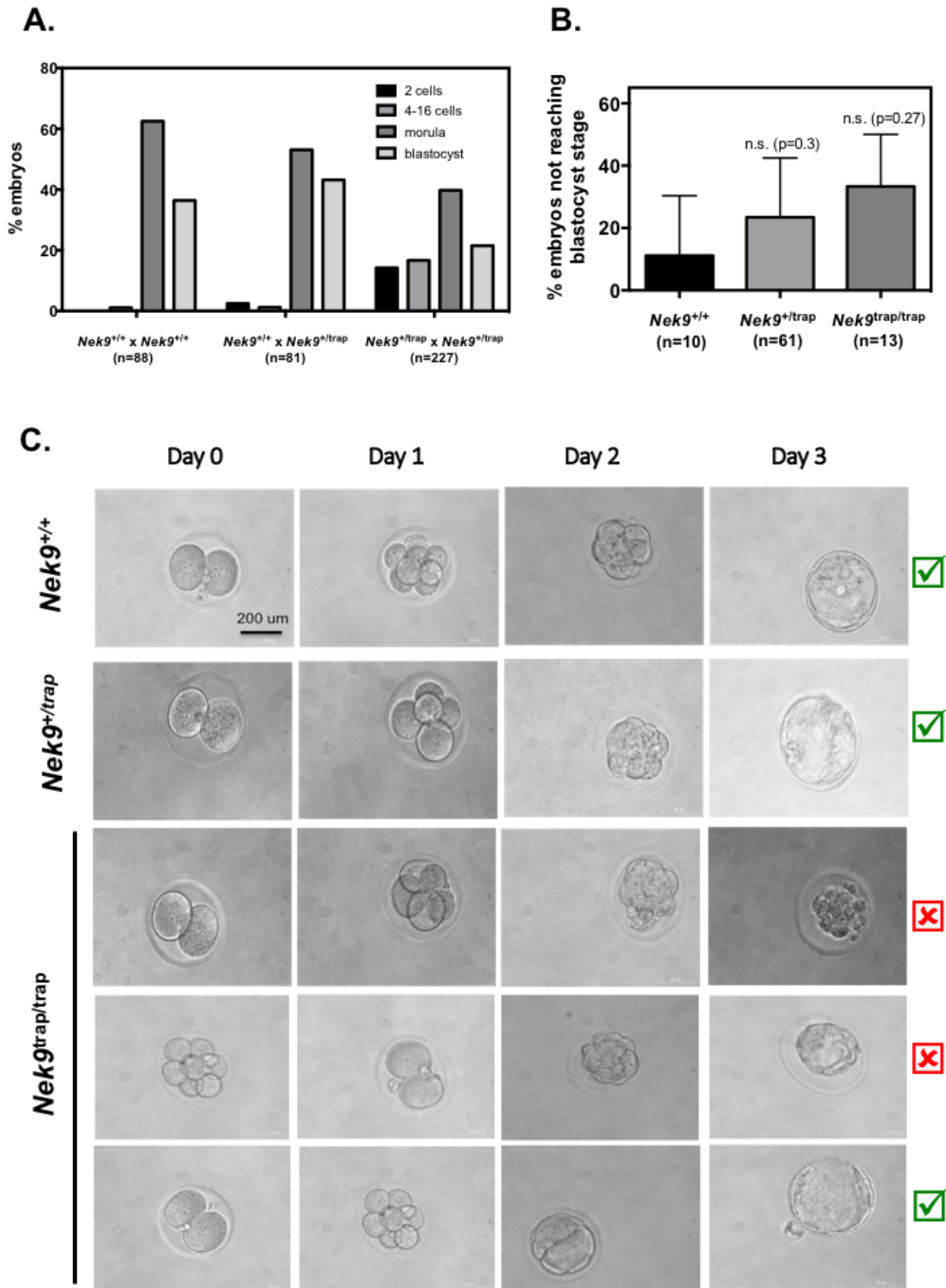


Figure 18: *Nek9^{trap/trap}* embryos have a lower viability than their WT counterparts. **A)** Developmental stage of E4.5 embryos resulting from the indicated three different intercrosses after 3 days in culture (2 cells, 4-16 cells, morula or blastocyst). n=88 embryos from *Nek9^{+/+}* x *Nek9^{+/+}* (6 females), n=81 embryos from *Nek9^{+/+}* x *Nek9^{+/trap}* (6 females) and n= 227 embryos from *Nek9^{+/trap}* x *Nek9^{+/trap}* (10 females); **B)** E1.5 embryos were isolated from *Nek9^{+/trap}* intercrosses, cultured for three additional days and genotyped by PCR. The percentage of E4.5 embryos that did not reach blastocyst stage after 3 days in culture is shown (embryos pooled from 3 independent experiments); **C)** Representative images of embryos from B with the indicated genotypes. ✓ and ✗ indicates if embryos reached the expected blastocyst stage or not.

To confirm this, we decided to perform similar crosses and harvest embryos for genotyping after three days in culture. To genotype embryos, we developed a nested-PCR strategy. After initial problems with reproducibility, possibly caused by allele drop-out (the preferential amplification of one of a pair of heterozygous alleles) and/or the contamination with wild type DNA, we modified our assay conditions (new primers pairs, PCR in sterile conditions), and decided to perform two PCRs on parallel from each sample (50% of sample each, see experimental methods). In this manner we managed to repeat several extractions having reproducible genotyping results. We recorded morphology and viability during culture and related it to genotype. Most of the wild-type embryos formed normal morulas and blastocysts. On the other hand, a considerable fraction of *Nek9^{trap/trap}* embryos didn't reach blastocyst stage (Figure 18B-C). The differences between wild type and *Nek9^{trap/trap}* embryos failed to reach statistical significance, something that we attribute to variability of our PCR results and/or low sample number.

We next performed additional *Nek9^{+/trap}* intercrosses, collected embryos that did reach the blastocyst stage after 3 days of culture and assessed mitotic structures by fluorescence microscopy (IF), staining DNA, tubulin and centrosomes (pericentrin). After that, embryos were recovered and genotyped (we didn't succeed to genotype embryos by IF with available anti-Nek9 antibodies).

In this independent set of experiments, and as expected from our previous results (see Figure 18B), less *Nek9^{trap/trap}* embryos than expected reached blastocyst stage. Additionally, we found less mitotic cells in *Nek9^{trap/trap}* blastocysts, of which 60% showed multipolar spindles with extra centrosomes (vs. 0% in control embryos). Thus, *Nek9^{trap/trap}* embryos that formed blastocysts showed a higher frequency of mitotic abnormalities that may result in death during the first days of development (although the low

RESULTS

numbers of embryos assayed preclude strong conclusions from our results). Interestingly, a small number of mitosis in heterozygous *Nek9*^{+/*trap*} embryos also showed multipolar spindles although these embryos were observed at the expected ratios (Figure 19).

	<i>Nek9</i> ^{+/+}	<i>Nek9</i> ^{+/<i>trap</i>}	<i>Nek9</i> ^{<i>trap</i>/<i>trap</i>}
Embryos reaching blastocyst stage (n=37)	32% (12) expected 25% (9)	54% (20) expected 50% (19)	14% (5) expected 25% (9)
Mitosis with multipolar spindle % (multipolar/total)	0% (0/19)	13,3% (2/15)	60% (3/5)

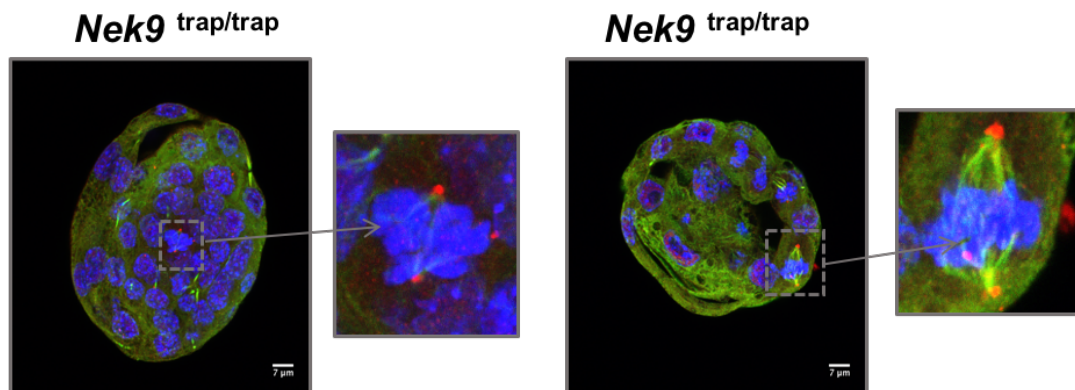


Figure 19: Mitotic abnormalities found in *Nek9*^{+/*trap*} embryos. E1.5 embryos were isolated from *Nek9*^{+/*trap*} intercrosses and cultured for three additional days. Embryos that reached blastocyst stage were recovered, stained and genotyped after imaging. The percentage of each genotype (found vs. expected) among the collected embryos is shown. The number of mitosis present in these embryos and the percentage of mitosis showing multipolar spindles is also shown, together with representative immunofluorescences of *Nek9*^{*trap*/*trap*} embryos. Centrosomes were stained for pericentrin (red), microtubules for alfa-tubulin (green) and DAPI for DNA (blue). n=37 embryos pooled from 2 different experiments. Scale bar 7 μ m.

Characterization of *Nek9*^{+/*trap*} mutant mice

As stated, *Nek9*^{+/*trap*} mice developed normally and were fertile. Furthermore, *Nek9*^{+/*trap*} embryonic fibroblasts (MEFs) proliferated well in culture and did not display obvious defects during cell cycle progression (see below). To check whether the expression in heterozygosity of *Nek9* results in the onset of any pathology affecting the viability of the animals at late

RESULTS

stages of life (specially tumors) we aged a cohort of *Nek9*^{+/+} and *Nek9*^{+/^{trap}} animals. *Nek9*^{+/^{trap}} mice displayed a slightly shorter tumor-free life span than controls (Figure 20A), and at the age of around 12 months presented an increase in macroscopic spontaneous pathologies compatible with neoplastic proliferations in different organs and tissues (Figure 20B). In particular, a histological study carried out with the assistance of the IRB Barcelona Histopathology Facility revealed that, when compared to control animals, *Nek9* mutant mice displayed a slightly increased frequency of colon (0% in controls and 2,2 % in mutants) and hepatic (0% in controls and 8,7% in mutants) tumors, although a lower frequency of pulmonary tumors (8,8 % in controls and 2,2 in mutants) (Figure 20C and Table 4).

	# animals		% animals	
	<i>Nek9</i> (+/+)	<i>Nek9</i> (+/-)	<i>Nek9</i> (+/+)	<i>Nek9</i> (+/-)
Dead/sacrificed before 20 months	5	13	14,7	28,3
Pathology not apparent/not determined*	4	8	11,8	17,4
Solitary kidney/kidney necrosis	0	4	0,0	8,7
Lymphoid hyperplasia	0	2	0,0	4,3
Cancer (all types)	1	1	2,9	2,2
Lymphoma	1	0	2,9	0,0
Non-lymphatic tumors	0	1	0,0	2,2
Hepatic	0	1	0,0	2,2
Pulmonar	0	0	0,0	0,0
Colon	0	0	0,0	0,0
Sacrificed at 20 months	29	33	85,3	71,7
Pathology not apparent/not determined*	0	4	0,0	8,7
Solitary kidney/kidney necrosis	0	0	0,0	0,0
Lymphoid hyperplasia	25	16	73,5	34,8
Cancer (all types)	5	11	14,7	23,9
Lymphoma	2	6	5,9	13,0
Non-lymphatic tumors	3	5	8,8	10,9
Hepatic	0	3	0,0	6,5
Pulmonar	3	1	8,8	2,2
Colon	0	1	0,0	2,2
All animals	34	46	100,0	100,0
Pathology not apparent/not determined*	4	12	11,8	26,1
Solitary kidney/kidney necrosis	0	4	0,0	8,7
Lymphoid hyperplasia	25	18	73,5	39,1
Cancer (all types)	6	12	17,6	26,1
Lymphoma	3	6	8,8	13,0
Non-lymphatic tumors	3	6	8,8	13,0
Hepatic	0	4	0,0	8,7
Pulmonar	3	1	8,8	2,2
Colon	0	1	0,0	2,2

Table 4: Specific pathologies found in *Nek9*^{+/+} and *Nek9*^{+/^{trap}} mice after 20 months aging experiment (* autolytic samples that couldn't be analyzed).

Splenomegaly with splenic lymphoid hyperplasia and pulmonary bronchi alveolar lymphoid tissue (BALT) hyperplasia were frequently presented in both *Nek9*^{+/*trap*} animals and in WT mice. Both findings were generally considered unspecific and frequently observed in aged laboratory rodents, especially in those housed in conventional animal facilities, although, the splenic hyperplasia of the lymphoid tissue might also be compatible with a preneoplastic lesion of lymphoid tissue. Other histological lesions found in this study and considered incidental findings frequently found in aging mice were renal tubular vacuolation, membrane proliferative glomerulonephritis, focal areas of necrosis of the adipose tissue, liver angiectasia, extramedullary hematopoiesis, liver microgranulomas, hepatic lipidosis and acidophilic macrophage pneumonia (Haines et al., 2001). Unfortunately, some of the samples obtained from death animals (frequently *Nek9*^{+/*trap*} animals) presented advanced autolysis that compromised the histologic diagnosis (pathology not apparent/not determined* in table 4)

Lymphoma is the most common contributing cause of morbidity or mortality in old mice (Haines et al., 2001). Our results showed that 20 months *Nek9*^{+/*trap*} animals presented a slightly higher incidence of lymphomas than its control counterparts, an observation that we hypothesize may be related to the described high levels of expression of Nek9 in the lymphatic system of wild type animals (Human Protein Atlas, www.proteinatlas.org). Conversely, we observed that Nek9 expression is significantly reduced in *Nek9* hemizygous mice (Figure 20E).

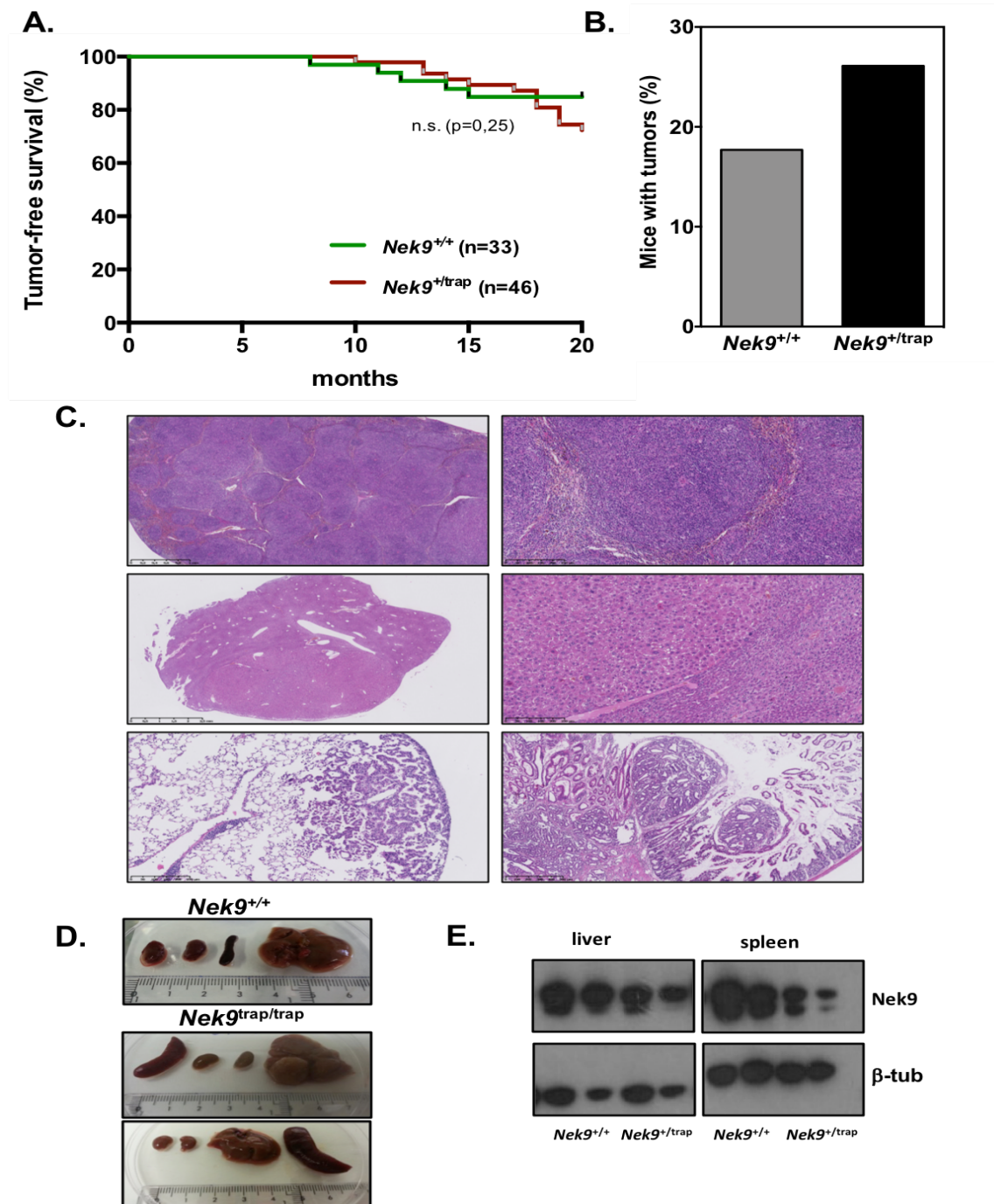


Figure 20: Nek9-deficient mice showed a tendency to develop tumors. **A)** Tumor-free survival curve of *Nek9*^{+/+} and *Nek9*^{+/trap} mice indicating a slight but non-significant reduction in the tumor-free life span of *Nek9* heterozygous mice ($p=0.25$, Log-rank or Mantel-Cox test); **B)** Percentage of tumor-bearing mice at 20-months ($n=33$ *Nek9*^{+/+} animals, $n=46$ *Nek9*^{+/trap} animals); **C)** Representative tumors found in *Nek9*^{+/trap} mice: lymphoma in the spleen (left and right top panels), hepatic (left and right middle panels), pulmonary (left bottom panel) and colon cancer (right bottom panel); **D)** Representative spleen, kidneys and liver of aged animals with the indicated genotypes are shown, note the presence of splenomegaly and a tumor of considerable size in one of the livers in *Nek9*^{+/trap} animals; **E)** Nek9 expression in the indicated tissues was determined by western blots using specific antibodies. β -tubulin is used as a loading control.

RESULTS

Interestingly, a high percentage of *Nek9*^{+/*trap*} animals showed a range of kidney defects (extensive areas of renal necrosis and in some cases presence of a solitary kidney). Although no observable differences in size or overall structure were noted, brains of *Nek9*^{+/*trap*} mice were found to be significantly lighter than these of control mice (Figure 21) together with a significant higher body weight resulting from an accumulation of white adipose tissue subcutaneous, intraabdominal and epididymal, that our data suggests may be normal in structure. We did a glucose tolerance test, a standard procedure that addresses how quickly exogenous glucose can be cleared from blood. Impairment of glucose tolerance indicates problems with maintenance of glucose homeostasis (insulin resistance, carbohydrate metabolism, diabetes, etc) that can result in body weight gain. No defect in glucose tolerance was seen in our animals (Figure 22).

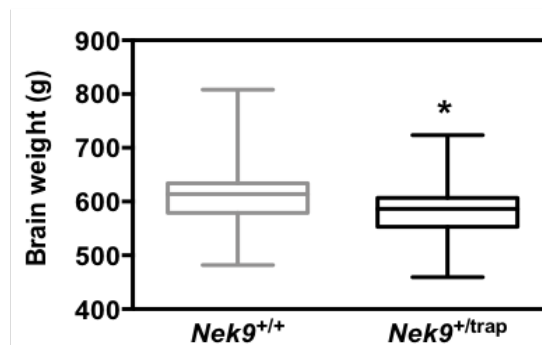


Figure 21: Brains of *Nek9*^{+/*trap*} mice are lighter than these of control mice. Brains were extracted from mice with the indicated genotypes just after sacrifice and weighted after fixation in 10% buffered formalin for 2 days (n=33 *Nek9*^{+/*+*} animals, n=26 *Nek9*^{+/*trap*} animals).

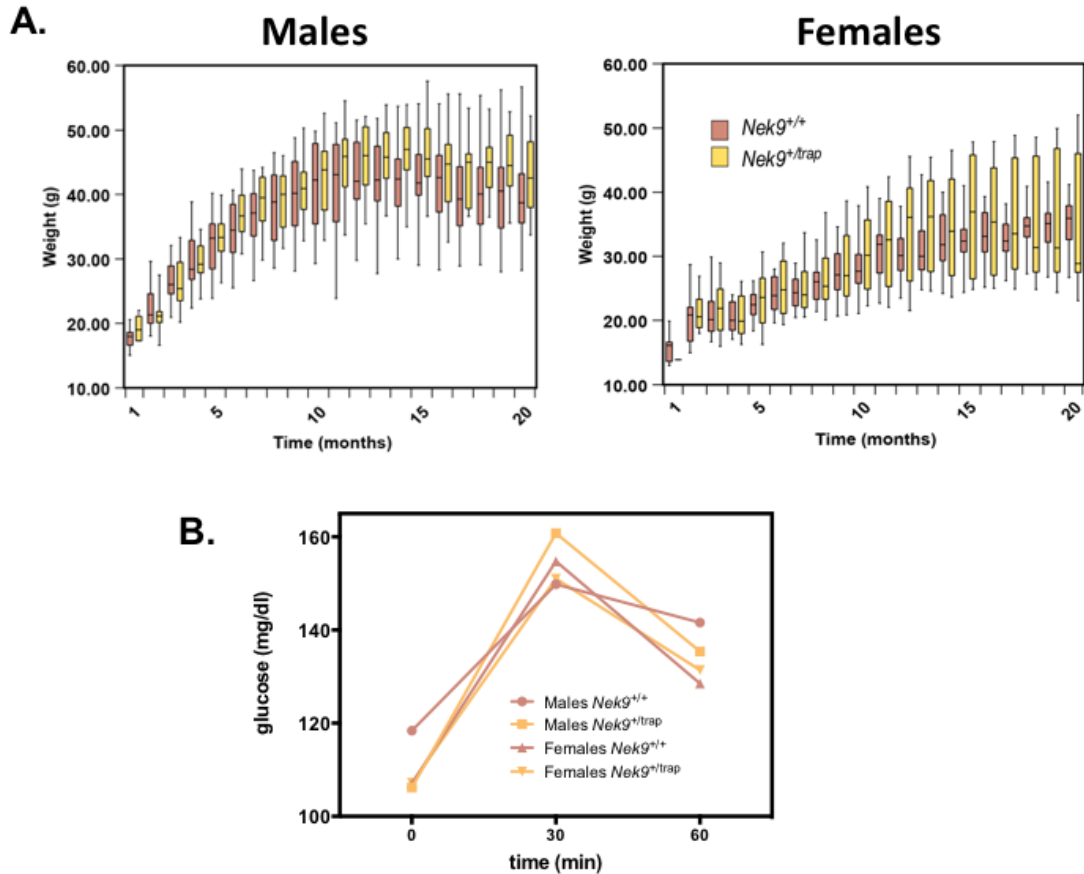


Figure 22: *Nek9^{+/trap}* mice have a considerable higher weight than control animals, and this is more pronounced in females. **A)** Animals were heighted one per month during the 20 months experiment (n=33 *Nek9^{+/+}* animals, 16 males and 17 females, n=46 *Nek9^{+/trap}* animals, 23 males and 23 females); **B)** Glucose tolerance test done in 5 males and 5 females of each genotype. 20% glucose solution, 2g of glucose/kg body mass or (μ l) = 10 x body weight (g) was injected intra-peritoneally. The blood glucose levels were then measured at 0 (time-point of injection), 30 and 60 minutes after injection by placing a small drop of blood on a new test strip and recording the measurements. Glucose levels should be below 140 mg/dl at 2 h. Levels between this and 200 mg/dl indicate “impaired glucose tolerance”, and any level above 200 mg/dl confirms a diagnosis of diabetes.

In view of our results interfering with Nek9 in different systems, and the apparition of different pathologies related to cellular transformation, we next performed an estimation of the incidence of aneuploidy in the aged animals by quantifying micronuclei in circulating erythrocytes, a standard test to indicate the existence of lagging chromosome fragments or whole chromosomes that have not been incorporated into the nucleus after mitosis (MacGregor et al., 1983). To do so, blood smear preparations are made and

RESULTS

stained with the DNA marker acridine orange. When a bone marrow erythroblast develops into a normochromatic erythrocyte (mature), the main nucleus is extruded. Thus, visualization of micronuclei is facilitated in these cells as a result of the lack of the main nucleus. We observed that the number of micronuclei is significantly higher in *Nek9*^{+trap} animals. This was associated to a higher number of immature erythrocytes. Usually, immature erythrocytes indicate excessive erythropoiesis in response to various stimuli such as acute hemorrhage, leukemias, anemia and metastatic cancer to the bone marrow. Our results thus suggest that *Nek9* haploinsufficiency results in chromosome segregation defects and possibly the onset of aneuploidy, and this may be related to the apparition of cancer. We confirmed this by karyotyping splenocytes of animals of different age (from 1 to 6 months), confirming that *Nek9*^{+trap} cells frequently showed gain or loss of chromosomes (Figure 23).

RESULTS

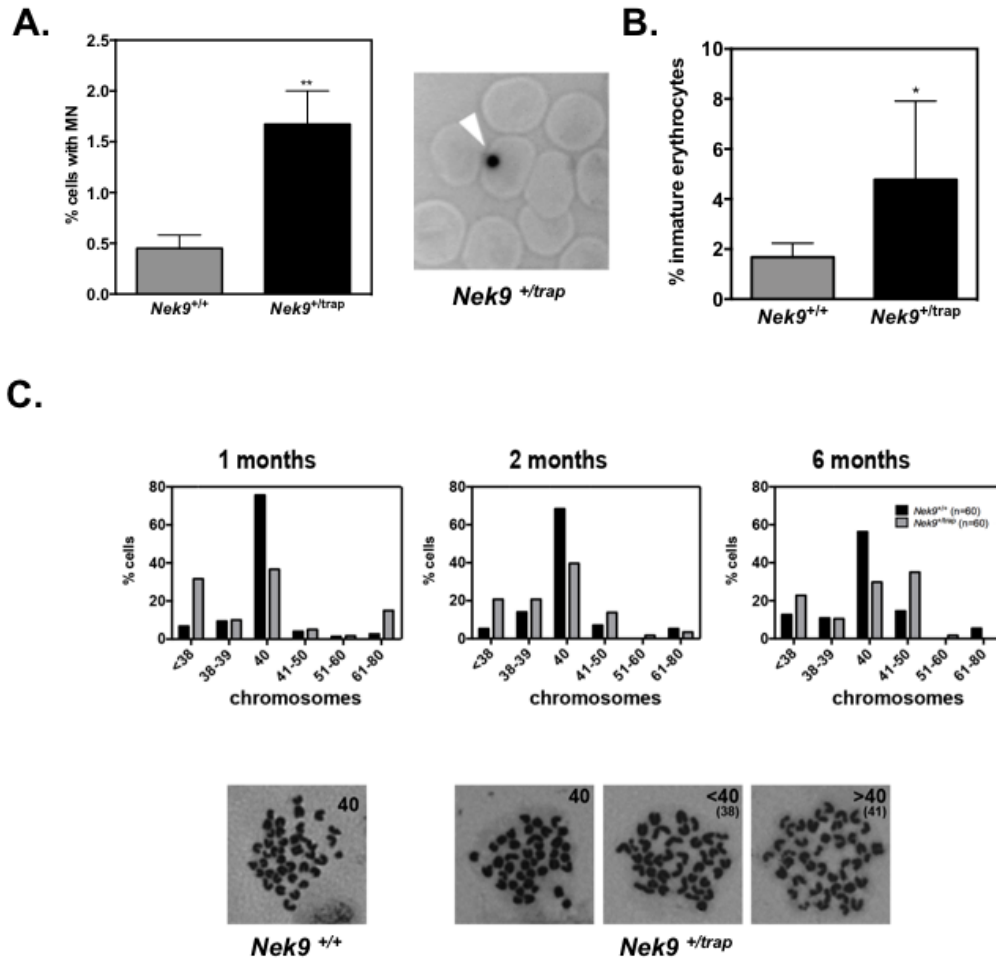


Figure 23: *Nek9* in heterozygosis results in aneuploidy. **A)** Percentage of circulating erythrocytes with micronuclei (6 different animals of each genotype at 20 months, 1000 cells counted per animal) and a representative micronuclei image in *Nek9*^{+/*trap*} erythrocytes stained with acridine orange; **B)** Percentage of immature erythrocytes (6 different animals of each genotype, 1000 cells counted per animal); **C)** Number of chromosomes in splenocytes, quantified in mitotic spreads at different ages (2 animals for each genotype, n=60 cells). Note that the major part of *Nek9*^{+/+} splenocytes had 40 chromosomes while *Nek9*^{+/*trap*} splenocytes showed a wide range of chromosome numbers.

Aneuploidy is a common characteristic of cancer cells. However, a part from driving tumorigenesis, aneuploidy can also inhibit it being crucial the cellular context and depending on the level of genomic damage that is induced (Weaver and Cleveland, 2008). Aneuploidy can activate p53, protecting organisms from developing tumors, and loss of p53 drastically accelerates tumor development (Li et al., 2010) and that is why p53-deficient

mice are chosen to study the effects of p53 loss on tumor progression mediated apoptosis and increased genomic instability (Donehower, 1996). Thus, taking advantage of the availability of *p53*-deficient mice (Jacks et al., 1994) (B6.129S2-Trp53tm1Tyj/J, a gift from Travis Stracker, IRB Barcelona), we decided to cross our animals with this model, to determine if the lack of the tumor suppressor resulted in a higher incidence of tumors. We aged a cohort of combined genotypes mice from *Nek9*^{+/*trap*}; *Trp53*^{+/-} intercrosses until 7 months to see if the absence of p53 increased significantly the apparition of cancer in *Nek9*^{+/*trap*} animals. Indeed, this is what we observed (Figure 24, Table 5). Although the incidence and type of tumor at the end of the experiment (7 months) was similar in *Nek9*^{+/*trap*}; *Trp53*^{-/-} and *Nek9*^{+/+}; *Trp53*^{+/-} animals, *Nek9*^{+/*trap*}; *Trp53*^{-/-} mice had a significantly shorter tumor-free life span than control animals being this paralleled with an increase in spontaneous pathologies at early age (Figure 24B-C), specifically different types of lymphomas and subcutaneous sarcomas. As a whole thymic lymphoma was the most common neoplasia observed in animals (57,1 % in *Nek9*^{+/+}; *Trp53*^{-/-} mice versus 66,7% in *Nek9*^{+/*trap*}; *Trp53*^{-/-} mice). This proliferative neoplastic change consisted of dense proliferation of lymphoid cells with loss of the normal thymus architecture (distinction of the cortex-medulla junction). Neoplastic cells presented lymphoblast appearance with round to oval nucleus and a moderate number of mitotic figures. Also, macrophages that had rests of phagocytized apoptotic lymphoid cells were present (tangible body macrophages, TBM) (Figure 24D). Invasion of the thymic capsule and peripheral tissues and organs (mediastinum, lungs, and pericardium) by the neoplastic cellular population was frequently observed.

.....

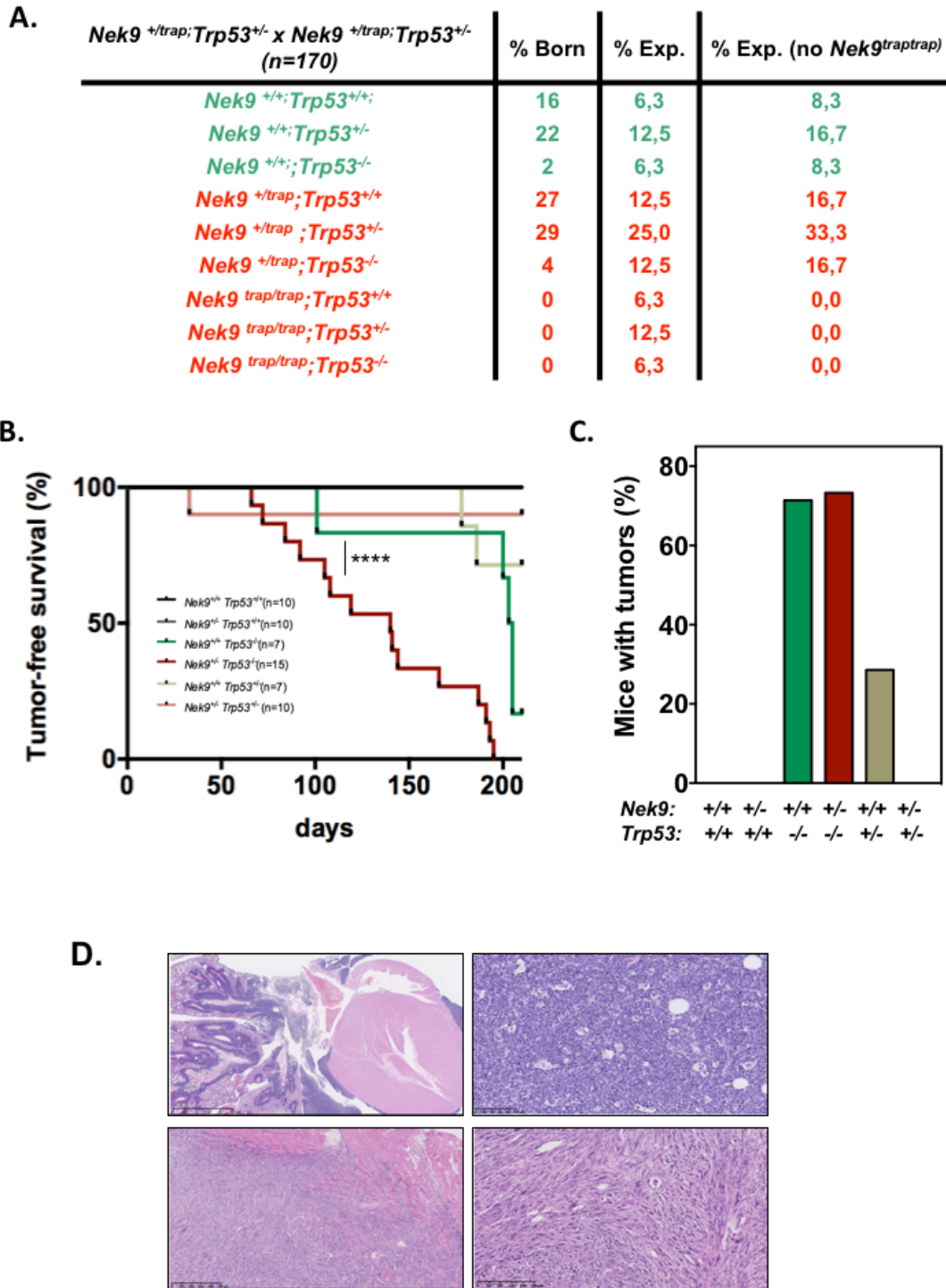


Figure 24: Effect of *Nek9* heterozygosity in p53-deficient mice. **A)** Results from *Nek9*^{+/*trap*};*Trp53*^{+/-} intercrosses. Percentage of born animals, the expected births and the expected births excluding inviable *Nek9*^{*trap**trap*} combinations; **B)** Tumor-free survival curve of all combined genotypes after 7 months, indicating a significant reduction in the life span of *Nek9*^{+/*trap*};*Trp53*^{+/-} as compared to wild type animals (Log-rank or Mantel-Cox test); **C)** Percentage of tumor-bearing mice in the different genotypes at the experiment endpoint; **D)** Representative tumors found: thymic lymphoma with infiltration in pericardium and lung (left above) with numerous tangible body macrophages (right above) and malignant subcutaneous sarcoma infiltrating subcutaneous muscle (bottom).

RESULTS

Our results could be related to the work of others with aneuploidy models and p53 mutant mice, where p53 loss drastically accelerates tumor development (Li et al., 2010), and suggest that the expression in heterozygosity of Nek9 results in aneuploidy and this subsequently in tumorigenesis affecting the viability of the animals, indicating that Nek9 may act as a haploinsufficient tumor suppressor. Interestingly Nek9 heterozygosity seemed to protect *Trp53*^{-/+} animals from tumors while Nek9 WT induce tumor formation in *Trp53*^{-/+} animals (Table 5 and Figure 24C). Further experiments will be needed to assess the significance of this observation.

		# animals					
		p53+/+ Nek9+/+	p53+/+ Nek9+/-	p53-/- Nek9+/+	p53-/- Nek9+/-	p53+/- Nek9+/+	p53+/- Nek9+/-
Total		10	10	7	15	7	10
Pathology not apparent/not determined*		10	10	0	0	5	9
Cancer (all types)		0	0	5	11	2	0
	Lymphoma	0	0	4	10	1	0
	Sarcoma	0	0	1	1	1	0
Other		0	0	1	4	0	1
	Skin lesions	0	0	0	2	0	0
	Unknown cause of death	0	0	0	2	0	1
		% animals					
		p53+/+ Nek9+/+	p53+/+ Nek9+/-	p53-/- Nek9+/+	p53-/- Nek9+/-	p53+/- Nek9+/+	p53+/- Nek9+/-
Total		100,0	100,0	100,00	100,00	100,0	100,0
Pathology not apparent/not determined*		100,0	100,0	0,00	0,00	71,4	90,0
Cancer (all types)		0,0	0,0	71,4	73,3	28,6	0,0
	Lymphoma	0,0	0,0	57,1	66,7	14,3	0,0
	Sarcoma	0,0	0,0	14,3	6,7	14,3	0,0
Other		0,0	0,0	14,3	26,7	0,0	10,0
	Skin lesions	0,0	0,0	0,0	13,3	0,0	0,0
	Unknown cause of death	0,0	0,0	0,0	13,3	0,0	10,0

Table 5: Specific pathologies found in Nek9 and p53-deficient mice after 7 months aging experiment (* autolytic samples that couldn't be analyzed).

Cellular effects of eliminating Nek9 expression in Mouse Embryonic Fibroblasts (MEFs)

In order to intensively characterize the phenotype resulting from totally or partially eliminating Nek9 expression, we aimed to perform more detailed studies using cultured MEF cells with different genotypes. As a first step towards this goal, we did a preliminary study of the phenotype resulting from the elimination of Nek9 expression in 3T3 or SV40 large T antigen-immortalized *Nek9^{flox/flox}* cells transduced with Cre expressing adenoviruses (produced in our group from virus originally from the Iowa University). However, immortalized cells rapidly became aneuploid and acquired aberrant centrosome numbers, and so the study described herein has been done completely in primary MEFs (passages P1 to P3). Using these, we took advantage of the possibility to abrogate the expression of Nek9 in a conditional manner by expressing the Cre recombinase in *Nek9^{flox/flox}* cells, and as an alternative system we eliminated Nek9 expression in *Nek9^{flox/flox};UBC-cre/ERT2* cells by incubation with 4-hydroxytamoxifen (4-OHT) (Figure 25). Identical results were obtained with both strategies, and unless indicated results presented herein correspond to *Nek9^{flox/flox};UBC-cre/ERT2* cells.

We thus derived *Nek9^{flox/flox};UBC-cre/ERT2* cells MEFs from E12.5 embryos and these cells were treated with 4-OHT 1 μ M to genetically abrogate the expression of Nek9 (resulting in *Nek9 ^{Δ/Δ}* MEFs), using already established conditions and monitored both by PCR and Nek9 western blot. Non-treated *Nek9^{flox/flox};UBC-cre/ERT2* cells were used as controls (wt cells treated with 4-OHT behave identically than non-treated).

The abrogation of Nek9 expression was done in non-cycling confluent cells maintained in low sera conditions. After 72 hours, cells were split and release

into the cell cycle by the addition of serum-containing media. Nek9 depletion was observed 24h after the release ($t=0$). Protein levels of Nek6 and Nek7, Nek9 downstream substrates were not affected, while p53 protein level had a slightly increase at 48h in Nek9-depleted cells (Figure 25).

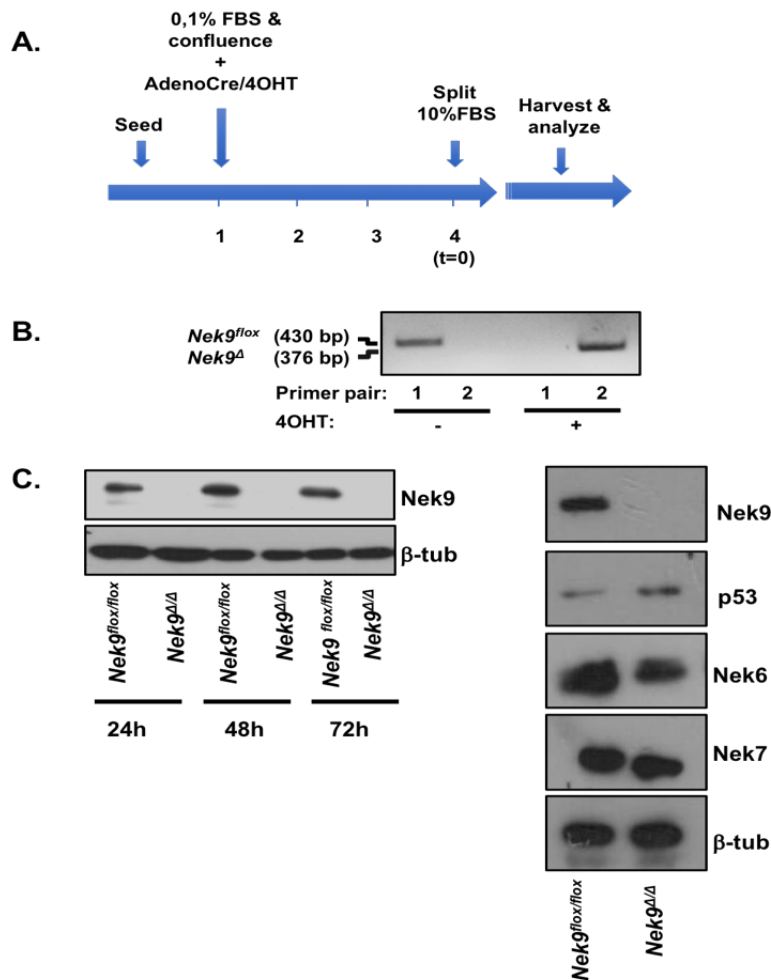


Figure 25: Abrogation of Nek9 expression in primary mice embryonic fibroblasts (MEFs). **A)** Schematic of the protocol followed for acute ablation of Nek9 in G0-arrested cells. *Nek9^{fllox/fllox}* cells were arrested by confluency in low serum and transduced with AdCre vector or treated with 4OHT. 72 hours later, cells were split into new medium supplemented with 10% fetal bovine serum to induce entry into the cell cycle and harvested for further analysis at different point times; **B)** Representative PCR showing the generation of the Nek9 null allele (*Nek9^Δ*) 48 hours after tamoxifen induction of Cre activity. The *Nek9^{fllox}* allele was genotyped using oligonucleotides pair 1 (FKW+S2R), whereas oligonucleotides pair 2 (FKW+S4R) was used to genotype the *Nek9^Δ* allele (see Table 3 in material and methods); **C)** Representative western blots showing Nek9 depletion at 24, 48 and 72 hours (first panel) after tamoxifen induction of Cre activity. β -tubulin is used as a loading control.

Nek9 depletion results in mitotic arrest and aneuploidy

Nek9^{Δ/Δ} cultures showed an impairment in their proliferation capacity when compared with control MEFs, being the doubling time of the cells in culture two-fold longer than control cells. This was associated to a slight tendency to have a higher mitotic index, suggesting cell cycle arrest or longer mitosis. However, no significant accumulation in prometaphase or other specific mitotic phase was observed, probably due to the high variability between experiments (Figure 26A-B). FACS cell cycle profiles of control and *Nek9^{Δ/Δ}* cultures were almost undistinguishable, with only a slight increase of the percentage of cells in G2/M detectable in Nek9-depleted cells at early point times. Importantly (see below) we didn't detect any increase in the percentage of cells with more than 4N DNA content (polyploid cells). No increase in the sub-G1 (less than 2N) population was either detected, suggesting that apoptosis does not occur in this population (Figure 26C).

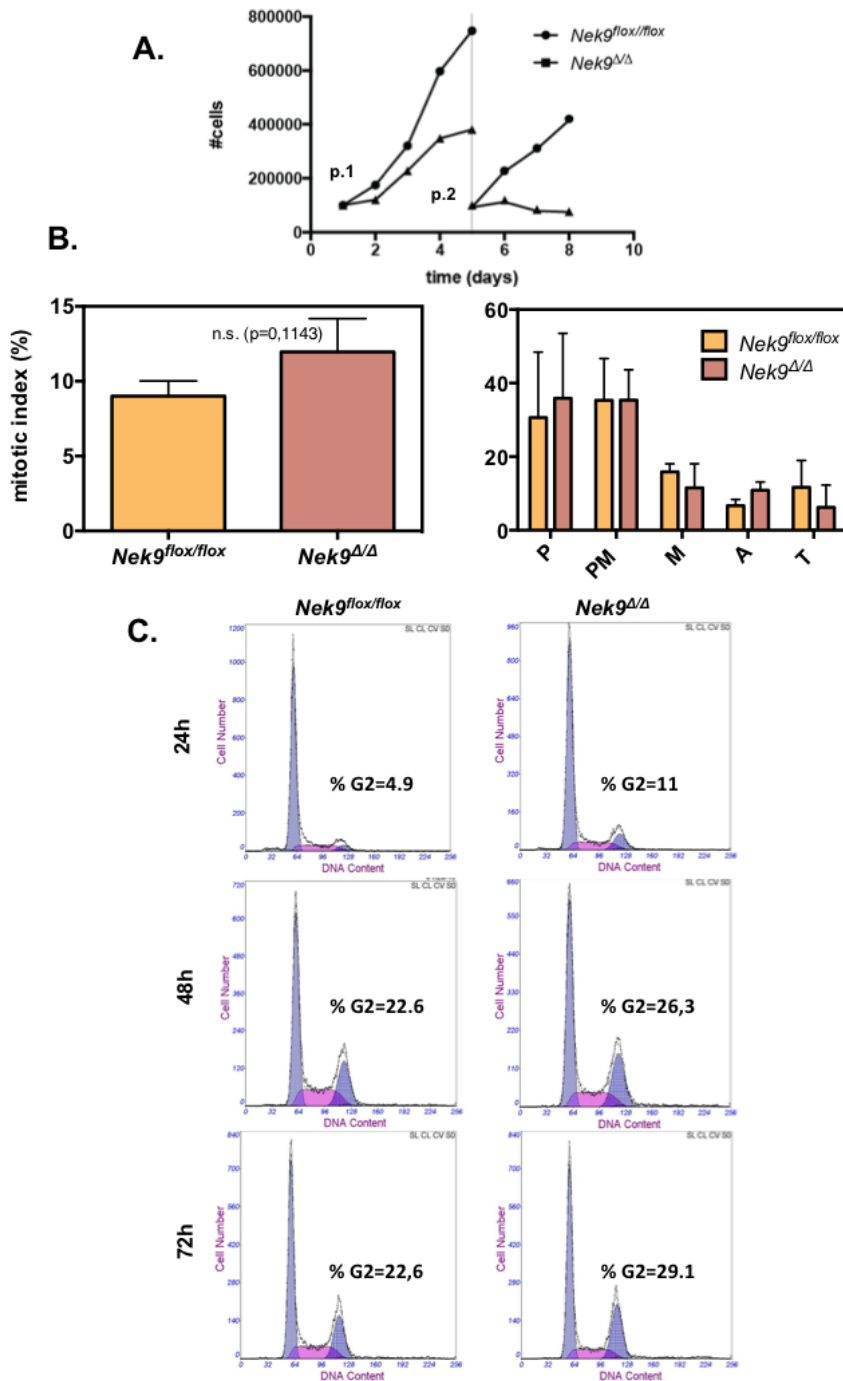


Figure 26: Nek9-depleted cell growth rate is reduced. **A)** Representative growth curve during 2 cell passages of control and Nek9-depleted cells. After 8 days in culture, Nek9-depleted cells stopped growing; **B)** For the indicated genotypes, the mitotic index (unpaired t-test was performed) and percentage of cells in each phase of mitosis were quantified by immunofluorescence with anti- β -tubulin plus DAPI (n=4 independent experiments; 100 cells quantified in each experiment). P=prophase, PM=prometaphase, M=metaphase, A=anaphase, T=telophase (unless indicated, here and henceforth, characterization of the phenotype is done in cells harvested 48h after the release into the cell cycle); **C)** Propidium iodide staining and analysis of DNA content by flow cytometry showed almost indistinguishable cell cycle profiles. Note that an accumulation of polyploid 4N and >4N cells was not detected.

We next studied entry and progression through mitosis by following MEFs in a time-lapse imaging experiment. The percentage of cells entering in mitosis (around 30%) was similar in *Nek9^{flox/flox}* and *Nek9^{Δ/Δ}* MEFs, suggesting that in these cells the kinase is not involved in the machinery controlling the G2 to M transition (Figure 27A). Control *Nek9^{flox/flox}* MEFs were able to carry out mitosis (in this case defined as time between apparent cell rounding and splitting into two daughter cells) in an average time of 41.5 minutes. In contrast, *Nek9^{Δ/Δ}* cells stayed in mitosis for an average time of 47 minutes, although several cells took much longer to complete mitosis. Additionally, 10% of *Nek9^{Δ/Δ}* MEFs cells (1% of *Nek9^{flox/flox}*) aborted mitosis, reverting to a single cell in most cases and 2.5% of the *Nek9^{Δ/Δ}* cells didn't finish mitosis before the experiment ended. Finally, 2.5% of cells both *Nek9^{flox/flox}* and *Nek9^{Δ/Δ}* died in mitosis (although we didn't observe caspase 3 activity by WB (Figure 27). So, with that, we confirmed our previous hypothesis of longer mitosis in Nek9-depleted cells, hence the higher mitotic index.

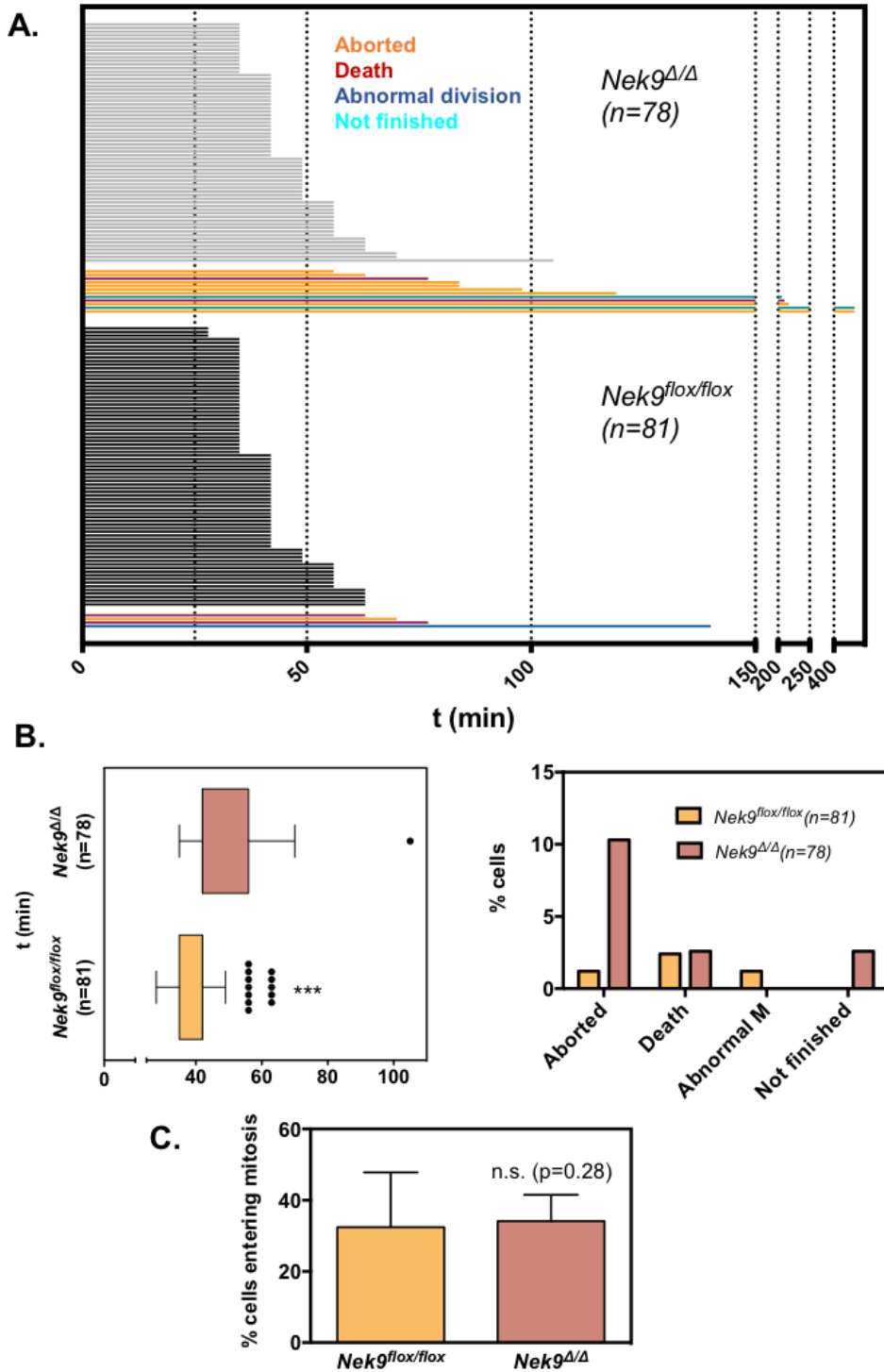


Figure 27: Nek9 depletion resulted in a significant increase of cell doubling time. **A)** Total number of cells entering mitosis in control or Nek9-depleted cells; **B)** Time in mitosis was quantified by live imaging and defined as time between apparent cell rounding and splitting into two daughter cells (n=78 mitosis in *Nek9^{flox/flox}* cells and n=81 mitosis in *Nek9^{Δ/Δ}* cells; aborted mitosis: cells that become round and after some time re-adhered without dividing; death: cells that become apoptotic; abnormal mitosis: division into three cells; not finished: cells that were in mitosis at the end of the recording; **C)** Time in mitosis of all cells that completed mitosis for the indicated genotypes and their classification.

We noticed that Nek9-deficient cultures contained a high percentage of cells with multiple micronuclei (20% cells vs 5% in control cells), a similar phenotype to that previously observed in *Nek9^{+/trap}* erythrocytes. These micronuclei almost always contained centromeres, thus suggesting whole chromosome segregation abnormalities resulting in aneuploidy (Figure 28A). We also found a high percentage of anaphases with lagging chromosomes (around 40% of anaphases in *Nek9^{Δ/Δ}* vs <1% in *Nek9^{flox/flox}*), although we did not find a significant number of binucleated cells, and telophases with DNA bridges (>15% telophases in *Nek9^{Δ/Δ}* vs <5% in *Nek9^{flox/flox}*) (Figure 28B).

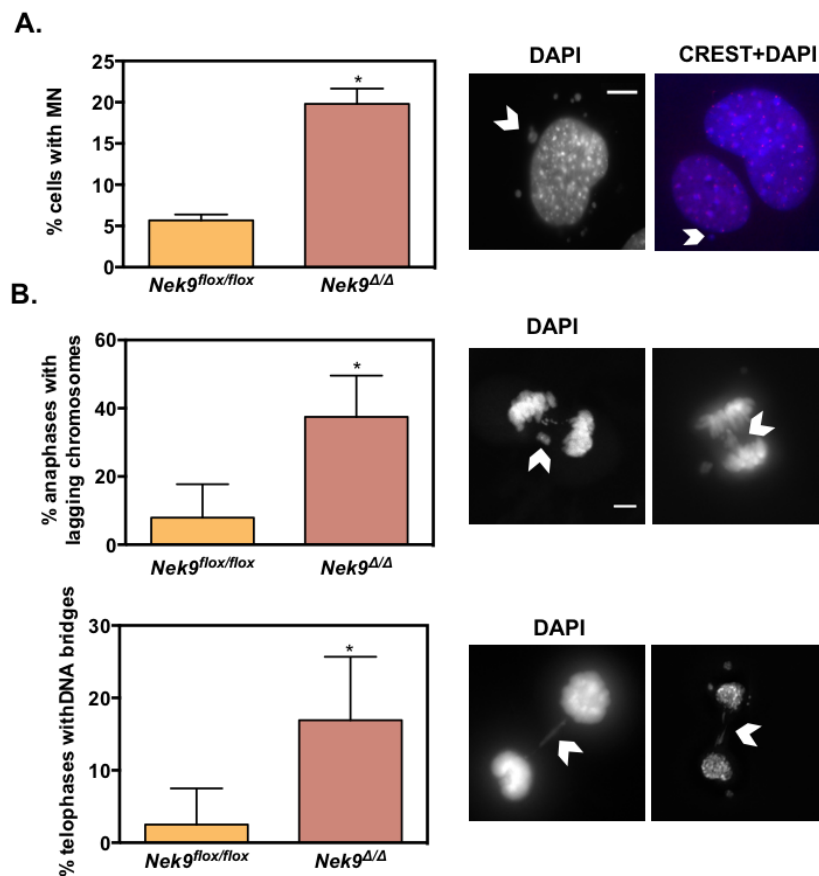


Figure 28: Nek9 depletion result in abnormal chromosome segregation. **A)** Accumulation of abnormal cells with micronuclei, n=4 independent experiments; 100 cells quantified in each experiment; right, staining with a centromere marker, right (CREST antibody in red, DAPI in blue) **B)** Percentage of anaphases with lagging chromosomes (30 *Nek9^{flox/flox}* and 45 *Nek9^{Δ/Δ}* cells from three independent experiments) and telophases with DNA bridges (30 *Nek9^{flox/flox}* and 45 *Nek9^{Δ/Δ}* cells from three independent experiments). Examples are shown (DAPI staining in grey). Scale bar 5 μm.

Our results suggested that the lack of Nek9 could result in aneuploidy, similarly to what we observed in haploinsufficient mice cells. To confirm this, we performed karyotypes. Indeed, *Nek9*^{Δ/Δ} cells frequently showed gain (50% in *Nek9*^{Δ/Δ} vs 20% in *Nek9*^{flx/flx}) or loss (25% in *Nek9*^{Δ/Δ} vs 5% in *Nek9*^{flx/flx}) of chromosomes effectively being aneuploid (Figure 29).

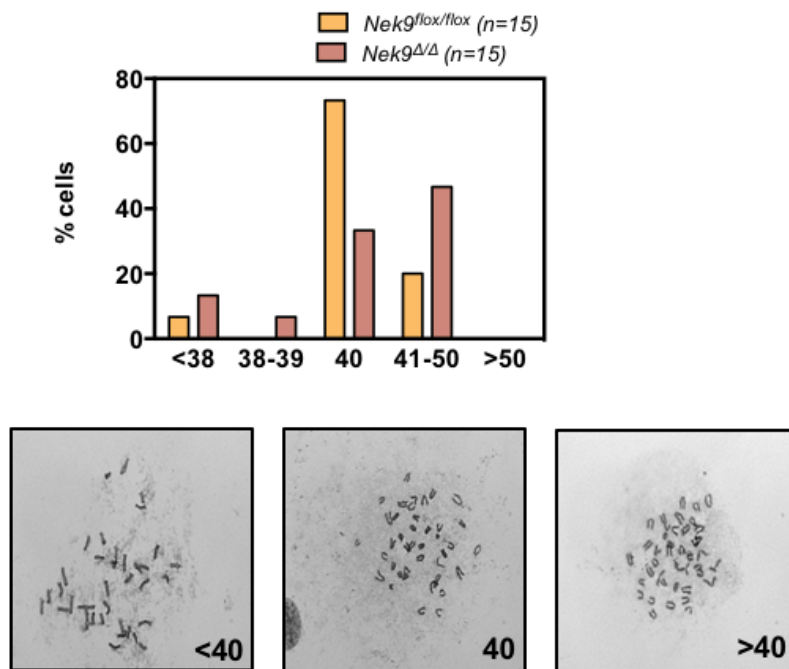


Figure 29: Nek9-depleted MEFs become aneuploidy. Number of chromosomes in MEFs with the indicated genotypes were quantified in mitotic spreads (n=15 cells for each genotype)

Nek9 depletion results in the apparition of multiple centrosomes and aberrant mitotic figures

We next sought to understand the origin of the observed mitotic defects and aneuploidy. Surprisingly, we observed that, upon Nek9 depletion, the number of γ -tubulin (Figure 30) or pericentrin (see below) foci increased significantly, suggesting centrosome amplification (something that was confirmed using additional centrosome markers, see below). As is

RESULTS

shown in Figure 30, we found a significant number of *Nek9*^{Δ/Δ} cells with 3, 4 or more than 4 centrosomes, including cells with up to more than 12 centrosomes (cells with only one nucleus were quantified and centrosomes were detected with γ -tubulin) at 48h post-release, that progressively increased from 24 hours to 72 hours post-release. In fact, 25% of *Nek9*^{Δ/Δ} cells had more than 2 centrosomes in comparison to <10 % of *Nek9*^{flox/flox} cells.

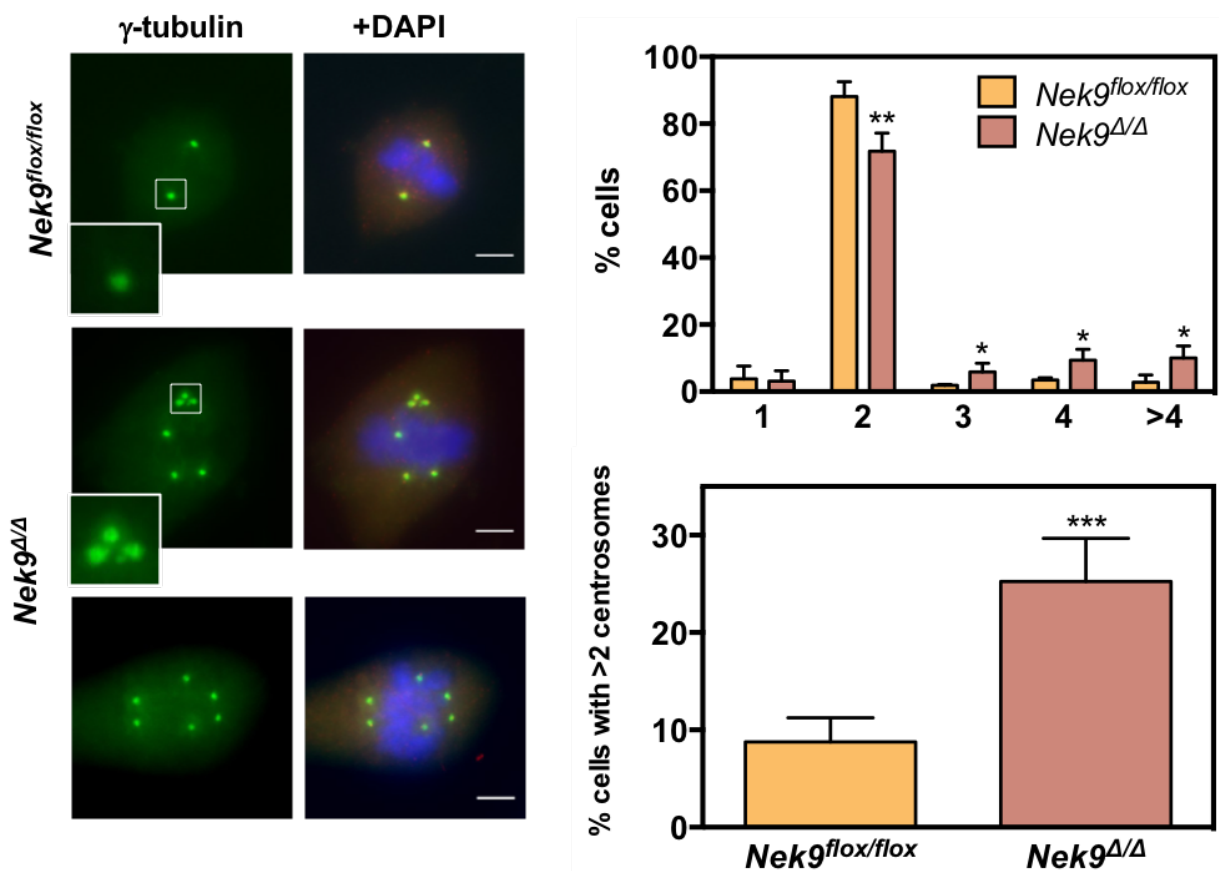


Figure 30: Nek9 depletion leads to centrosome amplification in MEFs. Frequency of *Nek9*^{flox/flox} and *Nek9*^{Δ/Δ} MEFs cells with the indicated number of centrosomes stained with γ -tubulin (plus DAPI). Multinucleated cells, present at low frequency in both control and Nek9-depleted cultures were not considered. Representative immunofluorescence images showing mitotic cells with extra centrosomes are shown. n=4 independent experiments, 100 cells per experiment. Unpaired t-test was performed. Scale bar 5 μ m.

Next, we examined whether enforced expression of Nek9 could rescue the observed centrosome overduplication. To address this, *Nek9^{flox/flox}* cells were first treated with 4-OHT and subsequently infected with pBABE-FLAG lentivirus expressing wild-type Nek9. The number of γ -tubulin foci in *Nek9 ^{Δ/Δ}* MEFs was markedly decreased by Nek9 re-expression (from 17,5% to 7,5% of cells showing more than two foci) but not by infection with the empty vector, strongly suggesting that Nek9 prevents centrosomal amplification (Figure 31).

Finally, as an additional control, *Nek9^{flox/flox}* (Cre-ERT2 negative) cells were treated with 4OHT. This did not result in an increase of the number of γ -tubulin foci in contrast to what we observed with Cre-ERT2 positive *Nek9^{flox/flox}* cells (and neither, as expected, in the downregulation of Nek9 expression). Additionally, as mentioned above and supporting the direct relation of Nek9 with the observed phenotype, *Nek9^{flox/flox}* cells transduced with AdenoCre, that did result in the efficient abrogation of Nek9 expression in a 4OHT independent manner, showed division defects, aneuploidy and amplification of the foci of different centrosome markers (data not shown).

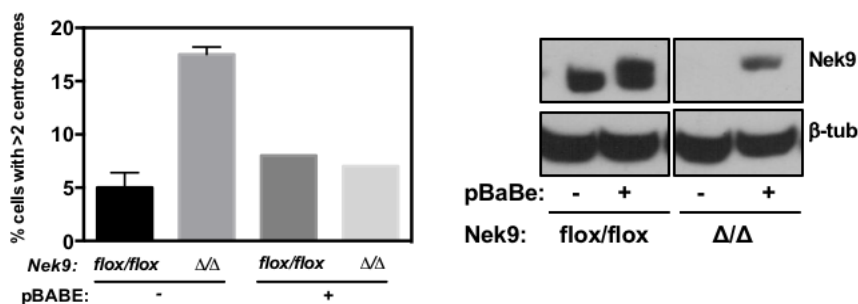


Figure 31: The number of centrosomes in *Nek9 ^{Δ/Δ}* MEFs was markedly decreased by re-expression of Nek9. *Nek9^{flox/flox}* and *Nek9 ^{Δ/Δ}* MEFs were infected with pBaBe retrovirus expressing Nek9 or the empty vector and selected by puromycin resistance. After confirming Nek9 depletion by WB (β -tubulin is used as a loading control), cells with more than two centrosomes were quantified by IF using γ -tubulin as a centrosome marker. n=2 independent experiments, 100 cells per experiment.

When the cell undergoes mitosis, the duplicated centrosomes separate in order to organize the poles of a bipolar mitotic spindle, resulting in accurate chromosome separation and the maintenance of genomic stability. Centrosome abnormalities such as the amplification of centrosome numbers, frequently lead to abnormal spindle formation, although cells have mechanisms to minimize this, such as the clustering or inactivation of extra centrosomes (Wang et al., 2014). Thus, we analyzed the appearance of the mitotic spindles in mitotic Nek9-depleted cells. We observed an increase in prophase cells with more than 2 centrosomes (30% in *Nek9^{Δ/Δ}* vs <5% in *Nek9^{flox/flox}*), and prometaphase/metaphase cells with multipolar mitotic spindles (40% in *Nek9^{Δ/Δ}* vs 5% in *Nek9^{flox/flox}*), spindles with clustered centrosomes (40% in *Nek9^{Δ/Δ}* vs 10% in *Nek9^{flox/flox}*) and what seem to be inactivated centrosomes (Figure 32). Thus, our results suggest that extra centrosomes observed in Nek9-deficient cells result in abnormal mitotic configurations. This may result in aneuploidy in part through the production of merotelic attachments, as these incorrect chromosome attachments are not detected by the SAC and, if these are uncorrected by anaphase onset, the probability of chromosome mis-segregation increases, resulting in whole chromosome aneuploidy. Furthermore, chromosomes with unresolved merotelic attachments usually get trapped in the cleavage between dividing cells, leading to chromosome breakage and consequently aneuploidy (Orr et al., 2015). In fact, as previously shown, we found anaphases or telophases with lagging chromosomes and DNA bridges (Figure 28), frequently associated to an abnormal number of centrosomes (Figure 32C).

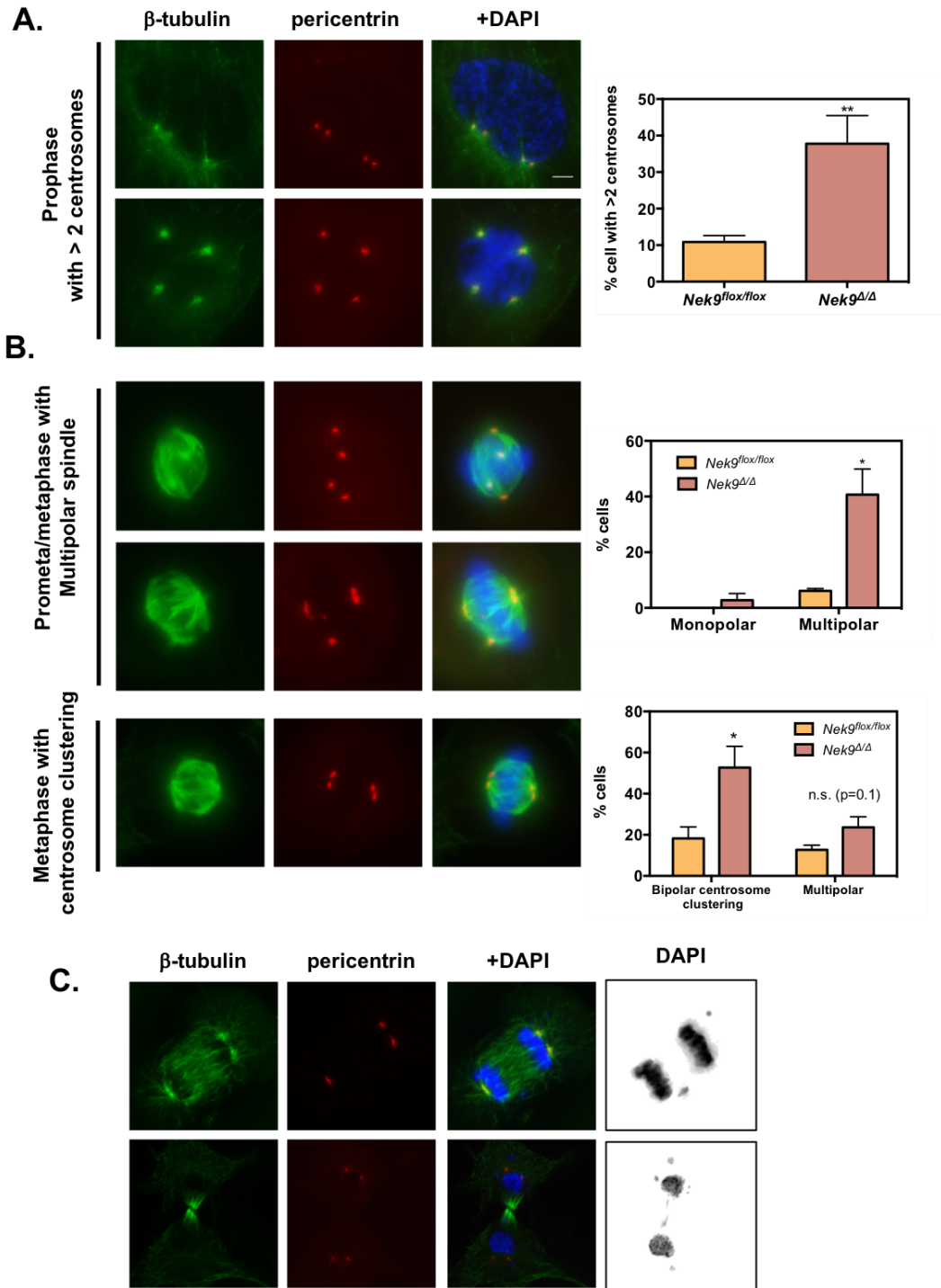


Figure 32: Representative immunofluorescence images of mitotic spindle abnormal conformations observed in *Nek9^{Δ/Δ}* MEFs, stained by anti- β -tubulin (mitotic spindle), pericentrin (centrosomes) and DAPI (DNA). **A)** Frequency of prophase cells with more than 2 centrosomes; **B)** Quantification of the incidence of multipolar spindles in prometaphase or metaphase cells (n=3 independent experiments, 50 cells per experiment) **and** quantification of the incidence of pseudo-bipolar with centrosome clustering and multipolar spindles in metaphase cells with more than two centrosomes (n=3 independent experiments, 50 cells per experiment); **C)** Representative IF of an anaphase with lagging chromosomes and telophase with DNA bridge, both with centrosome clustering. Scale bar 5 μ m.

Amplified centrosomes in Nek9-deficient cells have a close to normal structure, as demonstrated by the containing of different PCM makers such as pericentrin, CDK5RAP2, Cep192, NEDD1 and γ -tubulin in prophase centrosomes (Figure 33). Interestingly, although only significant in the case of Cep192 and NEDD1, there was a tendency towards a decrease in intensity of PCM proteins in prophase centrosomes in Nek9-depleted cells. This could be related to the previously described role of Nek9 during centrosome maturation (Sdelci et al., 2012) and may contribute to the observed mitotic abnormalities. Another explanation could be that as with an increased number of centrosomes, the PCM is redistributed among them.

Thus, PCM staining suggest that what we observed were indeed centrosomes. To finally establish this (and rule out other possible explanations such as centrosome fragmentation), we stained cells with centrin, a centriole marker. Figure 34A shows that indeed, extra PCM foci observed in Nek9-depleted cells contained centrioles, at least two per foci, although in some cases more than two were observed (see below). Our results thus established that Nek9 depletion results in the amplification of centrosome numbers.

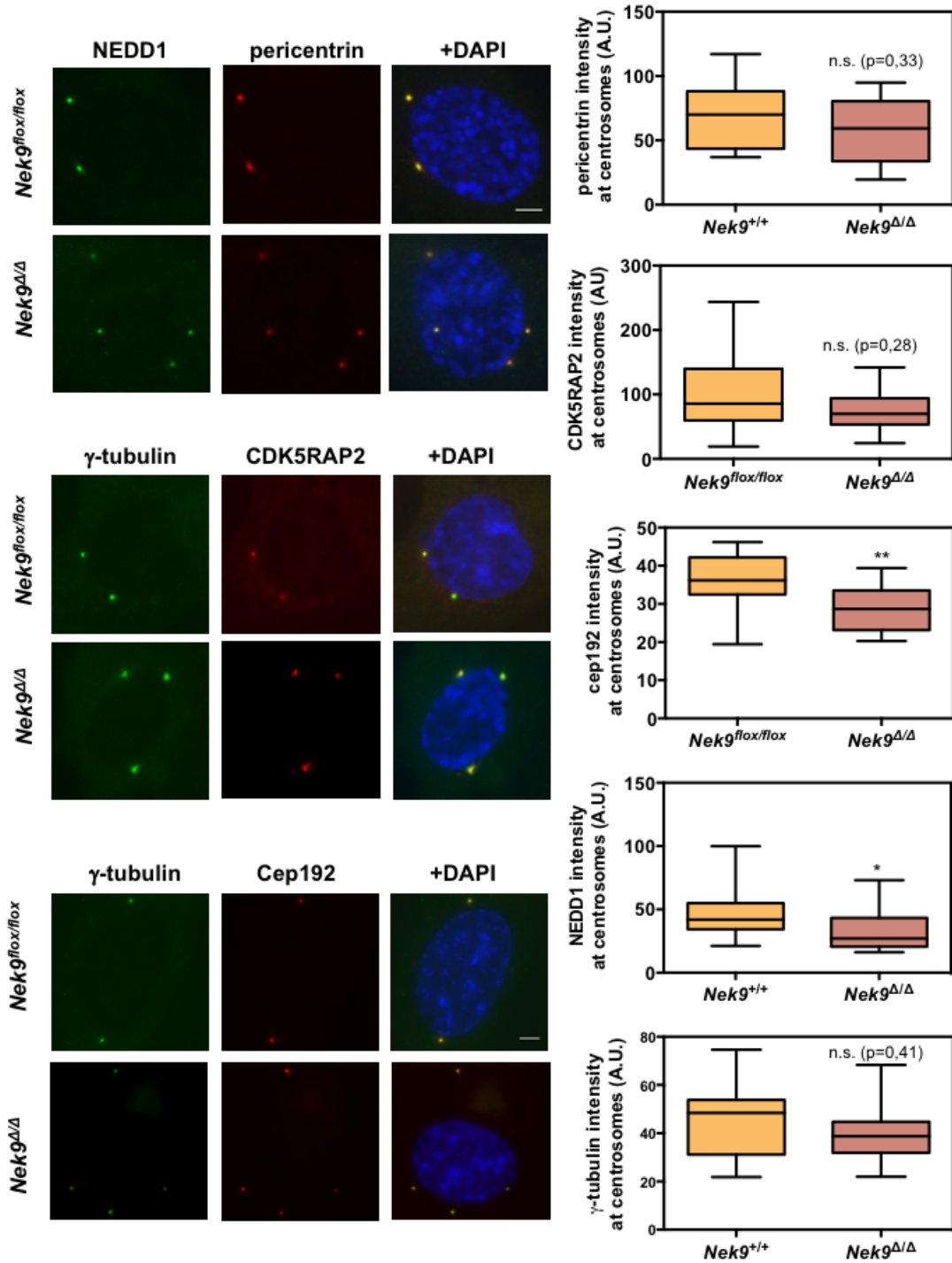


Figure 33: Centrosomes in *Nek9^{Δ/Δ}* cells recruited different PCM components. Quantification of pericentrin, CDK5RAP2, Cep192, NEDD1 and γ -tubulin intensity at mitotic centrosomes. Example cells with the corresponding antibodies plus DAPI are shown in each case. n=45 prophase cells from 3 different experiments. Prophases were identified using DAPI staining, by assessing chromosome condensation and the presence of apparently intact nuclei. Scale bar 5 μ m.

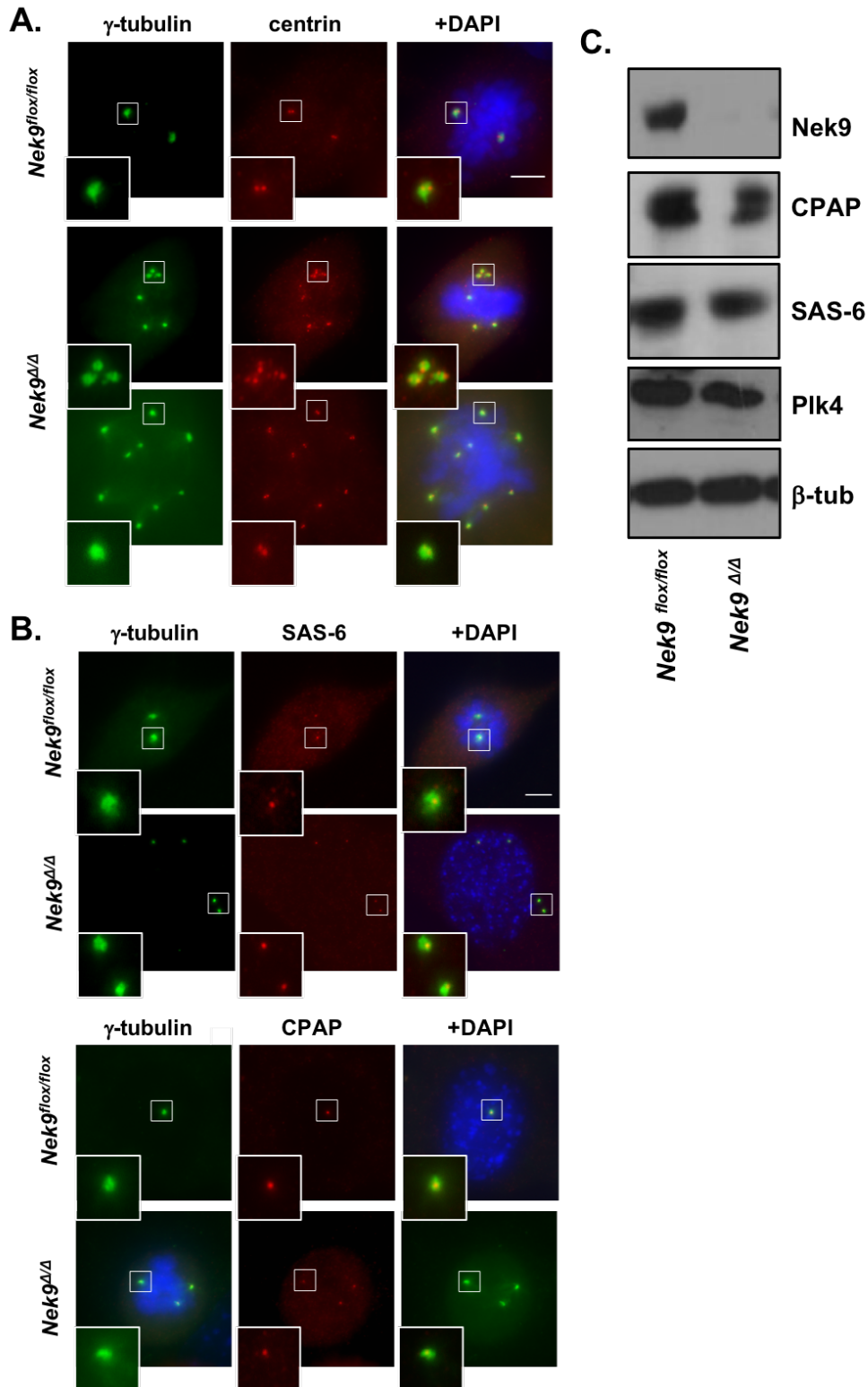


Figure 34: Centrosomes in *Nek9 $\Delta\Delta$* MEFs contain centrioles. **A)** Representative immunofluorescence images showing extra centrosomes in *Nek9 $\Delta\Delta$* cells, stained for centrin. Scale bar 5 μ m; **B)** Representative immunofluorescence images showing extra centrosomes in *Nek9 $\Delta\Delta$* cells, stained for detection of the centriolar components SAS-6 and CPAP. Scale bar 5 μ m; **C)** Western blot showing that Nek9 depletion did not affect protein levels of the duplication factors SAS-6, CPAP and Plk4. β -tubulin is used as a loading control.

Nek9-depleted cells contain an excess of Centrobilin-positive centrioles

Our data suggest that centrosome number did not increase as a result of failed mitosis, as we did not see a correlation with multinucleation or polyploid. It thus may be possible that abrogation of Nek9 expression results in a deregulation of the centriole/centrosome duplication cycle. We thus studied different centriolar proteins with the aim to understand whether centriole duplication was normal in Nek9-depleted cells.

We first stained centrosomes for the daughter centriole markers SAS-6 and CPAP (human SAS-4) (Figure 34B), observing that each centrosome contained only one SAS-6 or CPAP positive centriole as expected. Although not obvious changes in the amounts of these proteins were observed by immunofluorescence, to address if it was a result of abnormal expression of known centriole duplication factors such, SAS-6 or CPAP but also Plk4 (in our hands not observable in MEF cells by IF) in Nek9-deficient cells, we quantified the levels of these proteins by western blot. No obvious changes in the levels of any of the proteins were observed. (Figure 34C).

As we advanced above, *Nek9*^{Δ/Δ} MEFs centrosomes contained extra centrioles with different configurations including paired centrioles, single centrioles and clusters of three or more centrioles (Figure 35). In *Nek9*^{Δ/Δ} mitotic cells we found around 50% of cells with more than 4 centrioles per cell (~10% in *Nek9*^{flox/flox}). We also quantified the percentage of centrosomes with more than 2 centrioles in interphase cells, that was >15% in *Nek9*^{Δ/Δ} and around 2.5 % in *Nek9*^{flox/flox} cells. In our hands, the anti-centrin antibody resulted in some cases in multiple non-specific centrin *foci* in the cytoplasm making it difficult to quantify the results, so only *foci* that were clearly centrioles (i.e. surrounded by PCM) were considered in the quantifications.

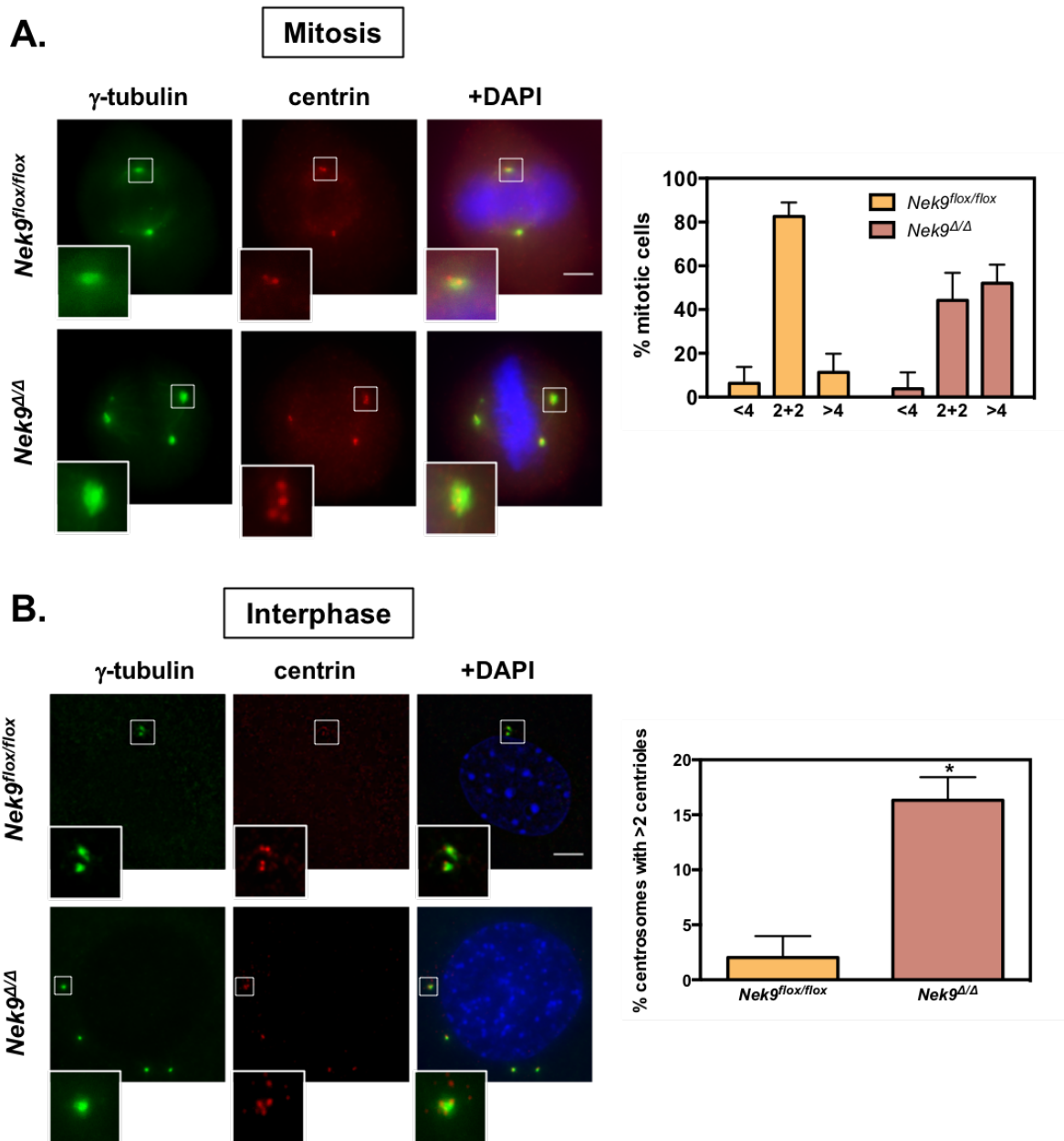


Figure 35: Nek9 depletion leads to multiple centrosomes with several different centriole configurations. **A)** Representative immunofluorescence images of mitotic MEFs immunostained with the indicated antibodies are shown. Centrioles (i.e. centrin foci associated to γ -tubulin) per cell in mitosis are quantified as follows: <4, 2+2 (2 centrioles per mitotic pole) or >4. n=4 independent experiments, 50 cells per experiment; **B)** Representative immunofluorescence images of interphase MEFs immunostained with the indicated antibodies are shown. Percentage of centrosomes with more than 2 centrioles. n=4 experiments, 50 cells per experiment. Scale bar 5 μ m.

While characterizing the *Nek9^{flox/flox}* cells, we realized that a significant percentage of centrioles present were positive for centrobilin, a daughter centriole marker (Zou et al., 2005). Centrobilin participate in an

undefined manner in the initiation of new centriole structures and facilitates the elongation and stability of centrioles via its interaction with tubulin (Gudi et al., 2011). As a Nek2 substrate, it has been reported to have a role in stabilizing the microtubule network (Jeong et al., 2007) and in regulating the assembly of functional mitotic spindles (Jeffery et al., 2010b). Centrobin is recruited to the procentrioles during S phase. During S, G2, and M phases, the cell shows two centrobin-positive centrioles, the newly assembled procentrioles/daughter centrioles. After mitosis, cells have one centrobin positive centriole, the daughter centriole assembled in the previous cell cycle. Upon reentering S phase, centrobin on the daughter centriole assembled in the previous cycle becomes undetectable, the molecular basis of this not being clear (Zou et al., 2005).

Mitotic control *Nek9^{flox/flox}* cells have a centrobin positive centriole (one daughter centriole) per each centriole pair. However, in *Nek9^{ΔΔ}* cells, we observed a significant increase in the number on centrobin positive centrioles (~60% of centrioles in *Nek9^{ΔΔ}* vs 50% in *Nek9^{flox/flox}* were centrobin positive, resulting in around 40% of *Nek9^{ΔΔ}* (vs <2% of *Nek9^{flox/flox}*) cells showing at least one diplosome with both centrioles positive for centrobin (Figure 36). In fact, different centriole configurations were observed with cells frequently having groups of more than two centrioles, all of them centrobin positive. Furthermore, the levels of centrobin assessed by western blot were slightly increased upon Nek9 removal, although the detection was difficult and the results variable between different experiments probably due to the small amount of centriolar centrobin in cells (Bauer et al., 2016) (Figure 36D).

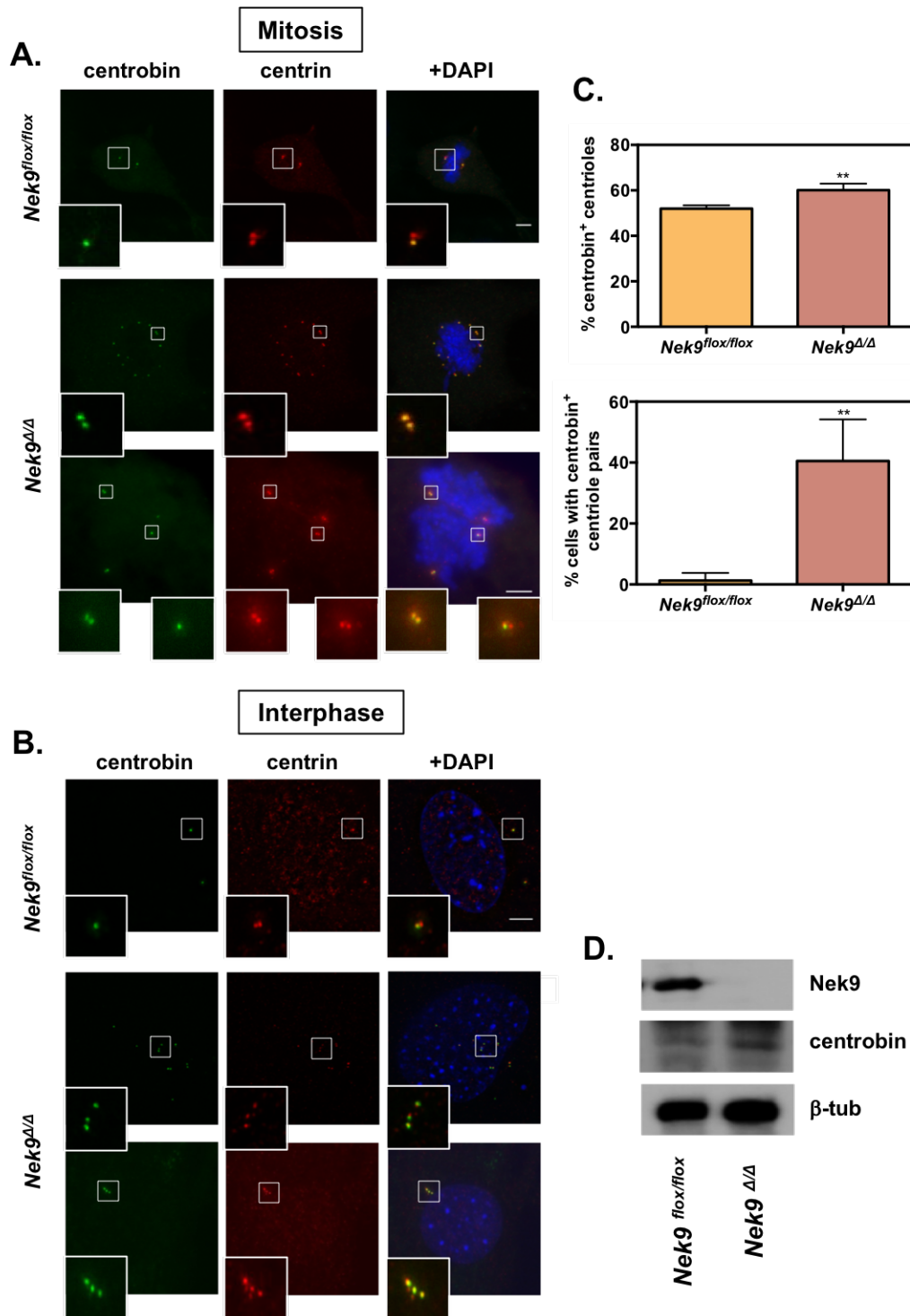


Figure 36: Centrobin positive centrioles were significantly increased in Nek9-depleted cells. **A)** Representative immunofluorescence images of mitotic MEFs immunostained with the indicated antibodies. Scale bar 5 μ m; **B)** Representative immunofluorescence images of interphase MEFs immunostained with the indicated antibodies. Scale bar 5 μ m; **C)** Percentage of centrobin positive centrioles and cells with centrobin positive centriole pairs. n=4, 30 cells per experiment; **D)** Representative western blot showing Nek9 depletion. Centrobin protein levels were slightly increased upon Nek9 absence. β -tubulin is used as a loading control.

Hence, Nek9 depletion may cause the production of multiple ‘daughter’ centrioles (something that our results with CPAP and SAS-6 do not seem to corroborate) or impede the removal of centrin from new mother centrioles just before reentering S phase. Centrin excess has been shown to cause the accumulation of CPAP, something that we have not observed, and defective long centrioles (Gudi et al., 2014, 2015), something that in some isolated cases we have seen but does not seem to be prevalent in *Nek9^{ΔΔ}* cells.

Despite the increase in the number of centrin positive centrioles, we did not notice the same increase using another daughter centriole marker, SAS-6 (Figure 37 and see also Figure 34). In fact, we observed a slight decrease (45% in *Nek9^{ΔΔ}* vs 55% in *Nek9^{flox/flox}* cells; n=1) in the percentage of SAS-6-positive centrioles, as the total number of centrioles in Nek9-depleted cells was higher, but roughly the same number of SAS-6 positive centrioles were observed. *Nek9^{flox/flox}* cells, almost entirely showed one SAS-6 positive procentriole per each centriole pair, ~10% with two centrin foci and 1 SAS-6 focus (corresponding to cells in G1) and ~90% with two centrin and SAS-6 foci (corresponding to S/G2/M cells with duplicated centrosomes). In contrast only 45% of *Nek9^{ΔΔ}* cells showed this configuration. The rest had more than 4 centrioles that however, were frequently associated with only one or two SAS-6 foci, suggesting that a fraction of the centrin positive centrioles observed in Figure 36 are not positive for SAS-6 (we were unable to do IFs simultaneously with these two centriolar proteins to document this). Interestingly, a significant number of cells (26,7%) did show centriole groups with three SAS-6 foci, hinting to a possible mechanism for centriole amplification.

Centrosome overduplication can result from two different mechanisms: the dysregulation of canonical templated centriole duplication, and the *de novo* formation of centrioles. In general, centrioles amplified through the canonical duplication cycle tend to form a cluster of daughters around a single mother centriole, whereas centrioles amplified by the *de novo* pathway tend to be dispersed in cytoplasm (Bettencourt-Dias and Glover, 2007).

Our observations seemed to point to canonical amplification (i.e. existence of groups of centrioles). To further elucidate this, we stained cells with centrobins plus C-Nap1, a mother centriole marker (Figure 38). As expected, after mitosis, control G1 cells (when only 2 centrioles are present) displayed two C-Nap1 positive centrioles, being only one of them centrobins positive, corresponding to the daughter centriole assembled in the previous S phase, whose centrobins will become undetectable upon reentering S phase. Thus, in S-G2-M (when already 4 centrioles are present) cells displayed two C-Nap1 positive centrioles and two centrobins positive centrioles, the newly assembled procentrioles. Interestingly, in *Nek9 Δ/Δ* cells we observed single C-Nap1 foci (mother centrioles) associated by several (usually two but in some cases three) centrobins foci. This resulted in an increase in centrobins positive centrioles in relation to C-Nap1 positive ones in *Nek9 Δ/Δ* cells, being 1.3 the average of centrobins positives centrioles vs C-Nap1 positive centrioles in *Nek9 Δ/Δ* and 0.8 in *Nek9^{fllox/fllox}* cells, respectively. As using SAS-6 we do not observe an excess of daughter centrioles (Figure 37), we hypothesize that what we observe are mother centrioles positive for centrobins associated to one or two daughter centrioles (also centrobins positive). Furthermore, we propose that the accumulation of defective removal of centrobins from the new mother centriole just after mitosis, induce new rounds of centriole duplication from the same mother centrioles generating a cluster of amplified centrioles.

RESULTS

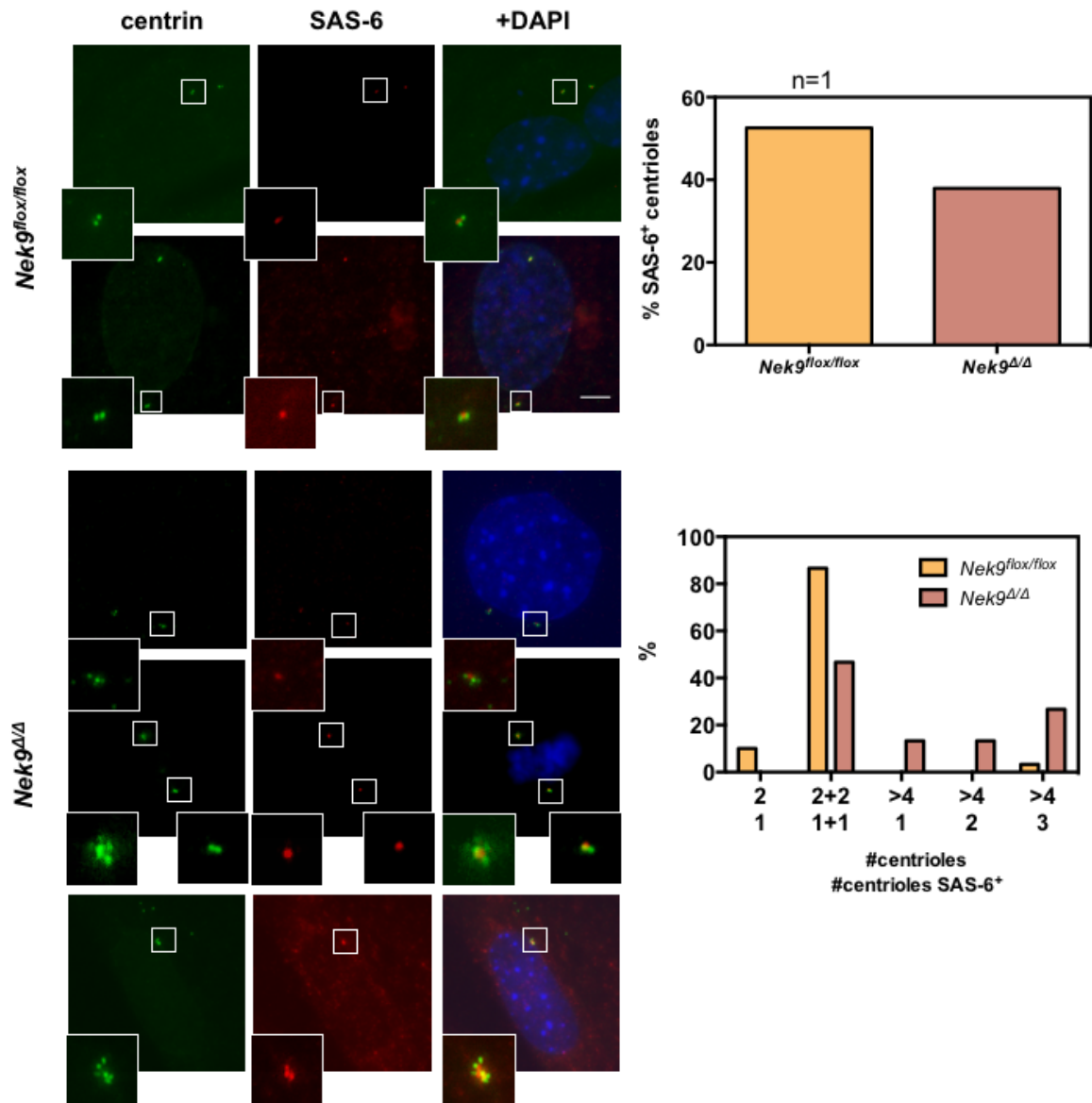


Figure 37: Representative immunofluorescence images of *Nek9^{flox/flox}* and *Nek9^{Δ/Δ}* MEFs immunostained with the indicated antibodies are shown. One SAS-6 positive centriole was present in each centriole pair. Percentage of centrosomes SAS-6 positives were quantified (total number or indicated configuration). Extra centrosomes in *Nek9*-depleted cells were not all positives for SAS-6 daughter centriole marker (one experiment, 100 cells). Scale bar 5 μ m.

RESULTS

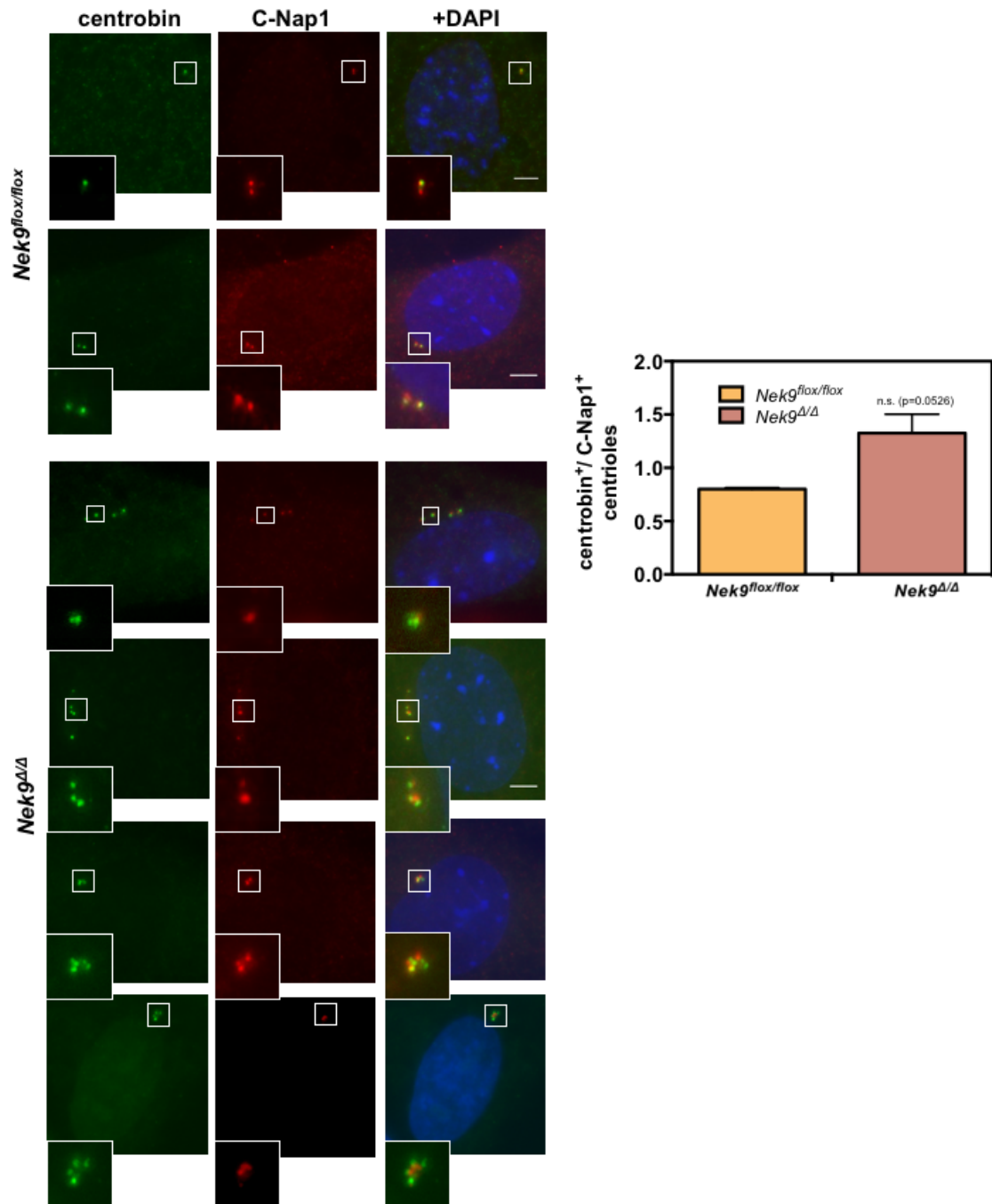


Figure 38: Representative immunofluorescence images of *Nek9^{flox/flox}* and *Nek9^{Δ/Δ}* MEFs immunostained with the indicated antibodies are shown. Quantification of centrobins positive centrioles versus C-Nap1 positive centrioles. The ratio between both is represented. n=2, 50 cells per experiment; unpaired t-test was performed. Scale bar 5 μ m.

Centrobin positive centrioles in *Nek9*^{Δ/Δ} cells favor the production of shorter cilia and multi-ciliated cells

The hypothesis that the lack of Nek9 results in mother centrioles positive for centrobin is supported by preliminary observations showing that centrobin positive centrioles in *Nek9*^{Δ/Δ} cells are able to function as basal bodies of cilia when arrested by serum starvation (Figure 39). We observed cilia (labeled with the ciliary marker Arl13b) that apparently were growing from centrobin positive centrioles (>20% of cilia showing Arl13b and centrobin signal overlap or continuity in *Nek9*^{Δ/Δ} cells vs 2% in *Nek9*^{flox/flox} cells), although we could not assure unequivocally that they were basal bodies without the use of other markers. Additionally, in some *Nek9*^{Δ/Δ} cells it was possible to observe cilia with two centrobin foci in their base. Although the number of cells producing cilia did not change in respect to control cells (around 60%), cilia in *Nek9*^{Δ/Δ} cells were frequently shorter (2,2 um vs 2,97 um in average in *Nek9*^{flox/flox}). Furthermore, we observed that 20% of *Nek9*^{Δ/Δ} cells were multi-ciliated (vs 2% in *Nek9*^{flox/flox}), something that may be related to the previously described centriole amplification.

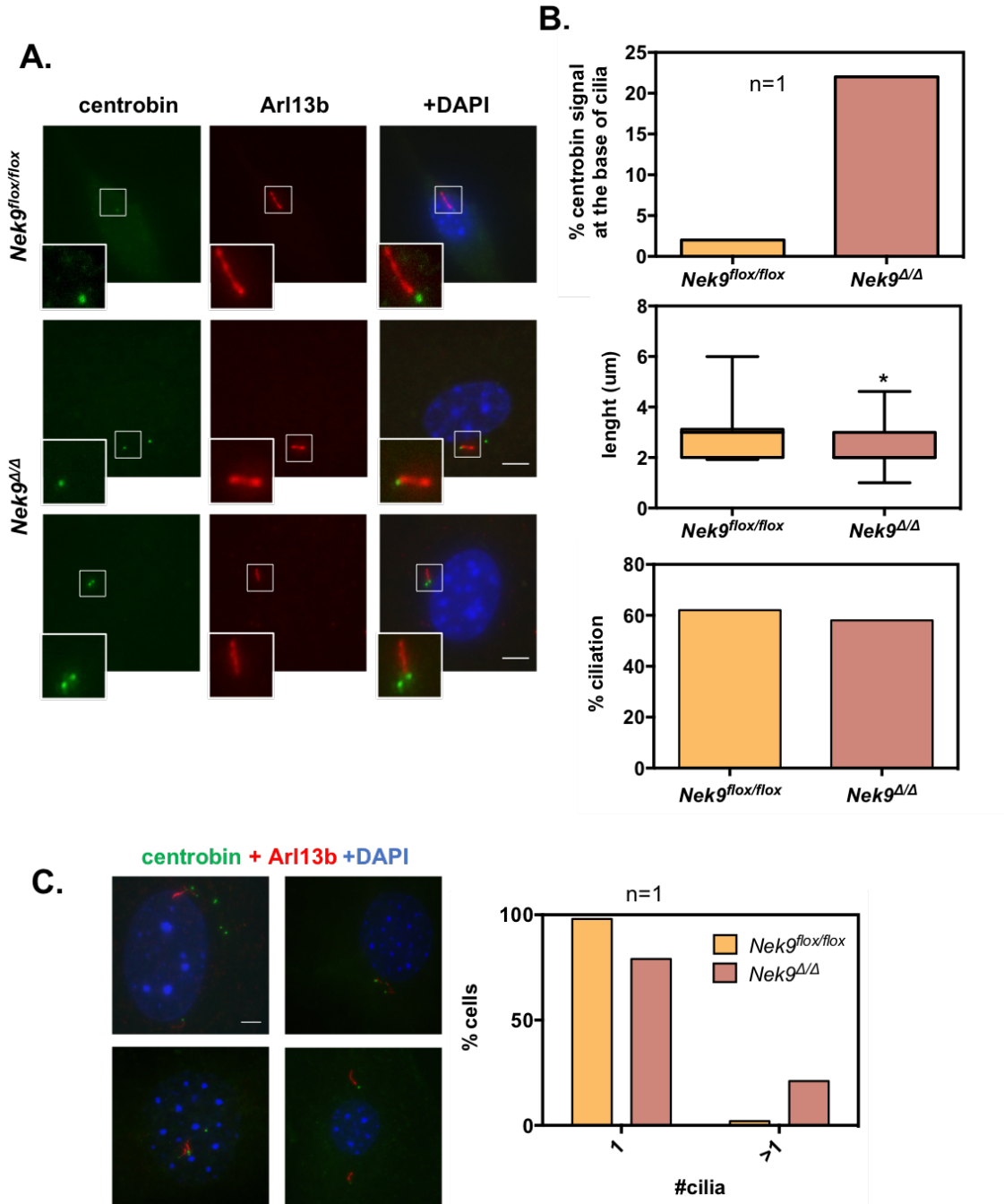


Figure 39: Cilia formation in G0 arrested *Nek9*-depleted cells. **A)** Representative immunofluorescence images of *Nek9^{flox/flox}* and *Nek9^{Δ/Δ}* MEFs immunostained with the indicated antibodies are shown; **B)** Percentage of ciliation between control and *Nek9*-depleted cells, cilia length quantification and percentage of centrobin signal at the base of cilia in *Nek9* absence (one experiment, 100 cells); **C)** Percentage and representative immunofluorescence images of multiciliated *Nek9^{Δ/Δ}* MEFs immunostained with the indicated antibodies are shown. One experiment, 100 cells. Scale bar 5 μ m.

Nek9 depletion in human cells

Cell viability is affected upon Nek9 depletion

In parallel to the described results, and to ascertain if the phenotype resulting from the depletion of Nek9 was not an isolated event observed in MEFs, we used two transformed human cell lines, U2OS and HeLa to study the result of depleting Nek9 by siRNA. Upon Nek9 depletion, both cell types showed an impairment in their proliferation capacity when compared with control cells. Surprisingly, and in contrast to what we observed in MEFs, the respective mitotic indexes were not increased, and in fact we observed a slight decrease in the percentage of mitotic cells in both cell lines. A clonogenic survival assay additionally showed that Nek9 downregulation was deleterious in both cases (Figure 40).

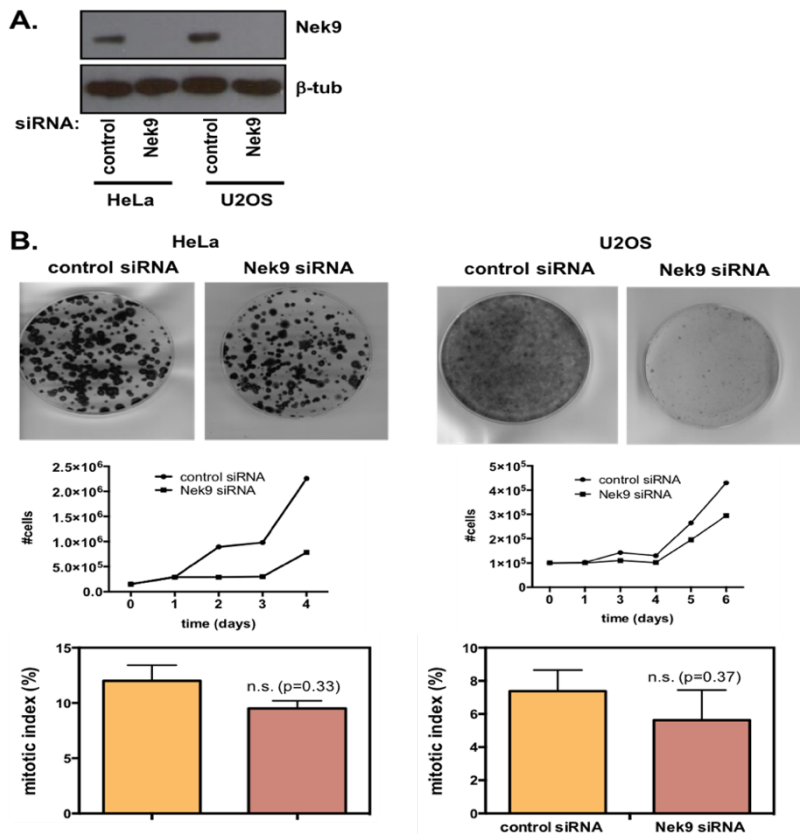


Figure 40: Nek9 abrogation in human cell lines. **A)** Representative western blot confirming Nek9 depletion 48h after siRNA transfection in HeLa and U2OS cells. β -tubulin is used as a loading control; **B)** Colony formation assay, growth curve and mitotic index in control or Nek9 siRNA transfected HeLa cells (n=2,100 cells per experiment) and U2OS cells (n=4, 100 cells per experiment).

U2OS but not HeLa cells phenocopy the effect on centrosomes of downregulating Nek9 levels observed in MEFs

Together with the proliferation defects, we observed that the downregulation of Nek9 resulted in centrosome amplification in U2OS but not HeLa cells (Figure 41). Thus, 7% of U2OS cells after Nek9 siRNA (vs 2% after control siRNA) showed more than two centrosomes while no amplification was detected in HeLa. Besides the increase in the number of centrosomes in U2OS, 48h post-transfection we also found a significant increase in the number of centrosomes with more than 2 centrioles (11% of centrosomes in Nek9 siRNA cells vs less than 1% in control cells).

We did not find abnormal expression of Plk4 or SAS-6 in U2OS after Nek9 depletion, and the extra centrioles were not SAS-6 positive. Control cells had one SAS-6 positive procentriole per each centriole pair (2;1 or 2+2;1+1 configurations) while in Nek9-depleted cells only the 70% showed this configuration. The rest of the cells showed more than 4 centrioles with only one or two of them being positive for SAS-6 (Figure 42).

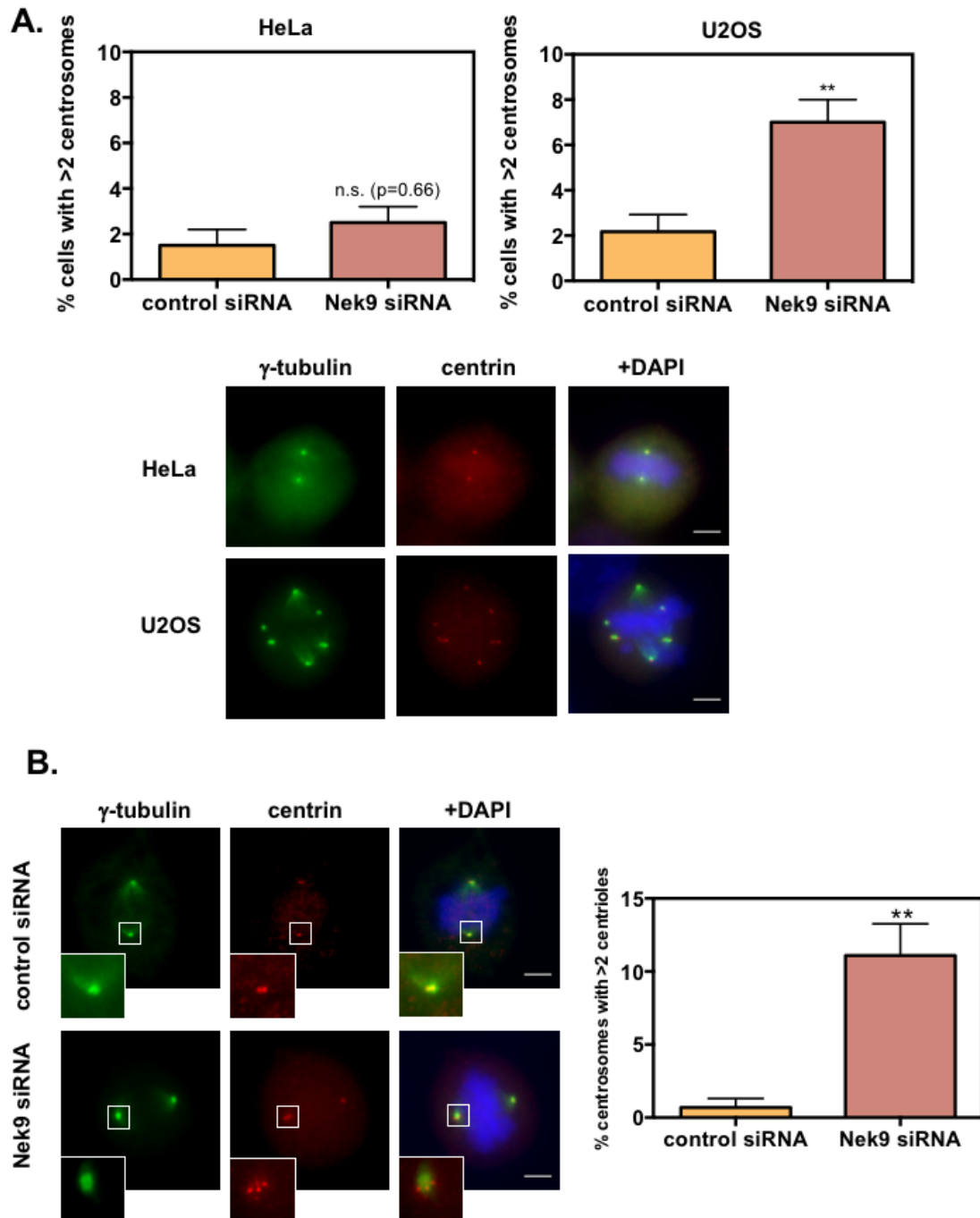


Figure 41: Nek9 depletion leads to centrosome amplification in U2OS but not in HeLa cells. **A)** Percentage of cells with more than 2 centrosomes 48h post-transfection in HeLa (n=2, 100 cells per experiment) and U2OS (n=3, 100 cells per experiment). Representative immunofluorescence images with the indicated antibodies are shown. Scale bar 5 μ m; **B)** Quantification of centrosomes with more than 2 centrioles upon Nek9 abrogation for 48 hours in U2OS cells (n=3, 50 cells per experiment, unpaired t-test was performed). Representative immunofluorescence images with the indicated antibodies are shown. Scale bar 5 μ m.

RESULTS

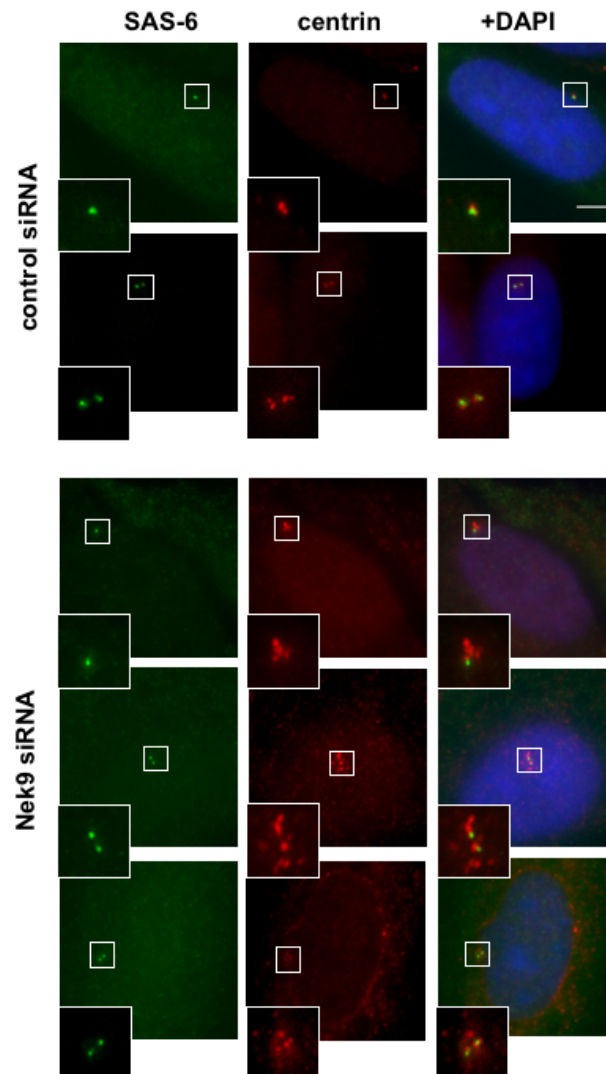
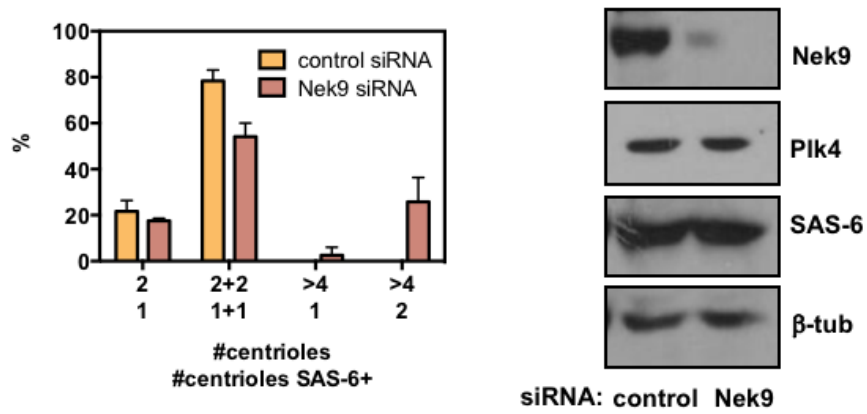


Figure 42: Centrin and SAS-6 configurations after control and Nek9 siRNA transfection in U2OS cell (48h post-transfection; n=2, 50 cells per experiment). Representative immunofluorescence images with the indicated antibodies are shown. Scale bar 5 μ m. Western blot showing that Nek9 depletion did not affected protein levels of the duplication factors SAS-6 and Plk4. β -tubulin is used as a loading control.

As in *Nek9^{ΔΔ}* cells, in U2OS where Nek9 was depleted by siRNA we noticed both in mitosis and in interphase, a significant increase in the number on centrobilin positive centrioles (50% of centrioles in control siRNA vs 70% in Nek9 siRNA cells), and the presence of centrobilin positive centriole pairs (35% of cells with a diplosome with both centrioles positive for centrobilin in Nek9 siRNA cells vs <5% in control cells) (Figure 43). As observed in MEFs, centrobilin levels as detected by western blot seemed to increase upon Nek9 downregulation, although these results not conclusive enough due to inter-experiment variability to be able to assure that this is the case (not shown).

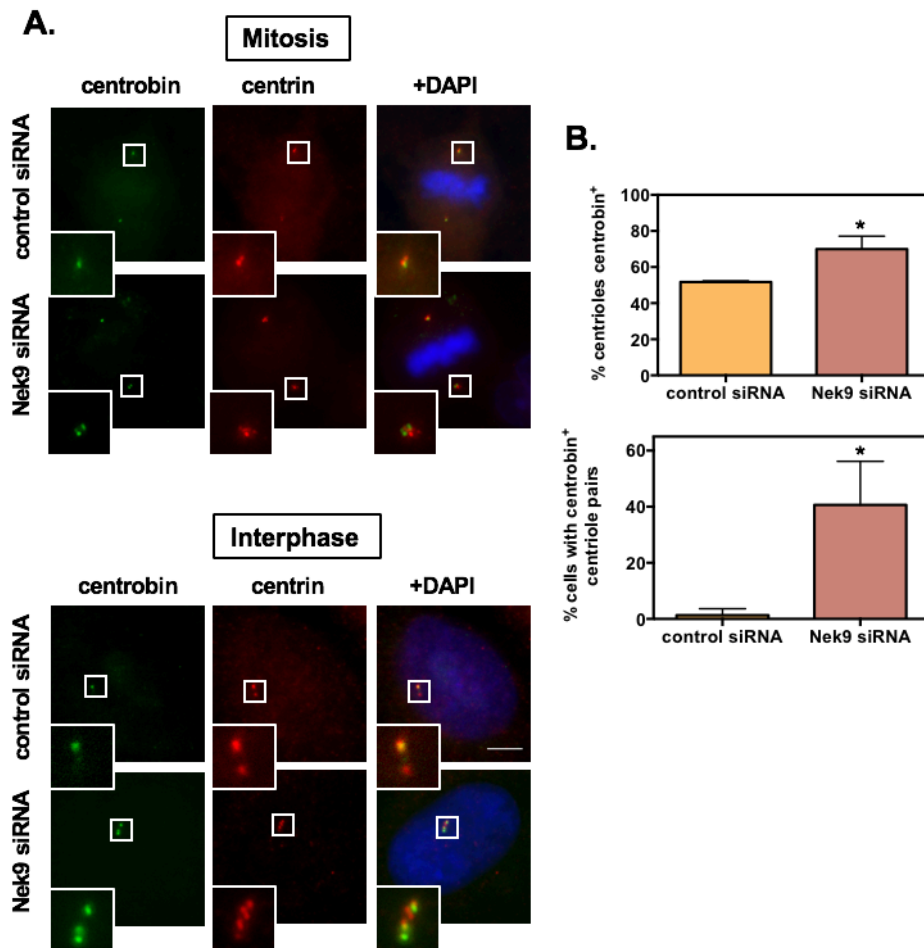


Figure 43: Excess of centrobilin positive centrioles in U2OS cells after Nek9 downregulation (48h post-transfection). **A)** Representative immunofluorescence images of mitotic and interphase cells immunostained with the indicated antibodies are shown. Scale bar 5 μ m; **B)** Percentage of centrobilin positive centrioles and cells with centrobilin positive centriole pairs. n=3, 50 cells per experiment; unpaired t-test was performed.

To finish the comparison between MEFs and U2OS, we also quantified C-Nap1 (mother centriole marker) in respect to centrobilin (daughter marker) positive centrioles, observing a similar increase in the number of centrobilin positive centrioles vs. C-Nap1 positive centrioles that we had previously observed in MEFs, being 1.2 the average of centrobilin positive centrioles per C-Nap1 positive centrioles in Nek9-depleted cells and 0.8 in control cells (Figure 44).

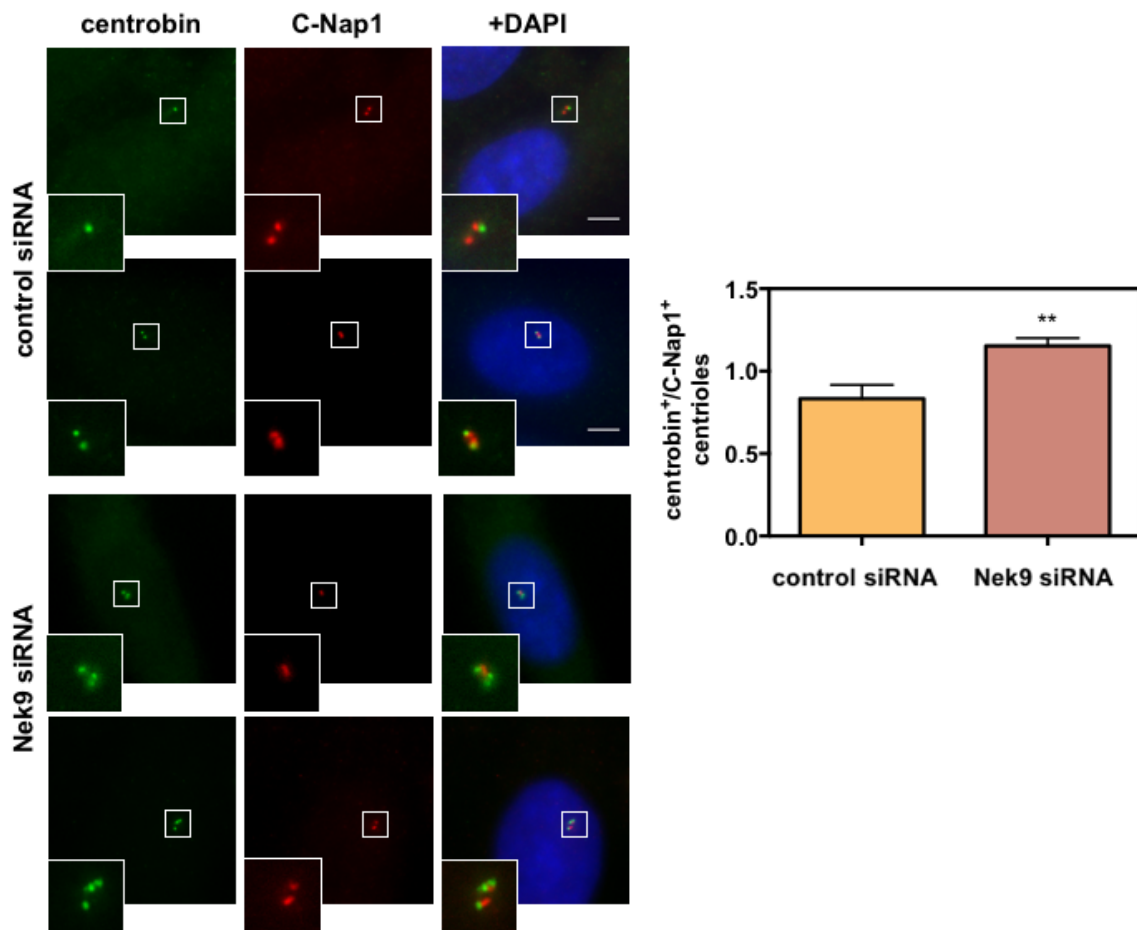


Figure 44: Representative immunofluorescence images of U2OS cells 48h post-transfection with control or Nek9 siRNAs, immunostained with the indicated antibodies are shown. Quantification of centrobilin positive centrioles versus C-Nap1 positive centrioles. n=3, 50 cells per experiment; unpaired t-test was performed Scale bar 5 μ m.

Centriole amplification upon Nek9 downregulation is Plk4-dependent

Being Plk4 the main regulator of centriole duplication, we also wanted to determine whether interfering with the activity levels of this kinase affects the ability of Nek9-depleted cells to increase centriole/centrosome numbers. In order to overexpress Plk4, we used a U2OS cell line that allows the temporally controlled expression of this kinase by tetracycline induction and examined centriole formation during cell-cycle progression (Figure 45). We could not detect changes in Plk4 levels by western blot (data not show), but already 12 h after Plk4 induction, approximately 40% of cells showed evidence of centriole amplification, both in control or Nek9-depleted cells, that progressively increased with time, with around 70% of cells showing multiple centrioles arranged in a manner reminiscent of the petals of a flower (rosettes) after 24 or 48h. This has been shown to correspond to multiple (pro)centrioles arranged around each parental centriole (Lopes et al., 2015). In these rosettes generated upon Plk4 induction most of the centrioles were SAS-6 and centrin positives. Nek9 RNAi did not result in an increase of the number of rosettes. Additionally, and as described, amplified centrioles from Nek9-depleted cells where Plk4 hadn't been induced were centrin but not SAS-6 positive, suggesting that the mechanism that results in centriole amplification in these cells is different to that of Plk4 overexpression.

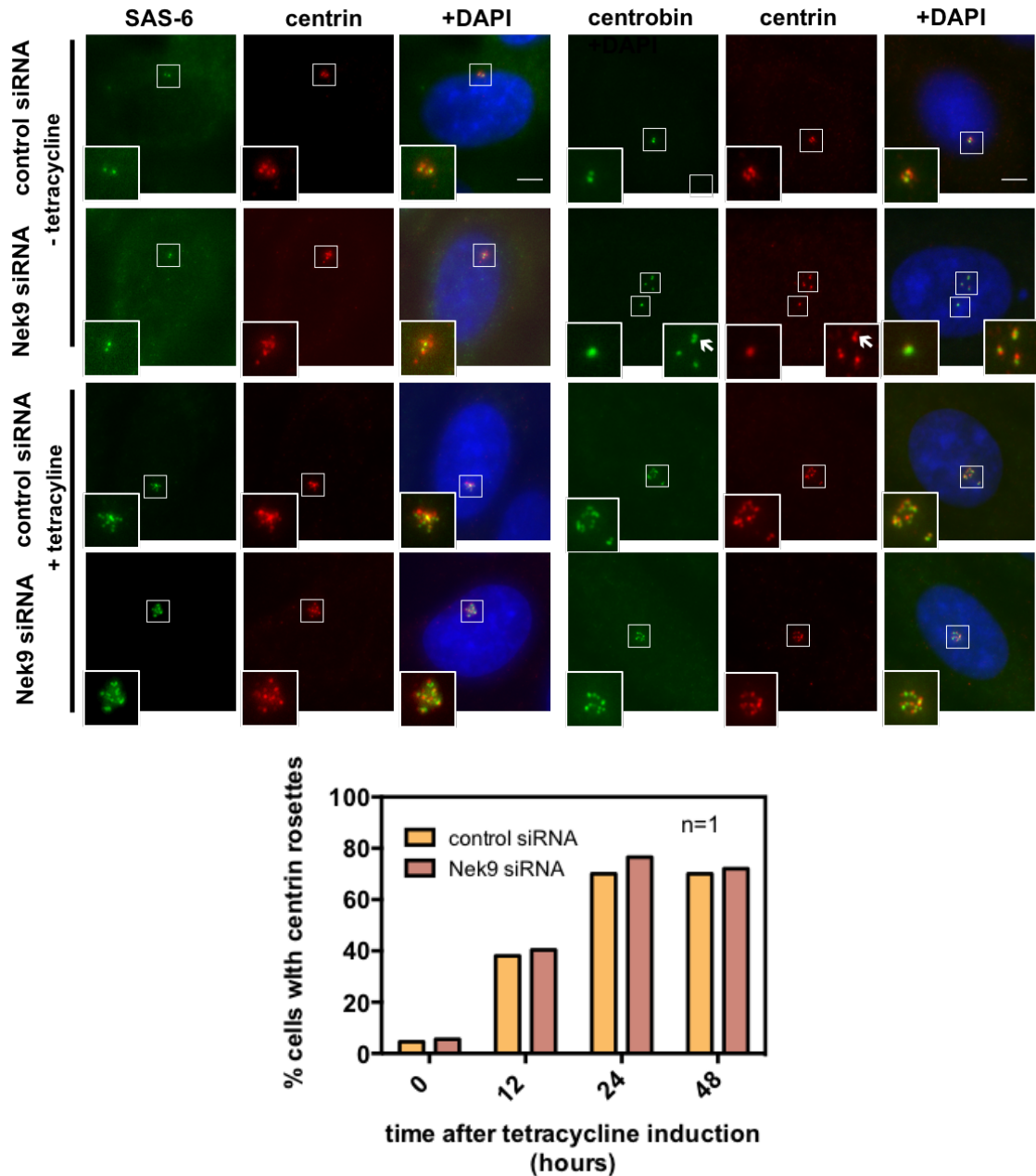


Figure 45: Representative immunofluorescence images of Plk4-inducible U2OS cells 48h post-transfection of control or Nek9 siRNAs, and immunostained with the indicated antibodies are shown. Percentage of cells forming centrin rosettes during 48h time course after tetracycline induction. t=0 before induction and 12, 24 and 48h after tetracycline induction (n=1, 100 cells). Scale bar 5 μ m. Arrowheads indicate a centrin positive centriole pair.

Conversely, we wanted to inhibit Plk4 activity and to do so we took advantage of centrinone B, a reversible inhibitor that triggers centrosome depletion in human cells (Wong et al., 2015). Figure 46A shows that after 48 hours in control siRNA transfected cells, 80% cells were found to have 2

RESULTS

centrosomes with 2 centrioles each (2+2 centrioles). When these cells were treated with centrinone B for 48 hours, the number of centrosomes and their respective centrioles were decreased. Under these conditions we found only 50% of cells with 2 centrosomes with 2 centrioles each (2+2). Instead, around 5% of the cells showed 2 centrioles in one centrosome and 1 centriole in the other (2+1) and 10 % one centriole per centrosome (1+1). Also, around 30% had one centrosome with only one centriole (1). In Nek9-depleted cells, almost 20% cells had more than 4 centrosomes with more than 2 centrioles each as expected from our previous results. After centrinone treatment, no cells with this configuration were observed. Instead, we found cells with two centrosomes but several abnormal centriole configurations (1+1, 2+1, 0+2). In addition, 40% cells had 1 centrosome with one centriole (1). Curiously, around 10% of these cells lacked centrioles. These data suggested that centriole amplification in Nek9-depleted cells depends on Plk4 activity. Interestingly it also shows that Nek9 depletion may accelerate centriole loss upon Plk4 inhibition.

We quantified in the same conditions the number of centrioles that were centrobilin positive (Figure 46B). We found that in control cells 40% of the cells had 2 centrioles, one centrobilin positive (2;1) and 60% had 4 centrioles, 2 centrobilin positives (2+2;1+1). When treated with centrinone B for 48 hours, 5% had 1 centriole, 1 centrobilin positive (1;1), 50% had 2 centrioles, one centrobilin positive (2;1), 5% 2 centrioles with no centrobilin (2;0) and 40% 4 centrioles, 2 centrobilin positives (2+2;1+1). On the other hand, in Nek9-depleted U2OS more than 20% had more than 4 centrioles that were centrobilin positives but when treated with centrinone B these cells lost centrioles. We instead found 25% cells with no centrobilin positive centrioles despite the cells still having 4 or 3 centrioles, suggesting that the extra centrobilin-positive centrioles were the firstly to be lost.

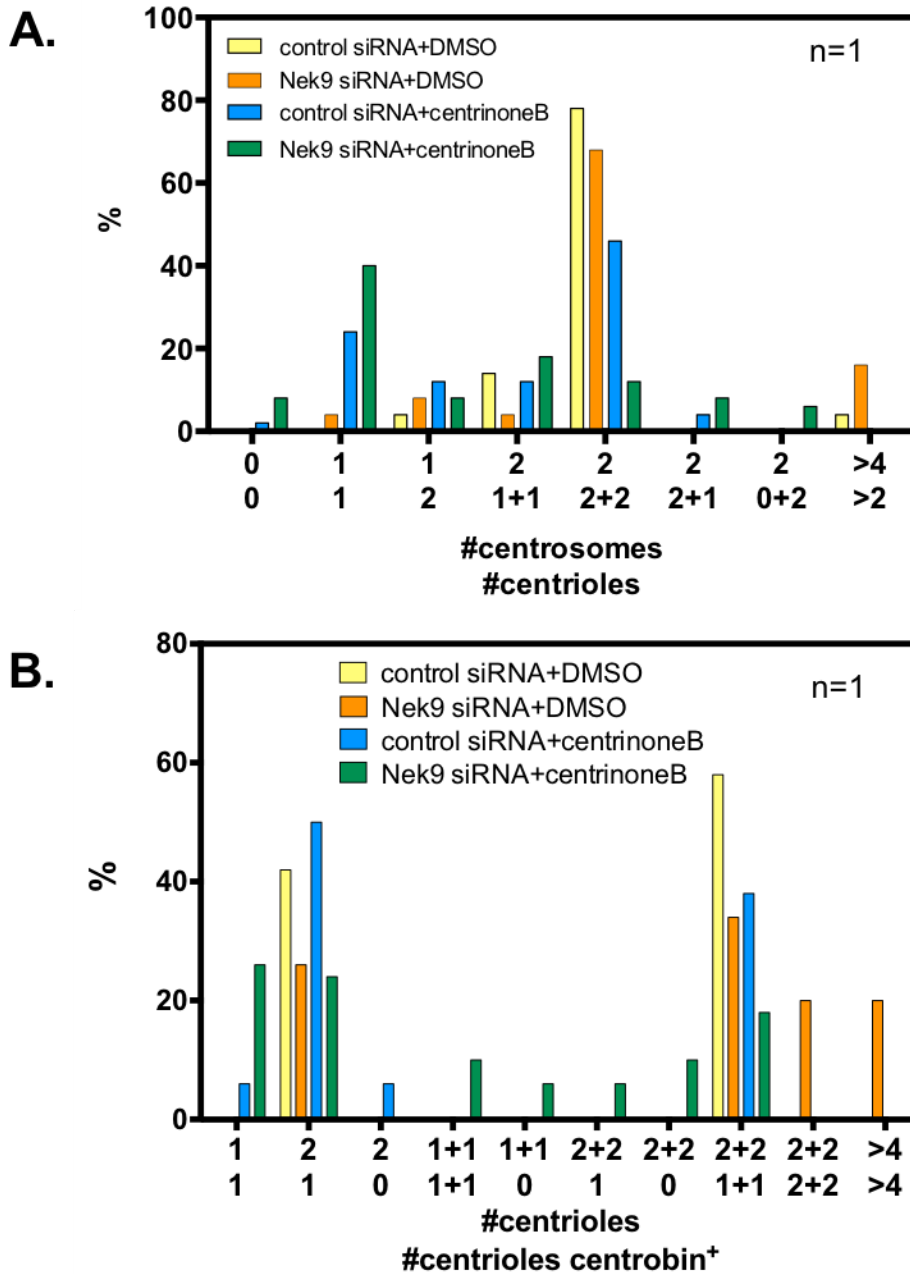


Figure 46: Centriole amplification in Nek9-depleted U2OS cells is Plk4 dependent. Control and Nek9 siRNA transfected cells were treated with DMSO or 500nM of the Plk4 inhibitor centrinone B (n=1, 100 cells), 48h transfection + 48h centrinone B treatment. **A)** Frequency of cells with the indicated number of centrosomes and centrioles identified with γ -tubulin and centrin antibodies, respectively; **B)** Frequency of cells with the indicated number of centrin positive centrioles.

Nek9 may control centriole number through centrobilin

We have the hypothesis that Nek9 has several unidentified roles during the cell cycle, and more specifically the late phases of mitosis, directly through the modification of the molecular behavior of different substrates by phosphorylation or indirectly as the activator of the downstream kinases Nek6/7.

In collaboration with Dr. Judit Villen (University of Washington, Seattle, US), we wanted to identify Nek9 substrates by monitoring phosphorylation sites on a proteome-wide scale. We compared changes in phosphosite composition after elimination of Nek9 in *Nek9^{flox/flox}* MEF cells infected with AdCre adenovirus (*Nek9^{+/+}* cells were used as controls) by SILAC (Stable Isotope Labeling by Amino acids in Cell culture). This technique gave us a global view of phosphosites that depend on the kinase for their phosphorylation, and thus, a list of substrates candidates.

One potential Nek9 substrate candidate that we found was centrobilin, the daughter centriole marker that according with our data is accumulated in amplified centrioles when Nek9 is depleted from both MEF and U2OS cells. Centrobilin was less phosphorylated in Nek9 null MEFs, what made us think about the possibility that Nek9 could phosphorylate centrobilin in late mitosis or G1, when it is known to be lost from the daughter centriole (Zou et al., 2005), thus being Nek9 implicated in the process of centrobilin release during centriole disengagement previous to the phase. According to our hypothesis, in the absence of Nek9, centrobilin would not be phosphorylated, remaining at daughter centrioles, and this through a yet to be determined mechanism would result in centriole amplification.

Centrobilin overexpression induces centriole amplification

Our data showed that the downregulation of centrobilin by RNAi interfered with centriole amplification resulting from Nek9 downregulation (not shown). We thus wondered what would happen if we overexpressed it. Thus, we expressed recombinant GFP-centrobilin in U2OS and HeLa cells. Our results showed the same effect observed upon Nek9 depletion. U2OS but not HeLa cells that were effectively GFP-centrobilin transfected, frequently contained more than four centrioles (15% of cells in interphase and 25% in mitosis in GFP-centrobilin transfected cells vs 5% cells in interphase and 2% in mitosis in GFP control transfected cells; only cells expressing low levels of GFP-centrobilin were considered). In addition, we confirmed that centrioles were also positive for GFP-centrobilin (Figure 47).

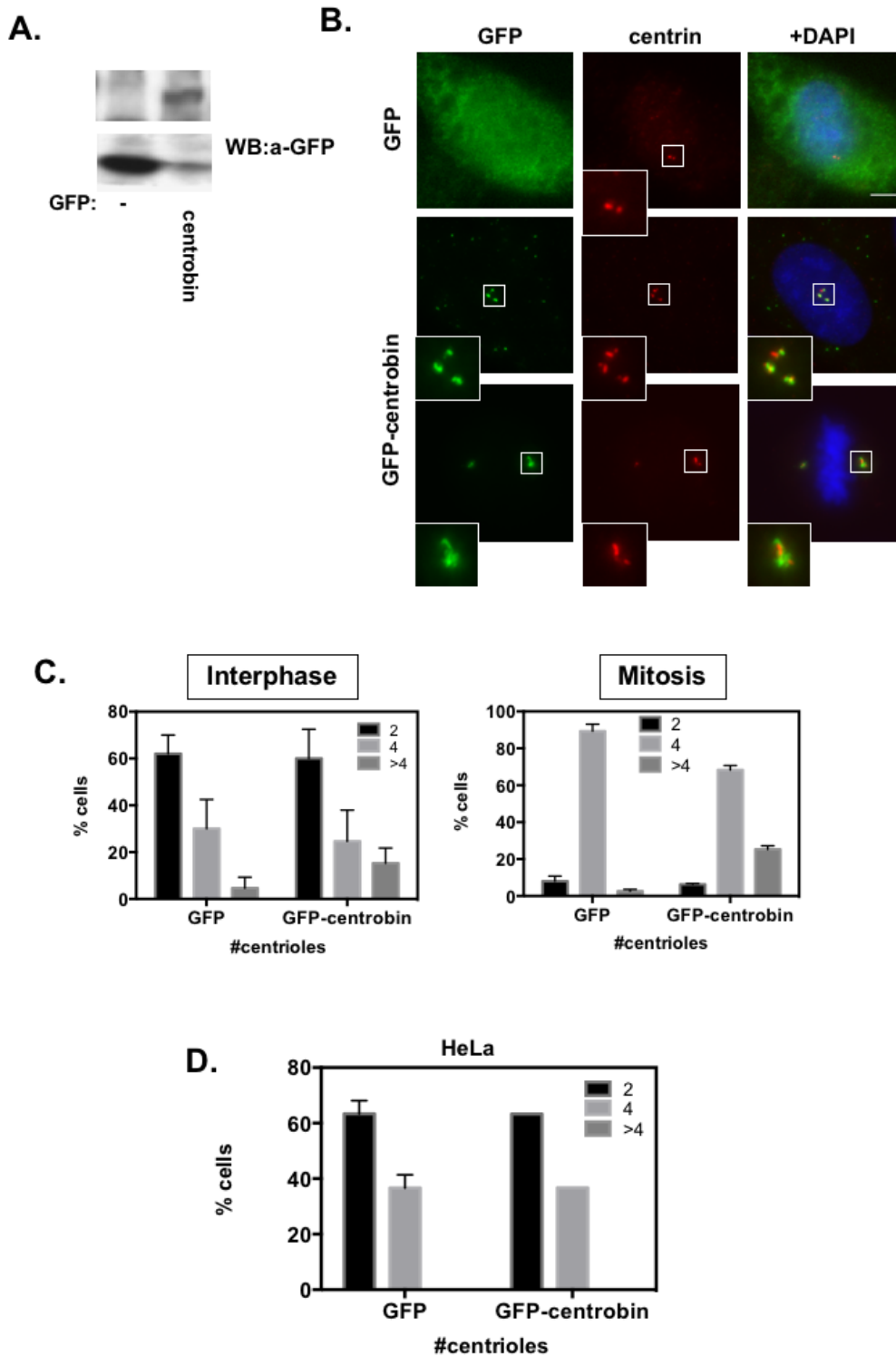


Figure 47: GFP-centrobin overexpression results in centriole amplification in U2OS cells. **A)** Anti-GFP western blot confirming GFP constructs expression; **B)** Representative immunofluorescence images of U2OS cells 24h post-transfection, immunostained with the indicated antibodies are shown. Scale bar 5 μ m; **C)** Percentage of interphase or mitotic cells with the indicated number of centrioles (n=3, 50 cells per experiment); **D)** Percentage of interphase HeLa cells with the indicated number of centrioles (n=2, 50 cells per experiment). In all cases cells expressing centrobin at levels in which the protein formed big aggregates in the cytoplasm were not considered.

Study of the possible phosphorylation of centrobilin by Nek9

In order to better understand the molecular basis of our observations, we next did a search for sites described to be postranslationally modified in centrobilin

(<https://www.phosphosite.org/proteinAction.action?id=9421>).

Unfortunately, the site that we identified by SILAC in mice cells (S776), although conserved, had not been identified as a site modified *in vivo* previously. Besides four Nek2 phosphorylation sites (Thr35, Ser36, Ser41 and Ser45) that had been exclusively confirmed *in vitro*, there were other residues that appeared several times modified *in vivo* in high throughput studies and could be putative Nek9 phosphorylation sites (conforming to the [FLWYV]XX[ST] sequence), Ser78, Ser80 and Ser837. Interestingly the last one was proximal to the site identified by SILAC in mouse centrobilin. Finally, we thought about the possibility that centrobilin degradation could be controlled by ubiquitination, and that this could depend on Nek9 phosphorylation. Indeed, several ubiquitination sites have been reported (Udeshi et al., 2013), one of them, K832, with several records in high throughput studies, close to Ser837 (Table 6).

Site	Sequence	PTM enzyme	in vivo	Conserved in mice	Nek9 site [FLWYV]XX[ST]	mutant
T35-p	NQVSSEVt ^s QLYAsL	Nek2	no	yes	yes	S4A/S4D
S36-p	QVSSEVt ^s QLYAsLR	Nek2	no	yes	yes	
S41-p	Vt ^s QLYAsLRLsRQA	Nek2	no	yes	yes	
S45-p	LYAsLRLsRQAEEATA	Nek2	no	yes	yes	
S62-p	QLYLPSt ^s PPHEGLD		yes	yes	yes	
S78-p	FAQELSRsL ^s VGLEK		yes	yes	yes	S2A/S2D
S80-p	QELSRsL ^s VGLEKNL		yes	yes	yes	
Y169-p	LEELFPRyT ^s LRPGP		yes	yes		
S171-p	ELFPRyT ^s LRPGPPL		yes	yes	yes	
S781-p	PEPPSSHsQGSGPSS		yes	yes	yes	
S790-p	GSGPSSGsPERGGDG		yes	yes	yes	
Y814-p	VSQLLRLyQARGWGA		yes	yes		
S837-p	YLkRLEHsGTDGRGD		yes	yes	yes	S837A/S837D
T230-p	AADRkkD ⁱ MIEQLDK		yes	yes		
S784-p	PSSHsQGSGPSSGsP		yes	yes		
S787-p	HsQGSGPSSGsPERG		yes	yes		
K832-ub	EDLLLYLkRLEHsGT		yes	yes	yes	K832M

Table 6: Described centrobilin PTM sites (phosphorylation/ubiquitination). Potential sites likely to be phosphorylated by Nek9 were indicated together with phospho-null and phosphor-mimetic mutants generated.

We thus next generated phospho-null and phospho-mimetic mutants for these potential posttranslational modification sites, by mutating serines or threonines residues to alanines or to aspartic acids, respectively, including GFP-centrobin[4A] or GFP-centrobin[4D] mutants that contained Thr35, Ser36, Ser41 and Ser45 residues, and GFP-centrobin[2A] or GFP-centrobin[2D] that contains Ser78 and Ser80. Finally, we produced GFP-centrobin[K832M] with the aim of interfering with the ubiquitination of this residue.

We next transfected all the centrobin constructs in U2OS to see if there was any change in centrobin amount or localization and whether they resulted in centriole amplification. Overexpressed GFP-centrobin frequently forms aggregates in the cytoplasm of cells and was not well extracted with the standard lysis buffer, so we used RIPA buffer. Even with this buffer the majority of the protein remained in the insoluble fraction (Figure 48A). None of the mutants had a significantly altered expression level or localization at centrioles (not shown) and centriole amplification was similar in all the mutants and equivalent to that observed with GFP-centrobin wild type. Despite these technical limitations, the highest levels of centriole amplification were observed with GFP-centrobin[4A]. Thus 40% of mitotic and 15% of interphase cells had more than 4 centrioles in comparison to a 30% found in mitosis or almost 10% in interphase when centrobin^{WT} was expressed. This effect was partially rescued with the phosphomimetic 4D (20% of mitotic cells with more than 4 centrioles and only 5% of interphase cells had more than 4 centrioles) which is also the better detected in the soluble fraction (Figure 48B). These results suggested that Thr35, Ser36, Ser41 and Ser45 residues as possible sites that have to be phosphorylated to avoid centriole accumulation of centrobin and subsequent centriole amplification.

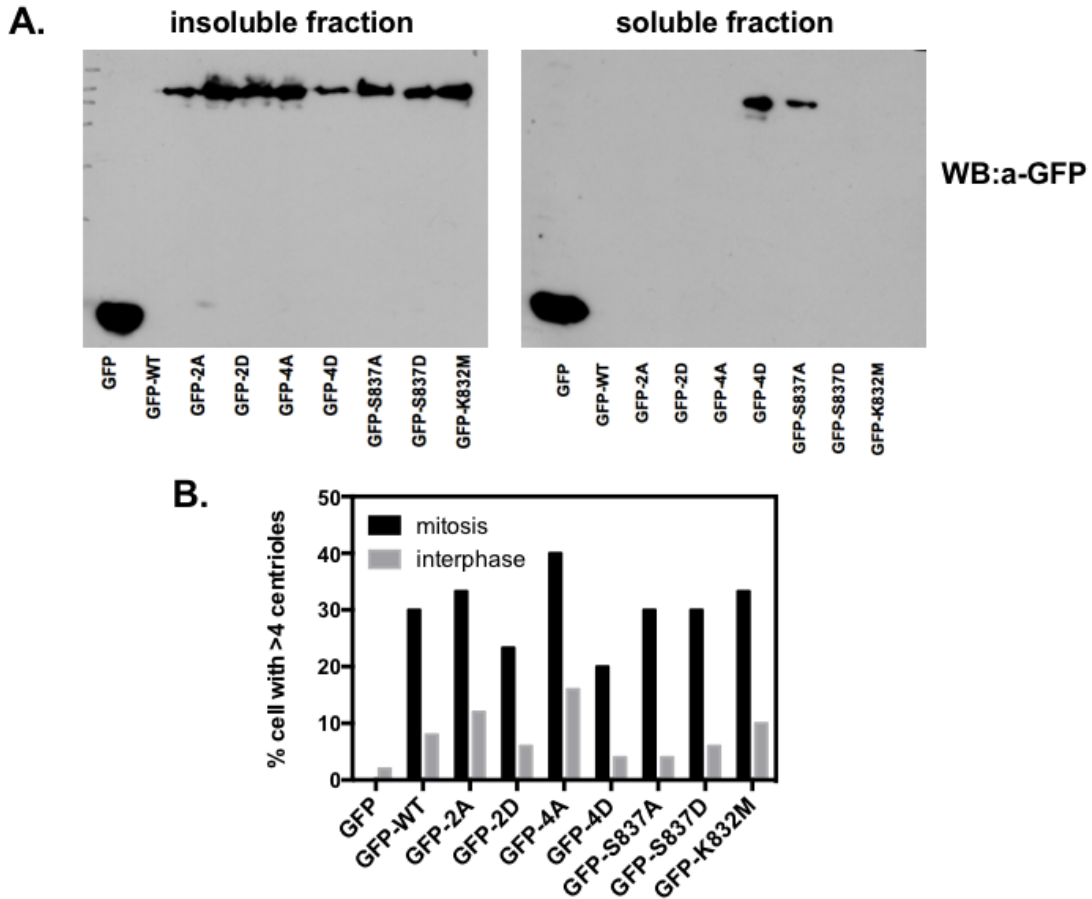


Figure 48: Centriole amplification observed upon overexpression of GFP-centrobin phospho-null and phospho-mimetic mutants in U2OS cells. **A)** Anti-GFP western blot of soluble and insoluble fractions after RIPA buffer protein extraction in U2OS cells transfected with all GFP-centrobin mutants.; **B)** The percentage of cells transfected with the indicated mutants that showed more than 4 centrioles were quantified in mitosis and interphase. Quantification was done by IF selecting only GFP positive cells (one experiment, 50 cells).

Nek9 interacts with centriolin

Our results suggest that Nek9 may control the amount of centriolin and (maybe as a result) its localization to centrioles. To address if Nek9 and centriolin interact *in vivo*, we performed an endogenous Nek9 immunoprecipitation. We observed that endogenous Nek9 immunoprecipitated together with centriolin (Figure 49A). To confirm the association, we transfected HeLa with FLAG-Nek9 plus FLAG-Nek6 as a control. Our results show that recombinant FLAG-Nek9 associates to endogenous centriolin. In contrast we could not detect association with

FLAG-Nek6 (Figure 49B). We next wanted to investigate whether the observed interaction was dependent on centrobins phosphorylation. To achieve this purpose, we transfected HeLa cells with GFP-centrobin and the phosphonull mutant 4A, the one that produced a higher level of centrosome amplification. As expected from the experiments described above, we detected an interaction between recombinant GFP-centrobin wild type and endogenous Nek9 (Figure 49C). Strikingly, we discovered that there was no association between centrobins 4A mutant and Nek9. Neither did we observe centrobins interaction with Plk1, Nek6 or Nek7.

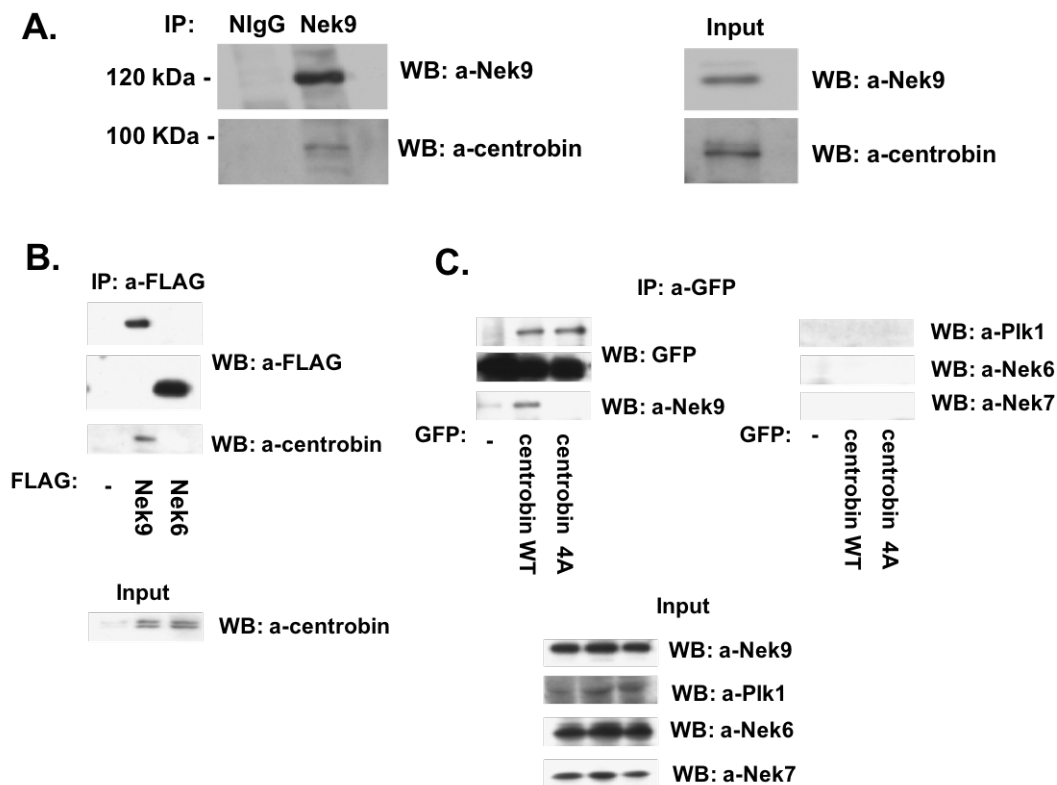


Figure 49: Nek9 associates with centrobins. **A)** Immunoprecipitation of endogenous Nek9 in HeLa cells and anti-centrobin western blot; **B)** Immunoprecipitation of FLAG-Nek9 and FLAG-Nek6 and anti-centrobin western blot; **C)** Immunoprecipitation of GFP-centrobin WT and GFP-centrobin 4A. Western blot for the indicated antibodies is shown.

RESULTS

ADDITIONAL RESULTS

ADDITIONAL RESULTS

High throughput screening for Nek9 inhibitors

The process of cell division has been long established as a targeting opportunity for cancer therapy. Interfering with DNA or tubulin with the aim of inducing either cell cycle arrest or abnormal mitosis and subsequent cell death is a proven strategy that results in differentially killing dividing cells while ideally not affecting differentiated cells. Targeting of mitotic regulators is emerging as a strategy that could complement or even substitute better established but less selective antiproliferative therapies that directly interfere with the cellular microtubule network such as paclitaxel, thus having several side effects.

With this in mind, we aimed to validate Nek9 as a putative antimitotic target by identification of small chemical inhibitors of its activity. Nek9 is by its enzymatic nature druggable, and regarding our results exposed before in different systems show that interfering with the different functions of the kinase can have strong antimitotic effects, possibly as the result of a significant induction of defective cell division and aneuploidy. Moreover, our group has recently shown that Nek9 signals between the mitotic kinase Plk1 and the kinesin Eg5 (Bertran et al., 2011; Eibes et al., 2018; Sdelci et al., 2012), both validated mitotic targets with several inhibitors presently undergoing clinical trials as antiproliferative agents.

We proposed to test whether, efficient inhibition of Nek9 results in cell cycle arrest and eventually the death of dividing cells (specially transformed cancer cells) while being innocuous to non-dividing cells. The effects of Nek9 inhibition was tested using a chemical genetics approach based in a strategy originally devised by the Shokat laboratory (University of California, San Francisco, <http://shokatlab.ucsf.edu>).

The project was developed in collaboration with Dr. Stefan Kubicek at PLACEBO, the Platform Austria for Chemical Biology at the Ce-M-M-, the Research Center for Molecular medicine of the Austrian Academy of

Sciences, where I stayed one month as a visiting student. We expressed and purified both inactive (but readily activable) and constitutively active Strep-Tagged Nek9 as well as biotinylated Nek7 and using PLACEBO available equipment we have screen part of PLACEBO library of chemicals for their capability to interfere with recombinant Nek9 autoactivation and phosphorylation of its substrate Nek7 in the presence of ATP/Mg²⁺. The modification of biotinylated Nek7 was detected using an available antibody that specifically recognizes phosphorylated Nek7 and streptavidin-coated AlphaScreen Donor beads plus AlphaScreen Protein A Acceptor beads (from PerkinElmer).

We screened a total of 1,165 compounds from 5 different compound collections: 1) NIH clinical collection, (2) Kinase collection, (3) CeMM library of unique drugs, (4) Collection of anti-cancer drugs and (5) Epigenetic compounds at concentrations ranging from 20 to 100 uM (0.2% DMSO). The positive control Staurosporin, a known protein kinase inhibitor was used at an assay concentration of 40 uM (0.2% DMSO).

Hits are defined as compounds that give > 50% inhibition compared to the DMSO controls. Thus, using these criteria, we identified 219 hits.

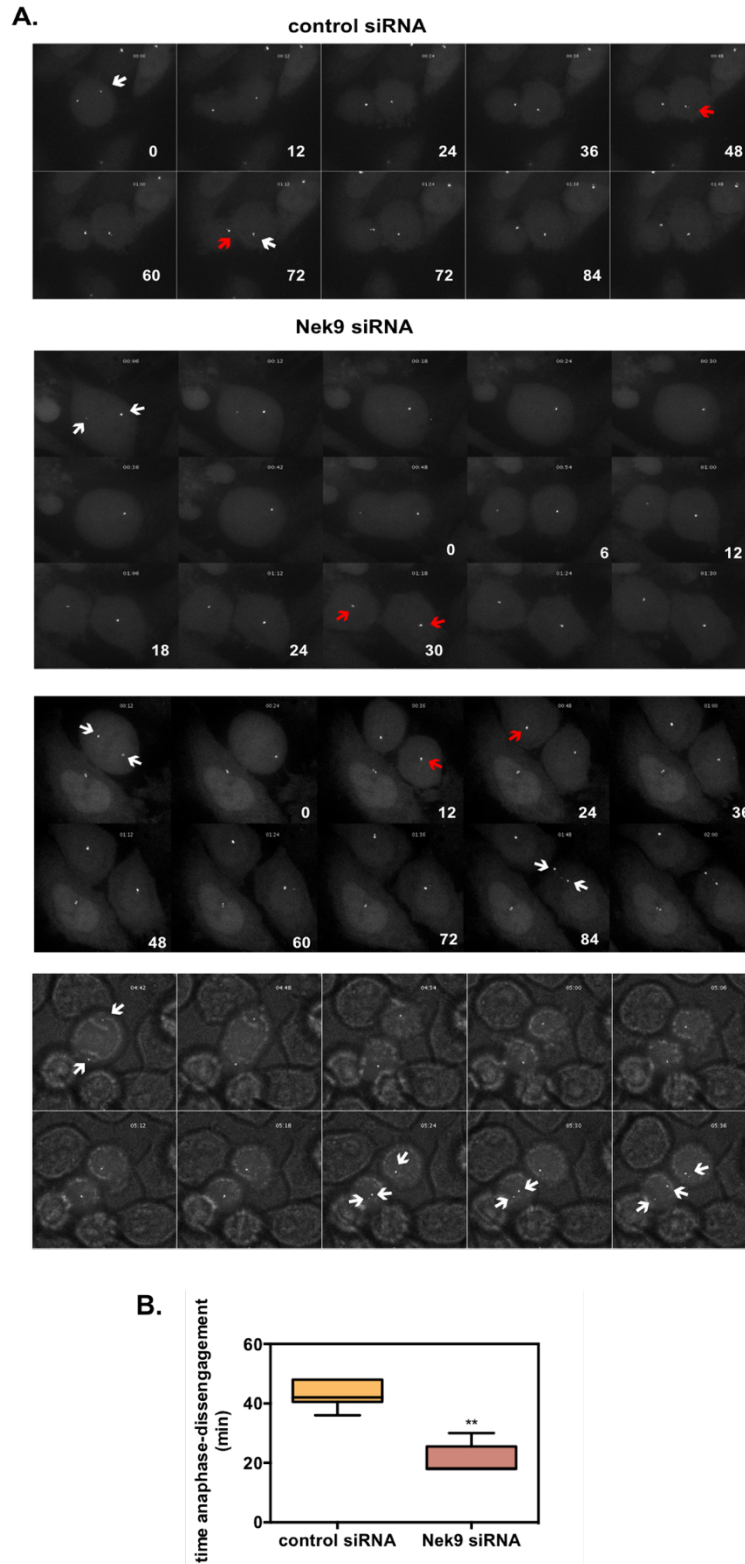
As an initial step, a positive obtained from the screen has been tested *in vivo* in human cells for its capability to mimic our observed phenotype of Nek9 inhibition, effectively mimicking the effects of depleting Nek9. However, more experiments have to be one with this and other compounds found in the screening.

Nek9 may be involved in centriole disengagement

It was described that orthogonal orientation of the centrioles was not the feature preventing centriole reduplication in human cells. Rather, centriole block to reduplication relies on a close association between a mother and a daughter centriole, which is established at the time of daughter centriole formation and is relieved in a Plk1-dependent manner. However, several centrosomal proteins, such as CPAP and centrobilin, have been reported to be required for the stabilization and elongation of daughter centrioles and that in its absence, cells cannot respond to Plk1 activity at the centrosome, preventing Plk1-dependent centriole distancing and disengagement (Shukla et al., 2015). We already mentioned the possibility of Nek9 role in G1 removing centrobilin from the centriole formed in the previous cycle. Hence, centrobilin accumulation upon Nek9 absence could induce premature centriole disengagement at the end of mitosis.

We followed the behavior of centrioles by long-term time-lapse microscopy in a U2OS GFP-centrin stable cell line after 48h control or Nek9 siRNA transfection. This analysis revealed that in Nek9 absence, centrioles disengaged prematurely after mitotic division, around 20 min after anaphase onset vs 40 min in control cells (Supplementary figure 4). Due to centrobilin accumulation in centrioles of cells where Nek9 had been depleted, it could be possible that Plk1-dependent daughter centrioles maturation occurs faster which leads to accumulation of PCM components around its proximal parts, stimulating distancing from the mother centrioles. Thus, mother centriole can initiate a new round of centriole duplication if the original daughter centriole is distanced enough.

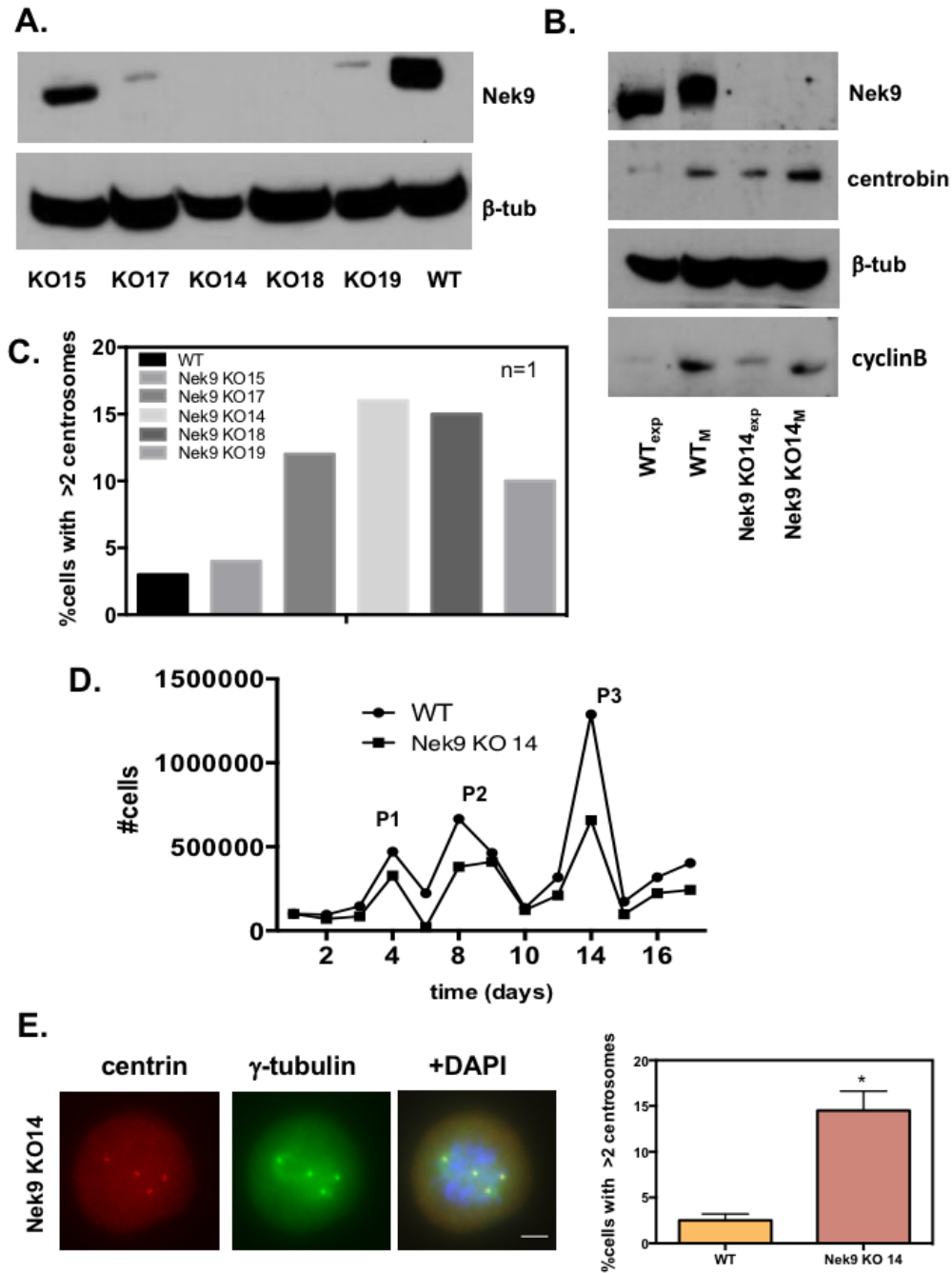
ADDITIONAL RESULTS



Supplementary figure 1: **A)** Representative time lapse images of mitotic U2OS GFP-centrin stable cell line 48h post-transfection of control or Nek9 siRNAs. Images were taken every 6 min (one experiment). Arrowhead pointing centrioles. **B)** Time (min) between anaphase onset and centriole disengagement (n=6 cells) and time (hours) in mitosis, since the cell became spherical until it divided in two cells (n=20 cells).

CRISPR/cas9, an additional model for Nek9 disruption

In parallel, we created a Nek9-depleted U2OS cell line by CRISPR/cas9 observing a phenotype similar i.e. centrosome amplification to that of genetically eliminating Nek9 expression in MEFs. We generated five different KO clones (KO 14, 15, 17,18 and 19) and its respective WT and analyzed the percentage of cells with more than two centrosomes. KO 15 did not amplify centrosomes, something that we expected since it still expressed Nek9, as shown by western blot. All others amplified centrosomes to a greater or lesser extent. We selected KO 14, the one with the highest amplification (>15% cells with >2 centrosomes) to perform next experiments. As previously shown for Nek9 siRNA U2OS, Nek9 abrogation resulted in proliferation defects. We did a growth curve with KO 14 during 17 days and 3 cell passages, observing a lower growth capacity in comparison with WT. At passage 2 and 3 we also quantified centrosomes, confirming the amplification phenotype (15% cells with >2 centrosomes). Finally, as Nek9 is activated in mitosis, we performed a mitotic arrest in U2OS KO 14 cells, that were incubated with 250 ng/ml nocodazole for 16 hours. Cells in mitosis (M) were collected after mitotic shake off, and untreated exponential growing cells (Exp) were used as a control. Mitotic arrest was confirmed by cyclinB expression. In the same way as in MEFs and U2OS Nek9-depleted centrin protein levels increased upon Nek9 depletion, especially in mitosis (Supplementary figure 2).



Supplementary figure 2: Generation and characterization of a CRISPR/SpCas9 Nek9 KO U2OS cell line. **A)** Representative western Blot showing Nek9 absence in different cell clones. β -tubulin is used as a loading control; **B)** U2OS KO cells were incubated with nocodazole (ND, 250 ng/ml) for 16 hours. Cells in mitosis (M) were collected after mitotic shake off, and cell extracts were analyzed by western blot with the indicated antibodies. Cyclin B levels are used as a marker for mitosis. β -tubulin is used as a loading control; **C)** Percentage of cells with more than 2 centrosomes observed in different KO clones, quantified using γ -tubulin antibody as a centrosome marker (one experiment, 100 cells); **D)** Growth curve during 3 cell passages in Nek9 KO cells (clon 14) compared with control cells. **E)** Representative immunofluorescence images of Nek9 KO (clon 14) immunostained with the indicated antibodies are shown. Frequency of cells with more than 2 centrosomes (n=2, 100 cells per experiment, an unpaired t-test was performed). Scale bar 5 μ m.

DISCUSSION

DISCUSSION

Nek9 null embryos die at early post-implantation stage

In the last few years, interference with Nek9 in different systems has suggested that the kinase has key roles during mitotic progression and more specifically in spindle organization. Our group have shown that expression of inactive forms of the kinase strongly interferes with cell division and in most cases results in cell death and that microinjection of anti-Nek9 antibodies into mitotic cells results in the disruption of spindle organization and prometaphase arrest or in some cases aberrant chromosome segregation followed by mitotic catastrophe or aneuploidy (Roig et al., 2002).

Also, Nek9 siRNA depletion results in a rapid increase of the percentage of cells in G2/M with a decreased spindle microtubule density and defects in chromosome alignment (Bertran et al., 2011; Sdelci et al., 2012). Thus, elimination of Nek9 expression has strong phenotypic results. We sought to study this in detail in the present thesis. To do so, we isolated *Nek9^{flox/flox}*;UBC-cre/ERT2 MEFs cells from mice and temporarily cultured them in the presence or absence of 4-hydroxytamoxifen (4-OHT) to achieve acute abrogation of Nek9 expression. In parallel we have also used siRNA to deplete Nek9 in human cells.

Nek9 is downstream of Plk1 in the mitotic signaling network (Bertran et al., 2011), and it has been described that depletion of both alleles of Plk1 in mice results in embryonic lethality after the eight-cell stage due to extensive mitotic aberrations (Lu et al., 2008b; Wachowicz et al., 2016). Something similar happen with Aurora A, another mitotic serine/threonine kinase that localize at centrosomes and mitotic spindles. Aurora A null mice die early during embryonic development before the 16-cell stage because of spindle assembly problems (Lu et al., 2008c). Thus, we wondered whether Nek9 depletion could have a similar effect. However, in the case of Nek9,

embryos did not arrest in any specific stage. Although some the *Nek9*^{-/-} embryos didn't reach blastocyst stage, others developed as normal blastocysts (although in some cases with mitotic abnormalities) and may thus implant and die at some time before birth, as suggested by the absence of viable embryos at E12.5. Thus, we guess that Nek9 ablation is lethal in embryos at early post-implantation stages, similar to what happens in the case of kinesin Eg5, which is phosphorylated by Nek6/7 (activated by Nek9), necessary for prophase centrosome separation and normal mitotic spindle formation (Bertran et al., 2011; Eibes et al., 2018). Eg5 heterozygous mice, that are healthy, fertile, and show no detectable phenotype, whereas *Eg5*^{-/-} embryos die during early embryogenesis, prior to the implantation stage (Chauvière et al., 2008). Post-implantation studies will be needed to be carried out by isolating embryos from E8.5 to E14.5 and performing similar analysis to further study this. Additional histological studies of deciduas at E5.5-E8.5 could also be performed.

It is interesting to note that 13,3% of the mitosis in *Nek9*^{+/^{trap} embryos also showed multipolar spindles, however the number of born embryos was similar to the expected one (in contrast to *Nek9*^{trap/trap} animals). This suggests that the mitotic abnormalities observed did not enough affect viability in a negative manner. However, in *Nek9*^{trap/trap} lack of both Nek9 alleles probably results in an excess of mitotic abnormalities that could generate aneuploidy and its consequent genomic instability and DNA damage. The presence of aneuploidy is related to abnormalities in centrosome number and mitotic errors, that in fact is what we observed in *Nek9*^{+/^{trap} MEFs. Our preliminary results showed a slightly increase in the number of centrosomes in respect to *Nek9*^{+/⁺ with cell passages (data not shown), which therefore, could explain the mitotic abnormalities and premature lethality in *Nek9* KO embryos. Curiously, the same phenotype is observed after abrogating Nek9 expression in *Nek9*^{flox/flox}, MEFs,}}}

namely, extra centrosomes that generate mitotic errors, which at the end results in the appearance of aneuploidy.

In an extensive study of mouse gene knockouts, it has recently been described that *Nek9* knockout was viable at E9.5 but with a small or absent trophoblast compartment. Then, at or after mid-gestation (embryonic days 9.5–14.5) animals die because of placental dysmorphologies, such as small placenta, reduced cellular density, labyrinth vascularization defects and hemorrhagic areas (Perez-Garcia et al., 2018).

Recent reports have shown that recessive germline *Nek9* mutations cause skeletal disease. Homozygous nonsense mutations in *Nek9*, c.1489C>T (p.Arg497*), were found in aborted fetuses with a lethal skeletal dysplasia in two Irish Traveller families (Casey et al., 2016). In addition, a single affected individual has also been described with a homozygous *Nek9* mutation, demonstrating joint contracture and Legg-Calvé-Perthes disease (MIM: 150600), a form of avascular necrosis of the femoral head. Two members of this same family had a missense *Nek9* mutation, c.2042G>A; p.Arg681His, that provoke arthrogryposis, perthes disease, and upward gaze palsy (MIM:614262), a disease characterized by persistent joints flexure or contracture (Shaheen et al., 2016). As previously described, *Nek9* gain of function mutations are involved in nevus comedonicus (NC), a severe form of acne, disrupting normal follicular differentiation. Thus, *Nek9* has a role in the epidermis and the follicular homeostasis, but notably, NC syndrome also characterized by features skeletal abnormalities, including scoliosis, syndactyly or absence of fingers, and supernumerary digits. Somatic *Nek9* mutation in bone progenitors could explain all these described findings (Levinsohn et al., 2016), and could be related to the *Nek9* KO embryos lethality.

Nek9 haploinsufficiency mouse model

Nek9 haploinsufficiency resulted in chromosome segregation defects and in the generation of aneuploid cells. *Nek9*^{+/-} mice are also prone to develop a wide spectrum of tumor types, suggesting that Nek9 may function as a tumor suppressor protecting from genomic instability. A similar increase in the development of spontaneous tumors has been observed in haploinsufficient mouse models of other mitotic and kinetochore genes as well as for mitotic checkpoint genes including Aurora A, CenpE, Mad2, or Cdh1 (Schvartzman et al., 2010). *Nek9*^{+/-} mice cells accumulate aneuploidy with age indicating that their tissues are genetically unstable and has the origin in centrosomes abnormalities. This feature correlates with increased susceptibility to tumor development, supporting the idea that Nek9 deregulation might eventually act as a driving force of tumor development by the induction of aneuploidy, something that would be exacerbated in a p53 null background. Despite these defects, at the end, *Nek9*^{+/-} mice developed normally and are fertile, so being Nek9 an essential kinase for cell proliferation and animal life, a minimal threshold of Nek9 expression or function is sufficient for cell progression and thereby an interesting observation given the current relevance of Nek9 as a putative cancer target.

As it was expected, the frequency of tumors in animals heterozygous for Nek9 was increased in animals with compromised p53 expression. In contrast, Kurioka et al., 2014 observed that Nek9 depletion selectively inhibited proliferation in p53-deficient cancer cells. They showed that patients with intact Nek9 and mutant p53 proteins exhibited significantly poorer prognoses, suggesting that expression of Nek9 promotes tumor growth. However, they use siRNA to deplete Nek9, which cannot be compared with expressing Nek9 in heterozygosis. In the other hand, what

we noticed was that in *Trp53*^{-/+} animals Nek9 WT induce tumors while Nek9 in heterozygosity protect animals from tumorigenesis which goes more in the line of Kurioka et al., 2014 data.

Aneuploidy by promoting genomic instability and DNA damage, was proposed as a main cause of cancer, based on the fact that aneuploidy is a common characteristic of tumors (Weaver and Cleveland, 2008). Nek9 in heterozygosis results in aneuploidy as shown by the presence on micronuclei in circulating erythrocytes and the gain or loss of chromosomes observed in splenocytes from Nek9^{+/*trap*}, even at early stages, one month after birth. However, the observed aneuploidy is not reflected in the number of tumors observed in mice. It is now clear that the effects of aneuploidy are more complex than initially proposed. Aneuploidy can drive tumorigenesis, but not necessarily. Sometimes, aneuploidy actually suppresses tumors. Three factors have to be taken into account: the combination of chromosomes in the cell, if the cell is stably aneuploid or contains a karyotype that is evolving due to further chromosomal missegregation and the additional mutations (Weaver and Cleveland, 2008). For example, Li et al., 2010 reported that aneuploidy increase levels of intracellular reactive oxygen species, producing oxidative DNA damage, which activates ataxia-telangiectasia mutated (ATM) and finally induce p53 activation. Thus, although there is a concordance of aneuploidy and p53 absence in many tumors, the presence of aneuploid cells in some normal tissues indicates that there are exceptions to the involvement of p53 in aneuploid cells and specific interaction of the karyotype with the genetic context in different tissues may be important in how cells respond to aneuploidy (Thompson and Compton, 2010).

Other factor to consider is the severity of the aneuploidy. Highly aneuploid cells are removed by p53-mediated apoptosis, mildly aneuploid

cells may enter p53-mediated senescence and slightly aneuploid cells are difficult to transform. Hence, slightly and mildly aneuploid cells do not show tumorigenic risks. Tumors can develop only when some of the highly aneuploid cells lose p53. Upon p53 absence, these cells can divide, acquire additional mutations and start tumor generation. However, it takes a long time for tumors to develop in mice and the penetrance usually is not complete. However, when p53 is removed from the beginning, tumors develop faster and the penetrance highly increase (Li et al., 2010).

Impact in the centriole duplication cycle after Nek9 cell abrogation

We have done a complete characterization of the phenotype from Nek9 cell abrogation. Our results show that eliminating Nek9 results in problems in proliferation, abnormal mitosis and centrosome amplification, without being associated to multinucleation or polyploidy. Based on that, and without completely ruling out that other factors related to the different functions of Nek9 may be implicated, we think centrosome amplification is the major cause of the observed mitotic aberrations and subsequent aneuploidy and tumor predisposition in aged *Nek9*^{+/-} animals, as well as the observed aneuploidy in Nek-9 deficient cells.

Centrosome amplification in Nek9-depleted cells was not a result of S-phase arrest as we treated control and Nek9-depleted cells with Hydroxyurea (HU) observing an accumulative effect to the one caused by Nek9 abrogation (data not shown). These extra centrosomes have a normal PCM structure with tendency towards a decrease in intensity of some PCM proteins in prophase centrosomes. This could be related to the previously described role of Nek9 during centrosome maturation (Sdelci et al., 2012,

note that this study was done in HeLa cells) and may contribute to the observed mitotic abnormalities. Another explanation could be that due to the increase in the number of centrosomes, the PCM is redistributed among them.

We also confirmed that amplified centrosomes were not a consequence of fragmentation as they contained extra centrioles, that additionally had different configurations including paired centrioles, single centrioles and clusters of three or more centrioles. The presence of singlet centrioles could indicate that both centriole engagement and cohesion failed, opening the possibility of a deregulation in G1 centriole disengagement process that licenses the centrioles for centriole duplication instead of a failure in the duplication process per se. This may be related to the observation that HeLa cells do not amplify centrioles upon Nek9 downregulation. These cells have been shown not to amplify centrioles during S phase arrest as a result of Plk1 not being active in S, preventing centriole licensing and reduplication (Lončarek et al., 2010).

Our results suggest that centriole overduplication in cells lacking Nek9 is Plk4-dependent and use the classical pathway of centriole duplication. However, the extra centrioles are not all daughters or they don't contain the cartwheel protein SAS-6 or SAS-4/CPAP. The cartwheel is located at the proximal part of a centriole, coincident with centriolar proteins SAS-6 and STIL. In particular, SAS-6 has been shown to form the scaffold of the cartwheel. While the cartwheel is essential for centriole assembly, it is removed from newborn centrioles at the end of the cell cycle when they are converted to centrosomes. Centriole disengagement and centriole-to-centrosome conversion occur at late mitosis and enable centriole duplication, so it is possible that cartwheel removal may function in the same process. In fact, in unconverted or unmodified centrioles, resulted

from inhibiting Plk1-dependent conversion, cartwheel removal also fails. Thus, centriole duplication cannot occur even when they are disengaged (Wang et al., 2011).

Our data matches with the hypothesis that amplified centrioles found after Nek9 depletion lack SAS-6 as a result of the protein being immediately lost from newborn centrioles, which become mothers (modified or converted) and acquire the capability to reduplicate whether or not they are disengaged, although in fact, they probably disengage prematurely.

In Nek9 depleted cells, an abnormally high percentage of centrioles are positive for centrobilin. It is possible that, at some point, as a result of this centrioles lose engagement and become re-licensed to duplicate, as evidenced not only by the presence of singlet centrioles both C-Nap1 and centrobilin positive but also by the increased numbers of diplosomes (centriole pairs) that were both centrobilin positive. Somehow, an excess of centrobilin results in ‘daughter’ centrioles that became mothers and can reduplicate generating more ‘daughters’.

In view of our SILAC results, Nek9 may regulate centrobilin degradation by phosphorylation, so Nek9 absence may possibly cause an accumulation of centrobilin, disengagement, and result in the generation of new centrioles. In fact, we have confirmed Nek9-centrobilin interaction by immunoprecipitation. In order to define the possible Nek9 phosphorylation region within the centrobilin polypeptide, in collaboration with Nuria Gallisà, we carried out an *in vitro* kinase assay with N-terminal (1-200 aa) and C-terminal (590-903 aa) centrobilin fusion proteins as substrates in presence or absence of Nek9 recombinant protein, and preliminary results pointed to a possible Nek9-dependent phosphorylation of centrobilin (not shown).

Strikingly, we discovered that there was no association between GFP-centrobin[4A] mutant and Nek9, suggesting that for the interaction to take place, centrobin should be already phosphorylated.

Despite our great effort to generate GFP-centrobin mutants we could not manage to reach any conclusion, as none of the mutants had a significantly altered expression level or localization at centrioles (not shown) as compared to wild type protein, and centriole amplification was similar in all the mutants. As levels of centrobin at centrioles are small, this could be explained by the effects of overexpression, making difficult to observe any differences. In addition, we found difficulties detecting centrobin by WB apart from the overexpression, the results obtained were variable although they seem to indicate that centrobin levels increased upon Nek9 depletion and decrease with centrobin siRNA transfection.

As a possible molecular mechanism that explains our observations, we would like to point out that using proximity-dependent biotinylation (BioID), (Gupta et al., 2015) identified TRIM37 (an E3 ubiquitin ligase) as a centrobin interactor. Increasing evidence indicated that this protein is involved in the tumorigenesis of several cancer types (Brodtkorb et al., 2014). Interestingly, it is required to prevent centriole reduplication. Probably acts by ubiquitinating positive regulators of centriole reduplication (Balestra et al., 2013). Consistent with that, *TRIM37* knockout cells formed ectopic centrosomal-component foci that contain centrosomal components. Thus, TRIM37 has an important role in ensuring that Plk4 recruitment and PCM assembly occur only on the scaffold provided by mother centriole (Meitinger et al., 2016). In view of that, we hypothesize that TRIM37 could ubiquitinate centrobin, as it has some described ubiquitination sites, somehow in a way that depends on Nek9 phosphorylation, resulting in its release previous to the next centriole duplication phase. Thus, upon Nek9 depletion,

TRIM37 could not ubiquitinate centrin, that remains in the daughter centriole allowing new rounds of centriole reduplication.

Altogether, our results show that the depletion of Nek9 results in centrosome amplification. We propose a model in which the lack of Nek9 results in the accumulation of centrin at centrioles and this is accompanied with an excess centriole production. Extra centrioles would result in aneuploidy in cells and tumors at the organism level. We discuss the possibility that in Nek9-depleted cells centrioles lose engagement and become re-licensed to duplicate, possibly as a result of an excess of centrin, as evidenced not only by the presence of singlet centrioles but also by the increased numbers of centrin-positive pairs. In view of our SILAC and kinase assay results, Nek9 may regulate centrin degradation by phosphorylation, possibly through the control of its ubiquitination, so the absence of Nek9 may possibly cause an accumulation of centrin, centriole disengagement and duplication licensing, and result in the generation of new centrioles (Figure 50).

DISCUSSION

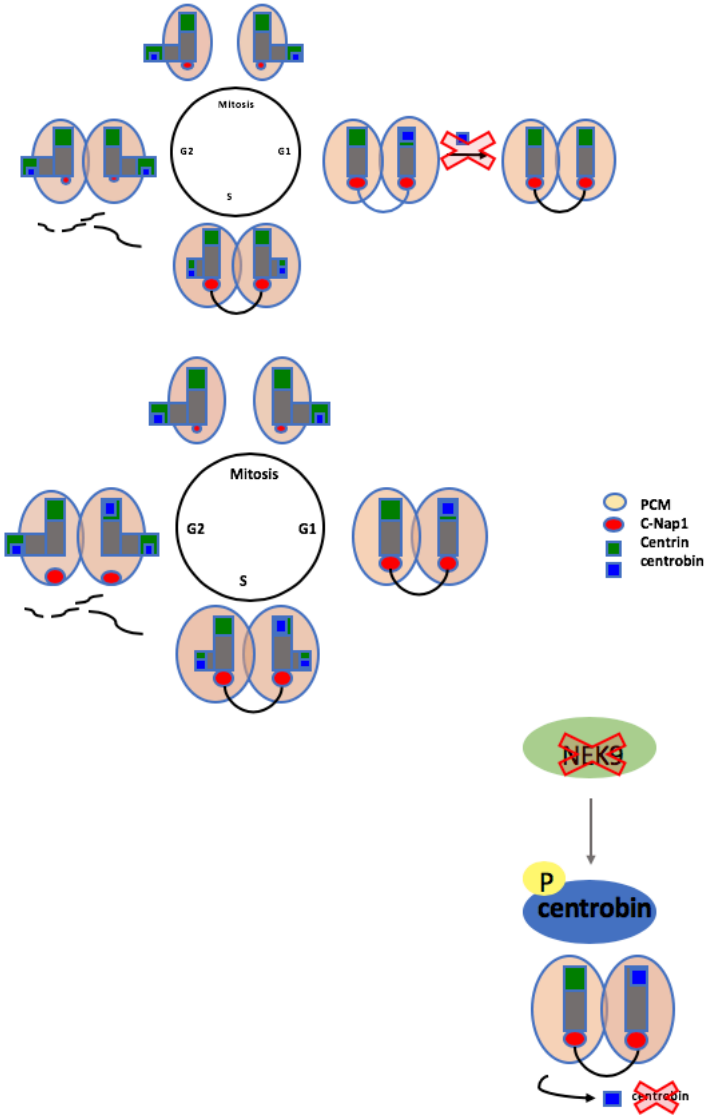


Figure 50: Proposed model for Nek9-centrobin function.

DISCUSSION

CONCLUSIONS

CONCLUSIONS

CONCLUSIONS

1. Nek9 abrogation is lethal in embryos during early development.
2. Pre-implantation embryos lacking Nek9 shows mitotic defects.
3. Nek9 haploinsufficiency results in chromosome segregation defects and the onset of aneuploidy, and this may be related to the apparition of tumors.
4. Tumor apparition frequency is remarkably increased in animals with compromised p53 expression.
5. Nek9 depletion impairs normal cell cycle progression and results in mitotic arrest.
6. Abnormal levels of Nek9 lead to the apparition of abnormal mitotic spindles.
7. Cell lacking Nek9 become aneuploidy.
8. Multiple centrosomes with abnormal centriole configurations are observed both in genetically engineered MEFs and human cells where Nek9 is absent or downregulated.
9. Centrosome amplification is not a result of fragmentation or of cytokinesis failure.
10. Nek9 depletion may cause an accumulation or a defective removal of centrin from new mother centrioles.
11. Extra centrioles are generated in Plk4-dependent manner.
12. Extra centrioles are “cartwheel-less” centrioles, lacking SAS-6
13. Centrin positive centrioles may favor the production of shorter cilia and multi-ciliated cells.
14. Centrioles with an excess of centrin may lose engagement and become re-licensed to duplicate, resulting in centriole amplification.
15. Centrin and Nek9 interact *in vivo*.
16. Nek9 may regulate centrin degradation by phosphorylation.

CONCLUSIONS

REFERENCES

REFERENCES

- Anderhub, S.J., Krämer, A., and Maier, B. (2012). Centrosome amplification in tumorigenesis. *Cancer Lett.* 322, 8–17.
- Andersen, J.S., Wilkinson, C.J., Mayor, T., Mortensen, P., Nigg, E.A., and Mann, M. (2003). Proteomic characterization of the human centrosome by protein correlation profiling. *Nature* 426, 570.
- Archambault, V., and Glover, D.M. (2009). Polo-like kinases: conservation and divergence in their functions and regulation. *Nat. Rev. Mol. Cell Biol.* 10, 265–275.
- Arquint, C., and Nigg, E.A. (2016). The PLK4–STIL–SAS-6 module at the core of centriole duplication. *Biochem. Soc. Trans.* 44, 1253–1263.
- Arquint, C., Sonnen, K.F., Stierhof, Y.-D., and Nigg, E.A. (2012). Cell-cycle-regulated expression of STIL controls centriole number in human cells. *J Cell Sci* 125, 1342–1352.
- Arquint, C., Gabryjonczyk, A.-M., Imseng, S., Böhm, R., Sauer, E., Hiller, S., Nigg, E.A., and Maier, T. (2015). STIL binding to Polo-box 3 of PLK4 regulates centriole duplication. *ELife* 4, e07888.
- Aydogan, M.G., Wainman, A., Saurya, S., Steinacker, T.L., Caballe, A., Novak, Z.A., Baumbach, J., Muschalik, N., and Raff, J.W. (2018). A homeostatic clock sets daughter centriole size in flies. *J Cell Biol* jcb.201801014.
- Azimzadeh, J. (2014). Exploring the evolutionary history of centrosomes. *Philos. Trans. R. Soc. B Biol. Sci.* 369.
- Azimzadeh, J., and Marshall, W.F. (2010). Building the Centriole. *Curr. Biol.* CB 20, R816–R825.
- Bahmanyar, S., Kaplan, D.D., DeLuca, J.G., Giddings, T.H., O’Toole, E.T., Winey, M., Salmon, E.D., Casey, P.J., Nelson, W.J., and Barth, A.I.M. (2008). β -Catenin is a Nek2 substrate involved in centrosome separation. *Genes Dev.* 22, 91–105.
- Balczon, R., Bao, L., Zimmer, W.E., Brown, K., Zinkowski, R.P., and Brinkley, B.R. (1995). Dissociation of centrosome replication events from cycles of DNA synthesis and mitotic division in hydroxyurea-arrested Chinese hamster ovary cells. *J. Cell Biol.* 130, 105–115.
- Balestra, F.R., Strnad, P., Flückiger, I., and Gönczy, P. (2013). Discovering regulators of centriole biogenesis through siRNA-based functional genomics in human cells. *Dev. Cell* 25, 555–571.
- Banterle, N., and Gönczy, P. (2017). Centriole Biogenesis: From Identifying the Characters to Understanding the Plot. *Annu. Rev. Cell Dev. Biol.* 33, 23–

49.

Barr, A.R., and Gergely, F. (2007). Aurora-A: the maker and breaker of spindle poles. *J. Cell Sci.* *120*, 2987–2996.

Barr, F.A., Silljé, H.H.W., and Nigg, E.A. (2004). Polo-like kinases and the orchestration of cell division. *Nat. Rev. Mol. Cell Biol.* *5*, 429–441.

Bartek, J., and Lukas, J. (2003). Chk1 and Chk2 kinases in checkpoint control and cancer. *Cancer Cell* *3*, 421–429.

Basei, F.L., Meirelles, G.V., Righetto, G.L., dos Santos Migueleti, D.L., Smetana, J.H.C., and Kobarg, J. (2015). New interaction partners for Nek4.1 and Nek4.2 isoforms: from the DNA damage response to RNA splicing. *Proteome Sci.* *13*, 11.

Baumann, C., Körner, R., Hofmann, K., and Nigg, E.A. (2007). PICH, a centromere-associated SNF2 family ATPase, is regulated by Plk1 and required for the spindle checkpoint. *Cell* *128*, 101–114.

Bayliss, R., Sardon, T., Vernos, I., and Conti, E. (2003). Structural Basis of Aurora-A Activation by TPX2 at the Mitotic Spindle. *Mol. Cell* *12*, 851–862.

Behrends, C., Sowa, M.E., Gygi, S.P., and Harper, J.W. (2010). Network organization of the human autophagy system. *Nature* *466*, 68–76.

Belham, C., Comb, M.J., and Avruch, J. (2001). Identification of the NIMA family kinases NEK6/7 as regulators of the p70 ribosomal S6 kinase. *Curr. Biol.* *11*, 1155–1167.

Belham, C., Roig, J., Caldwell, J. a, Aoyama, Y., Kemp, B.E., Comb, M., and Avruch, J. (2003). A mitotic cascade of NIMA family kinases. Ncrcc1/Nek9 activates the Nek6 and Nek7 kinases. *J. Biol. Chem.* *278*, 34897–34909.

Bertran, M.T., Sdelci, S., Regué, L., Avruch, J., Caelles, C., and Roig, J. (2011). Nek9 is a Plk1-activated kinase that controls early centrosome separation through Nek6/7 and Eg5. *EMBO J.* *30*, 2634–2647.

Bettencourt-Dias, M. (2013). Q&A: Who needs a centrosome? *BMC Biol.* *11*, 28.

Bettencourt-Dias, M., and Glover, D.M. (2007). Centrosome biogenesis and function: centrosomics brings new understanding. *Nat. Rev. Mol. Cell Biol.* *8*, 451.

Bettencourt-Dias, M., Rodrigues-Martins, A., Carpenter, L., Riparbelli, M., Lehmann, L., Gatt, M.K., Carmo, N., Balloux, F., Callaini, G., and Glover, D.M. (2005). SAK/PLK4 is required for centriole duplication and flagella

- development. *Curr. Biol.* *CB 15*, 2199–2207.
- Bettencourt-Dias, M., Hildebrandt, F., Pellman, D., Woods, G., and Godinho, S. (2011). Centrosomes and Cilia in Human Disease. *Trends Genet.* *TIG 27*, 307–315.
- Bhatnagar, S., Gazin, C., Chamberlain, L., Ou, J., Zhu, X., Tushir, J.S., Virbasius, C.-M., Lin, L., Zhu, L.J., Wajapeyee, N., et al. (2014). TRIM37 is a new histone H2A ubiquitin ligase and breast cancer oncoprotein. *Nature* *516*, 116–120.
- Bian, Z., Liao, H., Zhang, Y., Wu, Q., Zhou, H., Yang, Z., Fu, J., Wang, T., Yan, L., Shen, D., et al. (2014). Never in Mitosis Gene A Related Kinase-6 Attenuates Pressure Overload-Induced Activation of the Protein Kinase B Pathway and Cardiac Hypertrophy. *PLOS ONE* *9*, e96095.
- Blangy, A., Lane, H.A., d'Hérin, P., Harper, M., Kress, M., and Nigg, E.A. (1995). Phosphorylation by p34cdc2 regulates spindle association of human Eg5, a kinesin-related motor essential for bipolar spindle formation in vivo. *Cell* *83*, 1159–1169.
- Bolanos-Garcia, V.M. (2005). Aurora kinases. *Int. J. Biochem. Cell Biol.* *37*, 1572–1577.
- Bornens, M. (2012). The Centrosome in Cells and Organisms. *Science* *335*, 422–426.
- Bourke, E., Dodson, H., Merdes, A., Cuffe, L., Zachos, G., Walker, M., Gillespie, D., and Morrison, C.G. (2007). DNA damage induces Chk1-dependent centrosome amplification. *EMBO Rep* *603–609*.
- Boussif, O., Lezoualc'h, F., Zanta, M.A., Mergny, M.D., Scherman, D., Demeneix, B., and Behr, J.P. (1995). A versatile vector for gene and oligonucleotide transfer into cells in culture and in vivo: polyethylenimine. *Proc. Natl. Acad. Sci. U. S. A.* *92*, 7297–7301.
- Brodtkorb, M., Lingjærde, O.C., Huse, K., Trøen, G., Hystad, M., Hilden, V.I., Myklebust, J.H., Leich, E., Rosenwald, A., Delabie, J., et al. (2014). Whole-genome integrative analysis reveals expression signatures predicting transformation in follicular lymphoma. *Blood* *123*, 1051–1054.
- de Cárcer, G., Manning, G., and Malumbres, M. (2011). From Plk1 to Plk5. *Cell Cycle* *10*, 2255–2262.
- Carmena, M., and Earnshaw, W.C. (2003). The cellular geography of Aurora kinases. *Nat. Rev. Mol. Cell Biol.* *4*, 842–854.
- Carmena, M., Ruchaud, S., and Earnshaw, W.C. (2009). Making the Auroras glow: regulation of Aurora A and B kinase function by interacting proteins.

- Curr. Opin. Cell Biol. *21*, 796–805.
- Casey, J.P., Brennan, K., Scheidel, N., McGettigan, P., Lavin, P.T., Carter, S., Ennis, S., Dorkins, H., Ghali, N., Blacque, O.E., et al. (2016). Recessive NEK9 mutation causes a lethal skeletal dysplasia with evidence of cell cycle and ciliary defects. *Hum. Mol. Genet.* *25*, 1824–1835.
- Chan, J.Y. (2011). A Clinical Overview of Centrosome Amplification in Human Cancers. *Int. J. Biol. Sci.* *7*, 1122–1144.
- Chan, E.H.Y., Santamaria, A., Silljé, H.H.W., and Nigg, E.A. (2008). Plk1 regulates mitotic Aurora A function through β TrCP-dependent degradation of hBora. *Chromosoma* *117*, 457–469.
- Chang, J., Baloh, R.H., and Milbrandt, J. (2009). The NIMA-family kinase Nek3 regulates microtubule acetylation in neurons. *J. Cell Sci.* *122*, 2274–2282.
- Chauvière, M., Kress, C., and Kress, M. (2008). Disruption of the mitotic kinesin Eg5 gene (*Knsl1*) results in early embryonic lethality. *Biochem. Biophys. Res. Commun.* *372*, 513–519.
- Chen, H., Mohan, P., Jiang, J., Nemirovsky, O., He, D., Fleisch, M.C., Niederacher, D., Pilarski, L.M., Lim, C.J., and Maxwell, C.A. (2014). Spatial regulation of Aurora A activity during mitotic spindle assembly requires RHAMM to correctly localize TPX2. *Cell Cycle Georget. Tex* *13*, 2248–2261.
- Chen, Y., Chen, P.-L., Chen, C.-F., Jiang, X., and Riley, D.J. (2008). Never-in-mitosis related kinase 1 functions in DNA damage response and checkpoint control. *Cell Cycle Georget. Tex* *7*, 3194–3201.
- Cohen, P. (2002). The origins of protein phosphorylation. *Nat. Cell Biol.* *4*, E127–30.
- Cohen, S., Aizer, A., Shav-Tal, Y., Yanai, A., and Motro, B. (2013). Nek7 kinase accelerates microtubule dynamic instability. *Biochim. Biophys. Acta* *1833*, 1104–1113.
- Cross, R.A., and McAinsh, A. (2014). Prime movers: the mechanochemistry of mitotic kinesins. *Nat. Rev. Mol. Cell Biol.* *15*, 257–271.
- Cullati, S.N., Kabeche, L., Kettenbach, A.N., and Gerber, S.A. (2017). A bifurcated signaling cascade of NIMA-related kinases controls distinct kinesins in anaphase. *J Cell Biol jcb.201512055*.
- Cunha-Ferreira, I., Bento, I., and Bettencourt-Dias, M. (2009). From Zero to Many: Control of Centriole Number in Development and Disease. *Traffic* *10*, 482–498.

REFERENCES

- Dasso, M. (2002). The Ran GTPase: theme and variations. *Curr. Biol.* *CB 12*, R502-508.
- Desai, A., and Mitchison*, and T.J. (1997). Microtubule Polymerization Dynamics. *Annu. Rev. Cell Dev. Biol.* *13*, 83–117.
- Dodson, H., Bourke, E., Jeffers, L.J., Vagnarelli, P., Sonoda, E., Takeda, S., Earnshaw, W.C., Merdes, A., and Morrison, C. (2004). Centrosome amplification induced by DNA damage occurs during a prolonged G2 phase and involves ATM. *EMBO J.* *23*, 3864–3873.
- Doles, J., and Hemann, M.T. (2010). NEK4 STATUS INFLUENCES DIFFERENTIAL SENSITIVITY TO MICROTUBULE POISONS. *Cancer Res.* *70*, 1033–1041.
- Donehower, L.A. (1996). The p53-deficient mouse: a model for basic and applied cancer studies. *Semin. Cancer Biol.* *7*, 269–278.
- Donehower, L.A., Harvey, M., Slagle, B.L., McArthur, M.J., Montgomery Jr, C.A., Butel, J.S., and Bradley, A. (1992). Mice deficient for p53 are developmentally normal but susceptible to spontaneous tumours. *Nature* *356*, 215–221.
- Doxsey, S. (2001). Re-evaluating centrosome function. *Nat. Rev. Mol. Cell Biol.* *2*, 688.
- Du, J., Cai, X., Yao, J., Ding, X., Wu, Q., Pei, S., Jiang, K., Zhang, Y., Wang, W., Shi, Y., et al. (2008). The mitotic checkpoint kinase NEK2A regulates kinetochore microtubule attachment stability. *Oncogene* *27*, 4107–4114.
- Duncan, T., and Wakefield, J.G. (2011). 50 ways to build a spindle: the complexity of microtubule generation during mitosis. *Chromosome Res.* *19*, 321.
- Eibes, S., Gallisà-Suñé, N., Rosas-Salvans, M., Martínez-Delgado, P., Vernos, I., and Roig, J. (2018). Nek9 Phosphorylation Defines a New Role for TPX2 in Eg5-Dependent Centrosome Separation before Nuclear Envelope Breakdown. *Curr. Biol.* *28*, 121-129.e4.
- Elia, A.E.H., Cantley, L.C., and Yaffe, M.B. (2003). Proteomic screen finds pSer/pThr-binding domain localizing Plk1 to mitotic substrates. *Science* *299*, 1228–1231.
- Elowe, S., Hümmer, S., Uldschmid, A., Li, X., and Nigg, E.A. (2007). Tension-sensitive Plk1 phosphorylation on BubR1 regulates the stability of kinetochore microtubule interactions. *Genes Dev.* *21*, 2205–2219.
- Endicott, J.A., Noble, M.E.M., and Johnson, L.N. (2012). The structural basis for control of eukaryotic protein kinases. *Annu. Rev. Biochem.* *81*,

587–613.

Eyers, P.A., Erikson, E., Chen, L.G., and Maller, J.L. (2003). A Novel Mechanism for Activation of the Protein Kinase Aurora A. *Curr. Biol.* *13*, 691–697.

Fang, G., Zhang, D., Yin, H., Zheng, L., Bi, X., and Yuan, L. (2014). Centlein mediates an interaction between C-Nap1 and Cep68 to maintain centrosome cohesion. *J. Cell Sci.* *127*, 1631–1639.

Faragher, A.J., and Fry, A.M. (2003). Nek2A kinase stimulates centrosome disjunction and is required for formation of bipolar mitotic spindles. *Mol. Biol. Cell* *14*, 2876–2889.

Feige, E., and Motro, B. (2002). The related murine kinases, Nek6 and Nek7, display distinct patterns of expression. *Mech. Dev.* *110*, 219–223.

Feige, E., Shalom, O., Tsurriel, S., Yissachar, N., and Motro, B. (2006). Nek1 shares structural and functional similarities with NIMA kinase. *Biochim. Biophys. Acta BBA - Mol. Cell Res.* *1763*, 272–281.

Ferez, N.P., Gable, A., and Wadsworth, P. (2010). Mitotic functions of kinesin-5. *Semin. Cell Dev. Biol.* *21*, 255–259.

Firat-Karalar, E.N., and Stearns, T. (2014). The centriole duplication cycle. *Philos. Trans. R. Soc. Lond. B. Biol. Sci.* *369*, 20130460-.

Fletcher, L., Cerniglia, G.J., Yen, T.J., and Muschel, R.J. (2005). Live cell imaging reveals distinct roles in cell cycle regulation for Nek2A and Nek2B. *Biochim. Biophys. Acta BBA - Mol. Cell Res.* *1744*, 89–92.

Fong, C.S., Kim, M., Yang, T.T., Liao, J.-C., and Tsou, M.-F.B. (2014). SAS-6 Assembly Templated by the Lumen of Cartwheel-less Centrioles Precedes Centriole Duplication. *Dev. Cell* *30*, 238–245.

Fry, A.M. (2002). The Nek2 protein kinase: a novel regulator of centrosome structure. *Oncogene* *21*, 6184–6194.

Fry, A.M., Schultz, S.J., Bartek, J., and Nigg, E.A. (1995). Substrate Specificity and Cell Cycle Regulation of the Nek2 Protein Kinase, a Potential Human Homolog of the Mitotic Regulator NIMA of *Aspergillus nidulans*. *J. Biol. Chem.* *270*, 12899–12905.

Fry, A.M., Meraldi, P., and Nigg, E.A. (1998a). A centrosomal function for the human Nek2 protein kinase, a member of the NIMA family of cell cycle regulators. *EMBO J.* *17*, 470–481.

Fry, A.M., Mayor, T., Meraldi, P., Stierhof, Y.-D., Tanaka, K., and Nigg, E.A. (1998b). C-Nap1, a Novel Centrosomal Coiled-Coil Protein and Candidate Substrate of the Cell Cycle-regulated Protein Kinase Nek2. *J. Cell*

Biol. *141*, 1563–1574.

Fry, A.M., O'Regan, L., Sabir, S.R., and Bayliss, R. (2012). Cell cycle regulation by the NEK family of protein kinases. *J. Cell Sci.* *125*, 4423–4433.

Fry, A.M., Bayliss, R., and Roig, J. (2017). Mitotic Regulation by NEK Kinase Networks. *Front. Cell Dev. Biol.* *5*.

Fu, J., and Glover, D.M. (2012). Structured illumination of the interface between centriole and peri-centriolar material. *Open Biol.* *2*, 120104.

Fu, G., Ding, X., Yuan, K., Aikhionbare, F., Yao, J., Cai, X., Jiang, K., and Yao, X. (2007). Phosphorylation of human Sgo1 by NEK2A is essential for chromosome congression in mitosis. *Cell Res.* *17*, 608–618.

Fu, J., Lipinszki, Z., Rangone, H., Min, M., Mykura, C., Chao-Chu, J., Schneider, S., Dzhindzhev, N.S., Gottardo, M., Riparbelli, M.G., et al. (2015a). Conserved molecular interactions in centriole-to-centrosome conversion. *Nat. Cell Biol.*

Fu, J., Hagan, I.M., and Glover, D.M. (2015b). The Centrosome and Its Duplication Cycle. *Cold Spring Harb. Perspect. Biol.* *7*, a015800.

Fukasawa, K., Choi, T., Kuriyama, R., Rulong, S., and Vande Woude, G.F. (1996). Abnormal centrosome amplification in the absence of p53. *Science* *271*, 1744–1747.

Ganem, N.J., and Pellman, D. (2012). Linking abnormal mitosis to the acquisition of DNA damage. *J Cell Biol* *199*, 871–881.

Ganem, N.J., Godinho, S.A., and Pellman, D. (2009). A Mechanism Linking Extra Centrosomes to Chromosomal Instability. *Nature* *460*, 278–282.

Glover, D.M., Leibowitz, M.H., McLean, D.A., and Parry, H. (1995). Mutations in aurora prevent centrosome separation leading to the formation of monopolar spindles. *Cell* *81*, 95–105.

Godinho, S.A., and Pellman, D. (2014). Causes and consequences of centrosome abnormalities in cancer. *Philos. Trans. R. Soc. Lond. B. Biol. Sci.* *369*, 20130467-.

Gönczy, P. (2012). Towards a molecular architecture of centriole assembly. *Nat. Rev. Mol. Cell Biol.* *13*, 425–435.

Gönczy, P. (2015). Centrosomes and cancer: revisiting a long-standing relationship. *Nat. Rev. Cancer* *15*, 639–652.

Goshima, G., Nédélec, F., and Vale, R.D. (2005). Mechanisms for focusing mitotic spindle poles by minus end-directed motor proteins. *J. Cell Biol.* *171*, 229–240.

- Goshima, G., Mayer, M., Zhang, N., Stuurman, N., and Vale, R.D. (2008). Augmin: a protein complex required for centrosome-independent microtubule generation within the spindle. *J. Cell Biol.* *181*, 421–429.
- Gottardo, M., Pollarolo, G., Llamazares, S., Reina, J., Riparbelli, M.G., Callaini, G., and Gonzalez, C. (2015). Loss of Centrobin Enables Daughter Centrioles to Form Sensory Cilia in *Drosophila*. *Curr. Biol.* *25*, 2319–2324.
- Gruss, O.J., Carazo-Salas, R.E., Schatz, C.A., Guarguaglini, G., Kast, J., Wilm, M., Bot, N.L., Vernos, I., Karsenti, E., and Mattaj, I.W. (2001). Ran Induces Spindle Assembly by Reversing the Inhibitory Effect of Importin α on TPX2 Activity. *Cell* *104*, 83–93.
- Gudi, R., Zou, C., Li, J., and Gao, Q. (2011). Centrobin-tubulin interaction is required for centriole elongation and stability. *J. Cell Biol.* *193*, 711–725.
- Gudi, R., Zou, C., Dhar, J., Gao, Q., and Vasu, C. (2014). Centrobin-Centrosomal Protein 4.1-associated Protein (CPAP) Interaction Promotes CPAP Localization to the Centrioles during Centriole Duplication. *J. Biol. Chem.* *289*, 15166–15178.
- Gudi, R., Haycraft, C.J., Bell, P.D., Li, Z., and Vasu, C. (2015). Centrobin-mediated Regulation of the Centrosomal Protein 4.1-associated Protein (CPAP) Level Limits Centriole Length during Elongation Stage. *J. Biol. Chem.* *290*, 6890–6902.
- Gupta, A., and Kitagawa, D. Ultrastructural diversity between centrioles of eukaryotes. *J. Biochem. (Tokyo)*.
- Gupta, A., Tsuchiya, Y., Ohta, M., Shiratsuchi, G., and Kitagawa, D. (2017). NEK7 is required for G1 progression and procentriole formation. *Mol. Biol. Cell* *28*, 2123–2134.
- Gupta, G.D., Coyaud, É., Gonçalves, J., Mojarad, B.A., Liu, Y., Wu, Q., Gheiratmand, L., Comartin, D., Tkach, J.M., Cheung, S.W.T., et al. (2015). A dynamic protein interaction landscape of the human centrosome-cilium interface. *Cell* *163*, 1484–1499.
- Haines, D.C., Chattopadhyay, S., and Ward, J.M. (2001). Pathology of Aging B6;129 Mice. *Toxicol. Pathol.* *29*, 653–661.
- Hames, R.S., and Fry, A.M. (2002). Alternative splice variants of the human centrosome kinase Nek2 exhibit distinct patterns of expression in mitosis. *Biochem. J.* *361*, 77–85.
- Hanks, S.K., and Hunter, T. (1995). Protein kinases 6. The eukaryotic protein kinase superfamily: kinase (catalytic) domain structure and classification. *FASEB J. Off. Publ. Fed. Am. Soc. Exp. Biol.* *9*, 576–596.

- Haq, T., Richards, M.W., Burgess, S.G., Gallego, P., Yeoh, S., O'Regan, L., Reverter, D., Roig, J., Fry, A.M., and Bayliss, R. (2015). Mechanistic basis of Nek7 activation through Nek9 binding and induced dimerization. *Nat. Commun.* *6*, 8771–8771.
- Haren, L., Stearns, T., and Lüders, J. (2009). Plk1-dependent recruitment of gamma-tubulin complexes to mitotic centrosomes involves multiple PCM components. *PloS One* *4*, e5976.
- Hatch, E., and Stearns, T. (2010). *The Life Cycle of Centrioles*. Cold Spring Harb. Symp. Quant. Biol. *75*, 425–431.
- He, Y., Zeng, M.Y., Yang, D., Motro, B., and Núñez, G. (2016). NEK7 is an essential mediator of NLRP3 activation downstream of potassium efflux. *Nature* *530*, 354–357.
- Hetzer, M., Gruss, O.J., and Mattaj, I.W. (2002). The Ran GTPase as a marker of chromosome position in spindle formation and nuclear envelope assembly. *Nat. Cell Biol.* *4*, E177–E184.
- Hinchcliffe, E.H., and Sluder, G. (2001). “It Takes Two to Tango”: understanding how centrosome duplication is regulated throughout the cell cycle. *Genes Dev.* *15*, 1167–1181.
- Hirono, M. (2014). Cartwheel assembly. *Philos. Trans. R. Soc. Lond. B. Biol. Sci.* *369*, 20130458-.
- Holland, A.J., Fachinetti, D., Zhu, Q., Bauer, M., Verma, I.M., Nigg, E.A., and Cleveland, D.W. (2012). The autoregulated instability of Polo-like kinase 4 limits centrosome duplication to once per cell cycle. *Genes Dev.* *26*, 2684–2689.
- Holland, P.M., Milne, A., Garka, K., Johnson, R.S., Willis, C., Sims, J.E., Rauch, C.T., Bird, T.A., and Virca, G.D. (2002). Purification, Cloning, and Characterization of Nek8, a Novel NIMA-related Kinase, and Its Candidate Substrate Bicd2. *J. Biol. Chem.* *277*, 16229–16240.
- Hoogenraad, C.C., and Akhmanova, A. (2016). Bicaudal D Family of Motor Adaptors: Linking Dynein Motility to Cargo Binding. *Trends Cell Biol.* *26*, 327–340.
- Hoogenraad, C.C., Wulf, P., Schiefermeier, N., Stepanova, T., Galjart, N., Small, J.V., Grosveld, F., de Zeeuw, C.I., and Akhmanova, A. (2003). Bicaudal D induces selective dynein-mediated microtubule minus end-directed transport. *EMBO J.* *22*, 6004–6015.
- Hu, C.-E., and Gan, J. (2017). TRIM37 promotes epithelial-mesenchymal transition in colorectal cancer. *Mol. Med. Rep.* *15*, 1057–1062.

- Hudson, J.W., Kozarova, A., Cheung, P., Macmillan, J.C., Swallow, C.J., Cross, J.C., and Dennis, J.W. (2001). Late mitotic failure in mice lacking Sak, a polo-like kinase. *Curr. Biol.* *CB 11*, 441–446.
- Hunter, T. (2012). Why nature chose phosphate to modify proteins. *Philos. Trans. R. Soc. Lond. B. Biol. Sci.* *367*, 2513–2516.
- Hutterer, A., Berdnik, D., Wirtz-Peitz, F., Zigman, M., Schleiffer, A., and Knoblich, J.A. (2006). Mitotic activation of the kinase Aurora-A requires its binding partner Bora. *Dev. Cell* *11*, 147–157.
- Inanç, B., Dodson, H., and Morrison, C.G. (2010). A Centrosome-autonomous Signal That Involves Centriole Disengagement Permits Centrosome Duplication in G2 Phase after DNA Damage. *Mol. Biol. Cell* *21*, 3866–3877.
- Izquierdo, D., Wang, W.-J., Uryu, K., and Tsou, M.-F.B. (2014). Stabilization of cartwheel-less centrioles for duplication requires CEP295-mediated centriole-to-centrosome conversion. *Cell Rep.* *8*, 957–965.
- Januschke, J., Reina, J., Llamazares, S., Bertran, T., Rossi, F., Roig, J., and Gonzalez, C. (2013). Centrobin controls mother–daughter centriole asymmetry in *Drosophila* neuroblasts. *Nat. Cell Biol.* *15*, 241.
- Jeffery, J.M., Urquhart, A.J., Subramaniam, V.N., Parton, R.G., and Khanna, K.K. (2010a). Centrobin regulates the assembly of functional mitotic spindles. *Oncogene* *29*, 2649.
- Jeffery, J.M., Urquhart, A.J., Subramaniam, V.N., Parton, R.G., and Khanna, K.K. (2010b). Centrobin regulates the assembly of functional mitotic spindles. *Oncogene* *29*, 2649–2658.
- Jeffery, J.M., Grigoriev, I., Poser, I., van der Horst, A., Hamilton, N., Waterhouse, N., Bleier, J., Subramaniam, V.N., Maly, I.V., Akhmanova, A., et al. (2013). Centrobin regulates centrosome function in interphase cells by limiting pericentriolar matrix recruitment. *Cell Cycle* *12*, 899–906.
- Jeong, Y., Lee, J., Kim, K., Yoo, J.C., and Rhee, K. (2007a). Characterization of NIP2/centrobin, a novel substrate of Nek2, and its potential role in microtubule stabilization. *J. Cell Sci.* *120*, 2106–2116.
- Jeong, Y., Lee, J., Kim, K., Yoo, J.C., and Rhee, K. (2007b). Characterization of NIP2/centrobin, a novel substrate of Nek2, and its potential role in microtubule stabilization. *J. Cell Sci.* *120*, 2106–2116.
- Jiang, J., Yu, C., Chen, M., Tian, S., and Sun, C. (2015). Over-expression of TRIM37 promotes cell migration and metastasis in hepatocellular carcinoma by activating Wnt/ β -catenin signaling. *Biochem. Biophys. Res. Commun.*

464, 1120–1127.

Jiang, J., Tian, S., Yu, C., Chen, M., and Sun, C. (2016). TRIM37 promoted the growth and migration of the pancreatic cancer cells. *Tumour Biol. J. Int. Soc. Oncodevelopmental Biol. Med.* 37, 2629–2634.

Johnson, C.A., and Collis, S.J. (2016). Ciliogenesis and the DNA damage response: a stressful relationship. *Cilia* 5, 19.

Joukov, V., Walter, J.C., and De Nicolo, A. (2014). The Cep192-Organized Aurora A-Plk1 Cascade Is Essential for Centrosome Cycle and Bipolar Spindle Assembly. *Mol. Cell.*

Kamasaki, T., O'Toole, E., Kita, S., Osumi, M., Usukura, J., McIntosh, J.R., and Goshima, G. (2013). Augmin-dependent microtubule nucleation at microtubule walls in the spindle. *J. Cell Biol.* 202, 25–33.

Kandli, M., Feige, E., Chen, A., Kilfin, G., and Motro, B. (2000). Isolation and characterization of two evolutionarily conserved murine kinases (Nek6 and nek7) related to the fungal mitotic regulator, NIMA. *Genomics* 68, 187–196.

Kaneta, Y., and Ullrich, A. (2013). NEK9 depletion induces catastrophic mitosis by impairment of mitotic checkpoint control and spindle dynamics. *Biochem. Biophys. Res. Commun.* 1–8.

Kang, Y.H., Park, J.-E., Yu, L.-R., Soung, N.-K., Yun, S.-M., Bang, J.K., Seong, Y.-S., Yu, H., Garfield, S., Veenstra, T.D., et al. (2006). Self-regulated Plk1 recruitment to kinetochores by the Plk1-PBIP1 interaction is critical for proper chromosome segregation. *Mol. Cell* 24, 409–422.

Kapitein, L.C., Peterman, E.J.G., Kwok, B.H., Kim, J.H., Kapoor, T.M., and Schmidt, C.F. (2005). The bipolar mitotic kinesin Eg5 moves on both microtubules that it crosslinks. *Nature* 435, 114–118.

Kardon, J.R., and Vale, R.D. (2009). Regulators of the cytoplasmic dynein motor. *Nat. Rev. Mol. Cell Biol.* 10, 854–865.

Karlberg, S., Lipsanen-Nyman, M., Lassus, H., Kallijärvi, J., Lehesjoki, A.-E., and Butzow, R. (2009). Gynecological tumors in Mulibrey nanism and role for RING finger protein TRIM37 in the pathogenesis of ovarian fibrothecomas. *Mod. Pathol.* 22, 570–578.

Kastan, M.B., and Bartek, J. (2004). Cell-cycle checkpoints and cancer. *Nature* 432, 316–323.

Keller, D., Orpinell, M., Olivier, N., Wachsmuth, M., Mahen, R., Wyss, R., Hachet, V., Ellenberg, J., Manley, S., and Gönczy, P. (2014). Mechanisms of HsSAS-6 assembly promoting centriole formation in human cells. *J. Cell*

- Biol. 204, 697–712.
- Keller, L.C., Wemmer, K.A., and Marshall, W.F. (2010). Influence of centriole number on mitotic spindle length and symmetry. *Cytoskelet. Hoboken NJ* 67, 504–518.
- Kettunen, K.M., Karikoski, R., Hämäläinen, R.H., Toivonen, T.T., Antonenkov, V.D., Kuleshkaya, N., Voikar, V., Hölttä-Vuori, M., Ikonen, E., Sainio, K., et al. (2016). Trim37-deficient mice recapitulate several features of the multi-organ disorder Mulibrey nanism. *Biol. Open* 5, 584–595.
- Kim, J., Lee, K., and Rhee, K. (2015). PLK1 regulation of PCNT cleavage ensures fidelity of centriole separation during mitotic exit. *Nat. Commun.* 6, 10076–10076.
- Kim, S., Kim, S., Kim, S., and Rhee, K. (2011). NEK7 is essential for centriole duplication and centrosomal accumulation of pericentriolar material proteins in interphase cells. *J. Cell Sci.* 124, 3760–3770.
- Kirschner, M., and Mitchison, T. (1986). Beyond self-assembly: From microtubules to morphogenesis. *Cell* 45, 329–342.
- Kleylein-Sohn, J., Westendorf, J., Clech, M.L., Habedanck, R., Stierhof, Y.-D., and Nigg, E.A. (2007). Plk4-Induced Centriole Biogenesis in Human Cells. *Dev. Cell* 13, 190–202.
- Kong, D., Farmer, V., Shukla, A., James, J., Gruskin, R., Kiriyama, S., and Loncarek, J. (2014). Centriole maturation requires regulated Plk1 activity during two consecutive cell cycles. *J Cell Biol* 206, 855–865.
- Kornev, A.P., and Taylor, S.S. (2015). Dynamics driven allostery in protein kinases. *Trends Biochem. Sci.* 40, 628–647.
- Kraakman-van der Zwet, M., Overkamp, W.J.I., van Lange, R.E.E., Essers, J., van Duijn-Goedhart, A., Wiggers, I., Swaminathan, S., van Buul, P.P.W., Errami, A., Tan, R.T.L., et al. (2002). Brca2 (XRCC11) deficiency results in radioresistant DNA synthesis and a higher frequency of spontaneous deletions. *Mol. Cell. Biol.* 22, 669–679.
- Krause, A., and Hoffmann, I. (2010). Polo-like kinase 2-dependent phosphorylation of NPM/B23 on serine 4 triggers centriole duplication. *PLoS One* 5, e9849.
- Kurioka, D., Takeshita, F., Tsuta, K., Sakamoto, H., Watanabe, S.-I., Matsumoto, K., Watanabe, M., Nakagama, H., Ochiya, T., Yokota, J., et al. (2014). NEK9-dependent proliferation of cancer cells lacking functional p53. *Sci. Rep.* 4, 6111–6111.

REFERENCES

- Kwon, M., Godinho, S.A., Chandhok, N.S., Ganem, N.J., Azioune, A., Thery, M., and Pellman, D. (2008). Mechanisms to suppress multipolar divisions in cancer cells with extra centrosomes. *Genes Dev.* *22*, 2189–2203.
- Laurell, E., Beck, K., Krupina, K., Theerthagiri, G., Bodenmiller, B., Horvath, P., Aebersold, R., Antonin, W., and Kutay, U. (2011). Phosphorylation of Nup98 by multiple kinases is crucial for NPC disassembly during mitotic entry. *Cell* *144*, 539–550.
- Lee, K., and Rhee, K. (2012). Separase-dependent cleavage of pericentrin B is necessary and sufficient for centriole disengagement during mitosis. *Cell Cycle Georget. Tex* *11*, 2476–2485.
- Lee, J., Jeong, Y., Jeong, S., and Rhee, K. (2010a). Centrobin/NIP2 Is a Microtubule Stabilizer Whose Activity Is Enhanced by PLK1 Phosphorylation during Mitosis. *J. Biol. Chem.* *285*, 25476–25484.
- Lee, J., Jeong, Y., Jeong, S., and Rhee, K. (2010b). Centrobin/NIP2 is a microtubule stabilizer whose activity is enhanced by PLK1 phosphorylation during mitosis. *J. Biol. Chem.* *285*, 25476–25484.
- Lee, M.-Y., Kim, H.-J., Kim, M.-A., Jee, H.J., Kim, A.J., Bae, Y.-S., Park, J.-I., Chung, J.H., and Yun, J. (2008). Nek6 is involved in G2/M phase cell cycle arrest through DNA damage-induced phosphorylation. *Cell Cycle* *7*, 2705–2709.
- Lens, S.M.A., Voest, E.E., and Medema, R.H. (2010). Shared and separate functions of polo-like kinases and aurora kinases in cancer. *Nat. Rev. Cancer* *10*, 825–841.
- Levinsohn, J.L., Sugarman, J.L., McNiff, J.M., Antaya, R.J., and Choate, K.A. (2016). Somatic Mutations in NEK9 Cause Nevus Comedonicus. *Am. J. Hum. Genet.* *98*, 1030–1037.
- Li, M., Fang, X., Baker, D.J., Guo, L., Gao, X., Wei, Z., Han, S., van Deursen, J.M., and Zhang, P. (2010). The ATM–p53 pathway suppresses aneuploidy-induced tumorigenesis. *Proc. Natl. Acad. Sci. U. S. A.* *107*, 14188–14193.
- Lim, S., and Kaldis, P. (2013). Cdks, cyclins and CKIs: roles beyond cell cycle regulation. *Development* *140*, 3079–3093.
- Lin, Y.-C., Chang, C.-W., Hsu, W.-B., Tang, C.-J.C., Lin, Y.-N., Chou, E.-J., Wu, C.-T., and Tang, T.K. (2013). Human microcephaly protein CEP135 binds to hSAS-6 and CPAP, and is required for centriole assembly. *EMBO J.* *32*, 1141–1154.
- Ling, H., Hanashiro, K., Luong, T.H., Benavides, L., and Fukasawa, K.

- (2015). Functional Relationship among PLK2, PLK4 and ROCK2 to Induce Centrosome Amplification. *Cell Cycle Georget. Tex.*
- Liu, Q., Hirohashi, Y., Du, X., Greene, M.I., and Wang, Q. (2010). Nek2 targets the mitotic checkpoint proteins Mad2 and Cdc20: A mechanism for aneuploidy in cancer. *Exp. Mol. Pathol.* 88, 225–233.
- Liu, S., Lu, W., Obara, T., Kuida, S., Lehoczky, J., Dewar, K., Drummond, I.A., and Beier, D.R. (2002). A defect in a novel Nek-family kinase causes cystic kidney disease in the mouse and in zebrafish. *Development* 129, 5839–5846.
- Llamazares, S., Moreira, A., Tavares, A., Girdham, C., Spruce, B.A., Gonzalez, C., Karess, R.E., Glover, D.M., and Sunkel, C.E. (1991). polo encodes a protein kinase homolog required for mitosis in *Drosophila*. *Genes Dev.* 5, 2153–2165.
- Löffler, H., Bochtler, T., Fritz, B., Tews, B., Ho, A.D., Lukas, J., Bartek, J., and Krämer, A. (2007). DNA damage-induced accumulation of centrosomal Chk1 contributes to its checkpoint function. *Cell Cycle Georget. Tex* 6, 2541–2548.
- Löffler, H., Fechter, A., Liu, F.Y., Poppelreuther, S., and Krämer, A. (2013). DNA damage-induced centrosome amplification occurs via excessive formation of centriolar satellites. *Oncogene* 32, 2963–2972.
- Loncarek, J., and Bettencourt-Dias, M. (2017). Building the right centriole for each cell type. *J Cell Biol* jcb.201704093.
- Loncarek, J., and Khodjakov, A. (2009). Ab ovo or de novo? Mechanisms of centriole duplication. *Mol. Cells* 27, 135–142.
- Loncarek, J., Hergert, P., Magidson, V., and Khodjakov, A. (2008). Control of daughter centriole formation by the pericentriolar material. *Nat. Cell Biol.* 10, 322–328.
- Lončarek, J., Hergert, P., and Khodjakov, A. (2010). Centriole reduplication during prolonged interphase requires procentriole maturation governed by Plk1. *Curr. Biol. CB* 20, 1277–1282.
- Lopes, C.A.M., Jana, S.C., Cunha-Ferreira, I., Zitouni, S., Bento, I., Duarte, P., Gilberto, S., Freixo, F., Guerrero, A., Francia, M., et al. (2015). PLK4 trans-Autoactivation Controls Centriole Biogenesis in Space. *Dev. Cell.*
- Lowery, D.M., Lim, D., and Yaffe, M.B. (2005). Structure and function of Polo-like kinases. *Oncogene* 24, 248–259.
- Lu, L.-Y., Wood, J.L., Minter-Dykhouse, K., Ye, L., Saunders, T.L., Yu, X., and Chen, J. (2008a). Polo-like kinase 1 is essential for early embryonic

- development and tumor suppression. *Mol. Cell. Biol.* 28, 6870–6876.
- Lu, L.-Y., Wood, J.L., Minter-Dykhouse, K., Ye, L., Saunders, T.L., Yu, X., and Chen, J. (2008b). Polo-Like Kinase 1 Is Essential for Early Embryonic Development and Tumor Suppression. *Mol. Cell. Biol.* 28, 6870–6876.
- Lu, L.-Y., Wood, J.L., Ye, L., Minter-Dykhouse, K., Saunders, T.L., Yu, X., and Chen, J. (2008c). Aurora A is essential for early embryonic development and tumor suppression. *J. Biol. Chem.* 283, 31785–31790.
- Lüders, J. (2012). The amorphous pericentriolar cloud takes shape. *Nat. Cell Biol.* 14, 1126.
- Lüders, J., and Stearns, T. (2007). Microtubule-organizing centres: a re-evaluation. *Nat. Rev. Mol. Cell Biol.* 8, 161.
- Ma, N., Tulu, U.S., Ferenz, N.P., Fagerstrom, C., Wilde, A., and Wadsworth, P. (2010). Poleward transport of TPX2 in the mammalian mitotic spindle requires dynein, Eg5, and microtubule flux. *Mol. Biol. Cell* 21, 979–988.
- Ma, N., Titus, J., Gable, A., Ross, J.L., and Wadsworth, P. (2011). TPX2 regulates the localization and activity of Eg5 in the mammalian mitotic spindle. *J. Cell Biol.* 195, 87–98.
- Macůrek, L., Lindqvist, A., Lim, D., Lampson, M.A., Klompaker, R., Freire, R., Clouin, C., Taylor, S.S., Yaffe, M.B., and Medema, R.H. (2008). Polo-like kinase-1 is activated by aurora A to promote checkpoint recovery. *Nature* 455, 119–123.
- Maiato, H. (2010). Mitosis: wisdom, knowledge, and information. *Cell. Mol. Life Sci.* 67, 2141–2143.
- Maiato, H., Rieder, C.L., and Khodjakov, A. (2004). Kinetochore-driven formation of kinetochore fibers contributes to spindle assembly during animal mitosis. *J. Cell Biol.* 167, 831–840.
- Maliga, Z., Kapoor, T.M., and Mitchison, T.J. (2002). Evidence that monastrol is an allosteric inhibitor of the mitotic kinesin Eg5. *Chem. Biol.* 9, 989–996.
- Malik, S., Saito, H., Takaoka, M., Miki, Y., and Nakanishi, A. (2016). BRCA2 mediates centrosome cohesion via an interaction with cytoplasmic dynein. *Cell Cycle* 15, 2145–2156.
- Malumbres, M. (2014). Cyclin-dependent kinases. *Genome Biol.* 15, 122.
- Malumbres, M., and Barbacid, M. (2005). Mammalian cyclin-dependent kinases. *Trends Biochem. Sci.* 30, 630–641.
- Malumbres, M., and Barbacid, M. (2009). Cell cycle, CDKs and cancer: a changing paradigm. *Nat. Rev. Cancer* 9, 153–166.

- Manning, D.K., Sergeev, M., van Heesbeen, R.G., Wong, M.D., Oh, J.-H., Liu, Y., Henkelman, R.M., Drummond, I., Shah, J.V., and Beier, D.R. (2013). Loss of the ciliary kinase Nek8 causes left-right asymmetry defects. *J. Am. Soc. Nephrol. JASN* 24, 100–112.
- Mardin, B.R., Lange, C., Baxter, J.E., Hardy, T., Fry, A.M., and Schiebel, E. (2010). Components of the Hippo pathway cooperate with Nek2 kinase to regulate centrosome disjunction. *Nat. Cell Biol.* 12, 1166–1176.
- Matsuo, K., Ohsumi, K., Iwabuchi, M., Kawamata, T., Ono, Y., and Takahashi, M. (2012). Kendrin is a novel substrate for separase involved in the licensing of centriole duplication. *Curr. Biol. CB* 22, 915–921.
- Matsuoka, S., Ballif, B.A., Smogorzewska, A., McDonald, E.R., Hurov, K.E., Luo, J., Bakalarski, C.E., Zhao, Z., Solimini, N., Lerenthal, Y., et al. (2007). ATM and ATR Substrate Analysis Reveals Extensive Protein Networks Responsive to DNA Damage. *Science* 316, 1160–1166.
- Mayer, T.U., Kapoor, T.M., Haggarty, S.J., King, R.W., Schreiber, S.L., and Mitchison, T.J. (1999). Small molecule inhibitor of mitotic spindle bipolarity identified in a phenotype-based screen. *Science* 286, 971–974.
- McKenney, R.J., Huynh, W., Tanenbaum, M.E., Bhabha, G., and Vale, R.D. (2014). Activation of cytoplasmic dynein motility by dynactin-cargo adapter complexes. *Science* 345, 337–341.
- Meirelles, G.V., Silva, J.C., Mendonça, Y. de A., Ramos, C.H., Torriani, I.L., and Kobarg, J. (2011). Human Nek6 is a monomeric mostly globular kinase with an unfolded short N-terminal domain. *BMC Struct. Biol.* 11, 12.
- Meitinger, F., Anzola, J.V., Kaulich, M., Richardson, A., Stender, J.D., Benner, C., Glass, C.K., Dowdy, S.F., Desai, A., Shiau, A.K., et al. (2016). 53BP1 and USP28 mediate p53 activation and G1 arrest after centrosome loss or extended mitotic duration. *J. Cell Biol.* 214, 155–166.
- Melixetian, M., Klein, D.K., Sørensen, C.S., and Helin, K. (2009). NEK11 regulates CDC25A degradation and the IR-induced G2/M checkpoint. *Nat. Cell Biol.* 11, 1247–1253.
- Meraldi, P., and Nigg, E.A. (2001). Centrosome cohesion is regulated by a balance of kinase and phosphatase activities. *J. Cell Sci.* 114, 3749–3757.
- Meraldi, P., Lukas, J., Fry, A.M., Bartek, J., and Nigg, E.A. (1999). Centrosome duplication in mammalian somatic cells requires E2F and Cdk2–Cyclin A. *Nat. Cell Biol.* 1, 88–93.
- Meunier, S., and Vernos, I. (2011). K-fibre minus ends are stabilized by a RanGTP-dependent mechanism essential for functional spindle assembly.

- Nat. Cell Biol. *13*, 1406–1414.
- Meunier, S., and Vernos, I. (2015). Acentrosomal Microtubule Assembly in Mitosis: The Where, When, and How. *Trends Cell Biol.*
- Mi, J., Guo, C., Brautigan, D.L., and Larner, J.M. (2007). Protein Phosphatase-1 α Regulates Centrosome Splitting through Nek2. *Cancer Res.* *67*, 1082–1089.
- Mitchison, T., and Kirschner, M. (1984). Dynamic instability of microtubule growth. *Nature* *312*, 237–242.
- Moniz, L., Dutt, P., Haider, N., and Stambolic, V. (2011). Nek family of kinases in cell cycle, checkpoint control and cancer. *Cell Div.* *6*, 18–18.
- Morgan, D.O. (2007). *The Cell Cycle: Principles of Control* (New Science Press).
- Nakanishi, A., Han, X., Saito, H., Taguchi, K., Ohta, Y., Imajoh-Ohmi, S., and Miki, Y. (2007). Interference with BRCA2, which localizes to the centrosome during S and early M phase, leads to abnormal nuclear division. *Biochem. Biophys. Res. Commun.* *355*, 34–40.
- Nakazawa, Y., Hiraki, M., Kamiya, R., and Hirono, M. (2007). SAS-6 is a Cartwheel Protein that Establishes the 9-Fold Symmetry of the Centriole. *Curr. Biol.* *17*, 2169–2174.
- Neumayer, G., Helfricht, A., Shim, S.Y., Le, H.T., Lundin, C., Belzil, C., Chansard, M., Yu, Y., Lees-Miller, S.P., Gruss, O.J., et al. (2012). Targeting Protein for Xenopus Kinesin-like Protein 2 (TPX2) Regulates γ -Histone 2AX (γ -H2AX) Levels upon Ionizing Radiation. *J. Biol. Chem.* *287*, 42206–42222.
- Neumayer, G., Belzil, C., Gruss, O.J., and Nguyen, M.D. (2014). TPX2: of spindle assembly, DNA damage response, and cancer. *Cell. Mol. Life Sci.* *71*, 3027–3047.
- Nigg, E.A. (2002). Centrosome aberrations: cause or consequence of cancer progression? *Nat. Rev. Cancer* *2*, 815.
- Nigg, E.A., and Holland, A.J. (2018). Once and only once: mechanisms of centriole duplication and their deregulation in disease. *Nat. Rev. Mol. Cell Biol.*
- Nigg, E.A., and Raff, J.W. (2009). Centrioles, Centrosomes, and Cilia in Health and Disease. *Cell* *139*, 663–678.
- Nigg, E.A., and Stearns, T. (2011). The centrosome cycle: Centriole biogenesis, duplication and inherent asymmetries. *Nat. Cell Biol.* *13*, 1154–1160.

- Nigg, E.A., Čajánek, L., and Arquint, C. (2014). The centrosome duplication cycle in health and disease. *FEBS Lett.* *588*, 2366–2372.
- O’Connell, M.J., Krien, M.J.E., and Hunter, T. (2003a). Never say never. The NIMA-related protein kinases in mitotic control. *Trends Cell Biol.* *13*, 221–228.
- O’Connell, M.J., Krien, M.J.E., and Hunter, T. (2003b). Never say never. The NIMA-related protein kinases in mitotic control. *Trends Cell Biol.* *13*, 221–228.
- Ogungbenro, Y.A., Tena, T.C., Gaboriau, D., Lalor, P., Dockery, P., Philipp, M., and Morrison, C.G. (2018). Centrobin controls primary ciliogenesis in vertebrates. *J Cell Biol* jcb.201706095.
- Okuda, M., Horn, H.F., Tarapore, P., Tokuyama, Y., Smulian, A.G., Chan, P.-K., Knudsen, E.S., Hofmann, I.A., Snyder, J.D., Bove, K.E., et al. (2000). Nucleophosmin/B23 Is a Target of CDK2/Cyclin E in Centrosome Duplication. *Cell* *103*, 127–140.
- O’Regan, L., and Fry, A.M. (2009). The Nek6 and Nek7 protein kinases are required for robust mitotic spindle formation and cytokinesis. *Mol. Cell Biol.* *29*, 3975–3990.
- O’regan, L., Blot, J., and Fry, A.M. (2007). Mitotic regulation by NIMA-related kinases. *Cell Div.* *2*, 25–25.
- O’Regan, L., Blot, J., and Fry, A.M. (2007). Mitotic regulation by NIMA-related kinases. *Cell Div.* *2*, 25.
- O’Regan, L., Sampson, J., Richards, M.W., Knebel, A., Roth, D., Hood, F.E., Straube, A., Royle, S.J., Bayliss, R., and Fry, A.M. (2015). Hsp72 is targeted to the mitotic spindle by Nek6 to promote K-fiber assembly and mitotic progression. *J. Cell Biol.* *209*, 349–358.
- Oshimori, N., Ohsugi, M., and Yamamoto, T. (2006). The Plk1 target Kizuna stabilizes mitotic centrosomes to ensure spindle bipolarity. *Nat. Cell Biol.* *8*, 1095–1101.
- Otto, E.A., Trapp, M.L., Schultheiss, U.T., Helou, J., Quarmby, L.M., and Hildebrandt, F. (2008). NEK8 mutations affect ciliary and centrosomal localization and may cause nephronophthisis. *J. Am. Soc. Nephrol. JASN* *19*, 587–592.
- Pagan, J.K., Marzio, A., Jones, M.J.K., Saraf, A., Jallepalli, P.V., Florens, L., Washburn, M.P., and Pagano, M. (2015). Degradation of Cep68 and PCNT cleavage mediate Cep215 removal from the PCM to allow centriole separation, disengagement and licensing. *Nat. Cell Biol.* *17*, 31–43.

- Park, J., and Rhee, K. (2013). NEK2 phosphorylation antagonizes the microtubule stabilizing activity of centromeres. *Biochem. Biophys. Res. Commun.* *431*, 302–308.
- Parker, J.D.K., Bradley, B.A., Mooers, A.O., and Quarmby, L.M. (2007). Phylogenetic Analysis of the Neks Reveals Early Diversification of Ciliary-Cell Cycle Kinases. *PLOS ONE* *2*, e1076.
- Paweletz, N. (2001). Walther Flemming: pioneer of mitosis research. *Nat. Rev. Mol. Cell Biol.* *2*, 72.
- Perez-Garcia, V., Fineberg, E., Wilson, R., Murray, A., Mazzeo, C.I., Tudor, C., Sienerth, A., White, J.K., Tuck, E., Ryder, E.J., et al. (2018). Placentation defects are highly prevalent in embryonic lethal mouse mutants. *Nature*.
- Pines, J., and Rieder, C.L. (2001). Re-staging mitosis: a contemporary view of mitotic progression.
- Prosser, S.L., Sahota, N.K., Pelletier, L., Morrison, C.G., and Fry, A.M. (2015). Nek5 promotes centrosome integrity in interphase and loss of centrosome cohesion in mitosis. *J Cell Biol* *209*, 339–348.
- Puklowski, A., Homsy, Y., Keller, D., May, M., Chauhan, S., Kossatz, U., Grünwald, V., Kubicka, S., Pich, A., Manns, M.P., et al. (2011). The SCF–FBXW5 E3-ubiquitin ligase is regulated by PLK4 and targets HsSAS-6 to control centrosome duplication. *Nat. Cell Biol.* *13*, 1004–1009.
- Quarmby, L.M., and Mahjoub, M.R. (2005). Caught Nek-ing: cilia and centrioles. *J. Cell Sci.* *118*, 5161–5169.
- Quintyne, N.J., Reing, J.E., Hoffelder, D.R., Gollin, S.M., and Saunders, W.S. (2005). Spindle Multipolarity Is Prevented by Centrosomal Clustering. *Science* *307*, 127–129.
- Raaijmakers, J.A., and Medema, R.H. (2014). Function and regulation of dynein in mitotic chromosome segregation. *Chromosoma* *123*, 407–422.
- Raaijmakers, J.A., van Heesbeen, R.G.H.P., Meaders, J.L., Geers, E.F., Fernandez-Garcia, B., Medema, R.H., and Tanenbaum, M.E. (2012). Nuclear envelope-associated dynein drives prophase centrosome separation and enables Eg5-independent bipolar spindle formation. *EMBO J.* *31*, 4179–4190.
- Rapley, J., Nicolàs, M., Groen, A., Regué, L., Bertran, M.T., Caelles, C., Avruch, J., and Roig, J. (2008). The NIMA-family kinase Nek6 phosphorylates the kinesin Eg5 at a novel site necessary for mitotic spindle formation. *J. Cell Sci.* *121*, 3912–3921.
- Regué, L., Sdelci, S., Bertran, M.T., Caelles, C., Reverter, D., and Roig, J.

- (2011). DYNLL/LC8 protein controls signal transduction through the Nek9/Nek6 signaling module by regulating Nek6 binding to Nek9. *J. Biol. Chem.* *286*, 18118–18129.
- Reina, J., Gottardo, M., Riparbelli, M.G., Llamazares, S., Callaini, G., and Gonzalez, C. (2018). Centrobin is essential for C-tubule assembly and flagellum development in *Drosophila melanogaster* spermatogenesis. *J. Cell Biol.*
- Rhind, N., and Russell, P. (2012). Signaling Pathways that Regulate Cell Division. *Cold Spring Harb. Perspect. Biol.* *4*.
- Richards, M.W., O'Regan, L., Mas-Droux, C., Blot, J.M.Y., Cheung, J., Hoelder, S., Fry, A.M., and Bayliss, R. (2009). An Autoinhibitory Tyrosine Motif in the Cell-Cycle-Regulated Nek7 Kinase Is Released through Binding of Nek9. *Mol. Cell* *36*, 560–570.
- Rieder, C.L. (2005). Kinetochore fiber formation in animal somatic cells: dueling mechanisms come to a draw. *Chromosoma* *114*, 310–318.
- Rieder, C.L., and Khodjakov, A. (2003). Mitosis Through the Microscope: Advances in Seeing Inside Live Dividing Cells. *Science* *300*, 91–96.
- Roberts, A.J., Kon, T., Knight, P.J., Sutoh, K., and Burgess, S.A. (2013). Functions and mechanics of dynein motor proteins. *Nat. Rev. Mol. Cell Biol.* *14*, 713–726.
- Roig, J., Mikhailov, A., Belham, C., and Avruch, J. (2002a). Nercc1, a mammalian NIMA-family kinase, binds the Ran GTPase and regulates mitotic progression. *Genes Dev.* *16*, 1640–1658.
- Roig, J., Mikhailov, A., Belham, C., and Avruch, J. (2002b). Nercc1, a mammalian NIMA-family kinase, binds the Ran GTPase and regulates mitotic progression. *Genes Dev.* *16*, 1640–1658.
- Roig, J., Groen, A., Caldwell, J., and Avruch, J. (2005). Active Nercc1 Protein Kinase Concentrates at Centrosomes Early in Mitosis and Is Necessary for Proper Spindle Assembly. *16*, 4827–4840.
- Saladino, C., Bourke, E., Conroy, P.C., and Morrison, C.G. (2009). Centriole separation in DNA damage-induced centrosome amplification. *Environ. Mol. Mutagen.* *50*, 725–732.
- Salem, H., Rachmin, I., Yissachar, N., Cohen, S., Amiel, A., Haffner, R., Lavi, L., and Motro, B. (2010). Nek7 kinase targeting leads to early mortality, cytokinesis disturbance and polyploidy. *Oncogene* *29*, 4046–4057.
- Salina, D., Bodoor, K., Eckley, D.M., Schroer, T.A., Rattner, J.B., and Burke, B. (2002). Cytoplasmic Dynein as a Facilitator of Nuclear Envelope

- Breakdown. *Cell* 108, 97–107.
- Santamaría, D., Barrière, C., Cerqueira, A., Hunt, S., Tardy, C., Newton, K., Cáceres, J.F., Dubus, P., Malumbres, M., and Barbacid, M. (2007). Cdk1 is sufficient to drive the mammalian cell cycle. *Nature* 448, 811.
- Scheer, U. (2014). Historical roots of centrosome research: discovery of Boveri's microscope slides in Würzburg. *Philos. Trans. R. Soc. Lond. B. Biol. Sci.* 369, 20130469-.
- Schmidt, T.I., Kleylein-Sohn, J., Westendorf, J., Le Clech, M., Lavoie, S.B., Stierhof, Y.-D., and Nigg, E.A. (2009). Control of Centriole Length by CPAP and CP110. *Curr. Biol.* 19, 1005–1011.
- Schvartzman, J.-M., Sotillo, R., and Benezra, R. (2010). Mitotic chromosomal instability and cancer: mouse modelling of the human disease. *Nat. Rev. Cancer* 10, 102–115.
- Sdelci, S., Schütz, M., Pinyol, R., Bertran, M.T., Regué, L., Caelles, C., Vernos, I., and Roig, J. (2012). Nek9 phosphorylation of NEDD1/GCP-WD contributes to Plk1 control of γ -tubulin recruitment to the mitotic centrosome. *Curr. Biol. CB* 22, 1516–1523.
- Seki, A., Coppinger, J.A., Jang, C.-Y., Yates, J.R., and Fang, G. (2008). Bora and the kinase Aurora a cooperatively activate the kinase Plk1 and control mitotic entry. *Science* 320, 1655–1658.
- Shaheen, R., Patel, N., Shamseldin, H., Alzahrani, F., Al-Yamany, R., ALMoisheer, A., Ewida, N., Anazi, S., Alnemer, M., Elsheikh, M., et al. (2016). Accelerating matchmaking of novel dysmorphology syndromes through clinical and genomic characterization of a large cohort. *Genet. Med.* 18, 686–695.
- Shalom, O., Shalva, N., Altschuler, Y., and Motro, B. (2008). The mammalian Nek1 kinase is involved in primary cilium formation. *FEBS Lett.* 582, 1465–1470.
- Sherr, C.J., and Roberts, J.M. (2004). Living with or without cyclins and cyclin-dependent kinases. *Genes Dev.* 18, 2699–2711.
- Shin, W., Yu, N.-K., Kaang, B.-K., and Rhee, K. (2015). The microtubule nucleation activity of centrobilin in both the centrosome and cytoplasm. *Cell Cycle* 14, 1925–1931.
- Shukla, A., Kong, D., Sharma, M., Magidson, V., and Loncarek, J. (2015). Plk1 relieves centriole block to reduplication by promoting daughter centriole maturation. *Nat. Commun.* 6, 8077–8077.
- Silkworth, W.T., Nardi, I.K., Paul, R., Mogilner, A., and Cimini, D. (2012).

- Timing of centrosome separation is important for accurate chromosome segregation. *Mol. Biol. Cell* 23, 401–411.
- Sillibourne, J.E., Tack, F., Vloemans, N., Boeckx, A., Thambirajah, S., Bonnet, P., Ramaekers, F.C.S., Bornens, M., and Grand-Perret, T. (2010). Autophosphorylation of polo-like kinase 4 and its role in centriole duplication. *Mol. Biol. Cell* 21, 547–561.
- Skoufias, D.A., DeBonis, S., Saoudi, Y., Lebeau, L., Crevel, I., Cross, R., Wade, R.H., Hackney, D., and Kozielski, F. (2006). S-trityl-L-cysteine is a reversible, tight binding inhibitor of the human kinesin Eg5 that specifically blocks mitotic progression. *J. Biol. Chem.* 281, 17559–17569.
- Slevin, L.K., Nye, J., Pinkerton, D.C., Buster, D.W., Rogers, G.C., and Slep, K.C. (2012). The Structure of the Plk4 Cryptic Polo Box Reveals Two Tandem Polo Boxes Required for Centriole Duplication. *Struct. Lond. Engl.* 1993 20, 1905–1917.
- Sluder, G. (2005). Two-way traffic: centrosomes and the cell cycle. *Nat. Rev. Mol. Cell Biol.* 6, 743–748.
- Smith, S.C., Petrova, A.V., Madden, M.Z., Wang, H., Pan, Y., Warren, M.D., Hardy, C.W., Liang, D., Liu, E.A., Robinson, M.H., et al. (2014). A gemcitabine sensitivity screen identifies a role for NEK9 in the replication stress response. *Nucleic Acids Res.*
- Sonn, S., Jeong, Y., and Rhee, K. (2009). Nip2/centrobin may be a substrate of Nek2 that is required for proper spindle assembly during mitosis in early mouse embryos. *Mol. Reprod. Dev.* 76, 587–592.
- Sonnen, K.F., Schermelleh, L., Leonhardt, H., and Nigg, E.A. (2012). 3D-structured illumination microscopy provides novel insight into architecture of human centrosomes. *Biol. Open* 1, 965–976.
- Sonnen, K.F., Gabryjonczyk, A.-M., Anselm, E., Stierhof, Y.-D., and Nigg, E.A. (2013). Human Cep192 and Cep152 cooperate in Plk4 recruitment and centriole duplication. *J Cell Sci* 126, 3223–3233.
- Splinter, D., Tanenbaum, M.E., Lindqvist, A., Jaarsma, D., Flotho, A., Yu, K.L., Grigoriev, I., Engelsma, D., Haasdijk, E.D., Keijzer, N., et al. (2010). Bicaudal D2, Dynein, and Kinesin-1 Associate with Nuclear Pore Complexes and Regulate Centrosome and Nuclear Positioning during Mitotic Entry. *PLOS Biol.* 8, e1000350.
- Strebhardt, K., and Ullrich, A. (2006). Targeting polo-like kinase 1 for cancer therapy. *Nat. Rev. Cancer* 6, 321–330.
- Strnad, P., Leidel, S., Vinogradova, T., Euteneuer, U., Khodjakov, A., and

- Gönczy, P. (2007). Regulated HsSAS-6 levels ensure formation of a single procentriole per centriole during the centrosome duplication cycle. *Dev. Cell* *13*, 203–213.
- Sunkel, C.E., and Glover, D.M. (1988). polo, a mitotic mutant of *Drosophila* displaying abnormal spindle poles. *J. Cell Sci.* *89 (Pt 1)*, 25–38.
- Tan, B.C.-M., and Lee, S.-C. (2004). Nek9, a novel FACT-associated protein, modulates interphase progression. *J. Biol. Chem.* *279*, 9321–9330.
- Tan, R., Nakajima, S., Wang, Q., Sun, H., Xue, J., Wu, J., Hellwig, S., Zeng, X., Yates, N.A., Smithgall, T.E., et al. (2017). Nek7 Protects Telomeres from Oxidative DNA Damage by Phosphorylation and Stabilization of TRF1. *Mol. Cell* *65*, 818–831.e5.
- Tanenbaum, M.E., and Medema, R.H. (2010). Mechanisms of Centrosome Separation and Bipolar Spindle Assembly. *Dev. Cell* *19*, 797–806.
- Tanenbaum, M.E., Macůrek, L., Janssen, A., Geers, E.F., Alvarez-Fernández, M., and Medema, R.H. (2009). Kif15 Cooperates with Eg5 to Promote Bipolar Spindle Assembly. *Curr. Biol.* *19*, 1703–1711.
- Tarapore, P., and Fukasawa, K. (2002). Loss of p53 and centrosome hyperamplification. *Oncogene* *21*, 6234–6240.
- Taylor, S.S., and Kornev, A.P. (2011). Protein kinases: evolution of dynamic regulatory proteins. *Trends Biochem. Sci.* *36*, 65–77.
- Teixidó-Travesa, N., Villén, J., Lacasa, C., Bertran, M.T., Archinti, M., Gygi, S.P., Caelles, C., Roig, J., and Lüders, J. (2010). The γ TuRC Revisited: A Comparative Analysis of Interphase and Mitotic Human γ TuRC Redefines the Set of Core Components and Identifies the Novel Subunit GCP8. *Mol. Biol. Cell* *21*, 3963–3972.
- Thompson, S.L., and Compton, D.A. (2010). Proliferation of aneuploid human cells is limited by a p53-dependent mechanism. *J. Cell Biol.* *188*, 369–381.
- Tsai, M.-Y., Wiese, C., Cao, K., Martin, O., Donovan, P., Ruderman, J., Prigent, C., and Zheng, Y. (2003). A Ran signalling pathway mediated by the mitotic kinase Aurora A in spindle assembly. *Nat. Cell Biol.* *5*, 242–248.
- Tseng, B.S., Tan, L., Kapoor, T.M., and Funabiki, H. (2010). Dual detection of chromosomes and microtubules by the chromosomal passenger complex drives spindle assembly. *Dev. Cell* *18*, 903–912.
- Tsou, M.-F.B., and Stearns, T. (2006). Mechanism limiting centrosome duplication to once per cell cycle. *Nature* *442*, 947–951.
- Tsou, M.-F.B., Wang, W.-J., George, K.A., Uryu, K., Stearns, T., and

- Jallepalli, P.V. (2009). Polo kinase and separase regulate the mitotic licensing of centriole duplication in human cells. *Dev. Cell* *17*, 344–354.
- Tulu, U.S., Fagerstrom, C., Ferenz, N.P., and Wadsworth, P. (2006). Molecular Requirements for Kinetochore-Associated Microtubule Formation in Mammalian Cells. *Curr. Biol.* *16*, 536–541.
- Tutt, A., Gabriel, A., Bertwistle, D., Connor, F., Paterson, H., Peacock, J., Ross, G., and Ashworth, A. (1999). Absence of Brca2 causes genome instability by chromosome breakage and loss associated with centrosome amplification. *Curr. Biol.* *CB 9*, 1107–1110.
- Upadhyaya, P., Birkenmeier, E.H., Birkenmeier, C.S., and Barker, J.E. (2000). Mutations in a NIMA-related kinase gene, Nek1, cause pleiotropic effects including a progressive polycystic kidney disease in mice. *97*, 217–221.
- Uto, K., and Sagata, N. (2000). Nek2B, a novel maternal form of Nek2 kinase, is essential for the assembly or maintenance of centrosomes in early *Xenopus* embryos. *EMBO J.* *19*, 1816–1826.
- Vader, G., and Lens, S.M.A. (2008). The Aurora kinase family in cell division and cancer. *Biochim. Biophys. Acta BBA - Rev. Cancer* *1786*, 60–72.
- Vallee, R.B., McKenney, R.J., and Ori-McKenney, K.M. (2012). Multiple modes of cytoplasmic dynein regulation. *Nat. Cell Biol.* *14*, 224–230.
- Verhey, K.J., and Hammond, J.W. (2009). Traffic control: regulation of kinesin motors. *Nat. Rev. Mol. Cell Biol.* *10*, 765–777.
- Vicente, J.J., and Wordeman, L. (2015). Mitosis, Microtubule Dynamics and the Evolution of Kinesins. *Exp. Cell Res.* *334*, 61–69.
- Vidwans, S.J., Wong, M.L., and O'Farrell, P.H. (2003). Anomalous centriole configurations are detected in *Drosophila* wing disc cells upon Cdk1 inactivation. *J. Cell Sci.* *116*, 137–143.
- Wachowicz, P., Fernández-Miranda, G., Marugán, C., Escobar, B., and de Cárcer, G. (2016). Genetic depletion of Polo-like kinase 1 leads to embryonic lethality due to mitotic aberrancies. *BioEssays News Rev. Mol. Cell. Dev. Biol.* *38 Suppl 1*, S96–S106.
- Walczak, C.E., and Heald, R. (2008). Mechanisms of mitotic spindle assembly and function. *Int. Rev. Cytol.* *265*, 111–158.
- Wang, H., Xie, Y.-T., Han, J.-Y., Ruan, Y., Song, A.-P., Zheng, L.-Y., Zhang, W.-Z., Sajdik, C., Li, Y., Tian, X.-X., et al. (2012). Genetic polymorphisms in centrobilin and Nek2 are associated with breast cancer susceptibility in a Chinese Han population. *Breast Cancer Res. Treat.* *136*,

241–251.

Wang, H.-F., Takenaka, K., Nakanishi, A., and Miki, Y. (2011a). BRCA2 and nucleophosmin coregulate centrosome amplification and form a complex with the Rho effector kinase ROCK2. *Cancer Res.* *71*, 68–77.

Wang, W.-J., Soni, R.K., Uryu, K., and Tsou, M.-F.B. (2011b). The conversion of centrioles to centrosomes: essential coupling of duplication with segregation. *J. Cell Biol.* *193*, 727–739.

Wang, W.-J., Soni, R.K., Uryu, K., and Bryan Tsou, M.-F. (2011c). The conversion of centrioles to centrosomes: essential coupling of duplication with segregation. *J. Cell Biol.* *193*, 727–739.

Wang, X., Yang, Y., Duan, Q., Jiang, N., Huang, Y., Darzynkiewicz, Z., and Dai, W. (2008). sSgo1, a major splice variant of Sgo1, functions in centriole cohesion where it is regulated by Plk1. *Dev. Cell* *14*, 331–341.

Weaver, B.A., and Cleveland, D.W. (2008). The aneuploidy paradox in cell growth and tumorigenesis. *Cancer Cell* *14*, 431–433.

Weerd, B.C.M. van de, and Medema, R.H. (2006). Polo-Like Kinases: A Team in Control of the Division. *Cell Cycle* *5*, 853–864.

Weil, D., Garçon, L., Harper, M., Duménil, D., Dautry, F., and Kress, M. (2002). Targeting the kinesin Eg5 to monitor siRNA transfection in mammalian cells. *BioTechniques* *33*, 1244–1248.

Wells, C.I., Kapadia, N.R., Counago, R.M., and Drewry, D.H. (2017). In depth analysis of kinase cross screening data to identify chemical starting points for inhibition of the Nek family of kinases. *BioRxiv* 137968.

Winey, M., and O’Toole, E. (2014). Centriole structure. *Philos. Trans. R. Soc. Lond. B. Biol. Sci.* *369*.

Wittmann, T., Wilm, M., Karsenti, E., and Vernos, I. (2000). Tpx2, a Novel *Xenopus* Map Involved in Spindle Pole Organization. *J. Cell Biol.* *149*, 1405–1418.

Wittmann, T., Hyman, A., and Desai, A. (2001). The spindle: a dynamic assembly of microtubules and motors. *Nat. Cell Biol.* *3*, E28–E34.

Wong, Y.L., Anzola, J.V., Davis, R.L., Yoon, M., Motamedi, A., Kroll, A., Seo, C.P., Hsia, J.E., Kim, S.K., Mitchell, J.W., et al. (2015). Reversible centriole depletion with an inhibitor of Polo-like kinase 4. *Science* *348*, 1155–1160.

Wu, W., Baxter, J.E., Wattam, S.L., Hayward, D.G., Fardilha, M., Knebel, A., Ford, E.M., da Cruz e Silva, E.F., and Fry, A.M. (2007). Alternative splicing controls nuclear translocation of the cell cycle-regulated Nek2

- kinase. *J. Biol. Chem.* 282, 26431–26440.
- Xu, X., Weaver, Z., Linke, S.P., Li, C., Gotay, J., Wang, X.W., Harris, C.C., Ried, T., and Deng, C.X. (1999). Centrosome amplification and a defective G2-M cell cycle checkpoint induce genetic instability in BRCA1 exon 11 isoform-deficient cells. *Mol. Cell* 3, 389–395.
- Yang, J., Adamian, M., and Li, T. (2006). Rootletin Interacts with C-Nap1 and May Function as a Physical Linker between the Pair of Centrioles/Basal Bodies in Cells. *Mol. Biol. Cell* 17, 1033–1040.
- Yang, S.-W., Gao, C., Chen, L., Song, Y.-L., Zhu, J.-L., Qi, S.-T., Jiang, Z.-Z., Wang, Z.-W., Lin, F., Huang, H., et al. (2012). Nek9 regulates spindle organization and cell cycle progression during mouse oocyte meiosis and its location in early embryo mitosis. *Cell Cycle Georget. Tex* 11, 4366–4377.
- Yin, M.-J., Shao, L., Voehringer, D., Smeal, T., and Jallal, B. (2003). The Serine/Threonine Kinase Nek6 Is Required for Cell Cycle Progression through Mitosis. *J. Biol. Chem.* 278, 52454–52460.
- Yissachar, N., Salem, H., Tennenbaum, T., and Motro, B. (2006). Nek7 kinase is enriched at the centrosome, and is required for proper spindle assembly and mitotic progression. *FEBS Lett.* 580, 6489–6495.
- Zhang, Y., Foreman, O., Wigle, D.A., Kosari, F., Vasmatazis, G., Salisbury, J.L., van Deursen, J., and Galardy, P.J. (2012). USP44 regulates centrosome positioning to prevent aneuploidy and suppress tumorigenesis. *J. Clin. Invest.* 122, 4362–4374.
- Zheng, X., Ramani, A., Soni, K., Gottardo, M., Zheng, S., Ming Gooi, L., Li, W., Feng, S., Mariappan, A., Wason, A., et al. (2016). Molecular basis for CPAP-tubulin interaction in controlling centriolar and ciliary length. *Nat. Commun.* 7.
- Zitouni, S., Nabais, C., Jana, S.C., Guerrero, A., and Bettencourt-Dias, M. (2014). Polo-like kinases: structural variations lead to multiple functions. *Nat. Rev. Mol. Cell Biol.* 15, 433–452.
- Zitouni, S., Francia, M.E., Leal, F., Gouveia, S.M., Nabais, C., Duarte, P., Gilberto, S., Brito, D., Moyer, T., Kandels-Lewis, S., et al. (2016). CDK1 prevents unscheduled PLK4-STIL complex assembly in centriole biogenesis. *Curr. Biol. CB* 26, 1127–1137.
- Zou, C., Li, J., Bai, Y., Gunning, W.T., Wazer, D.E., Band, V., and Gao, Q. (2005). Centrobin: a novel daughter centriole-associated protein that is required for centriole duplication. *J. Cell Biol.* 171, 437–445.

SUPPLEMENTARY
TABLES

SUPPLEMENTARY TABLES

SUPPLEMENTARY TABLES

MEFs			
centrin	centrobin	<i>Nek9</i> ^{fl_{ox}/fl_{ox}} (%)	<i>Nek9</i> ^{Δ/Δ} (%)
2+2	1+1	62	48
1+1	1	36	20
2+2	2+2	0	10
2+2	2+1	0	12
2+2+1	2+1+1	0	2
2+2+1	2+1+1	0	4
1+2+3	1+1+2	0	2
2+2+2	2+1+1	2	2

centrobin	cnap1	<i>Nek9</i> ^{fl_{ox}/fl_{ox}} (%)	<i>Nek9</i> ^{Δ/Δ} (%)
2+2	1+1	0	14
2+1	1+1	2	8
1+1	1+1	54	22
1	1+1	44	18
1	1	0	8
1+3+2	1+1+1	0	4
2+2+2+2	1+1+1+1	0	10
2+2+1+1	1+1+1+1	0	8
3+2	1+1	0	4
1+2+2	1+1+1	0	2
2+1+1+1	1+1+1+1	0	2

U2OS			
centrin	centrobin	control siRNA(%)	<i>Nek9</i> siRNA(%)
2+2	1+1	96	68
1+1	1+1	2	0
2+2	2+2	0	20
4+2+4+2	2+2+2+2	0	2
2+3	2+2	0	4
2+1+1+2	1+1+1+1	0	2
4+5	2+5	0	2
4+4	2+2	0	2
centrobin	cnap1	control siRNA(%)	<i>Nek9</i> siRNA(%)
1	1+1	31,7	16,7
1+1	1+1	65,0	50,0
2+1	1+1	1,7	10,0
2+2	2+2	0,0	8,3
2+2	1+1	1,7	3,3
2+3+3	1+1+1	0,0	3,3
4+2	1+1	0,0	1,7
2+2+2+2	1+1+1+1	0,0	5,0
1+2+2	1+1+1	0,0	1,7

Table 7: Centriole configurations for the indicated centriole markers in control or *Nek9*-depleted MEFs or U2OS cells,

